PHD

Heat transfer in bubble columns

Rahimi, Rahbar

Award date:
1988

Awarding institution:
University of Bath

HEAT TRANSFER IN BUBBLE COLUMNS

Submitted by

Rahbar Rahimi

for the degree of

Doctor of Philosophy (PhD)

of the University of Bath

1988

ProQuest LLC
789 East Eisenhower Parkway
P.O. Box 1346
Ann Arbor, MI 48106-1346

Acknowledgment

I wish to express my sincere gratitude to Dr. R.W. Field, to whom I am deeply indebted for his valubale guidance during the course of this work.

I am grateful to the Ministry of Culture and Higher Education of Islamic Republic of Iran particularly members of Department of Chemical Engineering of University of Baluchistan in providing grant and opportunity for me to complete this work.

Thanks are also given to John Bishop for care he has taken in assembling the heater.

This is dedicated to my wife.

CONTENTS Page

SUMMARY

INTRODUCTION

1.- INTRODUCTION 1-1

1.1.-Description and Applications of Bubble Columns. 1-1

1.2.-Flow Patterns in Bubble Column. 1-3

1.1.-PREVIOUS NON-THEORTETICAL WORK ON HEAT TRANSFER 1-5

1.1.1.-Previous Experimental Work. 1-6

1.1.2.-Proposed Correlations. 1-11

1.1.3.-Comparison of Heat Transfer in Mechanically Agitated Vessels with that in Bubble Columns. 1-14

1.2.-PREVIOUS THEORETICAL WORK AND PROPOSED MECHANISMS FOR HEAT TRANSFER. 1-17

1.2.1.-Boundary Layer Models. 1-18

1.2.2.-Surface Renewal Models. 1-19

1.2.3.-Film-Surface Renewal Model. 1-28

1.2.4.-Other Concepts. 1-31

1.3.-CONCLUSION. 1-33

1.4.-SCOPE OF THE PRESENT WORK. 1-35

CHAPTER 2

2. -INTRODUCTION 2-1

2.1.-HYDRODYNAMICS OF BUBBLE COLUMN. 2-1

2.1.1- Bubble Size, Bubble Rise Velocity and Gas Hold-Up. 2-3

2.1.2- Liquid Circulation. 2-9

2.1.2.1- Energy Balance Method for Calculating Average Liquid Circulation Velocity. 2-10

2.2.- HEAT TRANSFER MODEL. 2-16

2.2.1.- Estimation of Parameters Involved in Heat Transfer Model, Equation 2.39. 2-20

2.2.1.1- Evaluation of Contact Time. 2-20

2.2.1.2- Evaluation of Film Thickness. 2-21

2.2.2.- Dimensionless form of Heat Transfer Equation. 2-22

TABLES

FIGURES

CHAPTER 3

3. -INTRODUCTION. 3-1

3.1.-DESCRIPTION OF THE APPARATUS. 3-1

3.1.1.- Column. 3-1

3.1.2.- Air Supply Line. 3-2

3.1.3.- Gas Distributor. 3-3

3.1.4.- Liquid Distributor. 3-3

3.1.5.- Heaters. 3-4

3.1.5.1- Heaters Rods. 3-4

3.1.5.2- Heater Bundle. 3-5

3.2.-EXPERIMENTAL PROCEDURES. 3-6

3.2.1.- Hold-Up Measurments. 3-6

3.2.2.- Heat Transfer Measurements. 3-7

3.3.-PRELIMINARY EXPERIMENTS. 3-10

3.3.1.- Effect of End Caps. 3-10

3.3.2.- Temperature Measurments. 3-10

TABLES

FIGURES

CHAPTER 4

HOLD-UP MEASUREMENTS

4.- INTRODUCTION. 4-1

4.1.-HOLD-UP MEASUREMENTS.- THEORY 4-2

4.1.1.- Introduction. 4-2

4.1.2.- Bed Expansion and Manometric Methods. 4-3

4.2.-MANOMETRIC LOCAL AND AVERAGE GAS HOLD-UP MEASUREMENTS. 4-5

4.2.1.- Manometric Method Discussion. 4-5

4.3.-AVERAGE HOLD-UP MEASUREMENTS FOR AIR-WATER SYSTEMS 4-7

4.3.1.- Effect of Liquid Height. 4-7

4.3.2.- Effect of Bulk Liquid Temperature. 4-8

4.3.3.- Effect of of Gas Distributor. 4-9

4.3.4.- Comparison of Experimental and Predicted Data. 4-11

4.4.-AVERAGE GAS HOLD-UP MEASUREMENTS FOR CMC SOLUTIONS. 4-12

4.4.1.- Effect of CMC Concentration on Gas Hold-Up. 4-13

4.4.2.- Effect of Gas Distributor. 4-14

4.4.3.- Effect of Bulk Liquid Temperature. 4-15

4.4.4.- Comparison of Experimental and Predicted Gas Hold-Up Data. 4-16

4.5.-Conclusion. 4-18

TABLES

FIGURES

CHAPTER 5

HEAT TRANSFER FROM SINGLE CYLINDRICAL HEATER

5.- INTRODUCTION. 5-1

5.1.-EFFECT OF SUPERFICIAL GAS VELOCITY ON THE HEAT TRANSFER COEFFICIENT. 5-2

5.2.-EFFECT OF LIQUID HEIGHT ON THE HEAT TRANSFER COEFFICIENT. 5-4

5.3.-EFFECT OF GAS DISTRIBUTOR TYPE AND GAS HOLD-UP. 5-7

5.3.1.- Effect of Gas Distributor Type. 5-7

5.3.2.- Effect of Average Gas Hold-Up. 5-9

5.4.-EFFECT OF HEATER POSITION IN COLUMN. 5-13

5.4.1.- Effect of Heater Vertical Position. 5-13

5.4.2.- Effect of Heater Radial Position. 5-15

5.5.-Effect of Heater Dimension and Orientation. 5-17

5.5.1.- Effect of Heater Vertical Length. 5-18

5.5.2.- Effect of Heater Orientation. 5-20

5.6.-EFFECT OF POWER INPUT TO THE HEATER AND HEATER SURFACE TEMPERATURE. 5-23

5.7.-EFFECT OF LIQUID PHASE VISCOSITY. 5-25

5.7.1.-Correlation of Experimental Data Based on Deckwer Model. 5-28

5.8.-SUMMARY. 5-29

TABLES

FIGURES

CHAPTER 6

HEAT TRANSFER FROM A BUNDLE OF HEATERS

6. -INTRODUCTION. 6-1

6.1.-EXPERIMENTS. 6-3

6.1.1.- Effect of the Tube Bundle End Plate Support. 6-4

6.1.2.- Effect of the Liquid Height. 6-5

6.1.3.- Effect of Vertical Position of the Heater. 6-5

6.1.4.- Effect of Horizontal Rotation of Bundle. 6-6

6.1.5.- Effect of Number of Rows and Columns within the Bundle. 6-6

6.1.6.- Effect of Tube Spacing. 6-7

6.2.-DISCUSSION OF THE RESULTS. 6-8

6.2.1.- Effect of the Tube Bundle End Plate. 6-8

6.2.2.- Effects of Water Height and Heater Bundle Position. 6-8

6.2.3.- Effect of Bundle Layout. 6-9

6.3.-CONCLUSIONS. 6-10

FIGURES

CHAPTER 7

FUTHER DISCUSSION OF RESULTS, THEORETICAL CONSIDERATIONS AND TEST OF THE MODEL

7.1.-INTRODUCTION. 7-1

7.1.1.-Comparison of Experimental Heat Transfer Coefficient Data. 7-2

7.1.2.-Comparison of the Existing Correlations with the Experimental Data. 7-3

7.1.3.-A General Consideration of Lewis et al Model. 7-5

7.2.-Evaluation of Parameters of the Present Model. 7-7

7.2.1.- Average Liquid Circulation Velocity. 7-7

7.2.2.- Heater Characteristic Length. 7-9

7.2.3.- Evaluation of Thermal Boundary Layer Thickness. 7-10

7.2.4.- The procedure for the Calculation of the Heat Transfer Coefficient for a Newtonian Fluid. 7-11

7.3.- COMPARISON OF THE MODEL WITH THE EXPERIMENTAL DATA AND THE PREVIOUS MODELS. 7-13

7.3.1.- Air-Water system. 7-13

7.3.2.- Other Systems. 7-14

7.3.3.- Comparison with Lewis et al (1982), Deckwer(1980) and Ruckenstein and Smigelschi(1965). 7-15

7.3.4.- Test of the Model in Dimensionless Form. 7-16

7.4.-APPLICATION OF THE MODEL TO NON- NEWTONIAN LIQUID. CMC SOLUTIONS 7-17

7.5.-SUMMARY. 7-20

7.6.-SUGGESTIONS FOR FURTHER WORK. 7-21

TABLES

FIGURES

APPENDIXES

APPENDIX A

A1.- CALCULATION OF SUPERFICIAL GAS VELOCITY. A-1

A2.- CALCULATION OF THE CORRECTED SURFACE TEMPERATURE. A-4

TABLES

FIGURES

APPENDIX B

HOLD-UP MEASUREMENTS - USE OF DIGITAL MANOMETER

APPENDIX C

DATA USED TO TEST NEW MODEL

C1-Comparison of The Prediction of The Present Model With the Experimental Values for Air-Water System. C-1

C2- Comparison of the Model Predictions with the Experimental Valuesfor Several Organic Liquids. C-8

APPENDIX D

CALCULATION INVOLVED CMC DATA

D1- Calculation of Heat Transfer Coefficient. D1-1

D2-Determination of The Best Values of Coefficients of Equation 2.47. D2-1

D3- Model Prediction of Heat Transfer Coefficient for CMC Solutions. D3-1

NOMENCLATURE.

REFERENCES.

SUMMARY

With the growth in biotechnology, bubble column behaviour is of increasing interest. Many of these applications as well as common applications involve transfer of heat.

Experimental investigation of heat transfer in bubble columns has been of interest to many workers, but only a few have taken a mechanistic approach. Furthermore most of the presented correlations do not represent the behaviour of systems over a wide viscosity range.

The Lewis et al model which was developed in Cambridge University is of value due to its sound theoretical basis and its ability to explain the behaviour of systems of low viscosity (see chapter1). In this work that model was tested, improved and hence a new procedure to predict heat transfer coefficients for Newtonian and non-Newtonian fluid has been presented. The new model can cover a wide range of liquid physical properties with viscosity as high as 180 cP and superficial gas velocies in the range of 10 to 120 mms^{-1}.

The model predictions are $\pm$25% accurate for Newtonian gas- liquid mixtures with 80% of the experimental data of several investigators lying within that error band. However the model predictions for CMC solutions of different concentrations are in

general about 35% higher than the experimental data (see chapter7). Nevertheless the model is of value and simple to use. The latter follows from the fact that the development of Lewis et al model was achived (a) by proposing a simplified equation to calculate the average liquid circulation velocity and (b) by developing the calculation of the film side heat transfer coefficient (see chapter 2).

Experimental investigation of heat transfer in bubble column confirmed the existence of a heater characteristic length and have shown its dependency upon the liquid viscosity (see chapter 5). During the course of this work a simple technique for measuring local gas hold-up was tested. This technique, however, was found to be applicable only to low gas flow rates of less than about 80 mms^{-1} (see chapter 4).

It was found that the vertical baffles reduce the heat transfer coefficient significantly whilst increasing the number of rows and columns in a tube bundle decreases the heat transfer coefficient only slightly. The existence of an optimum pitch to diameter ratio was realized (see chapter 6).

CHAPTER 1

INTRODUCTION

1. - Introduction

In this chapter after a general description of the various designs of bubble column, a review of previous work on heat transfer in bubble columns will be given. This will be followed by description of the scope of the present work.

1.1. - Description and Application of Bubble Columns.

Bubble columns are gas-liquid contactors in which the liquid phase is the continuous phase and the gas phase in the form of bubbles is the discontinuous phase. Different designs of bubble columns are schematically shown in Figure 1.1.

Figure 1.1(a) illustrates a simple bubble column in which the column is vertical and contains a batch liquid with gas being injected via a gas sparger at the base of the column. Alternatively both phases may be continuous. Figure 1.1(b) and

1.1(c) illustrates co-current and counter-current flow of both gas and liquid for multi-staged and multi-channel bubble column, respectively. Figure 1.1(d) is a schematic view of one form of a loop reactor in which a gas free liquid phase is separated from the mixture of gas-liquid by a centrally situated tube. In the downflow bubble column, Figure 1.1(e), gas is sparged into the top of the column.

Bubble columns containing a solid phase are called slurry reactors if both the solid and the gas phases are continuous. However, the term fluidized bed may be used when the solid phase is not continuous, Figure 1.1(f).

The choice between different designs is mostly based on the required gas and fluid residence times, which are the most important parameters in mass transfer operations, for example counter-current gas-liquid operations are desirable when relatively high gas conversions are desired.

Commercial bubble columns typically have diameters between 0.5 and 3 m and are up to 15 m long. The superficial gas velocity, U_g, is generally between 10 - 120 mms^{-1}.

Bubble columns are used in a variety of processes for chemical reactions or gas absorptions. A few examples of the current uses are summarized in Table 1.1. A more comprehensive list, however, was provided by Shah et al (1982). Except for biotechnology, food processing and pharmaceutical processes

where bubble columns reactors are often used in the processing of highly viscous and often non-Newtonian media, their use is with low viscosity media. Whilst design simplicity and low cost of maintenance make bubble column very attractive the relatively high pressure drop between gas inlet and outlet and the high amount of backmixing of both phases limits their use as absorbers and strippers. Backmixing, however, can be reduced by employing multi-channel columns.

Many of the reaction that are carried out in the bubble columns are highly exothermic and the rate of heat removal is therefore critical. Heat removal depends on the flow patterns arising from the imposed gas and liquid flow rates and the physical properties of the media.

1.2.- Flow Patterns in Bubble Columns.

Attention will be focused upon simple bubble columns of the type shown in Figure 1.1(a). The important variables that affect the bubble dynamics and flow regime in a bubble column are gas velocity, fluid properties, gas distributor and column diameter. Figure 1.2 shows the different flow regimes as a function of gas flow rate.

At low gas superficial velocities (usually less than 40 mms^{-1}) bubbles are small and uniform. Their nature depends on the physical properties of the liquid phase and gas distributor. Bubble coalescence are also small and distinct chains of rising

bubbles are observable. This regime is called bubbly flow. Figure 1.2(a) and Figure 1.2(b) show bubbly flow regimes when gas distribution is even and uneven, respectively. As the gas flow rate increases the bubble coalescence also increases. At the same time bubble breakage rate due to shearing effect of liquid motion becomes important, and so a mixture of large and small bubbles are produced. This regime in which the bubble paths are ill-defined is churn-turbulent and is shown in Figure 1.2(c). However, further increases in the gas flow rates can result in the formation of very large bubbles which almost fill the cross section of the column. Relatively small column diameter (less than 0.10 m) facilitates slug flow formation which is shown in Figure 1.2(d).

The rising bubbles causes the liquid to flow upward in the wakes of the bubbles. To satisfy continuity there is an equal downward flow of liquid. In addition to this relatively minor turnover of liquid, there is more major mixing of liquid in most bubble columns. This is caused by the distinct tendency of bubbles to flow preferentially in the central area of the column. The pressure difference between this region and the wall region causes liquid to flow upwards in the central area and downwards in the outer area. This is discussed in a greater detail in Chapter 2. This net circulative motion of the liquid creates a high degree of liquid mixing and therefore heat tranfer coefficients in bubble columns are high. The high degree of mixing is favourable in those cases where there is a need for uniformity of temperature throughout the column. This

facilitates temperature control of temperatures sensitive reactions.

Knowledge of liquid circulation is an important parameter in convective heat transfer models for bubble columns. Liquid circulation will be further discussed in Chapter 2, but a review of previous correlations on the heat transfer in bubbble columns will be given in the next section.

1.1.- PREVIOUS NON-THEORETICAL WORK ON HEAT TRANSFER.

As mentioned earlier many applications involving bubble columns require the removal of heat. Heat removal may be achieved by the following three methods;

1.- Vaporization of the liquid phase.

2.- Passing the liquid phase through a conventional heat exchanger located externally to the column.

3.- Direct tranfer of heat from the bubbly mixture to either internal tubes or cooling jackets surrounding the wall.

The first two methods are conventional methods and will not be discussed. The third method which involves determination of bubble columns heat transfer coefficients is the subject of this thesis. Part one of this section concentrates on the previous

experimental work, whilst part 2 focuses on the proposed correlations in the literature.

1.1.1.- Previous Experimental Work.

Heat transfer in a simple bubble column can be considered to dependent on the following parameters;

a).- Physical properties of gas and liquid phase

b).- Volumetric flow rates of gas and liquid phase.

c).- Column dimensions.

d).- Geometry and orientation of the heater.

e).- Design of distributor plate.

The above parameters will be discussed in turn.

a).- Physical properties of gas and liquid phase.

Kubie (1974) investigated the effect of gas physical properties by using air, argon and carbon dioxide at atmospheric pressure. It was found that the effect of gas properties are negligible and could be neglected. It was concluded that this was due in part to the low thermal conductivity and heat capacity of the gas and also to the low mass of gas present in the column when compared with that of the liquid.

Table 1.2 shows the dependency of liquid properties upon heat transfer coefficient for a number of correlations. It is evident that the heat transfer coefficient depends on the liquid

thermal conductivity, k, heat capacity, C_p, and viscosity, μ. Of the above mentioned parameters the effect of viscosity is substantial as it has an affect on the hydrodynamics of the system. It also varies with temperature over a greater range than the other physical properties.

Liquid viscosity directly influences the thickness of the boundary layer on the heating or cooling elements. As an increase in viscosity leads to poorer mixing and also an increase in the boundary layer thickness, it is evident that the heat transfer coefficient will be reduced. This is shown in Table 1.2 by the negative index which is -0.33 in most cases.

Since physical properties are a function of temperature Burkel (1972) suggested that the physical properties should be referred to the surface temperature of the heating element in order to account for the effect of different heat fluxes. This was accounted for by the introduction of Sieder-Tate viscosity correction term, $(\frac{\mu}{\mu_w})^n$, in the experimental correlations. The reported index by Konsetove (1966) and Joshi et al (1980) is 0.14. Whilst Chen (1987) gave value of 0.25 for the index when modifying the Ruckenstein and Smigelschi (1965) correlation.

b).- Volumetric flow rates of gas and liquid.

It has been found that heat transfer coefficient, h, increases with increasing gas superficial velocity. Up to a value of 50 mms^{-1} there is a steady rate of increase, but the

rate of increase is less with further increases in gas superficial velocity. The heat transfer coefficient remains approximately constant above gas superficial velocities of $100 mms^{-1}$. This overall trend is general but various workers have reported different dependencies.

Table 1.2 shows that the index of superficial gas velocity, U_g, varies from 0.19 to 0.33. The variation of index is related to the prevailing flow regime in the bubble column. At low superficial gas velocities of less than 40 mms^{-1} the index is 0.33. This is confirmed by many investigators such as Ruckenstein and Smigelschi (1965). The low index of 0.19 is for gas flow rates of above 70 mms^{-1} as reported by Lewis et al (1982). However, many investigators have accepted the average index of 0.25 for all gas flow rates between 10 to 100 mms^{-1}.

c).- Effect of Column Dimensions.

It is evident from Table 1.2 that the heat transfer coefficient is considered to be neither a significant function of column diameter nor of liquid height. Fair (1962), Konsentove (1966) and Kubie (1974) are among those who investigated the effect of liquid height. They concluded that for an aspect ratio of greater than 1 (aspect ratio = liquid height / column diameter) the heat transfer coefficient is independent of column diamater and liquid height. However, Wendt et al (1984) reported that in a counter-current bubble column the column diameter does not affect the heat transfer coefficient as long as

the flow is homogeneous. With a heterogeneous flow an increase in diameter leads to higher heat transfer coefficient and the effect is more at a relatively high superficial gas velocity. It was reported that $h \propto D^{0.15}$. Their investigations were carried out in five columns of 0.196 m to 1.0 m in diameter. The columns height was varied between 3 and 10 m and the gas superficial velocity from 5 mms^{-1} to 1000 mms^{-1}.

d).- Geometry and Orientation of the Heater.

Almost all the investigators whose experimental equipment were comparable with the commercial size bubble columns either reported or assumed that heat transfer coefficient did not depend on the heater length and therefore no characteristic heater dimension has generally been reported. However, Mersmann (1977) in comparing the reported experimental data deduced that the scatter of heat transfer coefficient data may be due to the different heater lengths that were used.

Kubie (1974) who used a wire heating element, found that the heat transfer coefficient from a horizontal heater of diameter H_d was proportional to $H_d^{-0.357}$. Lewis et al (1982) reported that for air-water system, using cylindrical rods as heaters, the heat transfer coefficient decreased with increasing heater vertical dimension (diameter or length) up to 40 to 50 mm. After this, h, was unaffected by further increases in the vertical dimensions of heater. They have concluded that the heater characteristic length is the vertical length of the

heaters.

Kubie (1974) and Michael and Reichert (1981) have reported that the vertical distance of the heating element from the gas sparger does not have a significant effect upon heat transfer coefficient provided that it is more than 1.5 times thecolumn diameter from the base.

c).- Design of the Gas Distributor.

The influence of sparger design in the behaviour of a bubble column is rather complex. The optimum sparger design is related to the design parameter of interest and the optimum design for different design parameters is different. For example, to increase the gas-liquid interfacial area it is necessary to increase the gas hold-up and reduce the bubble size. This however can be obtained by decreasing the intensity of liquid circulation which in turn will reduce the heat transfer coefficient.

At low gas flow rates (less than 50 mms^{-1}) in the bubbly flow regime the effect of the sparger design on the heat transfer coefficient may be important. In this region whilst the bubble size is independent of the gas flow rate, the bubble frequency is proportional to the gas flow rate. Coalescence in the liquid is not high enough to govern the quality of the dispersion. Thus different spargers will give a different gas hold-up and hence liquid circulation will be different. For example a porous plate will give a higher gas hold-up and a lower circulation intensity

compared with a perforated plate.

However in the turbulent regime the gas distributor design is not important because the dispersion quality mainly depends on the mixing created by the liquid turbulence.

Indeed Kubie (1974) who used a perforated and porous plate gas distributor and Lewis et al (1982) who only used perforated plates have reported a non-significant effect of gas distributor on the heat transfer coefficient. However the effect of gas distributor on the heat trasfer coefficient will be further examined in chapter 5.

1.1.2.- Proposed Correlations.

Following Hart (1976) the empirical correlations base on the experimental observations can be divided into the following three groups;

a).- Dimensionless equations involving Nu, Re, Pr, for example Novasade (1954), Kolbel (1960).

b).- Dimensional equations which generally do not include the gravitaional constant, g, for example Fair(1967) , Yoshitoma (1965), Konsetove (1966), Fair et al (1962)

c).- Dimensionless equations that incorporate, g, for

example Kast (1962).

As a result of this review, Hart presented the following equation

$$St = 0.125\,(Re\,Fr)^{-0.25}Pr^{-0.6} \qquad \ldots 1.1$$

Subsequently Stiff and Weinspach (1978), Joshi et al (1982), Deckwer (1980) and Vant Reit et al (1984) have also reviewed the published correlations. Table 1.2 and Table 1.3 summarize both the theoretical and empirical correlations together with their applicability range.

In addition to reviewing the literature, Deckewer considered the mechanism of heat transfer (which is discussed further in section 1.2) and suggested the following design equation.

$$St = 0.1(ReFrPr^2)^{-0.25} \qquad \ldots 1.2$$

Michael and Reichert (1981) reported that equation 1.2 could also be used for slurry reactors.

However, it is worth noting that according to these equations the heat transfer coefficient increases steadily with increasing gas superficial velocity, whereas there is a clear tendency for the heat transfer coefficient to remain

approximately constant above a certain gas superficial velocity which is usually about 100 mms^{-1}. These equations also do not show the effect of heater length as indicated by the choice of the Stanton number, St, to represent heat transfer equations.

Mersmann (1976) approached (see also section 1.2.4)the problem of the decreasing dependency of heat transfer coefficient upon superficial gas velocity. He suggested that if the superficial gas velocity was more than 15% of the rise velocity of a single bubble then the heat transfer coefficient had reached a maximum. The equations that have been given for the maximum heat transfer coefficient are;

For $0.03 < Pr < 1$

$$h_{max} = 0.107k \left[\frac{g}{\nu\alpha} \right]^{0.333} Pr^{0.266} \qquad \ldots 1.3$$

For $1 < Pr < 100$

$$h_{max} = 0.120 \left(\frac{g^2}{\nu} \right)^{0.167} (k\rho C_p)^{0.50} \qquad \ldots 1.4$$

Considering that the bubble rise velocity for an air-water mixture is about 300 mms^{-1}, then the maximum heat transfer coefficient will according to the above criteria be obtained at the superficial gas velocity of about 50 mms^{-1}. This value of gas superficial velocity corresponds to the change of liquid mixture flow pattern from bubbly flow to churn-turbulent flow. However, as mentioned earlier the heat transfer coefficient does

not remain approximately constant until a superficial gas velocity of 100 mms^{-1} is exceeded.

Equations of the type shown in Table 1.2 are easy to use. Apart from Deckwer who theoretically justified the form of the equation, they are essentially a fit to experimental data. For their range of applicability predictions have a likely error of ± 20%. However, in general they do not give an insight into the possible mechanism of heat transfer and the effect of other parameters such as gas hold-up and heater position.

A few have attempted to obtain a more general equation from theoretical consideration. This aspect will be covered after the following sub-section.

1.1.3.- Comparison of Heat Transfer in Mechanically Agitated Vessels with that in Bubble Columns.

Fair (1962) mentioned that heat transfer in bubble columns is comparable with that in of mechanical agitated gas-liquid vessels. He also found that the vibration of horizontal perforated baffle plates increases the heat transfer coefficient by 10%.

Stieff and Weinspach (1978), who have made an extensive comparison of work on heat transfer in the stirred and non-stirred gas-liquid reactors, have found that heat transfer

for relatively short bubble columns is less than that of mechanically agitated vessels under conditions of bubbly flow. However, at higher flow rates, the effect of mechanical agitation is not significant. The following equations were presented, which applies to simultaneous gas and mechanical agitation of the stirred vessel. In the absence of mechanical agitaion $Re_n = 0$. It is defined as $Re_n = (\rho n D_R^2)/\mu$ where n is stirring speed and D_R is the impeller diameter, D_R assumes column diameter, D, in the absence of mechanical agitation in the following equations.

Heat transfer "wall-aerated"

$$St = 0.054 \left[(Re_G Fr_G Pr^2)^{1/3}\right]^{-A} \left(\frac{\mu}{\mu_w}\right)^{0.42} \qquad \ldots 1.5$$

where

$$A = (0.79 + 0.186 \times 10^{-5} Re_n)(Re_n + 1)^{0.107} \qquad \ldots 1.6$$

Heat transfer "coil-aerated"

$$St = 0.137 \left[(Re_G Fr_G Pr^2)^{1/3}\right]^{-B} \left(\frac{\mu}{\mu_w}\right)^{0.42} \qquad \ldots 1.7$$

where

$$B = (0.73 + 0.164 \times 10^{-5} Re_n)(Re_n + 1)^{0.047}$$

and

$$Re_G = \frac{\rho U_g D_R}{\mu} \quad ; Pr = \frac{\mu C_p}{k} \quad ; Fr_G = \frac{U_g^2}{g D_R} \quad \ldots 1.8$$

Their validity range was given as

$$0.5 \leqslant Re_G \leqslant 16000 \qquad 4 \leqslant Pr < 825 \qquad 1 \leqslant \frac{H}{D} \leqslant 3$$

$$1.6 \times^{-9} \leqslant Fr_G \leqslant 4\ 10^{-2} \qquad 0 \leqslant Re_n \leqslant 2.2 \times 10^{-5} \qquad \ldots 1.9$$

Heijnen, and Reit (1984) also considered the similarity between mechanically agitated vessels and bubble columns. It was considered that the heat transfer coefficient for air-water system bubble columns, following the correlation of Fair (1962) and Burkel (1972) could be given as

$$h = 9391\ U_g^{0.25} \left(\frac{\mu}{\mu_w}\right)^{-0.35} \qquad \ldots 1.10$$

For mechanically agitated vessels, h, could be calculated from the following equation

$$h = 930 \left(\frac{P}{V}\right)^{0.222} \left(\frac{\mu}{\mu_w}\right)^{-0.33} \qquad \ldots 1.11$$

Now, since the energy input rate (P/V) for bubble columns is, $\rho g U_g$, the similarity of heat transfer coefficient is clear from the above equations.

Finally Joshi et al (1980) assumed that the heat transfer coefficient in bubble columns could be related to either the correlations for heat transfer coefficient in mechanically agitated vessels or to the relevant single phase pipe flow equations provided that the average liquid circulation velocity was employed. Hence the following equations were given;

Comparison with the mechanically agitated vessels yielded:

$$\frac{hD}{k} = 0.48 \left| \frac{D^{1.33} g^{0.33} \rho (U_g - \epsilon U_b)^{0.33}}{\nu} \right|^{0.66} \left(\frac{C_P \mu}{k}\right)^{0.33} \left(\frac{\mu}{\mu_w}\right)^{0.14} \quad \ldots 1.12$$

Comparison with pipe flow gave:

$$\frac{hD}{k} = 0.031 \left| \frac{D^{1.33} g^{0.33} \rho (U_g - \epsilon U_b)^{0.33}}{\nu} \right|^{0.80} \left(\frac{C_P \mu}{k}\right)^{0.33} \left(\frac{\mu}{\mu_w}\right)^{0.14} \quad \ldots 1.13$$

1.2.- PREVIOUS THEORETICAL WORK AND PROPOSED MECHANISMS FOR HEAT TRANSFER.

Although there is quite a wide range of experimental data on heat transfer in bubble columns only a few theoretical studies are available. A mechanistic model of heat transfer in a bubble column requires a hydrodynamic model of the bubble column. In the absence of this knowledge semi-theoretical models are

inevitable.

As mentioned earlier, the presence of gas bubbles causes turbulence. This turbulence is responsible for the continuous mixing of the liquid phase. Due to the high degree of mixing heat transfer in bubble columns is high and the liquid is isothermal. Different heat transfer mechanisms have been proposed and these have been classified in four groups

1.- Boundary layer models.

2.- Surface renewal models.

3.- Film surface renewal models.

4.- Other concepts.

These will be examined in turn.

1.2.1.- Boundary Layer Models.

An often over looked work is that of Konsetove (1966) who assumed that due to the non-linear path of the rising bubbles, the liquid movements in the bubble columns are three dimensional. The high rate of heat transfer was caused by the high intensity of these movements. It was assumed that the liquid movements in various directions took an equal part in heat transfer and therefore the heat transfer coefficient was calculated as the sum of normal and parallel heat transfer coefficients.

$$h = \frac{1}{3}h_n + \frac{2}{3}h_p \qquad \ldots 1.14$$

Knowledge of, h_n and h_p are required and Konsetove adopted the following equations which were derived for heat transfer over a surface in a mechanically agitated systems;

$$Nu_n = \frac{h_n l}{k} = 1.14 Re^{0.50} Pr^{0.33} \left(\frac{\mu}{\mu_w}\right)^{0.14} \qquad \ldots 1.15$$

$$Nu_p = \frac{h_p l}{k} = 0.035 Re^{0.80} Pr^{0.33} \left(\frac{\mu}{\mu_w}\right)^{0.14} \qquad \ldots 1.16$$

The liquid movement size, l, was tentatively assumed to be proportional to either the column diameter or the diameter of the heating element depending on whether the heat transfer is to the column wall or to the pipe built into the column. It was assumed that;

For a heat transfer to a wall;

$$l = \frac{1}{6} D \qquad \ldots 1.17$$

and for a heat transfer to a coil;

$$l = D_p \qquad \ldots 1.18$$

Futhermore, knowledge of the average liquid movement velocity is required. The value of $Re = \frac{Ul\rho}{\mu}$ can then be calculated. To this end it was assumed that all the energy input to the column was dissipated in the liquid movement. Hence the following equation was derived for the average liquid velocity.

$$U = \epsilon^{0.5}\left(\frac{1}{2}gD\right)^{0.5}\frac{\rho}{\rho - \rho_g} \qquad \ldots 1.19$$

where

$$\epsilon = 0.04\left[U_g\left(\frac{g\sigma}{\rho - \rho_g}\right)^{-0.25}\right]^{2/3}\left(\frac{\rho_g}{\rho}\right)^{0.15} \qquad \ldots 1.20$$

Substituting back the values of l and U into the equations 1.15 and 1.16 and adding the results according to equation 1.14 will give an equation for the heat transfer coefficient.

It was found that a plot of this equation against the Reynolds number gave a straight line in the range of Re = 10^{-3} to 10^{-5}. With the use of experimental data for estimating constants the equation was simplified to:

a.- For heat transfer to the column wall

$$\frac{h}{k}\left(\frac{\nu^2}{g}\right)^{1/3}Pr^{-1/3}\left(\frac{\mu}{\mu_w}\right)^{-0.14} = 0.25\epsilon^{1/3} \qquad \ldots 1.21(a)$$

In dimensionless form this can be represented as;

$$St = 0.25\epsilon^{0.33}(ReFrPr^2)^{-0.33} \qquad \ldots 1.21(b)$$

b.- For heat transfer to coil or pipe;

$$\frac{h}{k}\left(\frac{\mu^2}{g}\right)^{1/3} Pr^{-1/3}\left(\frac{\mu}{\mu_w}\right)^{-0.14} = 0.18\,\epsilon^{1/3}\left(\frac{D}{D_p}\right)^{1/3} \qquad \ldots 1.22$$

While this theory correctly shows the minor dependency of heat transfer coefficient on the surface tension and gives a reasonable dependency upon viscosity and superficial gas velocity, the term $(D/D_p)^{1/3}$ is unsupported by experimental evidence. It shows an over dependency upon column diameter and the heater size.

The method adopted by Konsetove is the typical approach of early investigators. An equation for heat transfer to single phase liquid over flat plate was selected and then modied to take into account the effect of gas-liquid mixing.

Ruckenstein (1958) showed that heat transfer over flat plate is given by

$$Nu \approx Re\sqrt{\frac{f}{2}} Pr^{\frac{1}{3}} \qquad \ldots 1.23$$

where for laminar flow

$$f = 16Re^{-1} \qquad \ldots 1.24$$

and for turbulent flow

$$f = 0.046Re^{-0.2} \qquad \ldots 1.25$$

It was assumed by Ruckenstein and Smegilschi (1965) that a laminar boundary layer was formed along the wall of the heat transfer element. This consisted of short portions of length x Figure 1.3 . As elements of liquid come into contact with the surface they flow in a laminar motion over a short path of length x after which they leave the surface and lose their identity in the liquid phase. The process repeats itself at intervals of x. Dimensional considerations gave the following equations for x and circulations velocity, U_c

$$x \propto \left(\frac{\mu}{\rho}\right)^{0.667} (g\epsilon)^{-0.333} \qquad \ldots 1.26$$

$$U_c \propto \left(\frac{\mu}{\rho}\right)^{0.667} (g\epsilon)^{0.333} \qquad \ldots 1.27$$

The above equations, together with equation 1.23 and 1.24 or 1.25 will after simplification give the following equation

$$h = Ak\left(\frac{g\epsilon}{\nu}\right)^{0.5}\left(\frac{\nu}{\alpha}\right)^{0.33} \qquad \ldots 1.28$$

Ruckenstein and Smegilschi assumed that gas hold-up, ϵ, is given by;

$$\epsilon = \frac{U_g}{U_b}$$

and that U_b can be calculated from

$$U_b = 1.18\left(\frac{\sigma g}{\rho}\right)^{0.25}$$

Experimental data were used to evaluate the constant A and the final equation presented was ,as follows :

$$h = 0.28k\left(\frac{g\,\epsilon}{\nu\alpha}\right)^{1/3} \qquad \ldots 1.29$$

Field (1987) casted equation 1.29 into dimensionless form and obtained :

$$St = A\,\epsilon^{0.33}(Re\,Fr\,Pr^2)^{-0.333} \qquad \ldots 1.30$$

The similarity of this equation and equation 1.21(b), which has previously not been noted, is striking.

Chen (1987) showed that the range of applicability of equation 1.28 could also be improved by the use of the Nicklin (1962)
equation for calculation of gas hold-up and hence equation 1.29 can be represented as;

$$h = Ck\left(\frac{g}{\nu\alpha}\right)^{0.33}\left|\frac{U_g}{(1.2U_g + U_b)}\right|^{0.33} \qquad \ldots 1.31$$

Chen analyzied Lewis's et al data and found that the value of constant, C, decreased with increasing heater characteristic length, L_c. When this dimension reached about 40 to 50 mm, C remained virtually constant at value of 41.

Zehnere (1986) adopted the following equation for a free

falling liquid over a flat plate.

$$Nu = 0.18 Pe^{2/3} Pr^{-1/3} \qquad \ldots 1.32$$

This was modified to take into account the effect of bubbles that disturb the boundary layer.

It was postulated that the bubbles penetrate the boundary layer and reduce the thickness of the boundary layer at the point of contact Figure 1.3. This takes place at constant intervals equal to that of the distance between bubbles. This distance, l, assumed to be :

$$l = d_b \left(\frac{\pi}{6\epsilon}\right)^{\frac{1}{3}} \qquad \ldots 1.33$$

However, at the point of contact, where the boundary layer is thin, due to the low conductivity of gas, heat transfer coefficient is not high. Thus Zehner also postulated that the heat transfer coefficient is proportional to the liquid content of the column;

$$h = h_l f(\epsilon) \qquad \ldots 1.34$$

Where in the simplest form

$$f(\epsilon) = 1 - \epsilon \qquad \ldots 1.35$$

However, to calculate the Peclet number (Pe = Re Pr)

knowledge of liquid velocity is required. The following formula due to Zehner (1986) was used.

$$U_c = \left(\frac{1}{2.5}\frac{\Delta\rho}{\rho} g l D U_g\right)^{\frac{1}{3}} \qquad \ldots 1.36$$

This together with equation 1.33, enabled h to be calculated from equations 1.32 and 1.34.

$$h = 0.18(1-\epsilon)\left(k^2 \rho C_p \frac{U_c^2}{l\mu}\right)^{\frac{1}{3}} \qquad \ldots 1.37$$

where l and U_c are given by 1.33 and 1.36, respectively.

It should be noted that whilst this equation gives a correct dependency of h upon $Ug^{0.22}$ for high superficial gas velocity, it assumes that the distance between the bubbles, l, are constant. This condition can only be met at very low superficial gas velocity.

Boundary layer models which have been described in this section require knowledge of a characteristic length and also a characteristic velocity. These difficulties were overcome by Kast (1963) who recogized that the usual concept of a boundary layer does not apply to the bubble agitated systems or play only a rather unimportant role. Surface renewal models, which are described below, are more appropriate.

1.2.2.- Surface Renewal Models.

Kast (1963) suggested that due to the high turbulence in bubble columns, it is unrealistic to asssume the existance of a liquid film at the heater surface. Deckwer (1980) developed this concept and his model envisages that in the vicinitiy of the heater surface there is a steady regular flow of liquid eddies from the bulk of liquid to the wall and vice versa Figure 1.3(c). This condition resembles Highbie's surface renewal model of mass transfer. The elements of liquid have a contact time, τ, at the surface. The assumption of unsteady one dimensional heat conduction into the liquid on the heater surface required the solutions of the following heat conduction equation;

$$\frac{\partial T}{\partial t} = \alpha \frac{\partial^2 T}{\partial x^2} \qquad \ldots 1.38$$

Boundary conditions are;

$$T = T_s \quad \text{at} \quad x = 0 \quad t \geq 0 \qquad \ldots 1.39$$

$$T = T_b \quad \text{at} \quad x > 0 \quad t = 0$$

$$T = T_b \quad \text{at} \quad x = \infty \quad t = 0 \qquad \ldots 1.40$$

Solution of this standard equation predicts that

$$h \propto \left[\frac{k\rho C_p}{t}\right]^{\frac{1}{2}} \qquad \ldots 1.41$$

Having dismissed the length of the heater as a basis for the

characteristic length, Deckwer calculated the contact time from Kolmogoroff's theory of local isotropic turbulence (see for example Davies (1972)).

The length, l, and velocity scale, U_l, of the micro eddies were related to the energy input per unit mass , E, and the kinematic velocity of the liquid , ν , by equations 1.42 and 1.43.

$$l = (\frac{\nu^3}{E})^{0.25} \qquad \ldots 1.42$$

$$U_l = (\nu E)^{0.25} \qquad \ldots 1.43$$

Therefore contact time, τ , is given as;

$$\tau \alpha \frac{l}{U_l} \qquad \ldots 1.44$$

Combination of equation 1.41 and 1.42 to 1.44 gives;

$$h \alpha (\frac{k\rho C_p E}{\nu})^{1/2} \qquad \ldots 1.45$$

In order to calculate the energy dissipated in the generation of fluctuations, Deckwer like Konsetove assumed that all the input energy of the gas was dissipated in the liquid fluctuations. Hence energy dissipation per unit mass of the liquid, E, could be inserted in the equation 1.45.

$$E = \rho g U_g \qquad \ldots 1.46$$

Substituting for E from 1.46 into 1.45 one obtains

$$St = A(ReFrPr^2)^{-0.25} \qquad \ldots 1.47$$

The constant of equation 1.47 was later calculated from experimental data and was found to be 0.1.

The above model can explain the dependency of heat transfer coefficient upon the thermal properties of the liquid. However the functional relationship for the operating parameter U_g is $h \alpha U_g^{0.25}$. This incorrectly remains constant over the whole range of superficial gas velocity. Also these models are generally not applicable to high viscosty liquids. This is either due to the wrongly chosen hydrodynamic model (For example assumption of all input energy by gas dissipated in liquid circulation) or neglect of the effect of the boundary layer which is dominant for high viscosity liquids.

1.2.3.- Film Surface Renewal Model.

The Lewis et al (1982) model for heat transfer in a bubble column is based on a consideration of film resistance and surface renewal. It was assumed that adjacent to the surface of the heater there is a very thin liquid film through which there is a steady state conduction of heat, Figure 1.3. Heat was subsequently transfered from the outer edge of the film to packets of liquid by unsteady state diffusion of heat.

Therefore this model was represented mathematically as follows;

$$\frac{\partial\theta}{\partial t} = \alpha\frac{\partial^2\theta}{\partial x} \qquad \ldots 1.48$$

It is subject to the following boundary conditions;

$$t = 0 \qquad \theta = \theta_\infty \qquad \ldots 1.49$$

$$x = 0 \qquad k\frac{\theta}{\delta} = k\frac{\partial\theta}{\partial x} \qquad \ldots 1.50$$

$$x = \infty \qquad \theta = \theta_\infty \qquad \ldots 1.51$$

where x is the distance from outer edge of the boundary layer, α is the liquid thermal diffusivity, θ is the temperature difference between surface and liquid at x, θ_∞, is the value of θ for x = oo, k is the liquid thermal conductivity and δ is the thickness of the liquid layer adjacent to the surface.

In light of the high turbulence in a bubble column, it was reasonable to assume that the proposed boundary layer was turbulent and the thin liquid film was the laminar sublayer. The solution of equations 1.48 to 1.51 also requires knowledge of the contact time of the packets of liquid with the laminar sub-layer. This was calculated by dividing the characteristic heater length by the average circulation velocity of the liquid.

The characteristic heater lengths were found experimentally

to be the vertical dimension of the heater up to a value of 45 mm.

As for the circulation velocity the average liquid circulation velocity given by Field and Davidson (1980) was used. Therefore the final equation was given as;

$$h = \left[\frac{\delta}{k} + \left[\frac{\pi L_c}{(4k\rho C_p U_{cF})} \right]^{-1/2} \right]^{-1} \qquad \ldots 1.52$$

where

$$L_c = 0.045 \text{ m}$$

$$U_{cF} = 1.36 \left[Hg(U_g - \epsilon U_s) \right]^{\frac{1}{3}} \quad \text{for} \quad \frac{H}{D} > 1 \qquad \ldots 1.53$$

and

$$\delta = 0.03 \frac{\mu}{\rho} x 10^3 \qquad \mu < 4x10^{-3} \quad \text{Pa.s}$$

This model successfully combines boundary layer and surface renewal models, but its use requires a prior knowledge of gas hold-up and is only applicable to low viscosity liquids. It also requires the knowldege of a characteristic length, L_c, which has not been confirmed by other investigators, and might possibly be dependent upon the geometry of the overall system. The result of the current investigation into the applicability of the above rules regarding L_c will be given in chapter 7.

1.2.4.- Other Concepts.

Attempts have been made to model the heat transfer coefficient on a free convection mechanism.

In free convection, fluid motion is set as a result of the buoyancy force which is caused by the density difference generated by the temperature gradient near the heating element. This type of flow is characterized by the Grashof number, Gr,

$$Gr = \frac{g\beta l^3 \Delta T}{\nu^2} = \frac{g l^3 \Delta\rho}{\nu^2 \rho} \qquad \ldots 1.54$$

Where l is characteristic length, g is gravitational constant, ν is kinematic viscosity, $\Delta\rho$ is the difference between density of the liquid away from the heating element and near the heating element.

Mersmann (1977) postulated that for the bubbly flow the Gr number could be represented by Archimedes number, Ar, defined as;

$$Ar = \frac{g l^3 (\rho - \rho_g)}{\nu^2 \rho} \qquad \ldots 1.55$$

where ρ_g is gas density. At low pressure ρ_g is negligible and hence

$$Ar = \frac{g l^3}{\nu^2} \qquad \ldots 1.56$$

In the case of a turbulent boundary layer the heat transfer coefficient was calculated from the following relationship;

$$Nu = c(GrPr)^{\frac{1}{3}} \qquad \ldots 1.57$$

After replacing Gr number with Ar number and assuming $\frac{\Delta\rho}{\rho} \doteq 1$, the following equation was readily obtained.

$$h = c\left[\frac{k^2\rho C_p g}{\mu}\right]^{\frac{1}{3}} \qquad \ldots 1.58$$

The constant of that equation was found to be function of Pr number

$$c = 0.107Pr^{0.226} \qquad \ldots 1.59$$

substituting for c in equation 1.58 and simplifying gives;

$$h = 0.107k\left(\frac{g}{\nu\alpha}\right)^{\frac{1}{3}}Pr^{0.226} \qquad \ldots 1.60$$

This is said to be applicable when the superficial gas velocity is more than 15% of the rise velocity of the single bubbles or when the heat transfer coefficient has reached its maximum value.

Ruckenstein and Smigelschi (1965) also drew upon the above analogy and replaced the product of $g\beta\Delta T$ in equation 1.54 and 1.57 with $g\epsilon\frac{\rho-\rho_g}{\rho}$ .They found the constant c to be 0.13. Further information on the range of applicability of this

equation was not given.

1.3.- CONCLUSION.

Many investigators have studied heat transfer in gas-sparged reactors and presented considerable information on the parameters that influence the heat transfer coefficient as is evident from table 1.2.

An increase of the heat transfer coefficient with increases of the gas superficial velocity were reported by all investigators. However, most of the presented correlations indicate a steady unchanging increase of heat trasnfer coefficient with increasing gas flow rate. Deckwer's equation can also be faulted in this regard. The semi-theoretical equations presented by Lewis et al and Chen's version of Ruckenstein and Smigelschi equation are preferred. They show a correct functional relationship between heat transfer coefficient and gas superficial velocity.

The effect of heater element length is not clear and different conclusions in this regard are given. Lewis et al and Kubie experiments showed a heater length or diameter effect, but almost all other investigators did not confirm this. Even the results of Lewis et al and Kubie are not really comparable as the nature of their heaters were different.

The effect of gas hold-up has been neglected by many

investigators including Deckwer. Only Ruckenstein and Smigelschi, Kubie, Lewis et al and Zehner have considered this effect and thus it is worthy of more investigation.

Almost all investigators reported that the heat tranfer coefficient is independent of distributor design. This is more relevant in the churn-turbulent flow regime.

While the effect of the physical properties of the gas phase may be nelected, the effect of the liquid phase physical properties are profound. In particular an increase in the viscosity of the liquid will significantly reduce the heat transfer coefficient. The Lewis et al model is only applicable to low viscosity liquids.

Most of the reported data are for Newtonian low viscosity fluids and the available correlations were generally tested with Newtonian fluids only. Hence more work on this regard is required.

Finally it may be deduced that in spite of much available data on heat transfer in bubble columns, there is still no reliable mechanistic equation to cover the complete range of gas and liquid flow rates and physical properties.

1.4.- SCOPE OF THE PRESENT WORK.

The Lewis et al model (1982) is a model which is derived from basic principles. However, this model is applicable to the low viscosity liquids and is not tested independently.

Thererfore the aim of this work was (a)to test this model and (b) to seek to improve the theoretical basis of the model so as to take account of high viscosity liquids and (c) to propose a procedure to calculate heat transfer coefficient for gased non-Newtonian fluids. The effect of heater length and cosideration of a bundle of heaters, as well as other paramters of the system, such as gas distributor and gas hold-up were also investigated.

Chaper 2 of this thesis is devoted to the theoretical aspects of the work. After describing the experimental set up and procedure in chapter 3, gas hold-up measurements will be considered in chapter 4. Heat transfer from a single immersed cylindrical heater and a set of experiments on a bundle of heaters will be considered in chapter 5 and 6. Whilst in chapter 7 the new procedures for calculating heat transfer coefficients in bubble columns are presented.

*

Table 1.1 Bubble Column Applications

Main product/process	Reactants	Reference
Organic Processes:		
Acetaldehyde	ethylene, air	Petroleum Process Handbook (1965)
Acetic acid	acetaldehyde, air	Sittig (1967), Kostyak *et al* (1962)
Acetic anhydride	acetaldehyde, air	Yau *et al* (1968)
Propylene oxide	propylene, air	Prengle & Barona (1970)
Fatty acids	paraffin wax, air	" " "
Vinyl acetate	ethylene, air	" " "
Cumene-phenol	cumene, air	Sittig (1967), Armstrong (1968)
Cyclohexane	benzene, hydrogen	Davidson & Amick (1956)
Oxo (hydroformylation)	olefin, hydrogen, carbon monoxide	Fair (1967)
Carbon tetrachloride	carbon disulphide, chlorine	Sittig (1967)
Inorganic processes:		
Ammonium nitrate	ammonia, nitric acid	Fair (1967)
Barium chloride	barium sulphide, chloride	Gupta & Sharma (1967)
Recovery of H_2S (absorption-oxidation process)	sodium carbonate, iron oxide, air	Goar (1968)
Biochemical processes:		
Production of single cell protein	various substrates	Rosenzeig & Ushio (1974) Sittig & Heine (1977)
Production of primary and secondary metabolites	-	Smith & Greenshields (1974)
Waste treatment - deep shaft process	-	

Table 1.2 Dependency of heat transfer coefficient upon system parameters for some previous equations of the form $h \propto k^i \rho^j C_p^k \mu^\ell g^m U_g^n$

Equation	i	j	k	ℓ	m	n	Ref
$St=0.1(ReFrPr^2)^{-0.22}$	0.44	0.78	0.5	-0.22	0.22	0.33	1
$St=0.124(ReFrPr^{2.5})^{-0.22}$	0.55	0.78	0.45	-0.33	0.22	0.34	2
$St=0.11(ReFrPr^{2.5})^{-0.22}$	0.55	0.78	0.45	-0.33	0.22	0.34	3
$St=0.11(ReFrPr^{2.48})^{-0.23}$	0.57	0.76	0.43	-0.33	0.24	0.30	4
$*St=0.28\epsilon^{0.33}(ReFrPr^2)^{-0.33}$	0.66	0.67	0.34	-0.33	0.33	0.34†	5
$*St=0.25\epsilon^{0.33}(ReFrPr^2)^{-0.33}$	0.66	0.67	0.34	-0.33	0.33	0.34†	6
$St=0.134(ReFrPr^{2.6})^{-0.25}$	0.65	0.75	0.35	-0.4	0.25	0.25	7
$St=0.175(ReFrPr^{2.4})^{-0.25}$	0.6	0.75	0.4	-0.35	0.25	0.25	8
$St=0.135(ReFrPr^{2.4})^{-0.27}$	0.52	0.73	0.48	-0.25	0.27	0.19	9
$*St=0.1(ReFrPr^2)^{-0.25}$	0.5	0.75	0.5	-0.25	0.25	0.25	10
Average	0.57	0.74	0.42	-0.31	0.258	0.293	

* based in part upon theoretical considerations
† $\epsilon = U_g/U_b$ assumed

REFERENCES

1 Kast (1962)
2 Kölbel (1964)
3 Shaykhutdinov *et al* (1971)
4 Burkel (1972)
5 Ruckenstein and Smigelschi (1965)
6 Konsetov (1966)
7 Kawase and Moo-Young (1987)
8 Hart (1976)
9 Louisi (1979)
10 Deckwer (1980)

Table 1.3.- Summary of Major Heat Transfer Work : Equations and Experimental Equipments

References	Column Height m	Column Diameter m	Sparger	Heater	Flow Type	U_g mms^{-1}	U_l mms-1	System	Equation
Fair(1962)	3.0	0.457 1.070	Sieve plate 47 holes 0.08-0.762 mm in dia.	wall side	co-current	up to 45.7	0.8-6	air-water	$h = 8846U_g^{0.22}$
Ruckenstein & Smigelschi (1965)	-	0.08	28 Capillary tubes in 4 rows, rectangular column	wall side	Batch co-current	up to 110	low	air-water	$h = 0.28k(\frac{g\epsilon}{\nu\alpha})0.33$
Shaykhutdi-nove et al (1971)	4.34	0.4	Sieve plate, 1 mm thick, 0.7 mm dia. holes	wall side colling & heating	co-current upward	2-1000	3.6-16.3	air-water glycerine	$St = A.0.11(ReFrPr^{2.5})^{-.22}$ A= 1 for liquid height 1 to 4 m
Kubie(1974)	-	-	Porous plate Sieve plate holes 1 to 12 mm in diameter	immeresed heater 138 mm long, 2.15 to 10.5 mm in diameter	Batch	3-500	-	water, heptane, ethyl-glycol, glycerol-air, Ar, Co_2	$Nu[pr^{1/3}Gal^{1/6}(1-\epsilon)^{0.25}]^{-1} = ARe^{0.117}$ A=1.2 Re < 10 A= 1.05 10<Re<5000

Continued...

References	Column Height m	Column Diameter m	Sparger	Heater	Flow Type	U_g mms^{-1}	U_l mms-1	System	Equation
Hart(1976)	0.61	0.099	Single vertical nozzel	wall side	counter current	0.254-21.34	-	air-water ethylene glycol	$J_H = 0.125(\frac{U_g\rho}{\mu g})^{-0.25}$ $J_H = \frac{h}{C_p U_g \rho}(\frac{C_p\mu}{k})^{0.60}$
Nishikawa et al(1977)	1.8	0.051 -0.15	nozzel dia. 1.6 to 3 mm	jacket wall, immeresed cooling coil	co-current	up to 270	15	water, glycerine CMC-air	$\frac{h}{\rho C_p}(\rho^2\Delta\rho\mu g)^{1/3}(\frac{C_p\mu}{k})^{2/3}\mu^{-0.05} = 0.054U_g^{0.25}$ $U_l < 54$ m/h $U_g < 1000$ m/h
Lewis et al(1982)	1.0	0.292	Sieve Plates (a)-Centeral area aerated 129 holes of 1 mm dia. (b)-whole cross - section aerated 196 holes of 1.9mm in dia.	immeresed diameter 30 or 50 mm, length 10 to 150 mm	Batch	up to 180	-	air-water N_2-cumene N_2-glycol	$h = \left\{\frac{\delta}{k} + \left\{\frac{\pi L_c}{4k\rho C_p U_c}\right\}^{1/2}\right\}^{-1}$ $L_c = 0.045$ m $\frac{H}{D} > 1$ $U_c = 1.36[Hg(U_g - \epsilon U_s)]^{1/3}$ $\delta = 0.03\frac{\mu}{\rho}x10^3$ $\mu < 4\times10^{-3}$

Continued...

References	Column Height m	Column Diameter m	Sparger	Heater	Flow Type	U_g mms^{-1}	U_l mms-1	System	Equation
Deckwer et al(1980)	-	-	sintered plate	immeresed heater	Batch	<40	-	N_2-slurry t_b=300 ^oC	$St = 0.1(ReFrPr^2)^{-0.25}$
Micheal & Richert (1981)	1.5	0.1	(a) Sieve plate 25 holes of 0.8 mm in diameter, (b)Sinterd plate.	immeresed length 65 mm,dia. 19 mm	Batch	120	0	ethylene + solids	$St = 0.1(ReFrPr^2)^{-0.25}$ solid content < 30% wt
Holcombe et al(1983)	1.8	0.078	Reducing section filled with 0.003 m OD glass sphere	cooling water jacket and heating rod.	co-current	0.88 9.8	0.097 0.014	N_2-water	$St = 0.1(ReFrPr_l^2)^{-0.26}$. $Exp(2.4x10^{-4}Re_l)$ $U_l<0.05$ $U_g<0.1ms^{-1}$

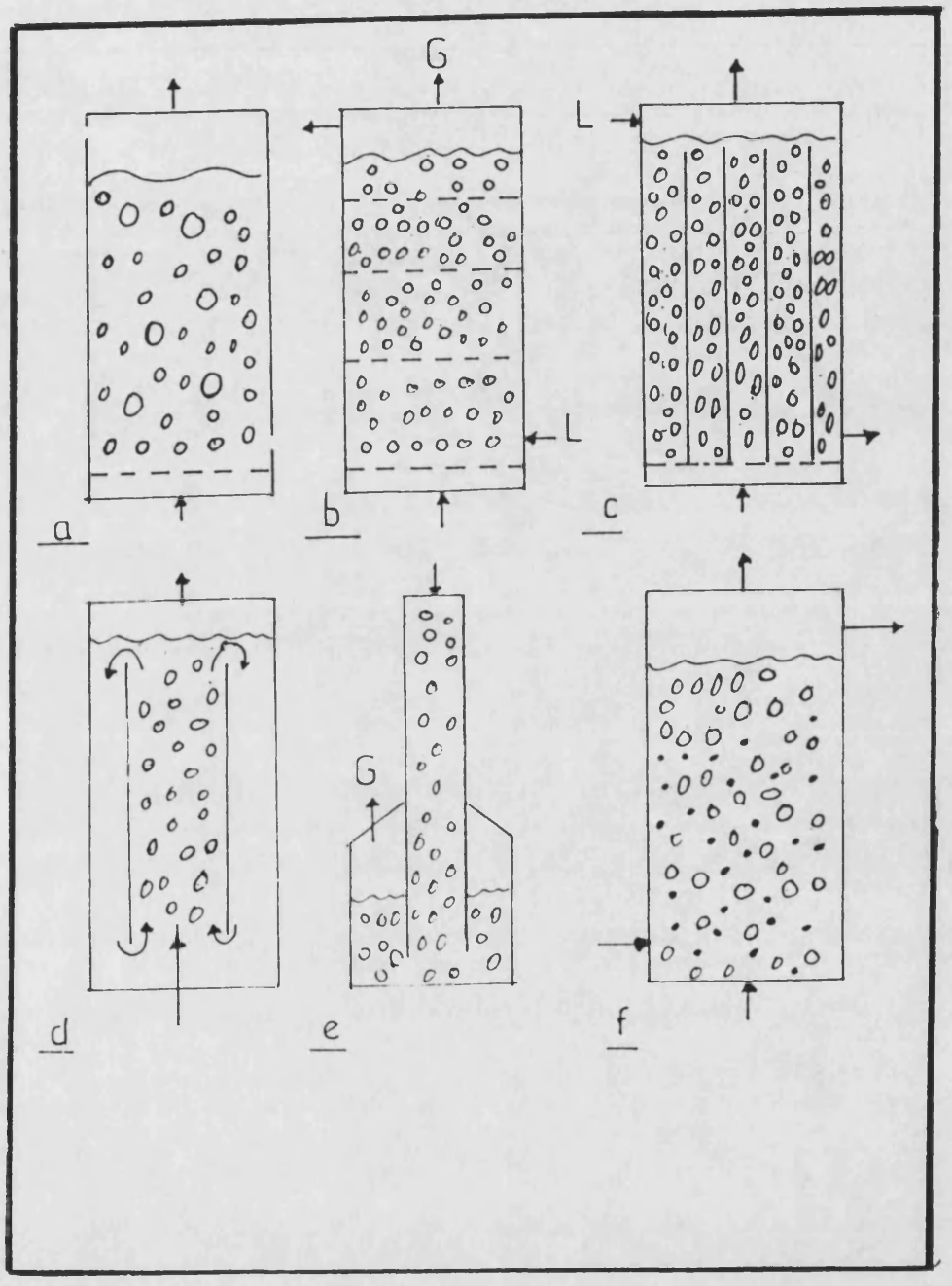

Figure 1.1.- Schematic view of some designs of bubble column. Description given in text.

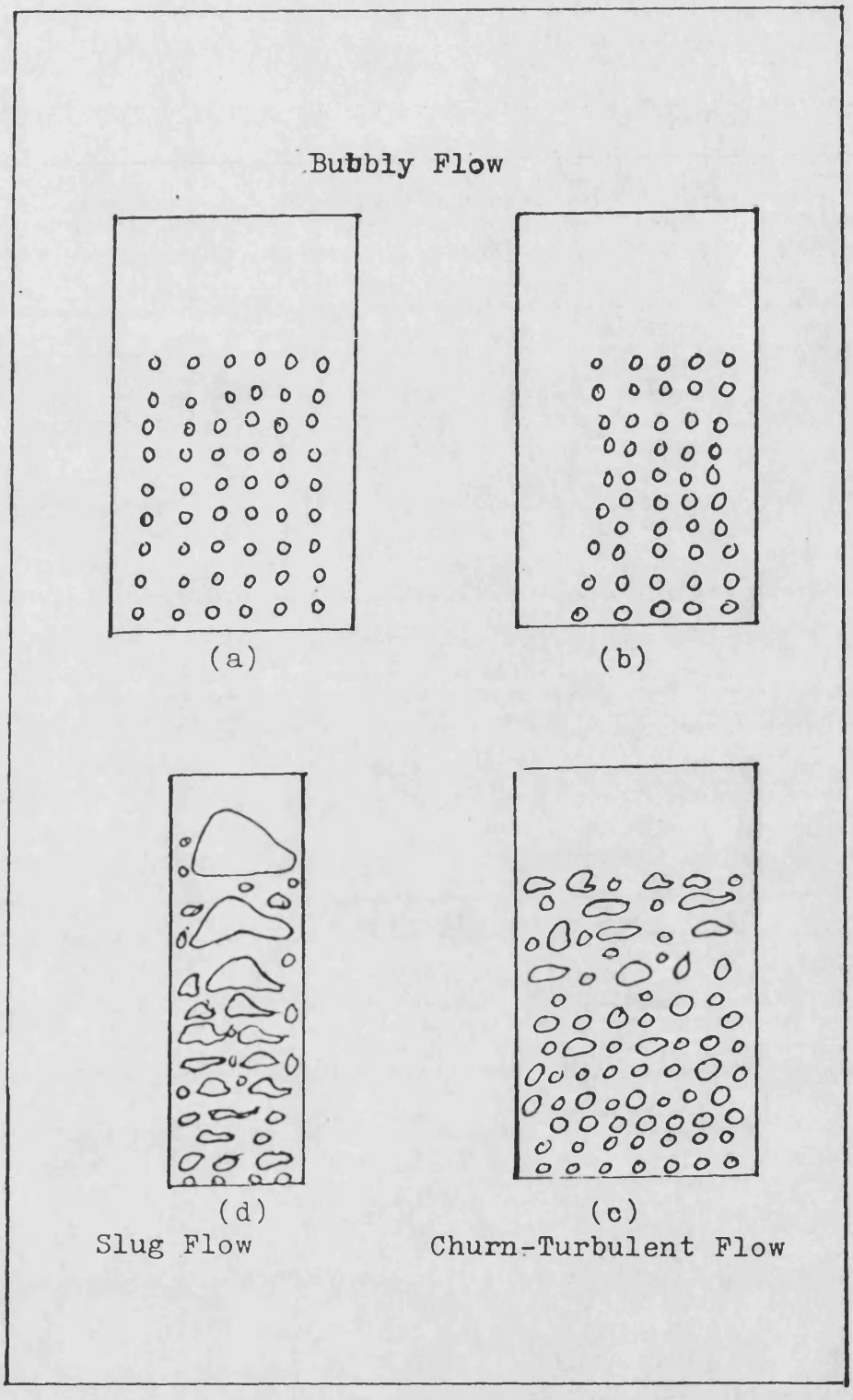

Figure 1.2.- Different flow patterns in bubble column. Description given in text.

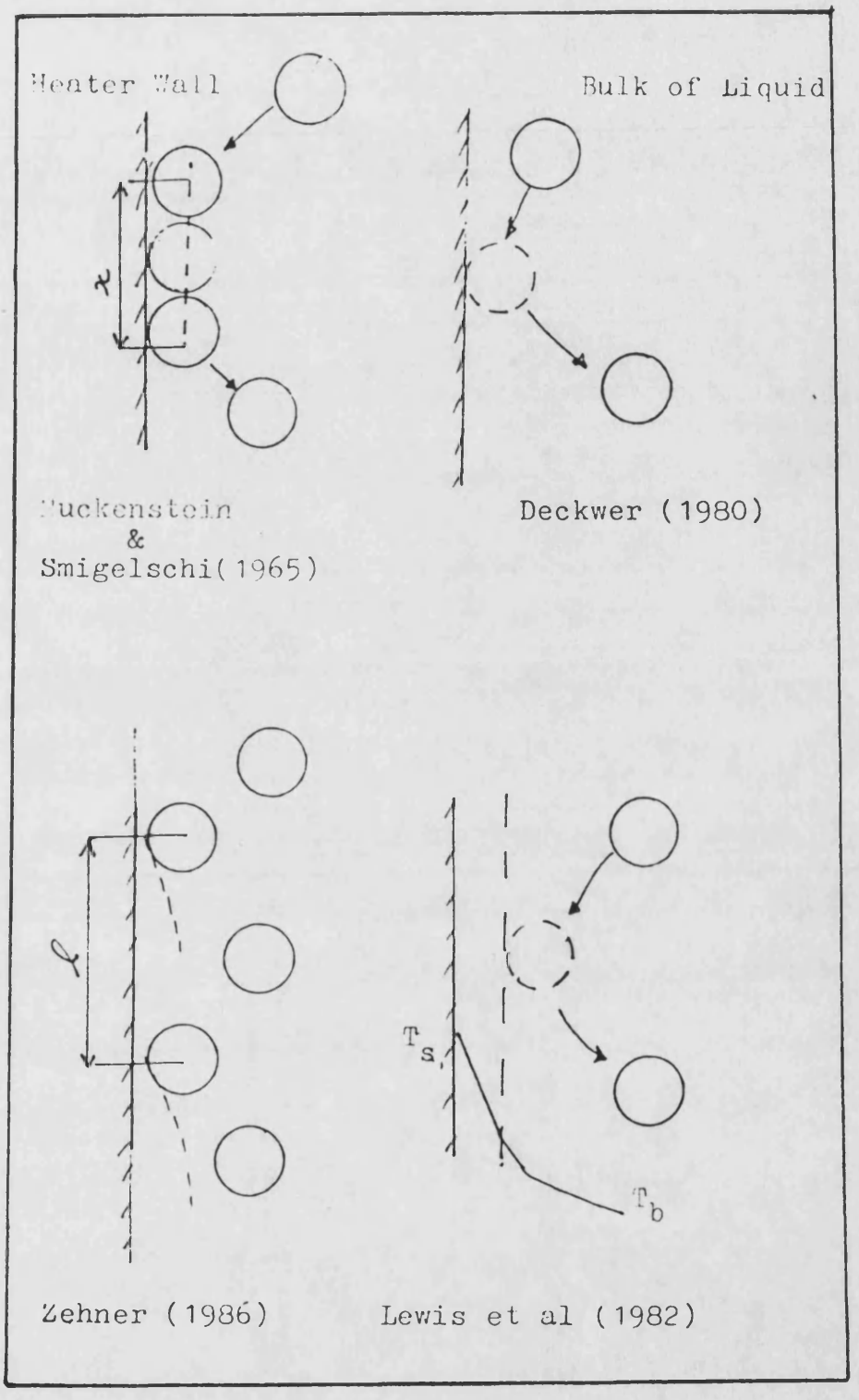

Figure 1.3 A picture of proposed mechanism of heat transfer in bubble column.

CHAPTER 2

BUBBLE COLUMN HEAT TRANSFER - A THEORETICAL APPROACH

2.- INTRODUCTION.

Whilst a number of workers have considered the various parameters affecting heat transfer coefficient, it was concluded at the end of the previous chapter that a sound truly theoretical heat transfer equation has yet to be developed. Therefore, it was considered appropriate to adopt a hydrodynamic model in order to obtain a theoretical equation for heat transfer in bubble column. Hence after introducing the chosen hydrodynamic model of bubble column, the heat transfer mechanism will be described and the resulting equation for the heat transfer coefficient will be obtained.

2.1.- HYDRODYNAMICS OF BUBBLE COLUMN.

Three distinct flow patterns, namely bubbly, churn-turbulent and slug flow, were introduced in section 1.2. Transition from bubbly to churn-turbulent and subsequently to slug flow depends mainly on the gas throughput and column diameter. Figure 2.1 is a qualitative representation of flow

regime on gas velocity and column diameter. It was reported that for air-water mixture transition from bubbly to churn-turbulent flow occurs at about $U_g > 40$ mms^{-1}.

In the churn-turbulent regime bubbles are of varying form and are very mobile, while size may reach 100mm in diameter and if column diameter is less than 100 mm transition to slug flow is likely. In tall columns bubble slug flow may be observed for column diameter of upto 200 mm (Deckwer (1981)).

Anderson and Quinn (1970) who have studied flow transition in bubble columns have shown that it is possible to have bubbly flow regime at higher gas superficial velocity by introducing trace contaminants. However, it is important to note that their approach included a porous sparger. Such spargers generate small bubbles whose size and hence rise velocity are highly dependent upon the surface tension properties of the liquid.

A further classification of column behaviour were made by Shah and Joshi(1981). They divided column height into 3 regions. The short distance above gas distributor were named region 1. In this region effects of the gas distributor and gas flow rate on the bubble size is more pertinent. In region 2 bubble properties depend on the liquid flow pattern and on the liquid properties. This region occupies most of the column height. Region 3 characterises itself by bubble coalescence. The relative positions of these regions depends on the gas flow rate. As the gas flow rate increases coalescence occurs at an

earlier stage and hence the effect of gas distributor is less important.

It has been shown that due to the introduction of gas, a strong liquid circulation pattern is developed. The upflow of liquid occurs at the centre and there is downflow in the annular region near the wall. The liquid circulation velocity depends on the superficial gas velocity, column diameter, gas hold-up, bubble rise velocity and diameter, liquid viscosity and height of the gas-liquid mixture. No attempts have been made in this work to catalogue the very vast literature on this subject. Nevertheless, those aspects of hydrodynamics which are relevant to heat transfer in bubble columns, i.e. bubble rise velocity, holdup and liquid circulation will be discussed further.

2-1-1.- Bubble Size, Bubble Rise Velocity and Gas Hold-Up.

Bubble formation at the orifice was studied extensively by Davidson and Schuler (1960(a), 1960(b)). However in a bubble column, the size of the bubbles depends mainly on a balance between the coalescence and breakup rates in the liquid mixture phase.

In contrast to the churn-turbulent regime, the type of gas distributor plate has a significant effect on the bubble size in bubbly flow regime. A porous plate distributor produces smaller bubbles than a sieve plate because the bubble sizes with the

former depends on the surface tension whereas with the latter its mainly inertia that affects the initial bubble size.Neverthless the correlations for the initial bubble sizes at the orifice will not be considered due to the fact that they are only valid for a very short distance above the gas sparger.

Akita and Yoshida (1974) proposed the following correlation for the prediction of the average bubble diameter (defined as Sauter mean diameter, $d_{vs} = \frac{\sum d_b^3}{\sum d_b^2}$), of bubbles in a bubble column,

$$\frac{d_{vs}}{D} = 26 \left(\frac{D^2 g\rho}{\sigma}\right)^{-0.5} \left(\frac{gD^3}{\nu^2}\right)^{-0.12} \left(\frac{U_g}{\sqrt{gD}}\right)^{-0.12} \qquad ...2.1$$

Equation 2.1 is based on the data in columns up to 0.3 m in diameter and superficial gas velocities up to 70 mms^{-1}.

Although this correlation predicted dependency of, d_{vs}, to column diameter to be $D^{-0.3}$, for columns diameter of greater than 0.3 m average bubble size became independent of column diameter.

Joshi(1980) proposed that Calderbank (1967) equation for bubble size,

$$d_{vs} = 4.15 \left(\frac{\sigma^{0.6}}{(P/V)^{0.4} \rho^{0.2}}\right) \epsilon^{0.5} + 9 \times 10^{-4} \qquad ...2.2$$

where $$\left(\frac{P}{V}\right) = U_g \rho (1 - \epsilon) g \qquad ...2.3$$

is more appropriate when it is required to calculate bubble rise velocity from Grace et al equations (table 2.1(b)).

As bubble size increases, bubble rise velocity will increase and therefore gas $_{hold-up}$ will decrease. Bubble rise velocity could be calcuated either from Peebles and Garber's equations (Wallis (1969)) or from Grace et al (1976) equations. The latter often refered as Clift et al (1978) equations. These equations are given in Table 2.1 (a and b).

It is interesting to note that conditions in bubble column corresponds to region 4 of Peebles and Garber's equations. In this region in the abscence of severe coalescence, bubble rise velocity depends only on the physical properties of the liquid phase;

$$U_b = A\,(g\frac{\sigma}{\rho})^{0.25} \qquad \ldots 2.4$$

where Harmathy gives A to be 1.53 rather that 1.18 as suggested originally by Peebles and Garber.

In bubble flow regimes U_g <40 mms^{-1} the rise velocity of a single bubble may vary between 200 and 300 mms^{-1} and in churn-turbulent bubble rise velocity remains approximately constant and are considerably higher. Transition from bubbly flow to churn-turbulent is usually accompanied by a distinct

increase in the bubble rise velocity, U_b.

Defining slip velocity, U_s, as the relative velocity between the phases, its relationship to the liquid and gas velocities and the voidage can be expressed (Lapidus and Elgin (1957)) as,

$$U_s = \frac{U_g}{\epsilon} \pm \frac{U_L}{1-\epsilon} \qquad \ldots 2.5$$

For batch bubble columns in the bubbly flow regime and at low gas flow rates, $U_L \sim 0$, hence

$$U_s \approx \frac{U_g}{\epsilon} \qquad \ldots 2.6$$

Slip velocity can be expressed as function of bubble rise velocity and gas hold-up ϵ,

$$U_s = U_b f(\epsilon)$$

The simplest form of function $f(\epsilon)$ is given by Turner (1966) as $f(\epsilon)=1$. Other functional relationships are summarised in Table 2.2. Lockett and Kirkpatric (1975) examined the various functions and found that they are unsatisfactory at gas hold-up above 0.25. In bubbly flow regime or relatively low gas hold-up the difference between equations are small and the Turnner equation, $U_s=U_b$, is satisfactory in order to calculate liquid circulation velocity (See section 2.1.2.1).

Numerous investigators have studied variation of gas hold-up

with superficial gas velocity, for example Bach and Philhofer (1978), Hikita et al (1980) and Field (1980).

Gas hold-up is defined as the percentage of volume of the gas in the two or three phase mixture in the bubble column. As the superficial gas velocity, U_g, increases from a relatively low values the gas hold-up increases steadily. However, after the transition from bubbly to churn-turbulent flow the gas holdup increases at a lesser rate. The influence of the gas velocity, U_g and gas hold-up ϵ, can be expressed as $\epsilon \alpha U_g^n$. Shah et al (1982) reported that at low gas superficial velocity where bubbly flow exists, n varies between 0.7-1.2. In churn-turbulent flow for a sieve plate gas sparger n=0.5-0.7.

Some correlations for gas hold-up prediction are given in Table 2.3. Even though large number of correlations for gas hold-up have been proposed in the literature, the large scatter of the data does not allow a single correlation to be used. Field (1980) showed that the simple equation presented by Mashelkar (1970), equation 2.7, represents air-water system reasonably well. Chen (1987) has proposed the use of Nicklin equation, equation 2.8,

Mashelkar equation:

$$\epsilon = \frac{U_g}{2U_g + U_s} \qquad \ldots 2.7$$

Nicklin equation :

$$\epsilon = \frac{U_g}{1.2U_g + U_s} \qquad \ldots 2.8$$

A similar equation that was proposed by Hughmark (1967) is

$$\epsilon = \frac{U_g}{2U_g + 0.35(\rho\,\sigma/72)^{1/3}} \qquad \ldots 2.9$$

where ρ is density in gcm^{-3}, σ is surface tension in dyn cm^{-1} and U_g is superficial gas velocity in ms^{-1}.

This equation and Mashelkar equation, equation 2.7, were found to represent the present experimental air-water data (Chapter 4) reasonably well.

Data on high viscosity and non-Newtonian fluids are less common. Equations presented in this section are only suitable for low viscosity Newtonian fluids. However, it is reasonable to assume that an equation of the form

$$\epsilon = \frac{U_g}{n\,U_g + U_s} \qquad \ldots 2.10$$

is also applicable to high viscosity liquid,given that the constant n is a function of the viscosity of the liquid and gas distributor type (Kelkar and Shah (1985)).

It was found that for CMC solutions a value of n=2.6 gives a reasonable fit (See Chapter 4) to the gas hold-up data.

2.1.2.- Liquid Circulation.

Liquid circulation is an important parameter that has a direct effect on the mean gas residence time and the distribution of the gas. Furthermore, liquid circulation can help in the modelling of the heat transfer process in bubble columns (See Section 2.2).

Existence of strong overall upflow of liquid in the middle region and downflow of liquid near the wall were shown by Pavlov (1965) and Hills (1974) who measured the liquid circulation velocity.

Figure 2.2 shows a typical velocity profile of liquid flow in a bubble column. A reverse flow of liquid circulation, i.e. upflow of liquid near the wall and downflow of liquid in the middle region of the column was reported by Moo-Young et al(1987). The gas was introduced around the base near the wall and a cone directed the downcoming liquid towards the wall.The column used was 0.23m in diameter and 1.22m in height.The diameter of the draft tube used was 0.113 m and its height was 0.705 m.

Figure 2.3 gives maximum liquid velocity as a function of gas superficial velocity from several investigators. It shows that the magnitude of liquid circulation is very high compared with the gas superficial velocity.

Whalley (1974) and Joshi (1981) review of liquid circulation models divided the models into models based on the force balance, which requires solution of the equation of motion, and energy balance models which require knowledge of the energy dissipation rate. The latter is then used to calculate maximum vorticity and hence liquid velocity can be obtained from differentiation of the stream function.

Whalley (1974) compared these models. It was concluded that energy balance methods are in a better agreement with the experimental data. Furthermore, Joshi and Sharma (1976) have successfully used the energy balance method to predict gas hold-up and effective interfacial area in horizontal sparged contactors. Thus this model were adopted in this study and a brief explaination is given in the following sub-section.

2.1.2.1.- Energy Balance Method for Calculating Average Liquid Circulation Velocity.

Whalley (1971) showed that the energy input rate, E_i, to bubble columns is

$$E_i = A\, U_g\, P_1 \ln\left(\frac{P_1}{P_2}\right) \qquad \ldots 2.11$$

where P_1 and P_2 are pressure at the column base and top respectively. U_g should refer to the column base. This equation can for relatively short bubble columns, which give a low ΔP,

be approximated to

$$E_i = A\, U_g\, \Delta P \qquad \ldots 2.12$$

where ΔP is simply the hydrostatic pressure head.

Field (1980) recognized seven modes of energy dissipation in bubble columns and by order of magnitude analysis it was concluded that energy dissipation in the wakes behind the bubbles, E_1, and energy dissipation in the hydraulic jump at the liquid surface, E_2, are important. It was also reported that for liquid viscosities up to 20 cP the dissipation due to viscous drag at the column wall is negligible.

The energy dissipation in the wakes behind the bubbles, E_1, has been shown by Whalley (1971) to be

$$E_1 = \frac{\pi D^2}{4} H\epsilon(1-\epsilon)\, U_s \rho_L g \qquad \ldots 2.13$$

An energy balance in the presence of the liquid circulation requires the calculation of E_2 which is equal to the loss of kinetic energy without pressure recovery during the downward flow. Thus energy available for liquid circulation is

$$E = E_i - E_1 = \frac{\pi D^2}{4} H\rho g(1-\epsilon).(U_g - \epsilon U_s) \qquad \ldots 2.14$$

Whalley and Davidson (1974) have numerically solved the following equation given for irrotational axi-symmetric flow (Batchelor (1967))

$$\frac{\omega}{r} = k\psi \qquad \ldots 2.15$$

where vorticity, ω, and stream function, ψ, are defined as

$$U_r = -\frac{1}{r}\frac{\partial \psi}{\partial z} \qquad U_z = \frac{1}{r}\frac{\partial \psi}{\partial r} \qquad \ldots 2.16$$

$$\omega = \frac{\partial U_r}{\partial z} - \frac{\partial U_z}{\partial r} \qquad \ldots 2.17$$

and k is a constant.

The analytical solution of equation 2.15 as given by Field (1980) is

$$\psi^* = \frac{\psi}{\psi_o} = B\sin(\pi z^*)\,(a\frac{r^{*2}}{2})\sum_{k=1}^{k=\infty} A_k\,(V)(a\frac{r^{*2}}{2})^{k-1} \qquad \ldots 2.18$$

where $\psi^* = R(r^*).Z(z^*)$, $A_1 = 1$, $A_2 = V$ and for $k > 2$ the coefficients are given by $k(k-1)A_k = 2VA_{k-1} - A_{k-2}$,

$$r^* = \frac{r}{r_o} \qquad z^* = \frac{z}{H} \qquad V = \frac{(\frac{\pi D}{H})^2}{16a}$$

and

$$a^2 = kr_o^4$$

Therefore, by differentiating equation 2.18 according to equations 2.16, the velocity component in the column could be calculated. However, the unknown, ψ_o, could be obtained from

energy balance, E, equation 2.14. Hence ψ_0 is given as

$$\psi_0 = \left[\frac{1}{16\pi} \frac{D^4}{\rho(1-\epsilon)} \frac{E}{F(A^*)} \right]^{1/3} \quad \ldots.2.19$$

where

$$F(A^*) = \int_0^{A^*} \frac{1}{(r^{*2})} \left(\frac{dR}{dr^*} \right)^3 dr$$

and

$$A^* = \frac{A}{r_0}$$

Now the average circulation velocity, U_{cF}, is defined by

$$U_{cF} = \frac{1}{\pi} \frac{1}{A^2} \int_0^A u' 2\pi r \, dr \quad \ldots.2.20$$

where u' is the velocity at H/2 and A is the distance AM in Figure 2.2. By diferentiation of equation 2.18 Field (1980) showed that equation 2.20 becomes

$$U_{cF} = \left| \psi_0 a \frac{A^{*2}}{A^2} \right| \sum_{k=1}^{k=\infty} A_k.(V).(a\frac{A^{*2}}{2})^{(k-1)} \quad \ldots2.21$$

The unknown A^* is obtained from

$$\sum_{k=1}^{k=\infty} A_k.(V).k.(a\frac{A^{*2}}{2})^{(k-1)} = 0$$

as $\frac{dR}{dr^*}=0$ at A.

Substituting equation 2.19 into 2.21 for H/D>1 the function has the following value

$$U_{cF} = 1.47 \left[\frac{E}{D^2 \rho (1 - \epsilon)} \right]^{\frac{1}{3}} \qquad \ldots 2.22$$

Substituting for E from equation 2.14 into 2.22 gives an equation for the average liquid circulation velocity, equation 2.23.

$$U_{cF} = 1.36 [Hg(U_g - \epsilon U_s)]^{1/3} \qquad \ldots 2.23$$

where U_{cF} is the average liquid circulation velocity, H is the height of liquid, U_g is the superficial gas velocity and U_s is the slip velocity.

Equation 2.23 was mainly derived for inviscid liquid and for aspect ratios of H/D>1.

Joshi and Sharma (1979) stated that Whalley and Davidson's model predicts 2-3 times higher values of average liquid circulation velocity for H/D>1 and the existance of a single circulation cell for columns with H/D>3 is unrealistic.

By assuming a series of multiple ciruclation cells on top of each other, Joshi and Sharma (1979) and Joshi (1980) proposed the following equation for the calcuation of the average liquid circulation velocity in the bubble column

$$U_{cJ} = 1.31 [Dg(U_g - \epsilon U_s)]^{1/3} \qquad \ldots 2.24$$

where U_{cJ} is the average liquid circulation velocity and D is the column diameter.

The term $(U_g - \epsilon U_s)$ in equation 2.23 and 2.24 which is a measure of the available energy for liquid ciruclation, has proved difficult to predict. This is due to the large error that may arise from subtraction of the two relatively large values involved.

The solution of these equations also require a prior knowledge of average gas hold-up and the slip velocity. These were overcome in the present study in the following manner.

Assuming that variation of gas hold-up with superficial gas velocity is smooth and that gas hold-up can be calculated by equation of type 2.10 then it can be rewritten in the following form

$$(U_g - \epsilon U_s) = n\,\epsilon\,U_g$$

Hence equation 2.23 and 2.24 become,

$$U_{cFs} = 1.36\,(n\,\epsilon\,H\,g\,U_g)^{1/3} \qquad 1 < \frac{H}{D} < 3 \qquad \ldots 2.25$$

$$U_{cJs} = 1.31\,(n\,\epsilon\,D\,g\,U_g)^{1/3} \qquad \frac{H}{D} \geq 3 \qquad \ldots 2.26$$

where n is 2 or 1.2 for air-water system depending on use of equation 2.7 or 2.8 for calculation of gas hold-up, respectively.

It is interesting to note that the liquid circulation velocity as presented by equation 2·25 or 2·26 is almost like equation 1·36 which was derived by Zehner (1986).

2.2.- HEAT TRANSFER MODEL.

The high rate of heat flux obtainable in a bubble column is due to the liquid turbulence intensity generated by the bubbles. The boundary layer on the surface of the heater is considered turbulent with a laminar sub-layer. It was assumed that part of the heat resistance lies in the thermal boundary layer and that due to the very low thickness of the laminar sub-layer and hence the thermal boundary layer, the nature of heat transfer in this film is that of steady state heat conduction. However, heat transfer from the outside of laminar sub-layer to the "packets" of liquid in the two phase mixture is by unsteady diffusion of heat. Mathematical representation of these assumptions for one dimensional heat transfer is

$$\frac{\partial \theta}{\partial t} = \alpha \frac{\partial^2 \theta}{\partial x^2} \qquad \ldots 2.27$$

boundary conditions are

$$t = 0 \qquad \theta = \theta_\infty \qquad \ldots 2.28$$

$$x = 0 \qquad -k\left(\frac{\theta}{\delta}\right) = -k\frac{\partial\theta}{\partial x} \qquad \ldots 2.29$$

where θ is the temperature difference between the heater surface and the bulk temperature, θ_∞ is the temperature between the heater surface, t_s, and the bulk temperature, t_b, at $x = \infty$ and $x = 0$ is at the edge of the thermal boundary layer.

Solution of equation 2.27 for a flat plate was given by Carslaw Jaeger (1959) as;

$$\frac{\theta}{\theta_\infty} = \text{erf}\frac{x}{2\sqrt{\alpha t}} + e^{(\frac{1}{\delta})^2\alpha t} \cdot \text{erf}\left[\frac{x}{2\sqrt{\alpha t}} + \frac{\sqrt{\alpha t}}{\delta}\right] \qquad \ldots 2.30$$

The instantaneous heat transfer coefficient, h_i, may be defined as

$$q = h_i\theta_\infty = -k\left|\frac{\partial\theta}{\partial x}\right|_{\text{surface}} = -\left|\frac{k\theta}{\delta}\right|_{x=0} \qquad \ldots 2.31$$

Hence from equation 2-31 one obtains that

$$h_i = -\frac{k}{\delta}\frac{\theta_{x=0}}{\theta_\infty} \qquad \ldots 2.32$$

From equation 2.30

$$\frac{\theta_{x=0}}{\theta_\infty} = e^{(\frac{1}{\delta})^2 \alpha t} \operatorname{erfc} \frac{1}{\delta}\sqrt{\alpha t} \qquad \ldots 2.33$$

The average heat transfer coefficient, h, may be defined as

$$h = \frac{1}{\tau}\int_{\tau_o}^{\tau} h_i \, dt \qquad \ldots 2.34$$

Substituting for h_i from 2.32 and 2.33 in 2.34 and integrating by part, (Xavier (1979)) will give an equation to calculate the average heat transfer coefficient

$$h = \frac{h_f}{A^2}\left[\operatorname{erfc}(A)e^{A^2} - 1\right] + h_p \qquad \ldots 2.35$$

where

$$A = 2\frac{h_f}{\sqrt{\pi h_p}} \qquad h_f = \frac{k}{\delta} \qquad h_p = 2\left(\frac{k\rho Cp}{\pi\tau}\right)^{1/2}$$

When there is no film resistance, i.e. $\delta \rightarrow 0$, equation 2.35 result is similar to the surface renewal model (section 1.2.2)

$$\lim_{\delta \to 0} h = h_p = \left(\frac{4\, k\, \rho\, Cp}{\pi\tau}\right)^{\frac{1}{2}} \qquad \ldots 2.36$$

Field (1980) approximated equation 2.35 to an accuracy of better than 5% by considering the packet heat resistance, $1/h_p$, in series with the film resistance, $1/h_f$. Heat transfer in the

boundary layer was given by equation 2.37.

$$q = -k\frac{\theta}{\delta} = h_f\theta$$

or

$$h_f = \frac{k}{\delta} \qquad \ldots 2.37$$

Since it was assumed that

$$\frac{1}{h} = \frac{1}{h_f} + \frac{1}{h_p} \qquad \ldots 2.38$$

Then by substituting for h_f and h_p from 2.37 and 2.36 in 2.38 one obtains

$$h = \left[\frac{\delta}{k} + \sqrt{\frac{\pi\tau}{4\, k\rho Cp}}\right]^{-1} \qquad \ldots 2.39$$

Solution of equation 2.39 required the two unknowns, δ and τ to be known. These are given in following sub-sections by equation 2.40 and 2.46 respectively. The experimental results for heat transfer in bubble columns are given in chapter 5 whilst application of the theoretical model and the subsequent semi -theoretical simplified correlation are given in chapter 7.

2.2.1.- Estimation of Parameters Involved in Heat Transfer Model, Equation 2-39.

2.2.1.1.- Evaluation of Contact Time.

It was mentioned in section 1.1.1(d) that experimental observations of Lewis et al (1980) showed the existence of a characteristic heater length, L_c, for the transfer of heat in bubble columns. Packets of liquid which are brought in contact with of the films travel this length before detaching from the film and losing their identity.

Eventhough the upward movement of the liquid is a function of position, they could be approximated by taking the average liquid circulation velocity as the characteristic velocity. Therefore contact time is given by

$$\tau = \frac{L_c}{U_c} \qquad \ldots 2.40$$

In the present work value of L_c ,for Newtonian liquids,was found to be 31 mm with the use of equation 2.26 for the calculation of circulation velocity. Details are given in Chapter7.

2.2.1.2.- Evaluation of Film Thickness.

For single phase flow in a smooth tube the thickness of the turbulent boundary layer is given as (see for example Kay and Nedderman(1974), page 186),

$$y^+ = 5 \qquad \ldots 2.41$$

or

$$\delta = \frac{5\mu}{(\tau_w \rho)^{1/2}} \qquad \ldots 2.42$$

where $\tau_w = \frac{1}{2} f \rho U_c^2$ and $f = 0.046 Re^{-0.2}$ ...2.43,44

Lewis et al (1982) assumed that the film thickness is equivalent to the velocity boundary layer. This assumption applies only for a liquid with Pr=1. Therefore a more realistic assumption is that the resistance to the heat transfer is given by the thermal boundary layer. These two, however are related to each other,

$$\frac{\delta_t}{\delta} \approx Pr^{-\frac{1}{3}} \quad \text{for} \quad Pr \geqslant 1 \qquad \ldots 2.45$$

Hence substituting for δ from equation 2.42 together with equations 2.43 and 2.44 in equation 2.45 will give

$$\frac{\delta_t}{L_c} = 33 \left(\frac{\rho U_c L_c}{\mu} \right)^{-0.9} \left(\frac{\mu Cp}{k} \right)^{\frac{-1}{3}} \qquad \ldots 2.46$$

where δ_t can be used in equation 2.39 instead of δ

The applications of equation 2.46 is considered later in chapter 7.

2.2.2.- Dimensionless form of Heat Transfer Equation.

It was assumed that heat transfer coefficient in the bubble column can be approximated as

$$\frac{1}{h} = \frac{1}{h_f} + \frac{1}{h_p} \qquad \ldots 2.38$$

Assuming that $1/h_f$ term is constant and using equation 2.25 or 2.26 in order to calculate contact time in equation 2.39 one readily obtains

$$\frac{1}{h} = A + B(\epsilon U_g)^{\frac{-1}{6}} \qquad \ldots 2.47$$

where the constants A and B can be found experimentally.

However, multiplication of equation 2.38 by $\rho C_p U_c$ will give

$$\frac{\rho C_p U_c}{h} = \frac{\rho C_p U_c}{h_f} + \frac{\rho C_p U_c}{h_p}$$

or

$$\frac{1}{St} = \frac{1}{St_f} + \frac{1}{St_p} \qquad \ldots 2.48$$

but $$\frac{1}{h_f} = \frac{\delta_t}{k}$$

and

$$\frac{1}{h_p} = \sqrt{\frac{\pi L_c}{4k\rho C_p U_c}} = 0.89 \sqrt{\frac{L_c}{k\rho C_p U_c}}$$

where δ_t is given by equation 2.46 and U_c by 2.26.

Therefore

$$\frac{1}{St_f} = 33 Re^{0.1} Pr^{\frac{2}{3}}$$

and

$$\frac{1}{St_p} = 0.89 (Re\ Pr)^{\frac{1}{2}}$$

Hence

$$\frac{1}{St} = 33\ Re^{0.1}\ Pr^{\frac{2}{3}} + 0.89(Re\ Pr)^{\frac{1}{2}} \qquad \ldots.2.49$$

where $Re = \frac{\rho U_c L_c}{\mu}$ and $Pr = \frac{\mu Cp}{k}$

**

Region 1 $U_b = \frac{2R_b^2(\rho - \rho_g)}{9\mu}$	$Re_b < 2$
Region 2 $U_b = 0.33g^{0.76}(\frac{\rho}{\mu})^{0.52}R_b^{1.28}$	$2 < Re_b < 4.02G_1^{-2.214}$
Region 3 $U_b = 1.35(\frac{\sigma}{\rho R_b})^{0.50}$	$4.02G_1^{-0.214} < Re_b < 3.10G_1^{-0.25}$ or $16.32G_1^{0.144} < G_2 < 5.75$
* Region 4 $U_b = 1.18(\frac{g\sigma}{\rho})^{0.25}$	$3.10G_1^{-0.25} < Re_b$ or $5.75 < G_2$

Where $Re_b = \frac{2\rho U_b R_b}{\mu}$ $G_1 = g\frac{\mu^4}{\rho\sigma^4}$ $G_2 = \frac{g R_b^4 U_b^4 \rho^3}{\sigma^3}$

* The upper limit of region 4 is reached when the rise velocity is comparable with the value given by Davis and Taylor 1950) i.e

$$U_b = \sqrt{gR_b}$$

Table 2.1(a).- Bubble rise velocity of a single bubble in liquids (according to Peebles and Garber (1953)).

$$U_b = \frac{\mu}{\rho d_b} M^{-0.149} (J - 0.857)$$

$J = 0.94 H_1^{0.757}$, when $2 < H_1 < 59.3$

or $J = 3.42 H_1^{0.441}$ when $H_1 > 59.3$

$$H_1 = \frac{4}{3} E_o M^{-0.149} \left(\frac{\mu}{\mu_w}\right)^{-0.14}$$

$$J = Re_b M^{0.149} + 0.857$$

$$M = \frac{g\mu^4(\rho - \rho_g)}{\rho^2 \sigma^3} \quad ; \quad Re_b = \frac{d_b U_b \rho}{\mu} \quad ; \quad E_o = \frac{g(\rho - \rho_g) d_b^2}{\sigma}$$

Table 2.1(b).- Bubble rise velocity of a single bubble in liquids (according to Grace et al (1976)).

Turner (1966) $f(\epsilon) = 1$
Davidson and Harrison (1966) $f(\epsilon) = \frac{1}{1-\epsilon}$
Bridge et al (1964) $f(\epsilon) = (1-\epsilon)^{(n-1)}$ n=2 for small air bubbles in water
Marrucci (1965) $f(\epsilon) = \frac{(1-\epsilon)}{1-\epsilon^{5/3}}$
Wallis (1965) $f(\epsilon) = (1-\epsilon)^{2n-1}$ n=2 for small bubbles n=0 for large bubbles

Table 2.2.- Proposed $f(\epsilon)$ that can be used in equation $U_s = U_b f(\epsilon)$.

Hugmark (1967) $$\epsilon = \frac{U_g}{2U_g + 0.35(\frac{\rho\sigma}{72})^{1/3}}$$ multi-orifice D > 0.10 m
Batch and Pilhopher (1978) $$\frac{\epsilon}{1-\epsilon} = 0.115(\,Re\,Fr\,)^{0.23}$$ $$Re = \frac{U_g d_b \rho}{\mu} \quad ; \quad Fr = \frac{U_g^2}{d_b g}$$ Perforated plate ; D = 0.10 m
Akita and Yoshida (1973) $$\frac{\epsilon}{1-\epsilon^4} = 0.2(\frac{gD^2\rho}{\sigma})^{\frac{1}{8}}(\frac{gD^3}{\nu^2})^{\frac{1}{12}}(\frac{U_g}{\sqrt{g\,D}})$$ single nozzel sparger D=0.152 to 0.60 m Ug < 0.50 ms^{-1}
Kumar et al (1976) $$\epsilon = 0.728U - 0.485U^2 + 0.0975U^3$$ $$U = U_g(\frac{\rho^2}{\sigma g(\rho - \rho_g)})^{0.25}$$ multi orifice sparger D=0.05 to 0.10 m Ug< 0.14 ms^{-1}
Hikita et al(1980) $$\epsilon = 0.672(\frac{U_g\mu}{\sigma})^{0.578}(\frac{\mu^4}{\rho\sigma^3})^{-0.131}(\frac{\rho_g}{\rho})^{0.062}(\frac{\mu_g}{\mu})^{0.107}$$ single sparger D=0.10 m
Godbole et al (1982) $$\epsilon = 0.319U_g^{0.476}\mu^{-0.058} \qquad \mu<0.246 \text{ Pa.s}$$

Table 2.3- Some examples of proposed correlations in litrature to predict gas hold-up in bubble column.

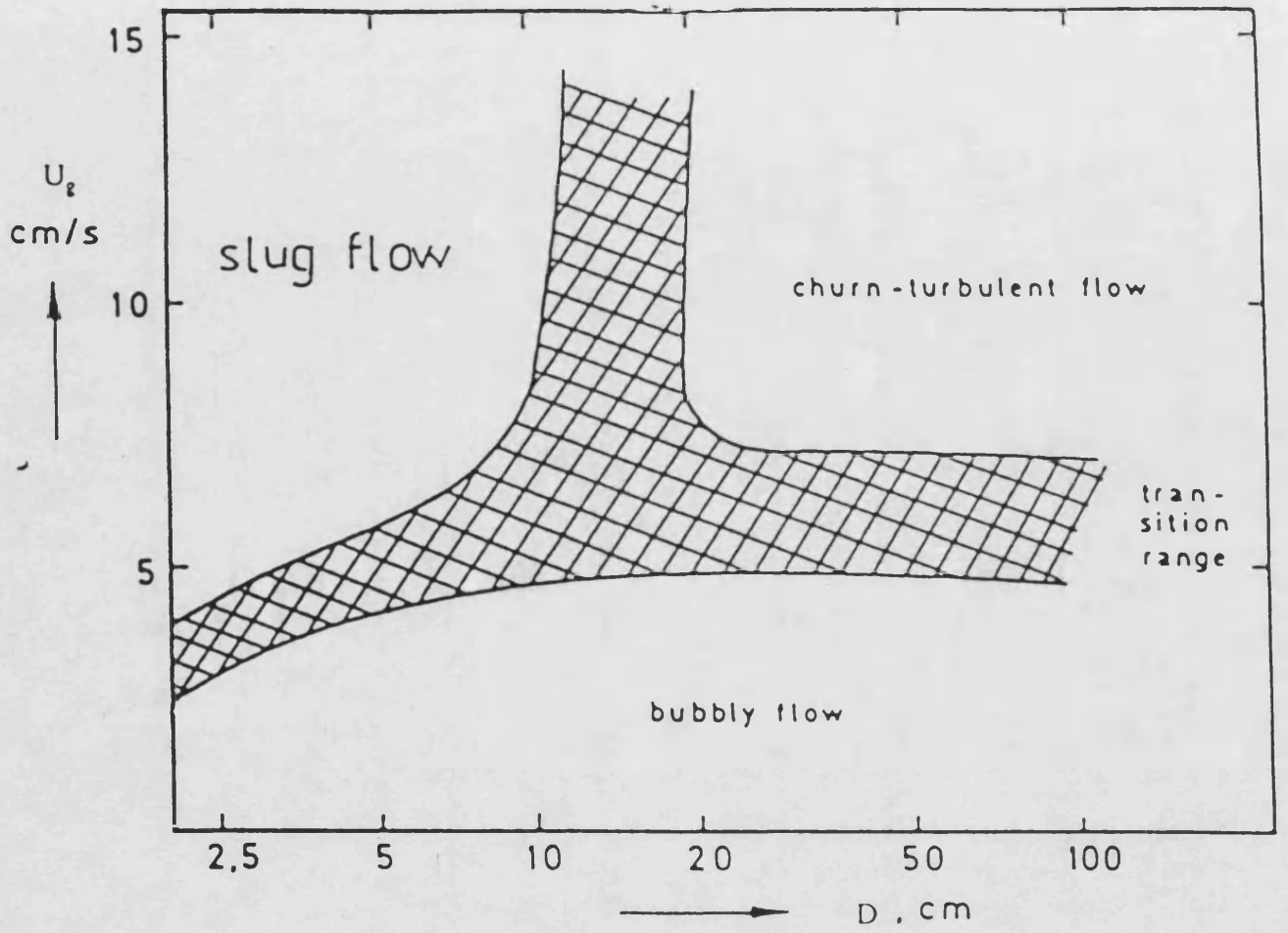

Figure 2.1.- Dependence of flow regime on gas velocity and column diameter, qualitatively for low viscosity liquids, Deckwer(1981).

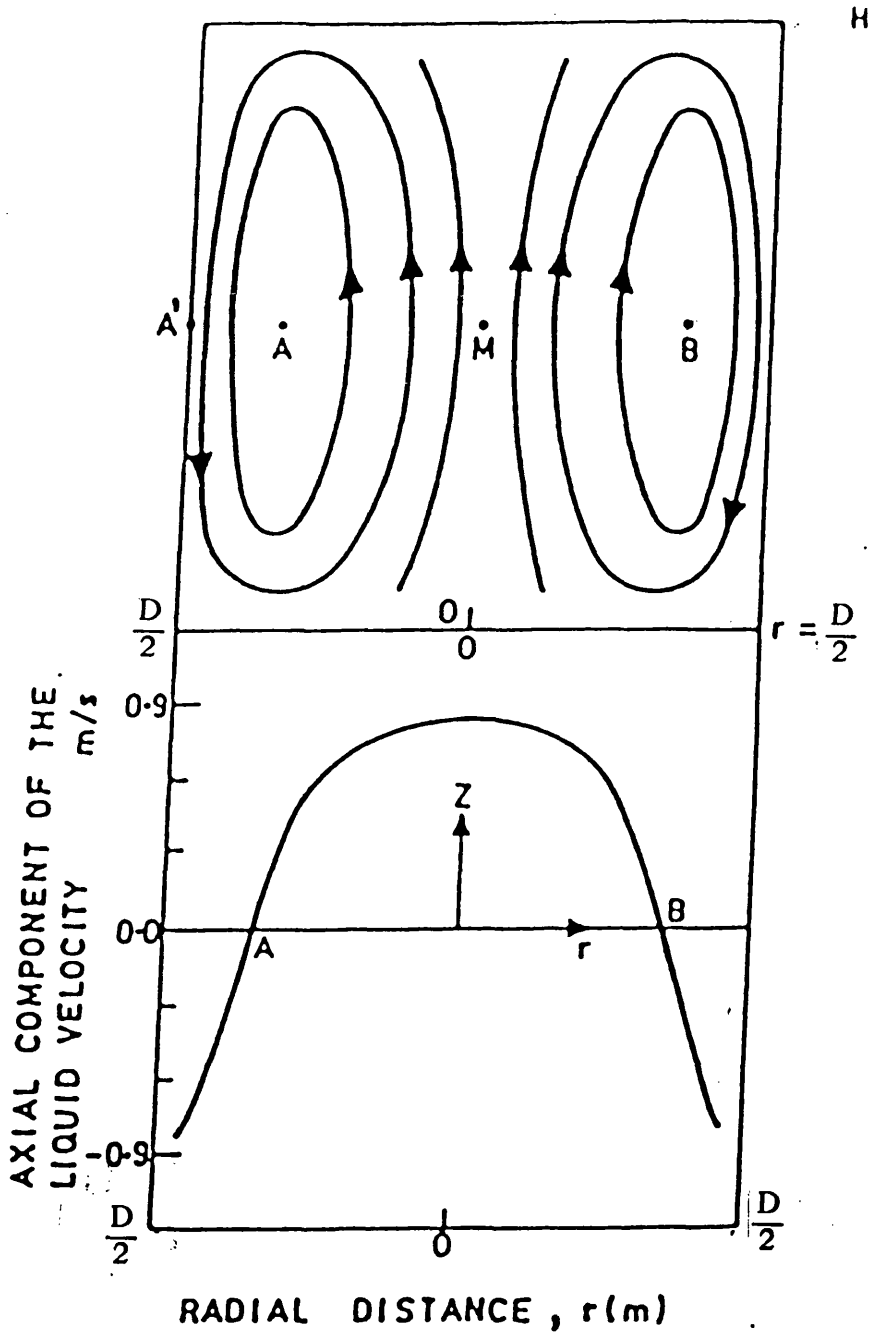

Figure 2.2.- Liquid circulation and velocity profile in a bubble column, an axisymmetric cell. D=1.0 m, H/D=1, U_g = 50 mms^{-1} . A, B: centres of vortices. Joshi and Sharma (1979).

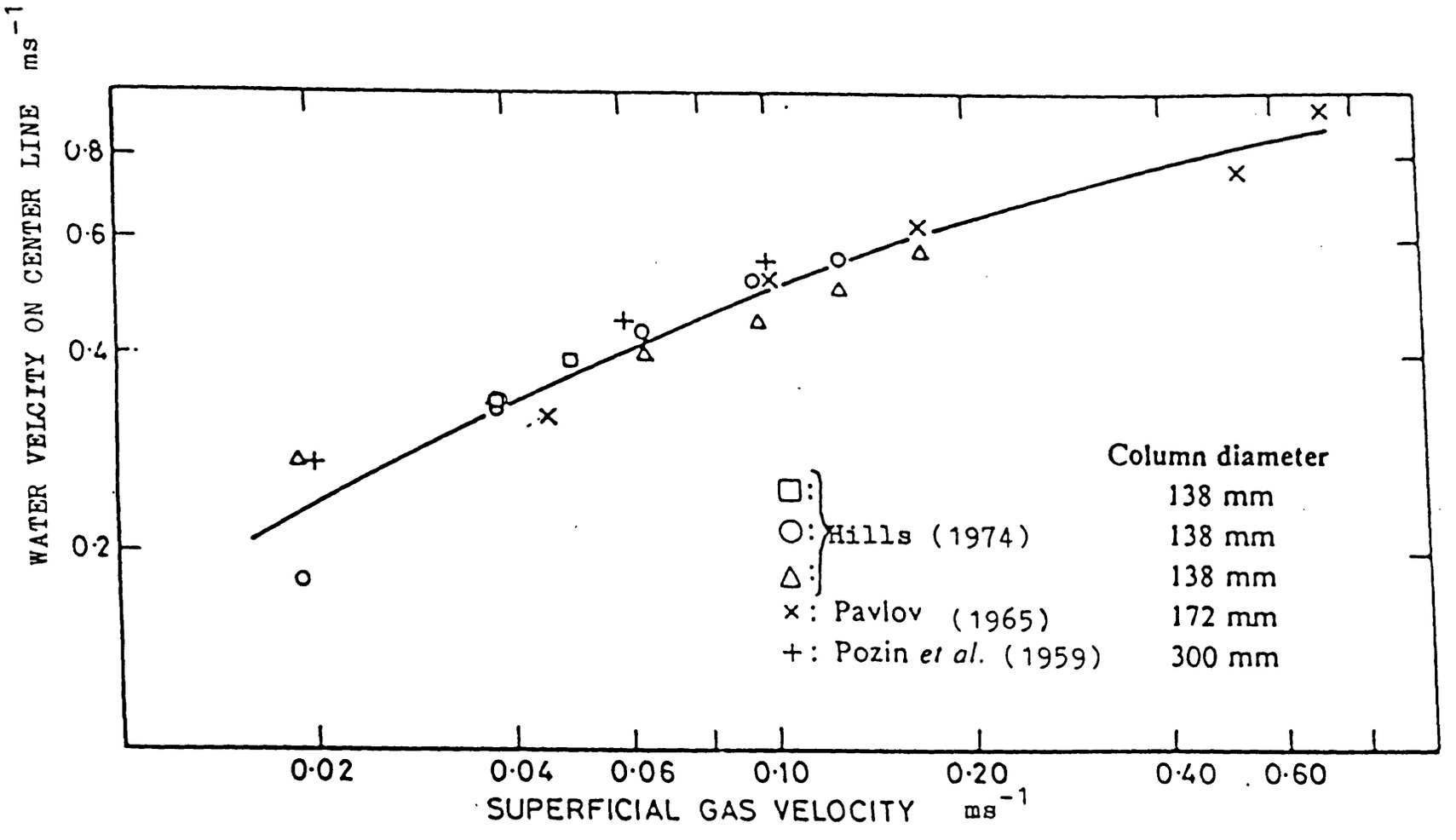

Figure 2.3.- Maximum liquid velocity as a function of gas rate. Hills (1974)

CHAPTER 3

EXPERIMENTAL EQUIPMENT AND PROCEDURES

3.- INTRODUCTION.

This chapter describes the details of the experimental apparatus and the experimental procedures for gas $_{hold-up}$ and heat transfer measurements.

3.1.- DESCRIPTION OF THE APPARATUS.

Figure 3.1 presents a diagram of the apparatus. The assembled equipment as used for the latter part of the work is shown in Figure 3.2 and it is described below.

3.1.1.- Column.

The column consists of a QVF glass section 1.50 m in height and 0.292 m in diameter bolted to a 0.1 m height metalic section. The metalic section of the column contained a liquid inlet to the

column and its dimensions are given in Figure 3.3(a).

The conventional metallic end section below the gas distributor plate, Figure 3.3(b), included air entry and liquid drainage ports. Its height is 0.30 m and the air inlet port is o.15 m from the base. There are no internal in the air box such as baffles. However, this box was assumed to be large enough to prevent pressure variations.

The air box and distributor plate and the liquid entry section of the column bolted together while the gas distributor plate was positioned in between. Rubber gasket of about 3 mm thick was used as sealant.

3.1.2.- Air Supply Line.

Mains air was passed through an air filter and pressure regulator valve and one of the two parallel rotameters before entering the column. Rotameters were manufactured by KDG Ltd and were of size 24 and 35. The floats type were Koronnite and Duraluminum. The supply line was 1 inch BSP. The manufacturer's calibration charts were used in order to calculate gas flow rates. A pressure indicator just above the rotameters enabled any necessary pressure correction to be made as detailed in Appendix A1.

3.1.3.- Gas Distributors.

Four different sieve plate distributors were employed as detailed in Table 3.1. The sieve plates were made of 3 mm thick aluminium sheets cut into 0.445 m diameter circle. Holes of 1 mm diameter were drilled into plates. Distributor 129a had 129 holes drilled evenly on a circular area of radius o.144 m and square pitch of 24 mm. Distributor 129b has 69 holes in a semi-circular pattern and was obtained by blocking half of distributor 129a. Distributor 57c was of the same type as 129a but the distance between holes were increased to 35 mm and hence the number of holes reduced to 57. Distributor 57c was in essence distributor 57a, but it was situated above distributor 129a with a gap of about 3 mm in between.

A fifth type of distributor was a sheet of porosint bronze type M-14 Grade C, of thickness 5.1 mm with nominal pore size of $<100\,\mu m$ manufactured by Sintered Products Ltd. It was cut to diameter of 0.285 m and supported to the aluminium ring.

3.1.4.- Liquid Distributor.

Figure 3.4(a) shows a schematic view of the liquid distributor. It was made of crossed shape copper tube of 17.7 mm (1/2 inch) diameter with 8 holes of 2 mm diameter on each limb.

Liquid could enter at the junction of the two tubes via a copper tube of 17.7 mm diamater as shown in Figure 3.4(b).

Liquid distribution position was 4 mm above the gas distributor.

3.1.5.- Heaters.

3.1.5.1.- Heater Rods.

The heaters were made of brass which has a thermal conductivity of 100 $W(mK)^{-1}$ at 33 ^{o}C. The different sizes of heaters are detailed in Table 3.2 and a diagram is given in Figure 3.5. The design is similar to that developed by Lewis et al (1982). The top end of the heaters were insulated by using tufnol of total lengths 50 mm. These are also shown in Figure 3.5(b). Whilst Figure 3.5(c) is the photograph of the assembled 30 by 60 mm heater.

The size and ratings of the cartrige heaters which were used in conjunction with the heater are given in Table 3.2.

Surface temperature of the heaters was measured by 4 type K (Cr-Al) thermocouples with accuracy of ± 0.1 ^{o}C. The thermocouples diameter was 1 mm. These thermocouples were positioned inside the heater and were connected to a digital type K thermometer.

In assembling the thermocouples and the heater cartridge care was taken to ensure that the thermocouple tip touches the thermocouple well end. Also to prevent heat losses, or liquid

entry, to the heater top of the heater cartridge was sealed with the silicon rubber.

Power was supplied via a Variac transformer and measured by a wattmeter. The circuit also contained as a safety device an insulating transformer with a 2 A ratings.

The temperature of the liquid could be raised to the desired level by a 3 KW heater. The liquid temperature was maintained within $\pm$ 2^{o}C manually.

The heaters were supported inside the column by 1.5 m long and 10 mm diameter galvanized tube. This was held in an adjustable clamp mechanism that could be positioned in any desired radial position.

The heaters themselves could be assembled horizontally or vertically as required and could be positioned at any required distance from the distributor.

Heater vibration was reduced in later experiments by adding an expansion bar to the galvanised tube. The expansion rod was about 30 mm above the heater.

3.1.5.2.- Heater Bundle.

Figure 3.6 is the photograph of the heater bundle. It

consisted of two aluminium end plates of 165 by 165 mm used to support the centrally positioned heater and surrounded by dummy heaters.

The dummies were made of wood and their lengths were 165 mm and their diameter were the same as heater itself being 30 mm. The heater length was 120 mm.

The heater bundles were arranged in a square pitch (in line arrangement). The different arrangements are as detailed in Table 3.3. Experiments were carried out with 9 or 25 heater dummies and a heater. Pitch to heater diameter ratios of 1.25, 1.5, 2.25 and 2.47 were used. A plan view of the position of the heater bundle in the column is shown in Figure 3.7.

3.2.- EXPERIMENTAL PROCEDURES.

3.2.1.- Hold-up Measurements.

The main objective of the early work was to measure local gas holdup. Local gas hold-up was measured using a manometric technique. The procedure was first to fill the column up to the desired height and then the manometer tubes were placed in one of the chosen positions that are shown in Figure 3.8. Care was taken to ensure that water in the manometer limbs were level. The vertical distance between manometer limbs were kept constant at 100 mm. They were held together by ordinary silicon tape.

The free end of manometers were connected to a micro digital air pressure indicator, Model MP6KMD manufactured by Air Ltd.

After aeration the changes in air pressure were recorded. Local gas holdup values were calculated using the method explained in chapter 4.

In all runs the average gas holdup was measured by the bed expansion method. The increase in the height of the liquid level due to aeration were calculated by measuring the liquid height before and after aeration with an accuracy of ± 1 mm. Gas holdup was then calculated from equation 3.1 with an estimated error of less than 7%.

$$\epsilon = \frac{H_o - H}{H_o} \qquad \ldots 3\text{-}1$$

H is the height of liquid before aeration and H_o is height of liquid after aeration.

The superficial gas velocity were referred to the conditions at the base of the column static pressure.

3.2.2.- Heat Transfer Measurements.

Measurements of heat transfer in the aerated water and CMC solutions were obtatined for a wide range of operational

conditions. The CMC solutions were prepared by dissolving CMC powder in water (the high viscosity type CMC sodium salt product of BDH was used). The rheological properties were measured with a Brookfield viscometer Model UCL at shear rates of from 0.3 to $73s^{-1}$. Physical properties of water and CMC solutions are given in Table 3.4. The aspect ratios of 2, 3 and 4 were used with a combination of heaters dimensions. Superficial gas velocities were calculated at the column base pressure and bulk liquid temperature (see Appendix A1 for details). The range was 12 to 120 mms^{-1}.

To measure the heat transfer coefficient the column was first filled with either water or a CMC solution in the approximate range of 100 to 10,000 ppm. The liquid depth was 0.6, 0.9 and 1.20 m, but most of the experiments were carried out at the aspect ratio of 3 corresponding to the liquid depth of 0.9 m. Then a measured air flow rate was supplied whilst the heater was put in the required location. Power was supplied via a Variac transformer to the cartridge heater, the amount being measured by a wattmeter. The supplied power was in the range of 45 to 180 W for the different heater dimensions in order to maintain a constant heat flux of 1519.5 Wm^{-2} for most runs.

The temperature of the heater was measured by four thermocouples which were fixed inside the heater between 0.7 to 3 mm from the surface. The average was correct as detailed in Appendix A2 to give surface temperature of the heater probe.

The temperature difference was calculated from the average heater surface temperature and the liquid temperature. The bulk liquid temperature was measured by a thermocouple suspended freely inside the column away from the heater surface.

For a given superficial air velocity, the heat transfer and holdup were measured. The latter by the bed expansion method. The heat transfer coefficient, h, was calcualated as .

$$h = \frac{Q}{A\,\Delta T} \qquad \ldots 3.2$$

where Q = power input to the heater, A = surfac area of the heater, . Δ T= temperature difference between the average heater surface and bulk of liquid.

The tufnol that was used for insulating the ends of the heater had a thermal conductivity smaller than 0.29 $W(mK)^{-1}$ which is less than that of water. Also the end cross sectional area of the brass rod is about 22% of the curved surface area. Therefore the error in the heat transfer measurements due to the heat transfer through tufnol ends are negligible.

The temperature difference along the surface of the heater was not investigated but it is known (Hart (1976)) to be negligible except near the ends and following Hart it was considered reasonable to measure the temperature of the heater surface at the middle of the heated section. However the

corrected individual temperatures were found to vary by about 2%.

3.3.- PRELIMINARY EXPERIMENTS.

3.3.1.- Effect of End Caps.

The effect of heater end insulators cap on the measured heat transfer coefficient was investigated by using both 50 mm and 100 mm long tufnol end cap with a 30 by 60 mm heater. The results that are shown in Figure 3.9 shows that the heat transfer coefficient data obtained with 100 mm insulator cap is on average only 4% higher than the data obtained with the 50 mm cup. This is considered to be within the experimental error and hence the effects of the end caps has been neglected.

3.3.2.- Temperature Measurements.

A comparison between positioning the thermocouples inside the heater and on the surface of the heater was made. The results for a 30 by 60 mm heater shown as variation of the calculated values of heat transfer coefficient with superficial gas velocity in Figure 3.10. It shows that positioning the thermocouple on the heater surface will give values that are on average about 4% lower. This was taken into account by reducing the calculated values of heat transfer coefficients by 4%. This only applied to some of data for 30 x 60 mm heater.

Table 3.1.- Characteristics of the sieve plates. All holes are 1 mm in diameter.

Plate	Number of holes	Arrangements
57a	57	57 holes on square pitch of 35 mm. Including centre hole.
57c	57	Plate 57a was put over plate 129a with 33 mm gap between them.
129a	129	129 holes on square pitch of 25 mm. Including centre hole.
129b	56	centre line plus half of plate 129 were blocked.

Table 3.2.- Dimensions of heaters and heater cartridges

Heater		Cartridge		
length mm	Diameter mm	length mm	diameter mm	ratings W
120	30	100	10	200
60	30	50	10	150
30	30	20	10	200

Table 3.3.- Detailes of bundles used.

No. of rows	No. of columns	* pitch	clearance mm
3	3	1.25	7
5	5	1.23	7
3	3	1.50	15
3	3	2.25	37.5
3	3	2.47	44

*pitch= (distance between the centers)/heater diameter.

Table 3.4(a).-Physical properties of water at selected temperatures

temperature ^{o}C	ρ kgm^{-3}	μ cP	C_p $J(kg/^{o}C)^{-1}$	k $W(mK)^{-1}$	σ Nm^{-1}
10	1000	1.3	4200	0.55	74.25
20	998	1.002	4181	0.60	72.75
30	995	0.7975	4178	0.61	71.18
50	998	0.5468	4180	0.64	67.91

Table 3.4(b).- physical properties of CMC solutions.

Density, heat capacity and thermal conductivity are that of water.

$$\mu = K(\gamma)^{n-1}$$

approximate concentration ppm	K Pas^n	n
100	0.002	0.857
500	0.004	0.831
1000	0.008	0.834
1500	0.011	0.877
2000	0.018	0.833
2500	0.024	0.810
3000	0.028	0.810
5000	0.087	0.810
10000	0.158	0.810

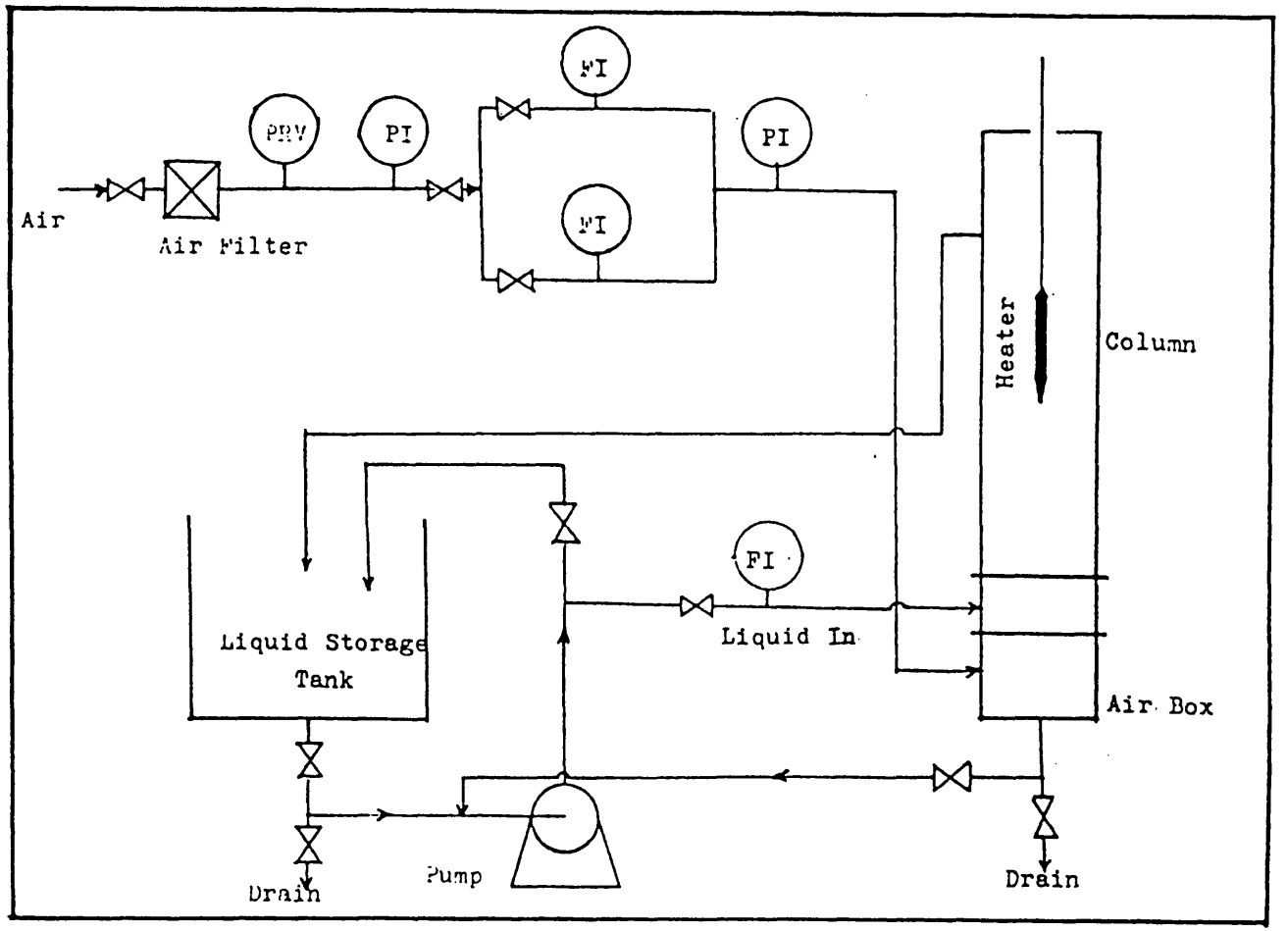

Figure 3.1.- Diagram of the Bubble Column Apparatus.

Figure 3.2.- Photograph of Experimental Set Up.

Figure 3.3 - Dimensions of liquid inlet and air box.

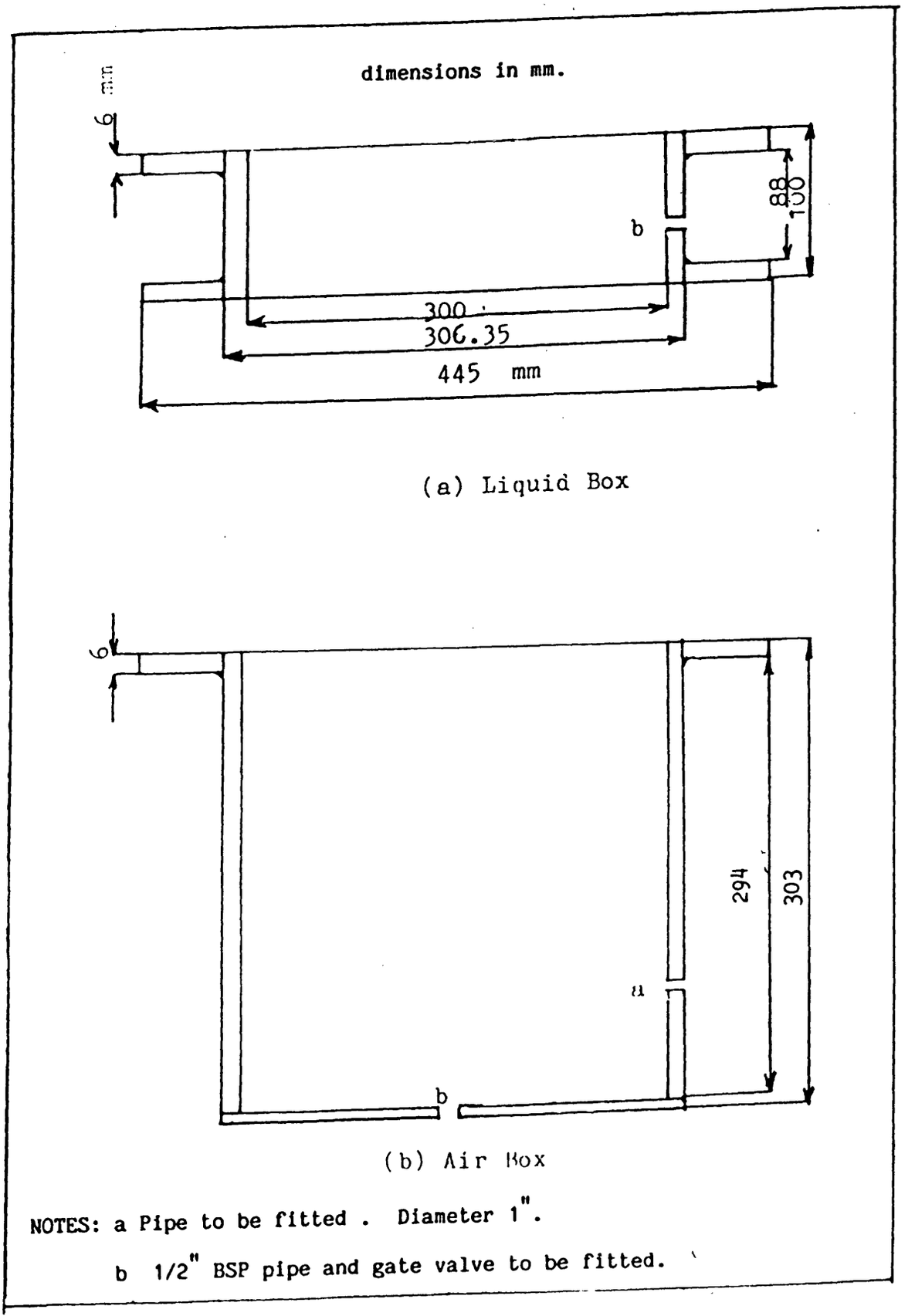

NOTES: a Pipe to be fitted . Diameter 1".

b 1/2" BSP pipe and gate valve to be fitted.

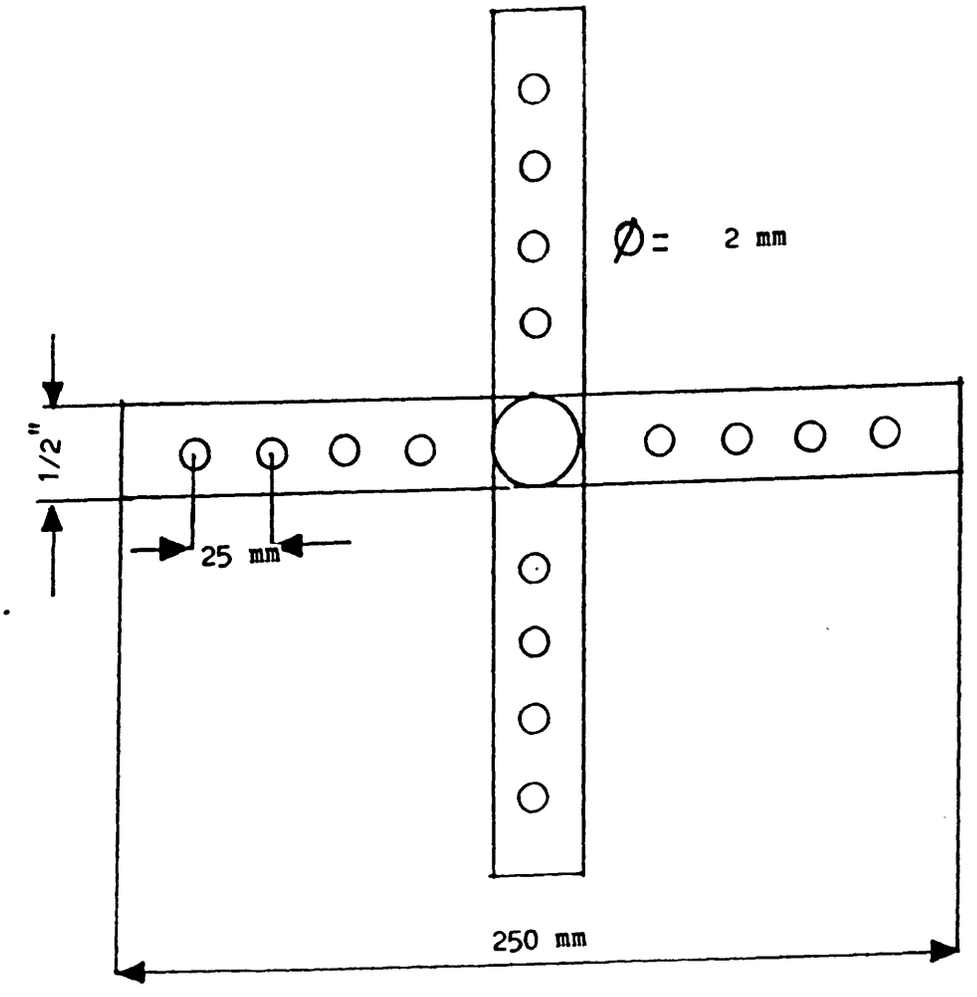

Figure 3.4 (a) - Schematic top view of the liquid distributor.

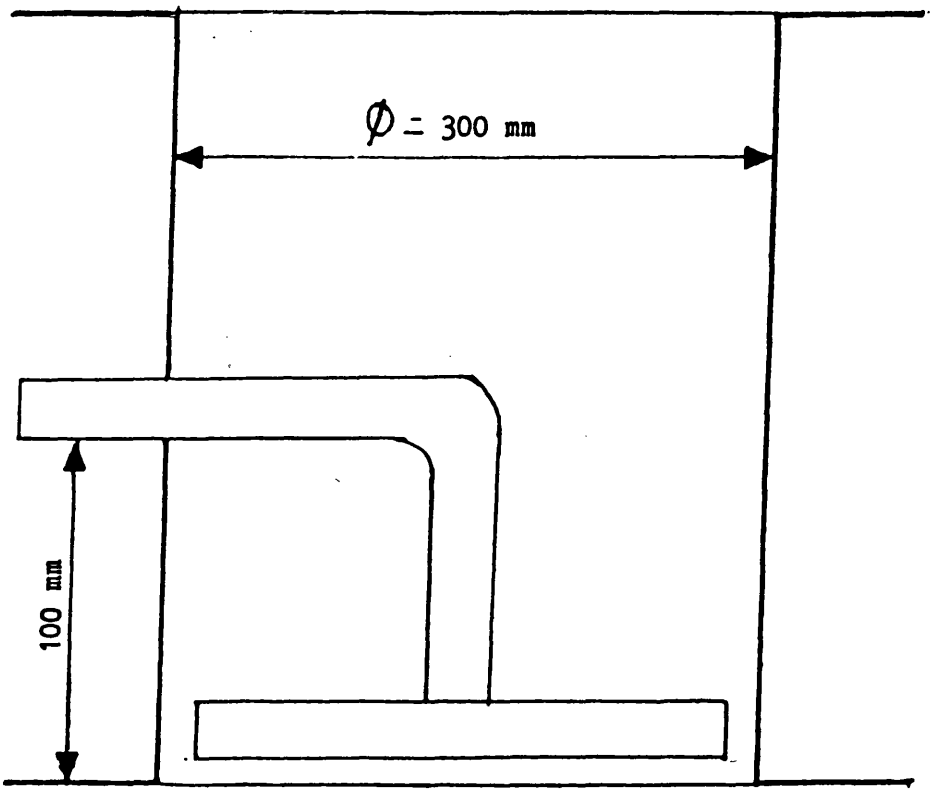

Figure 3.4 (b) - Position of liquid distributor inside liquid box.

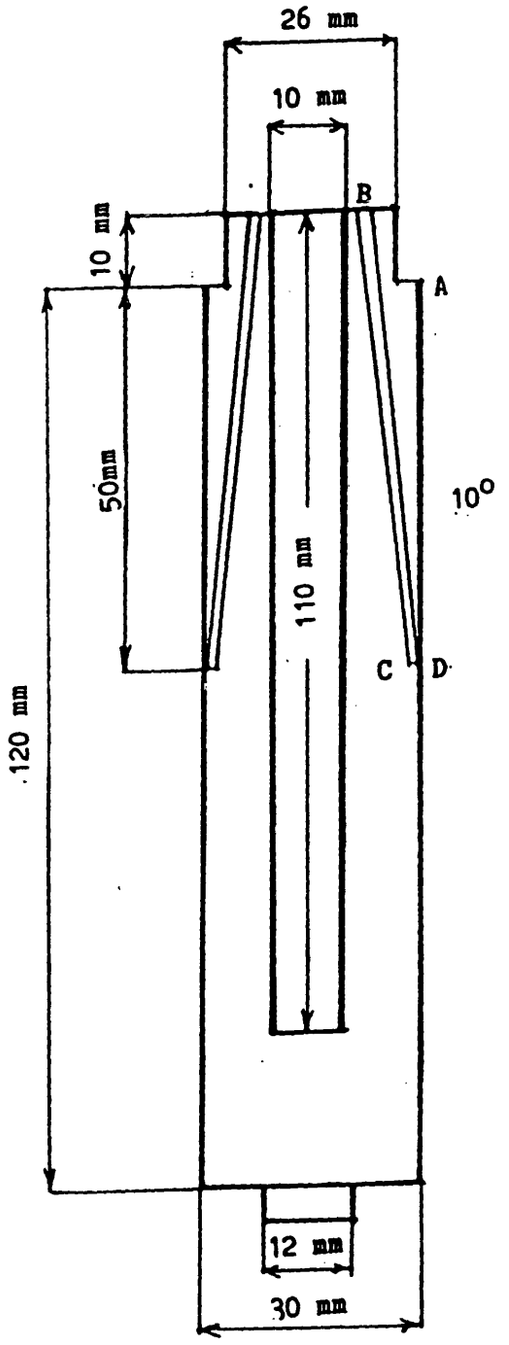

Figure 3.5 (a)- Diagram of main body of heater.

Dimensions in mm

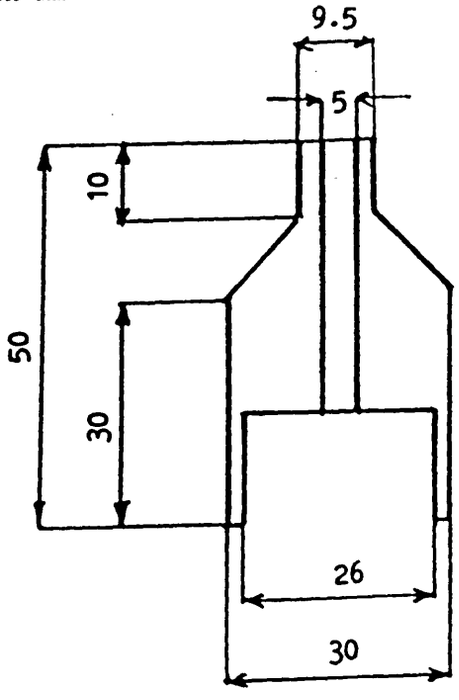

Top cap

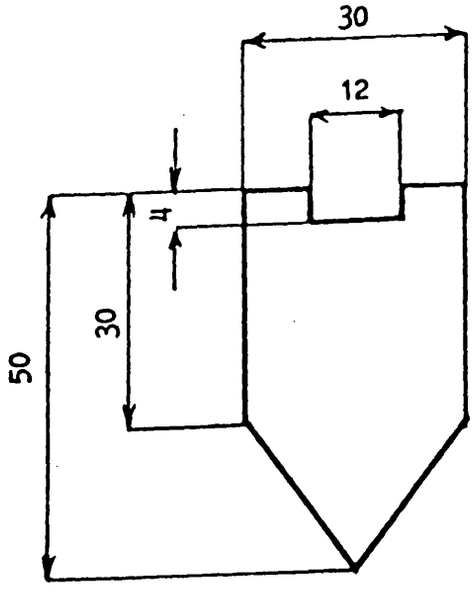

End cap

Figure 3.5 (b)- Diagram of heater caps.

Figure 3.5(c).- Photograph of the 30 by 60 mm Heater.

Figure 3.6.- Photograph of the Heater Bundle.

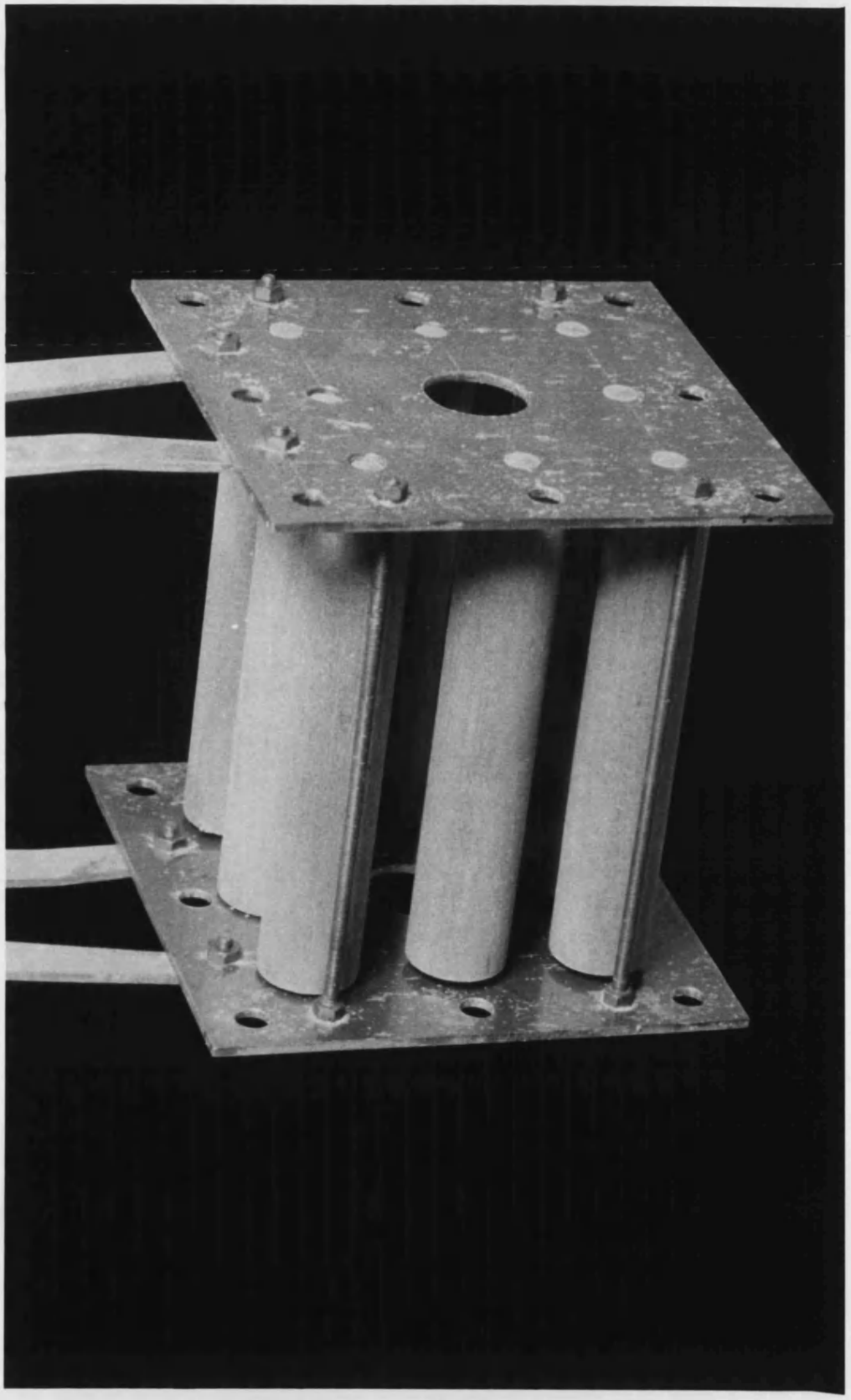

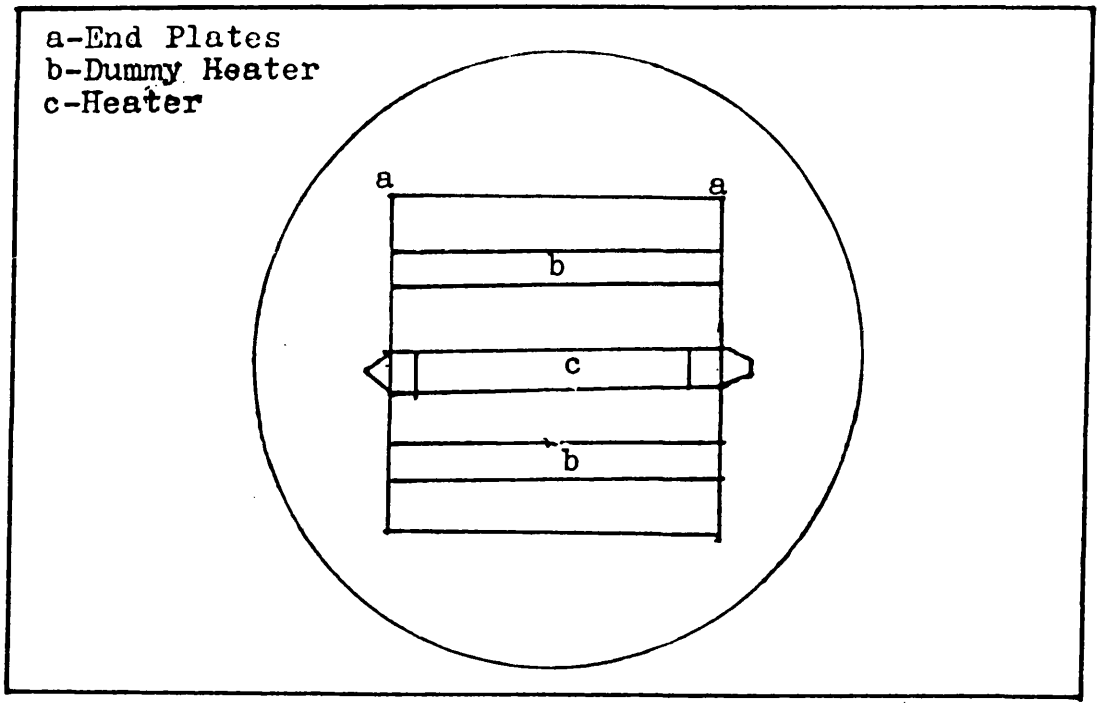

Figure 3.7 - Position of tube bundle in column viewed from above.

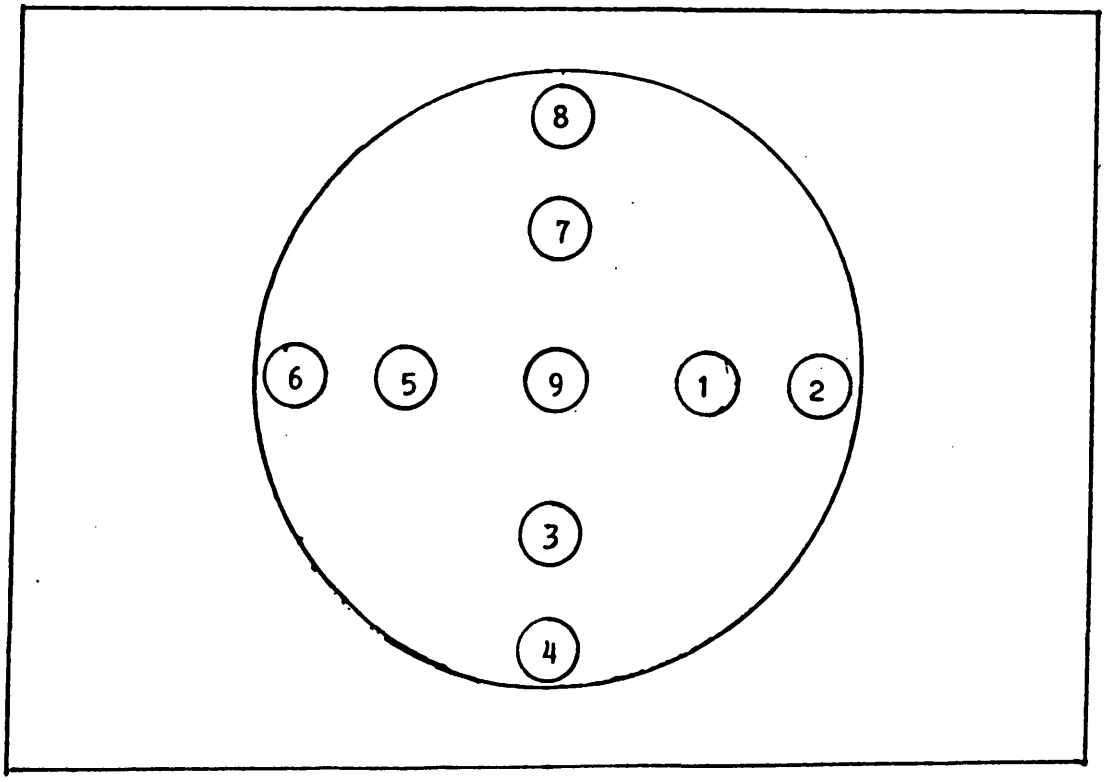

Figure 3.8 - Horizontal position of manometer limbs.

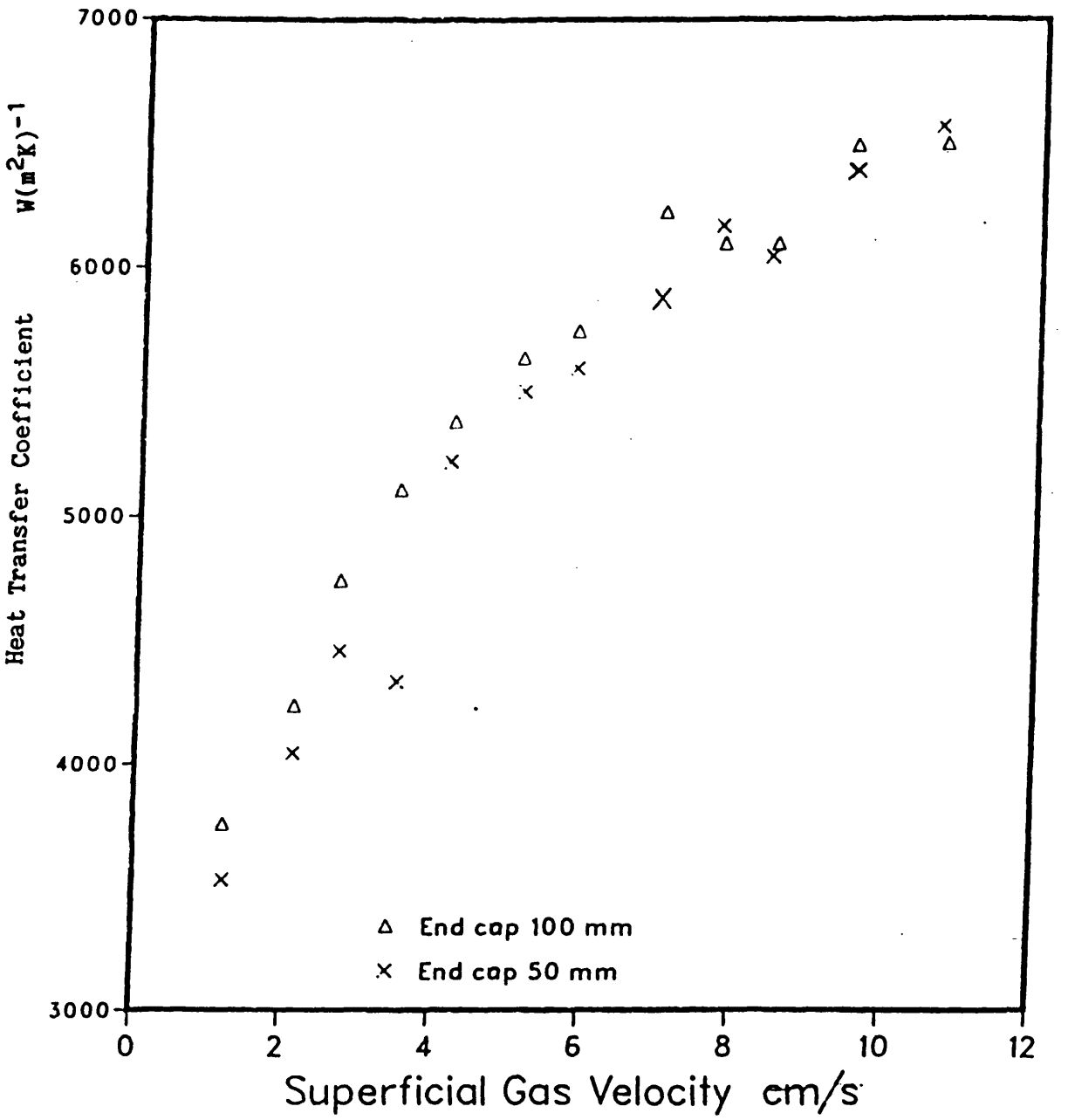

Figure 3.9 - Variation of heat transfer coefficient with superficial gas velocity. Effect of Insulator End Cap Length for 30 by 60 mm vertical heater. Water height was 0.90 m and 57c distributor was used.

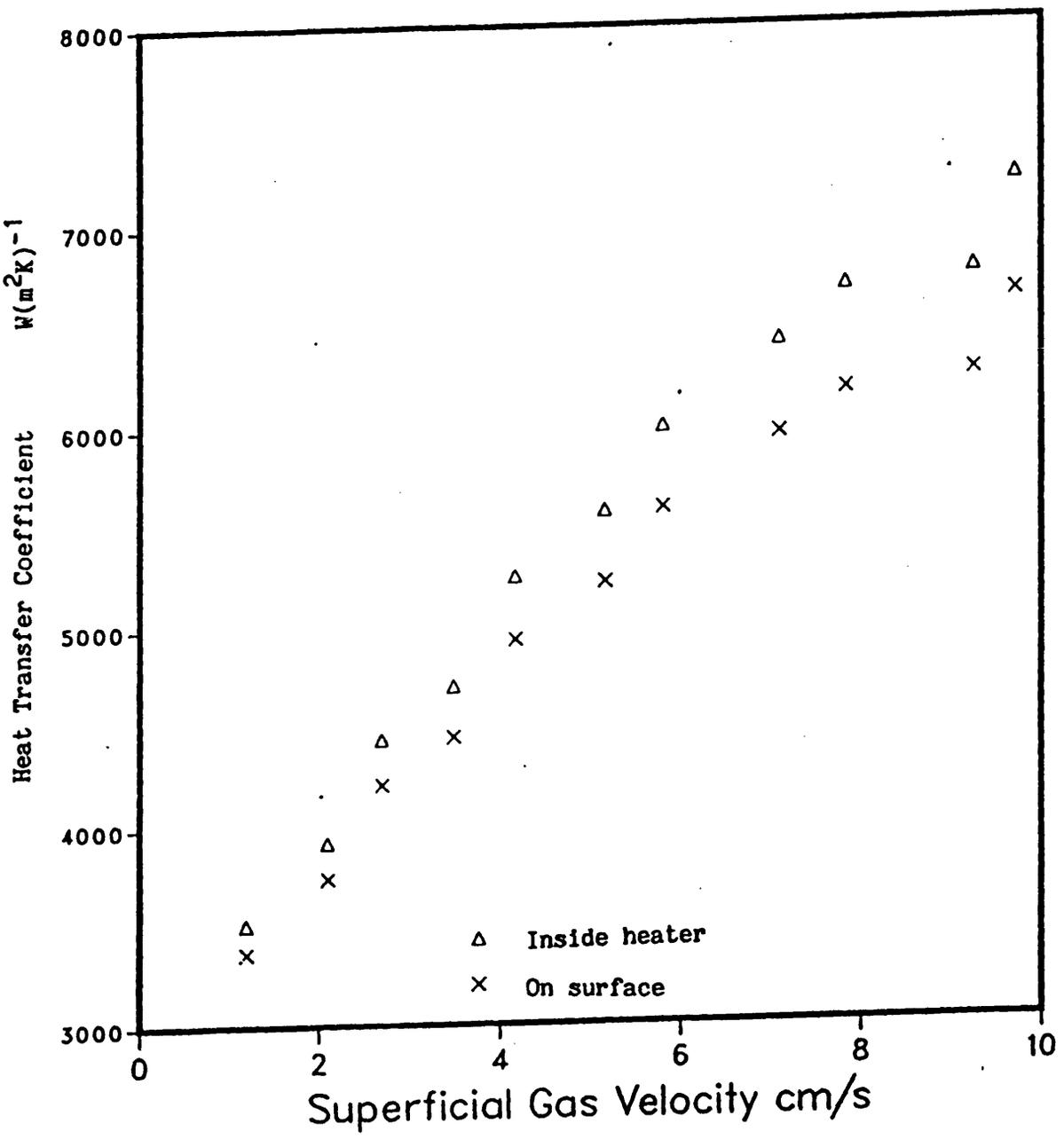

Figure 3.10 - Variation of heat transfer coefficient with superficial gas velocity. Effect of Thermocouple Position on surface and embedded for 30 by 60 mm vertical heater. Water height was 0.90m and 57a distributor was used.

Effect

CHAPTER 4

HOLD-UP MEASUREMENTS

4.- INTRODUCTION

Certain bubble column heat transfer models as described in chapter 2 include a dependency upon gas hold-up. However, gas hold-up is a non-adjustable parameter that depends on parameters such as the physical properties of the liquid mixture, type of gas sparger and gas throughput. Whilst studying parameters that could affect the heat transfer coefficient in bubble columns (which will be described in chapter 5) their effect on gas hold-up were also noted. Following a discussion of the results, suitable correlations that can represent the experimental hold-up data will be presented.

Attempts also were made to measure the radial and axial variation of local gas hold-up by use of a manometric method and the limited success was crucial to a better understanding of the extent of the parallelism between gas hold up and heat transfer in bubble columns.

4.1.- HOLD-UP MEASUREMENTS - THEORY

4.1.1.- Introduction

Some methods of gas hold-up measurements in bubble column are;

1-Bed expansion and gas disengagement method,eg. Akita and Yoshida(1973), Godbole et al (1982).

2- Manometric methods, eg. Hills(1976), Hikita and Kikuma(1974)

3-Different probes, eg. Optical probes (Nottenkamper et al(1983)) and capacitance probe (Lewis (1984)).

Nottenkamper et al reported that accuracy of these methods are comparable eventhough his optical probe hold-up data are consistantly 10% lower than data obtained by manometric methods and are within $\pm$10% accurate in comparison with data of other experimenters.

Whilst manometric and optical probe methods can be used for local and average gas hold-up measurements the bed expansion method can only be used for the latter.

Due to the easy application of the bed exansion and manometric methods, as described below, it was decided that these methods be used in this work.

4.1.2.- Bed Expansion and Manometric Methods

Gas hold up is defined as the volume fraction of the two phase mixture occupied by the gas phase. Therefore, in the bed expansion method average gas hold-up, ϵ , can be calculated by direct measurement of the liquid height before and after aeration.

$$\epsilon = \frac{H_o - H}{H_o} = \frac{\Delta H}{H_o} \qquad \ldots 3.1$$

However, in the manometric method this could be achieved by measuring hydrostatic presure at two points. Measurement of gas hold-up at a specific level is provided by the momentum balance for a two phase system. The momentum balance indicates that the total pressure drop of the aerated fluid is composed of contributions due to the liquid acceleration, wall friction and hydrostatic pressure of the aerated liquid.

Hills(1976) showed that contribution of acceleration and friction in case of batch bubble column are negligible. With this simplification, the variation of pressure with height is entirely due to hydrostatic head. Hence

$$\frac{\Delta P}{\Delta h} = -\rho g (1 - \epsilon) \qquad \ldots 4.1$$

Pressure is measured with a vertical tube manometer filled

with the column liquid. Then if ΔZ is the manometer reading then;

$$\rho g \frac{\Delta Z}{\Delta h} = \frac{\Delta P}{\Delta h} + \rho g \qquad \ldots 4.2$$

Therefore from equations 4.1 and 4.2 one obtains,

$$\epsilon = \frac{\Delta Z}{\Delta h} \qquad \ldots . 4.3$$

Where ΔZ is manometric reading and Δh is the distance between manometer tappings. $\frac{\Delta P}{\Delta h}$ is the pressure gradient.

In this work hold-up was measured indirectly by measuring the differential change in air pressure in two manometer limbs, which were connected to a digital pressure gauge.This was then related to the gas hold-up as indicated in Appendix B1. Gas hold-up calculated from equation 4.4

$$\epsilon = \frac{(P_{m2} - P_{m1})}{\rho g \, \Delta h} \left[1 + \frac{\rho g H_t}{P_{atm}} \right] \qquad \ldots . 4.4$$

Where $(P_{m1} - P_{m2}) = \Delta P_m$ is the measured pressure difference, P_{atm} is the atmospheric pressure, ρ is the density of the liquid phase, Δh is the distance between the manometer limbs and

H_t is the total length of each manometer limbs and its associated tubing.

4.2. - MANOMETRIC LOCAL AND AVERAGE GAS HOLD-UP MEASURMENTS.

Experiments were performed to check the validity of the above manometric method for use in local and average gas hold-up measurements.

The 0.292 m diameter column was filled with tap water to an initial height of 0.60 m. At two levels of 0.35 and 0.45 m from the 129a distributor and at different radial positions as indicated in Figure 3.1 gas hold-up was measured for various gas superficial velocities. The results are given in Table 4.1.

The average gas hold-up at each level, 0.35 or 0.45 m from gas distributor, is calculated by taking the average of the local gas hold up values at that level. The overall average is the mean of the average for each level. Table 4.1 also shows the average of gas hold-up measured by the bed expansion method.

4.2.1.- Manometric Method Discussion

Experimental data of Table 4.1 clearly shows that local gas hold-up is a function of position and assumes different values, but no trend is observable in the measured gas hold-up at the

different radial positions. This contradicts the reported observation that local gas hold-up is at its highest value at the column axis and its lowest value is near the column wall(See for example Hills(1974) and Nottenkamper et al(1983)). Nottenkamper, however, reported that local gas hold-up, measured by the optical probe, is independent of radial position at low gas flow rates for evenly distributed gas at the sparger. It should be noticed that these investigators employed column with aspect ratio of about 10 whilst the present study was carried out in a column with an aspect ratio of 2. Nevertheless, in accordance with both Hills and Nottenkamper an increase in gas hold-up with height is observable. The accuracy of this method is apparent from the almost equal values of gas hold-up measured by the bed expansion method and average gas hold-up calculated from the local gas hold-up values measurd by the manometric method.

As the gas flow rates increased above 90 mms^{-1} the pressure indicator response remained almost constant at all probe locations and did not vary with further increase in gas flow rates. This still awaits an explanation.

The vertical movements of the probe required that the column aeration be stopped so that the initial liquid level in the manometer and hence initial pressure be adjusted. This is necessary because the vertical movement changes the initial length H_t.

A change in the gas content above the liquid level in the manometer limbs was avoided by making the manometer tubing connetions air tight. Provision also made to prevent air bubble entry to the manometer limbs. To this effect different designs of manometer limbs that were employed are shown in Figure 4.1. It was found by trial and error that the design shown in Figure 4.1(d) satisfies the experimental requirements ; with the other designs bubbles entered the limbs.

4.3.- AVERAGE HOLD-UP MEASUREMENTS FOR WATER-AIR SYSTEM

4.3.1.- Effect of Liquid Height

Experiments to measure the average gas hold-up by the bed expansion method were carried out at three different unaerated water height of 0.6, 0.90 and 1.20 m. Bulk water temperatures were recorded and soften water was used . The results are shown in Figures 4.2 to 4.3.

Figures 4.2 and 4.3 show data of typical runs together with the average of runs for water height of 0.60 and 0.90 m, respectively. It is apparent that at gas flow rates above $90 mms^{-1}$ data are more scattered and are about $\pm$ 10% of the average value. This is mainly due to increased fluctuation of the liquid surface and slight foam formation at higher gas folw rates which

introduced higher errors in the measuring of the liquid height. The average gas hold-up for 0.90 m height water and the 57a distributor as a function of gas velocity is also shown in Figure 4.4. Figure 4.5 shows the variation of gas hold-up with superficial gas velocity for three values of liquid height. It shows that for gas velocity more than 30 mms^{-1} average gas hold-up incrases with increasing liquid height from 0.60 m to 1.20 m. This could be due to the increased rate of bubble coalesence and bubble breakage due to the shearing effect of water motion. The above effect may have an upper limit and at gas flow rates more than 100 mms^{-1} the average gas hold-up appears to become independent of water height due to the equilibrium reached between bubble coalesence and bubble breakage caused by the fluid motion.

4.3.2.- Effect of Bulk Liquid Temperature

Figure 4.6 shows the effect of temperature on gas hold-up for the limited temperature range investigated. An Increase of temperature in the range of 10 to 30 ^{o}C increased the gas hold-up by about 20%. This can partly be explained by change of physical and coalescing properties of the liquid phase. Table 4.2 shows the physical properties of water and the calculated bubble size and bubble rise velocity by equation 2.1 and 2.2 ,respectively. It shows that as temperature rises from 10 to 30 ^{o}C bubble diameter decreases from about 50 mm to 43 mm, a decrease of about 12%, but the bubble rise velocity decreases only 1%.

However viscosity of water decreases about 40% from 1.307 to 0.765 Pa.s as temperature increased from 10 to 30°C and the increased hold-up was related to viscosity. Lower gas hold-up with an increase of viscosity was explained by Eissa and Schugerl(1975).They reported that at low viscosity the drag forces are not large enough to cause bubble coalescence and hence bubble size distribution is more uniform and it size is smaller which results in higher gas hold-up.

4.3.3.- Effect of Gas Distributor

The effect of the gas distributor were investigated for a number of sieve plates and a single sintered plate distributor. The results are given in Figure 4.7.

Gas hold-up for 57a and 57c type distributor were found to be equal. As these two distributors differ from each other only with respect to the gas space below the distributor, it was concluded that the size of the gas chamber does not influence gas hold-up significantly.

Both the number of holes and its distribution have an effected on gas hold-up. Increasing the number of holes from 57 to 129 increased gas hold-up upto superficial gas velocity of 80 mms^{-1}. Above 80 mms^{-1}, in fully developed churn -turbulent flow regime, gas hold-up was unaffected by the number of holes

and their distribution. However , sintered plate gave gas hold-up of about 28% at superficial gas velocity of 80 mms^{-1}. This is about 60% higher than the corresponding values for the sieve plates. The smaller bubble sizes that were produced by the sintered plate distributor compared with the 57c distributor plate are shown in photographs of bubbles in Figure 4.8 and Figure 4.9,respectively. These are taken for a qualitative comparison of bubble size at gas flow rate of 12 mms^{-1}. The initial water height was 0.65 m.

The effect of maldistribution of gas at the column base has been shown in Figure 4.7 by data for 129b distributor. It showed that the gas hold-up decreased. This finding is in accordance with that of Freedman and Davidson(1969) who argued that lower gas hold-up results from an uneven distribution of gas, higher liquid circulation and consequently a higher coalescence rate. This in turn increases bubble rise velocity and therefore reduces gas hold-up. They also argued that this phenomena does not contradict Towell et al(1965) who reported that the distributor geometry did not have an effect on gas hold-up. The reason is that it can be argued that maldistribution of gas at the base increases the entrance region of a bubble column further and excluding data for this region would show , that for a sieve plate distributor, its design does not affect gas hold-up outside of the entrance region.

4.3.4.- Comparison of Experimental and Predicted Data

The Dependency of gas hold-up upon gas superficial velocity, U_g ,may be described by a power law equation of type $\epsilon = A\ U_g^B$ where A and B can be found experimentally. It was found that for water the dependency of gas hold-up on gas superficial velocity can be best presented by considering two regions.For low superficial gas velocities less than 40 mms^{-1}. B changes between 1 to 0.70 and A is constant with a standard deviation of $\pm$0.35%. At higher gas flow rates, 4< U_g <120 mms^{-1} the index varies between 0.4 to 0.70 and A remains constant at value of 0.06 with a rather high standard deviation of $\pm$2%. This range of dependency co-incides with the transition point from bubbly flow to churn turbulent flow. This transition point can be best obtained by locating the minimum in the curve of U_g / ϵ plotted aginst U_g. These ranges of dependency have been reported by many investigators(see for example the excellent review of Shah et al(1982)). Whilst value of B depends on the existing flow pattern, value of A mainly depends on the physical properties of the system and this account for nearly constant value of A for the present sets of data.

Mashelkar(1970) did not distingiushed between the region of low and high gas flow rates and arrived at equation 2.7 for the air water system , which is similar to the semi-theoretical equation developed by Niklin,equation 2.8 for slug flow in bubble columns.

As there are many existing correlations, produced for a wide spectrum of physical and operational conditions, it was thought appropriate to select and test an existing equation for the air-water system which was suitable to use with the heat transfer model developed in chapter 2. To this end Figure 4.10 and Figure 4.11 were produced.

Figure 4.10 and Figure 4.11 show experimental and predicted gas hold-up as a function of gas superficial velocity. Correlations are given in table 2.2 and the required physical properties are given in table 4.3. It is apparent from Figure 4.10 and Figure 4.11 that the predictions of the correlations are very different. It is also clear from Figure 4.12 and Figure 4.13 that the correlations given by Hughmark and Mashelkar, equation 2.9 and 2.7, respctively, could represent the present experimental data within $\pm 10\%$. In the Mashelkar equation the experimental value of bubble rise velocity of 310 mms^{-1}, which is the reciprocal of slope of the line shown in the Figure 4.4, was used.

4.4.- AVERAGE GAS HOLD-UP MEASUREMENTS FOR CMC SOLUTIONS

Experiments were carried out in a 0.30 m diameter bubble column which was filled up to the height of 0.90 m with CMC

solutions of different concentrations. The superficial gas velocity was varied between 10 to 100 mms^{-1}. The type 57c distributor was used in most runs. The sintered plate was only used to check the effect of distributor type with the 3000 ppm CMC solution.

The apparent viscosity, μ , of the CMC solutions was calculated with the help of an equation derived by Nishikawa et al(1987) where the average shear rate, γ , in the bubble columns is related to the gas superficial velocity, U_g , by equation 4.5.

$$\mu = K(\gamma)^{n-1} \qquad \ldots 4.5$$

$$\gamma = 5000 U_g \qquad U_g > 4\times10^{-3}$$

The units used are ms^{-1} for U_g , s^{-1} for γ and cP for μ . K and n are flow consistancy and flow behavior index, respectively. The apparent viscosity was used to correlate the gas hold-up data.

4.4.1.- Effect of CMC Concentration on Gas Hold-Up

Figure 4.14 shows the variation of gas hold-up with superficial gas velocity at different concentration of CMC solution.It is clear from Figure 4.14 that the gas hold-up shows an increase with gas velocity and that for CMC concentrations

higher than 1000 ppm the gas hold-up decreases with further increase in the concentration of the CMC solution. Higher concentrations of CMC solution correspond to higher apparent viscosity of the solution at any specific superficial gas velocity.

Figure 4.15 shows the effect of apparent viscosity on gas hold-up at three different superficial gas velocities of 10, 35 and 87 mms^{-1}. It shows that in the viscosity range of 1 to 12 cP at low gas flow rate of 12 mms^{-1} variation of gas hold-up with viscosity is negligible but at higher gas flow rates gas hold-up decreases at an apparent viscosity of about 3 cP. Batch and Pilhofer(1978), Kelkar and Shah(1983) and Godbole et al(1982) similar to Eissa and Schugerl (1975), explained this on the basis of hindered gas bubble motion in viscous fluids, in which at relatively low viscosity, drag forces are not large enough to cause bubble coalescence. These moderate forces have contributed to a more uniform distribution of bubbles and hence higher gas hold-ups.

4.4.2.- Effect of Gas Distributor

Figure 4.16 shows gas hold-up data as a function of superficial gas velocity for the sintered and 57c distributor plates. It shows that gas hold-up data obtained with the sintered plate are higher than that of sieve plates at low gas

superficial velocity but approaches that of sieve plate at higher gas velocity.

Visual observations showed that for the sintered plate distributor and at a low superficial gas velocity the bubbles are smaller in size than that of a sieve plate distributor. This was also the case with water.

The finer bubbles lead to a lower bubble rise velocity for the sintered plate and hence higher gas hold-up. However, as the superficial gas velocity increases the rate of bubble coalesence also increases which in turn caused the bubble rise velocity to increase.This causes a decrease in gas hold-up.Finally an equilibrium between bubble coalesence and bubble breakage due to circulative movements of the liquid mixture will be developed. Hence at higher gas flow rates, gas hold-up become independent of distributor type. Nevertheless,the initial fine and more uniform bubbles that were produced by the sintered plate delayed the transition of bubbly flow to churn turbulent flow.

4.4.3.- Effect of Bulk Liquid Temperature

The variation of gas hold-up with temperature for a limited range of temperature is given in Figure 4.17. It was found that in the experimental range of 18 to 36 ^{o}C gas hold-up is on

average 15% higher for data of 36 ^{o}C than for data of 18 ^{o}C. This is mainly because the viscosity of the liquid has been decreased by the increase of temperature. An explanation was given in section 4.3.2.

4.4.4.- Comparison of Experimental and Predicted Gas Hold-up Data for CMC Solutions.

Table 4.4 gives some current correlations for the prediction of gas hold-up for non-Newtonian solutions. Most investigators such as Godbole(1982) and Vatil et al(1987) correlated experimental data in a power low model in which the effect of apparent viscosity of the solution was taken into account. Whilst both Godbole et al(1982, 1984) and Hauge et al(1987) reported that for non-Newtonian solutions gas hold-up decreases with increasing column diameter, the latter recognized the variation of bubble size and hence bubble rise velocity and gas hold-up with column aspect ratio. This effect prevails up to aspect ratio of 3. Further increases in the aspect ratio does not have an obvious effect on the gas hold-up.

Experimental gas hold-up data of the present study showed that the dependency of gas hold-up on the superficial gas velocity and viscosity, μ , for 57c distributor and the aspect ratio of 3 is; $\epsilon \alpha U_g^{0.65} \mu^{-0.5}$ where U_g varies between 10 to 100 mms^{-1}.

Kelkar and Shah (1985) presented experimental gas hold-up data obtained in a 0.154 m diameter and 3.35 m tall bubble column with an equation based on the theoretical consideration of Zuber and Findley (1965) for churn-turbulent flow regime. The final equation presented as;

$$\epsilon = \frac{U_g}{n\,U_g + U_b} \qquad \ldots 4.6$$

where n represents the non-uniformity of radial distribution of the gas and U_b is indicative of a qualitative estimantion of single buble rise velocity. It was reported that n is independent of solutions concentrations and is about 2.6. However, as solutions concentration increases from about 100 ppm to 2300 ppm the viscosity of liquid increases and hence U_b increases from 0.104 to 0.328 ms^{-1}.

The experimental data were compared with both the correlation developed by Godbole et al (1982) and the above equation of Kelkar and Shah (1985). The results presented in Figure 4.18 are for a 3000 ppm CMC solution. It is apparent that the equation developed by Kelkar and Shah correlated the present data reasonably well and hence it was selected to represent the hold-up data of the present study.

4.5.- CONCLUSION.

The manometric method presented in this work was successfully used for low gas flow rates to measure radial and vertical local gas hold-up. The measured data did not show the reported trend of highest hold-up at the column axis and lowest hold-up at the column wall. However as expected there was an increase of axial gas hold-up with height. The average gas hold-up from the manometric and bed expansion methods are in good agreement suggesting that the local gas hold-up measurements are accurate.

It was found that experimental data can be best presented by either Hugmark or Mashelkar correlations. The predictions are within $\pm$10% accurate. Therefore use of these equations with the heat transfer model is justifiable.

It was found that for CMC solutions gas hold-up is a strong function of apparent viscosity and that an increase of viscosity reduces gas hold-up. It was also found that an equation similar to Hugmark equation represented by Kelkar and Shah can be used to correlate CMC data. This will be subsequently be used in the heat transfer model described in chapter 2.

****

U_g mms^{-1}	vertical distance from base m	horizontal position									average gas holdup manometric method.	average gas hold up bed expansion method.
		1	2	3	4	5	6	7	8	9		
12.	0.35	0.046	0.046	0.046	0.046	0.047	0.046	0.038	0.058	0.035	0.049	0.040
	0.45	0.059	0.062	0.053	0.046	0.046	0.054	0.058	0.059	0.043		
26.5	0.35	0.076	0.082	0.098	0.082	0.078	0.091	0.070	0.078	0.058	0.085	0.088
	0.45	0.083	0.077	0.100	0.094	0.095	0.106	0.106	0.095	0.066		
34.0	0.35	0.107	0.118	0.127	0.106	0.106	0.137	0.086	0.088	0.077	0.112	0.114
	0.45	0.104	0.119	0.131	0.115	0.122	0.119	0.125	0.122	0.099		
48.9	0.35	0.146	0.178	0.170	0.166	0.125	0.179	0.131	0.128	0.103	0.154	0.152
	0.45	0.166	0.154	0.163	0.178	0.170	0.148	0.184	0.152	0.133		
67.2	0.35	0.178	0.178	0.176	0.170	0.155	0.209	0.143	0.162	0.131	0.170	0.172
	0.45	0.178	0.178	0.190	0.180	0.181	0.179	0.187	0.178	0.145		
81.6	0.35	0.190	0.186	0.191	0.190	0.175	0.218	0.154	0.182	0.131	0.186	0.184
	0.45	0.190	0.196	0.202	0.203	0.196	0.191	0.202	0.190	0.154		

Table 4.1.- Local gas hold-up measured by the manometric method for a tap water height of 60 cm. distributor was 129. The horizontal positions are indicated in Figure 3.8.

t	ρ	σ	μ	^1U_b	^2U_b	$^3d_{vs}$	$^4d_{vs}$
^oC	kgm^{-3}	Nm^{-1}	Pa.s	ms^{-1}	ms^{-1}	mm	mm
10	999.7	74.22	1.307	0.251	0.254	4.80	8
20	997.9	72.75	1.002	0.250	0.249	4.5	7.7
30	995.3	71.18	0.765	0.249	0.220	4.3	7.6

Notes : 1. equation 2.4
2. Table 2.1(b)
3. equation 2.1
4. equation 2.2

Table 4.2.- Physical properties,bubble diameter and rise velocity of water for U_g= 0.07 ms^{-1} D=0.292 m.

Density of water at 18 ^oC	= 997	kgm^{-3}
Surface tension	= 73 x 10^{-3}	Nm^{-1}
Viscosity	= 1.028 x 10^{-3}	Pa.s
Bubble rise velocity from slope of Figure 4.4 for U_g < 0.04 ms^{-1}	= 0.31	ms^{-1}

Table 4.3.- Data used in predicting hold -up values plotted in Figure 4.10 and 4.11.

Table 4.4.- Some correlations for prediction of gas hold-up in non-Newtonian fluids.

1- Godbole et al (1982)

$$\epsilon = 0.225 U_g^{0.532} \mu^{-0.146}$$

2- Godbole et al (1984)

$$\epsilon = 0.207 U_g^{0.6} \mu^{-0.19}$$ For churn –turbulent regime

3- Kelkar et al (1985)

$$\epsilon = \frac{U_g}{n(U_g + U_L) + U_b}$$

n and U_b can be found experimentally

4- Guy et al(1986)

$$\epsilon = 0.386 Ga Fr_o^{0.84} \left(\frac{d_o}{D}\right)^{2.075}$$

$$Ga = \frac{\rho g^2 D^3}{\mu^2} \qquad Re_o = \frac{\rho U_o d_o}{\mu} \qquad Fr = \frac{U_g}{(g d_o)^{0.5}}$$

$$d_b = 2.92 Re_o^{-0.1} Fr_o^{0.42} d_o$$

5- Moo- Young et al(1987)
for polyacrylamide solutions.

$$\epsilon = 0.24 n^{-0.6} \left(\frac{U_g}{\sqrt{gD}}\right)^{(0.84 - 0.14n)} \times \left(\frac{g D}{\nu^2}\right)^{0.01K}$$

$$\nu = \frac{K}{\rho}\left(\frac{2U_g}{D}\right)^{(n-1)}$$

6- Vatai et al(1987)

$$\epsilon = 0.95 \left(\frac{U_g \mu}{\sigma}\right)^{0.769} \left(\frac{\mu^4 g}{\rho \sigma}\right)^{-0.170} \left(\frac{\rho_g}{\rho_L}\right)^{0.062} \left(\frac{\mu_g}{\mu_a}\right)^{0.107}$$

7- Hauque et al (1987)

$$\epsilon = 0.50 \left(\frac{U_b}{(gD/2)^{0.50}}\right)^{0.4} \left(\frac{U_g}{U_b}\right)^{0.8}$$

U_b calculated from Clift et al relationship.

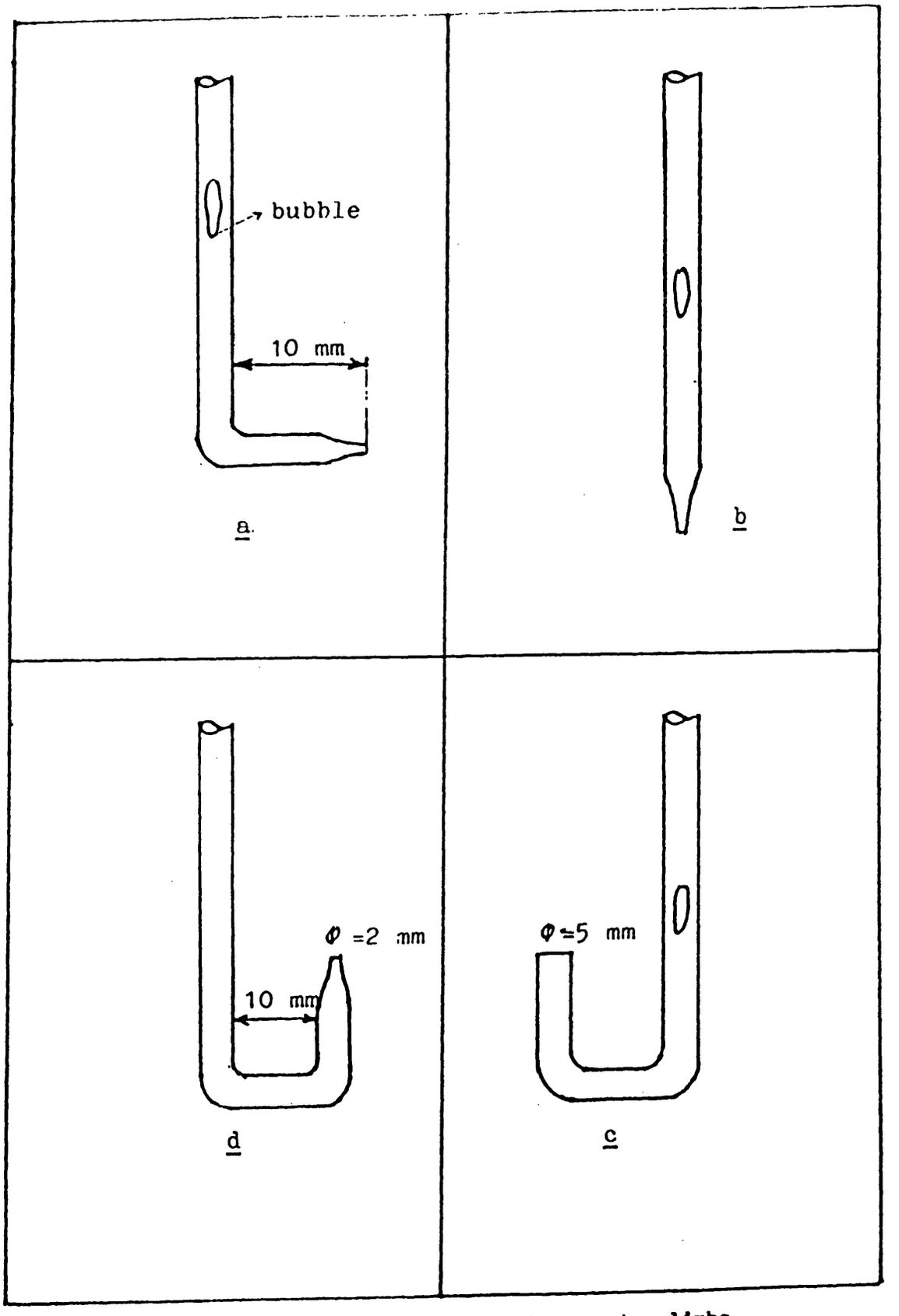

Figure 4.1.- Different designs of manometer limbs that were used with the digital manometer.

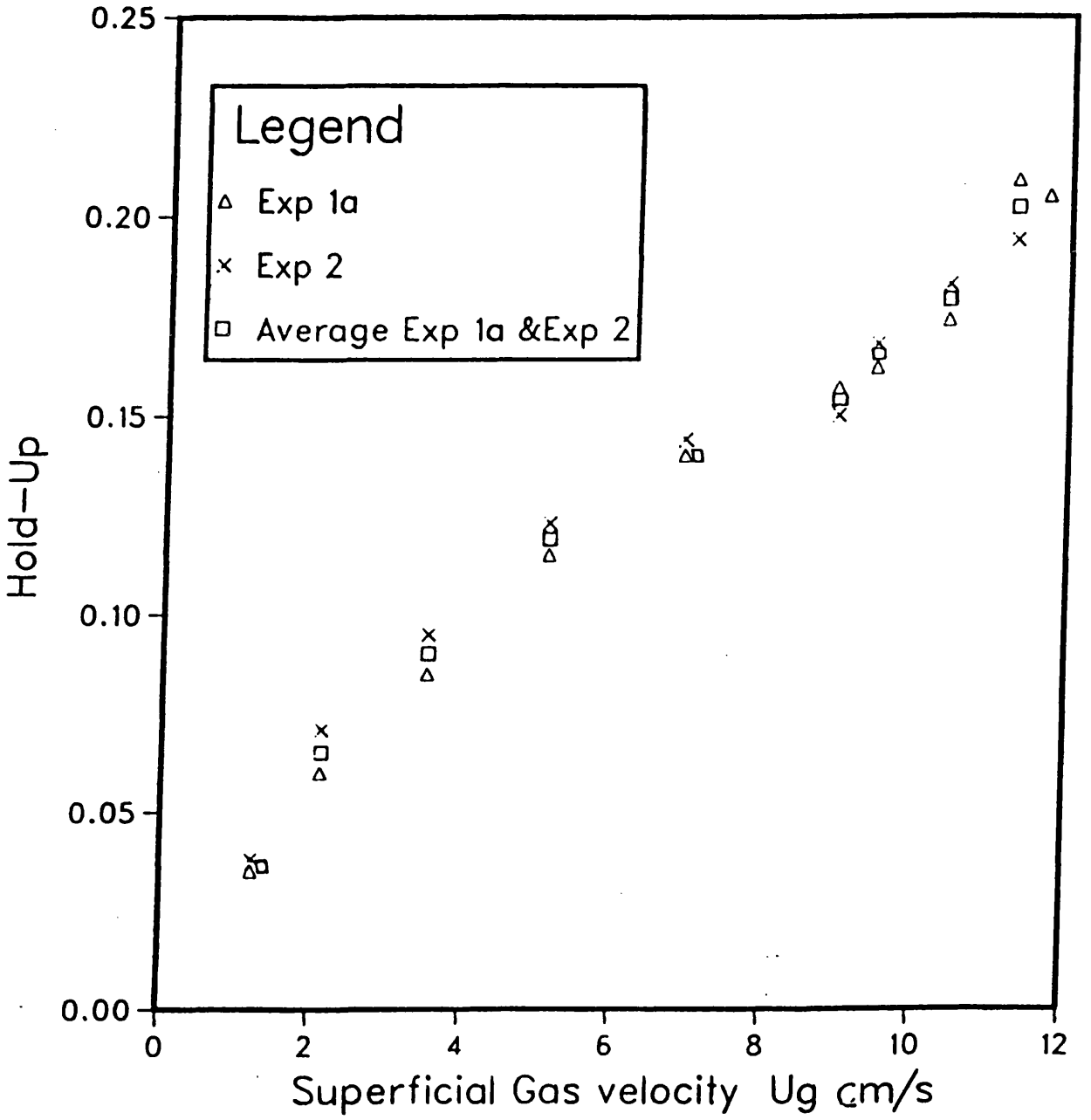

Figure 4.2. - Average gas hold-up variation with superficial gas velocity for a water height of 60 cm, temperature 17 -18 ^{o}C. Distributor used 57a.

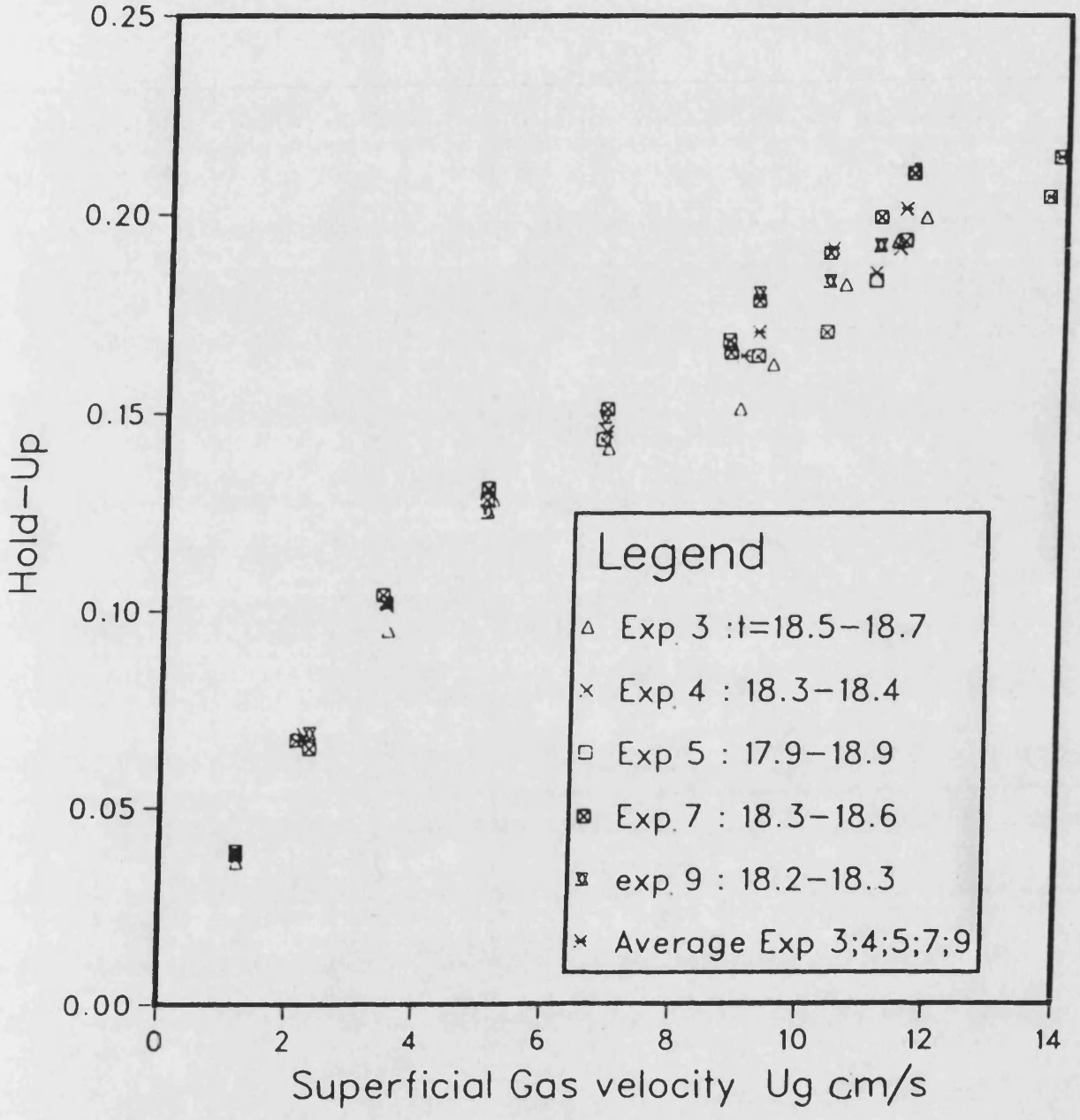

Figure 4.3. - Average gas hold-up variation with superficial gas velocity for a water height of 90cm Temperature 17.9 - 18.7 ^{o}C. Distributor used 57a.

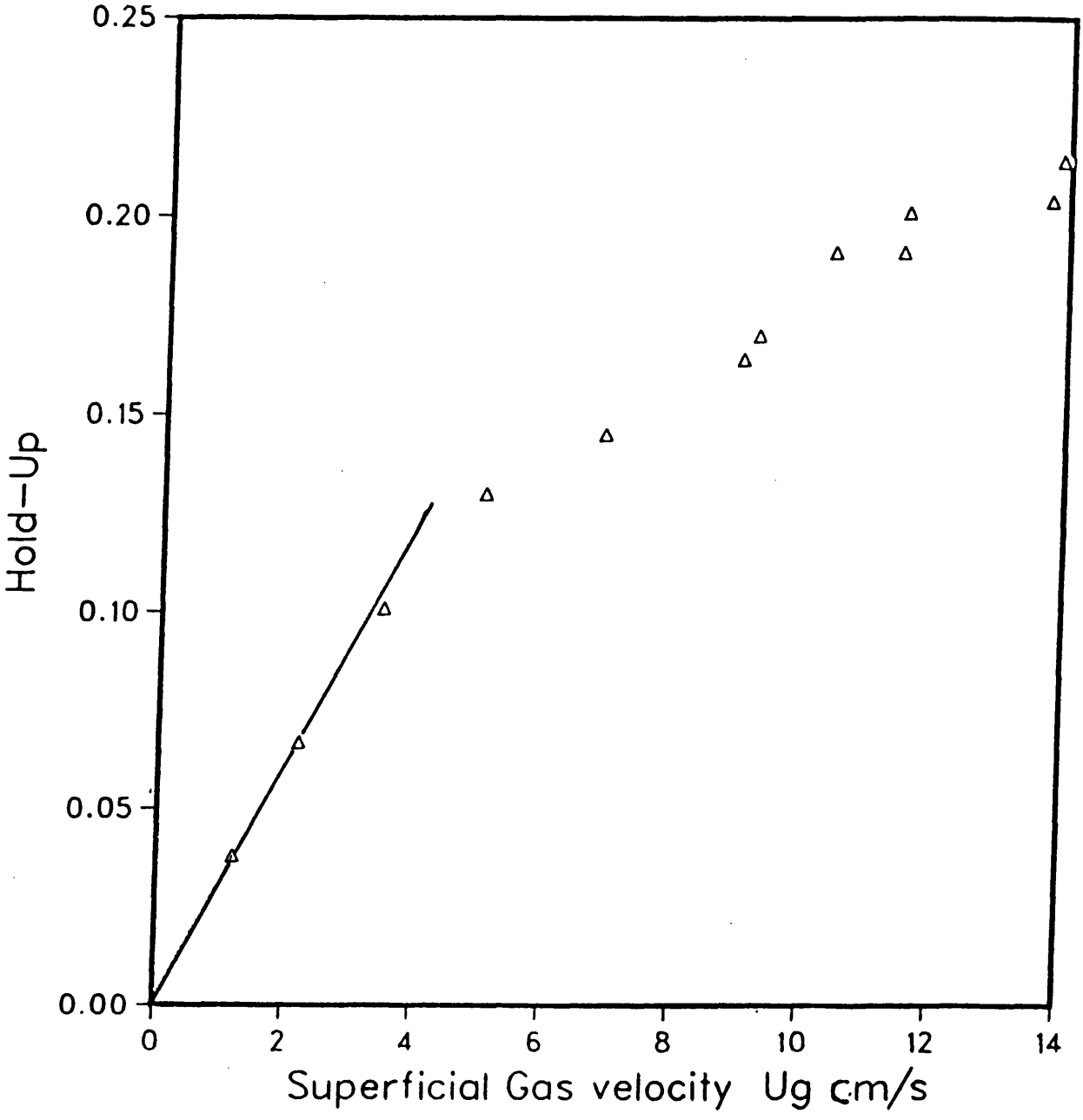

Figure 4.4.- Average gas hold-up variation with superficial gas velocity for a water height of 90cm , temperature 18.2- 18.7 °C. Distributor used 57a.

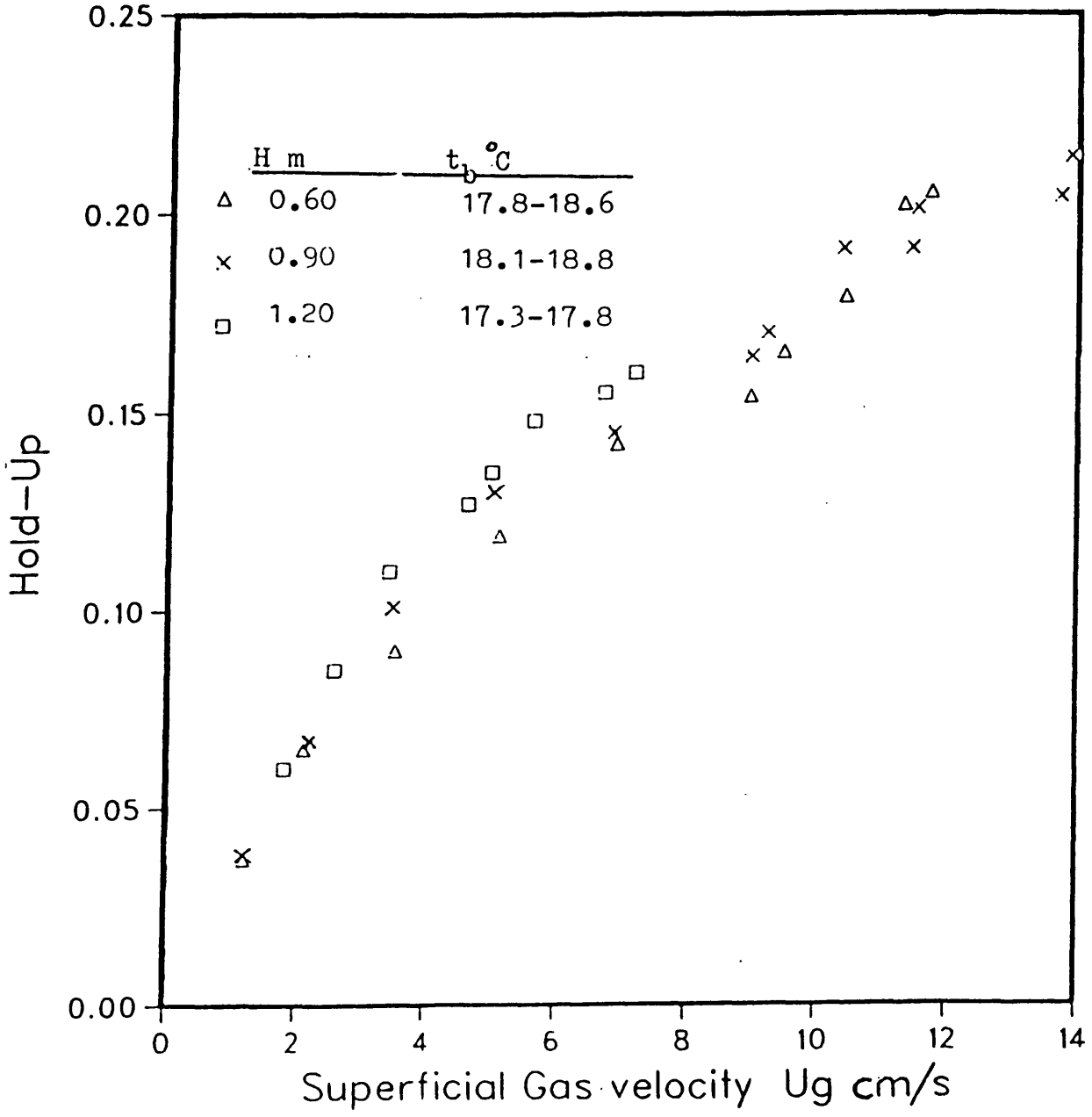

Figure 4.5.- Effect of water height upon average gas hold - up. Variation of gas with superficial gas velocity, temprature 17- 19 °C. Distributor used 57a.

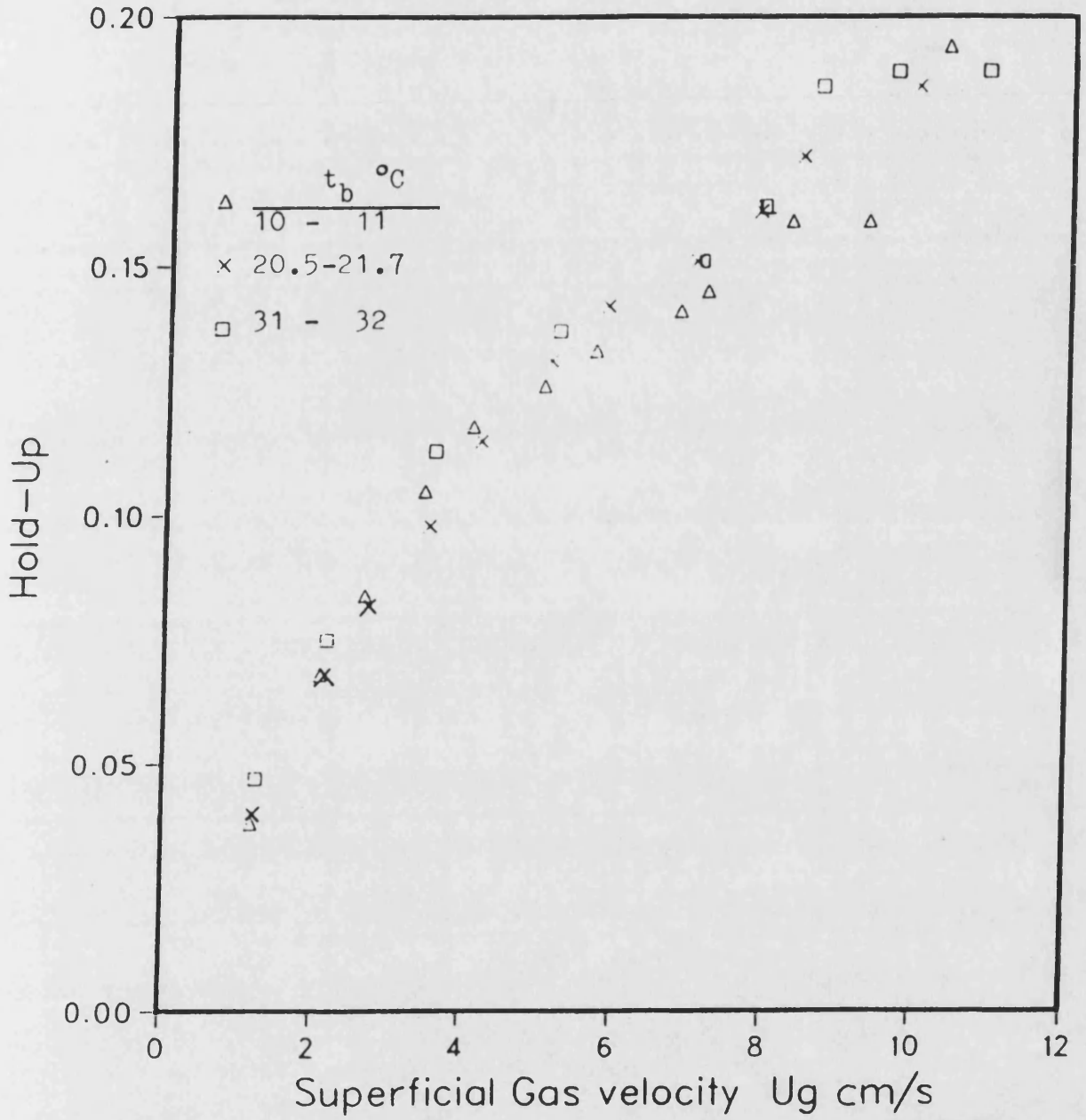

Figure 4.6.- Effect of water temperature upon average gas hold-up. Variation of average gas hold-up with superficial gas velocity for a water height of 90 cm . Distributor used 57c.

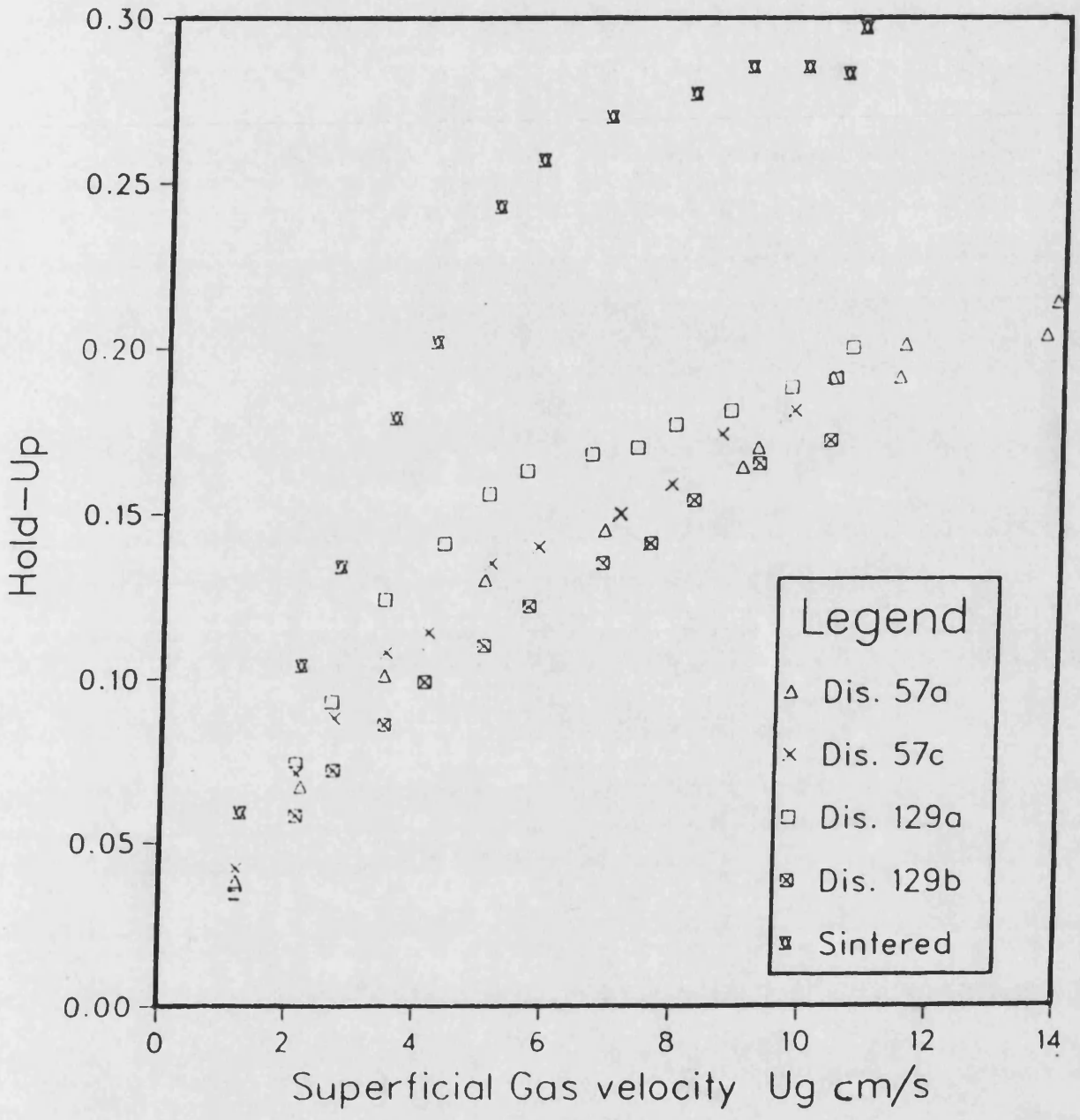

Figure 4.7.- Effect of gas distributor upon average gas hold-up . Variation of gas hold-up with superficial gas velocity for a water height of 90 cm, temprature 18.1- 18.8 ^{o}C.

Figure 4.8.- Photograph of bubbles . Scale 3:2
Sintered plate used. U_g= 12 mms^{-1} , hold-up= 0.06
aerated water height 65 cm .

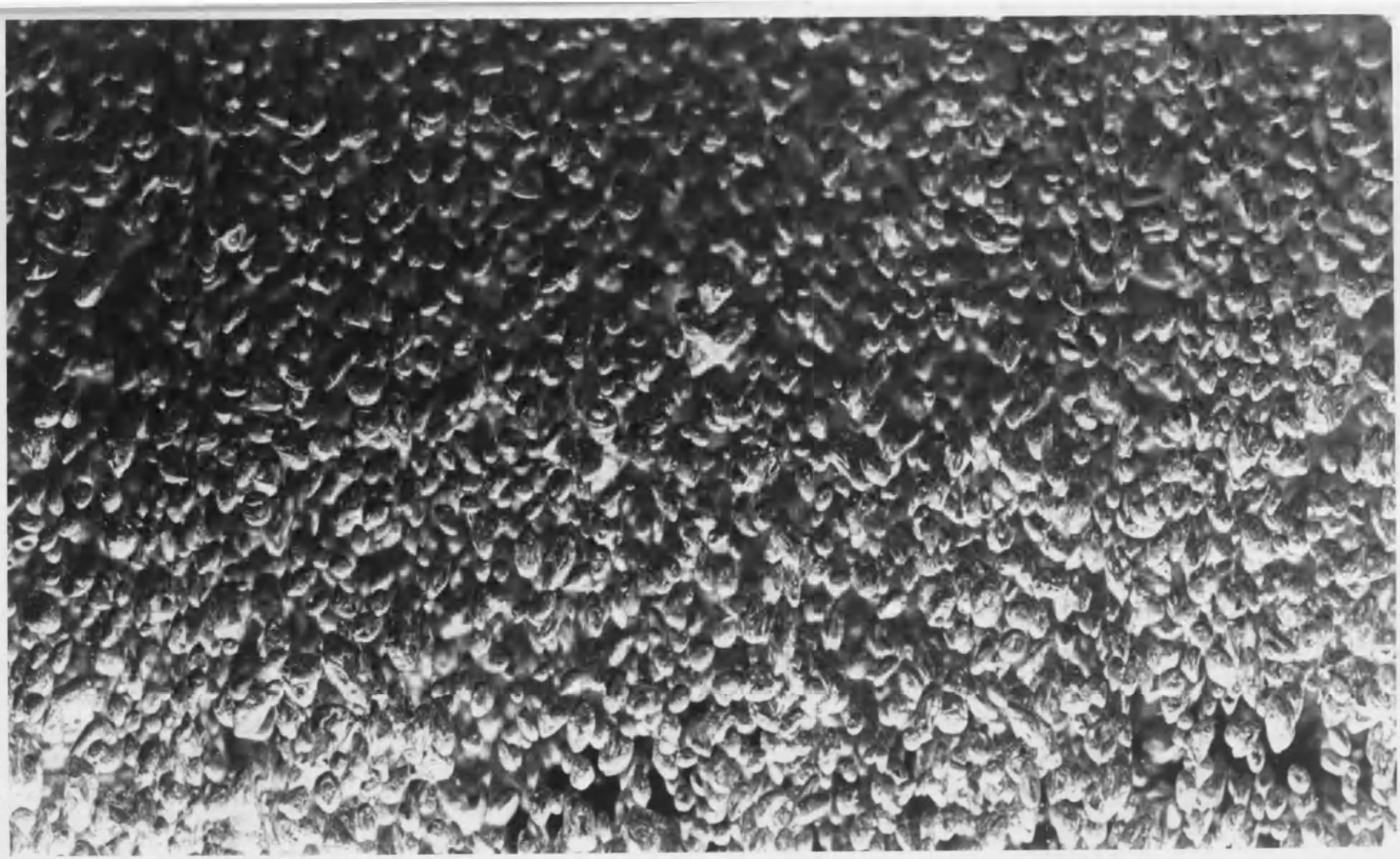

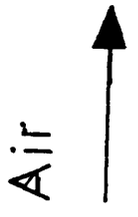

Figure 4.9.-Photograph of bubbles. Scale 3:2
Sieve plate used. U_g= 12 mms^{-1} , hold-up= 0.04
aerated water height 65 cm.

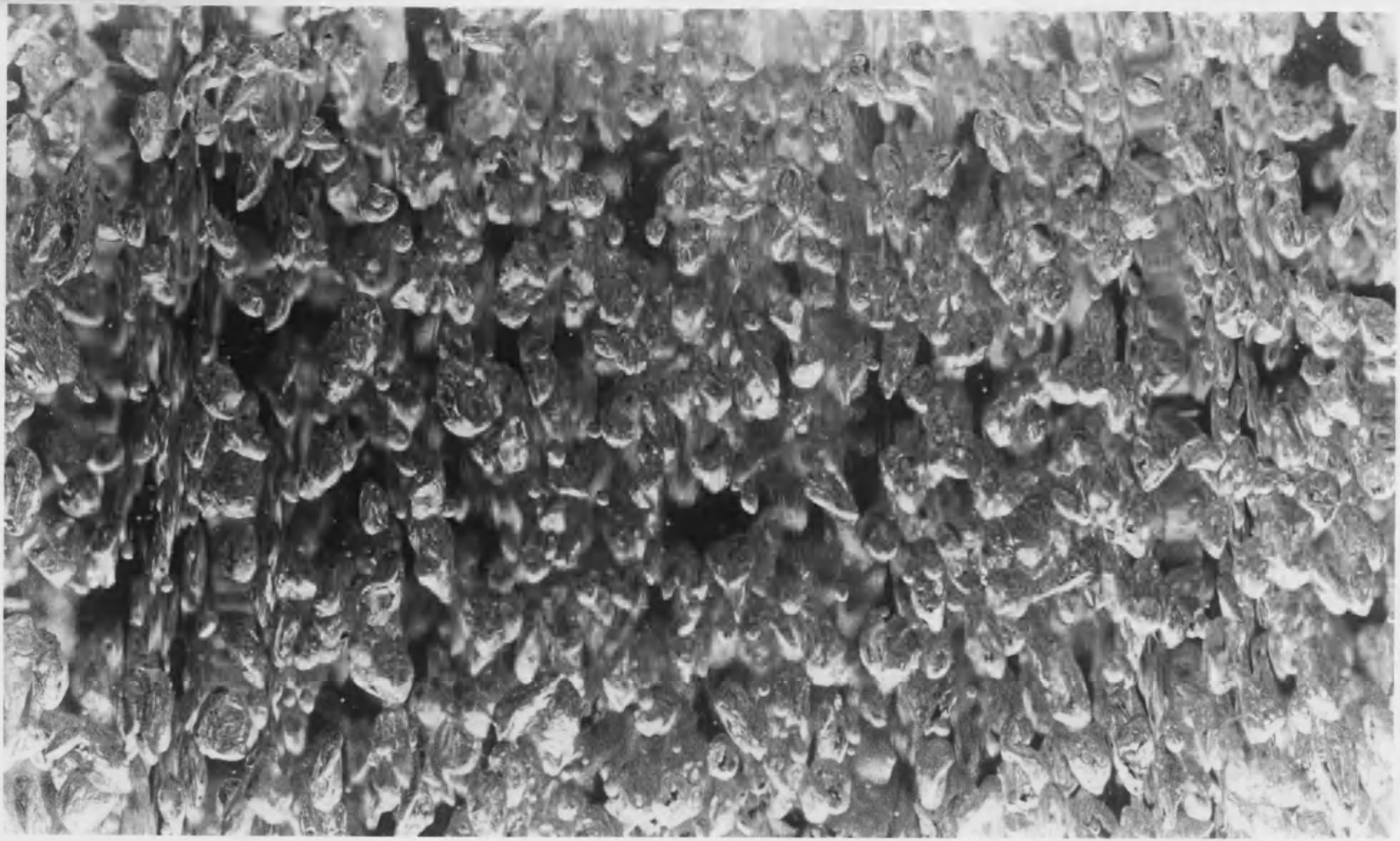

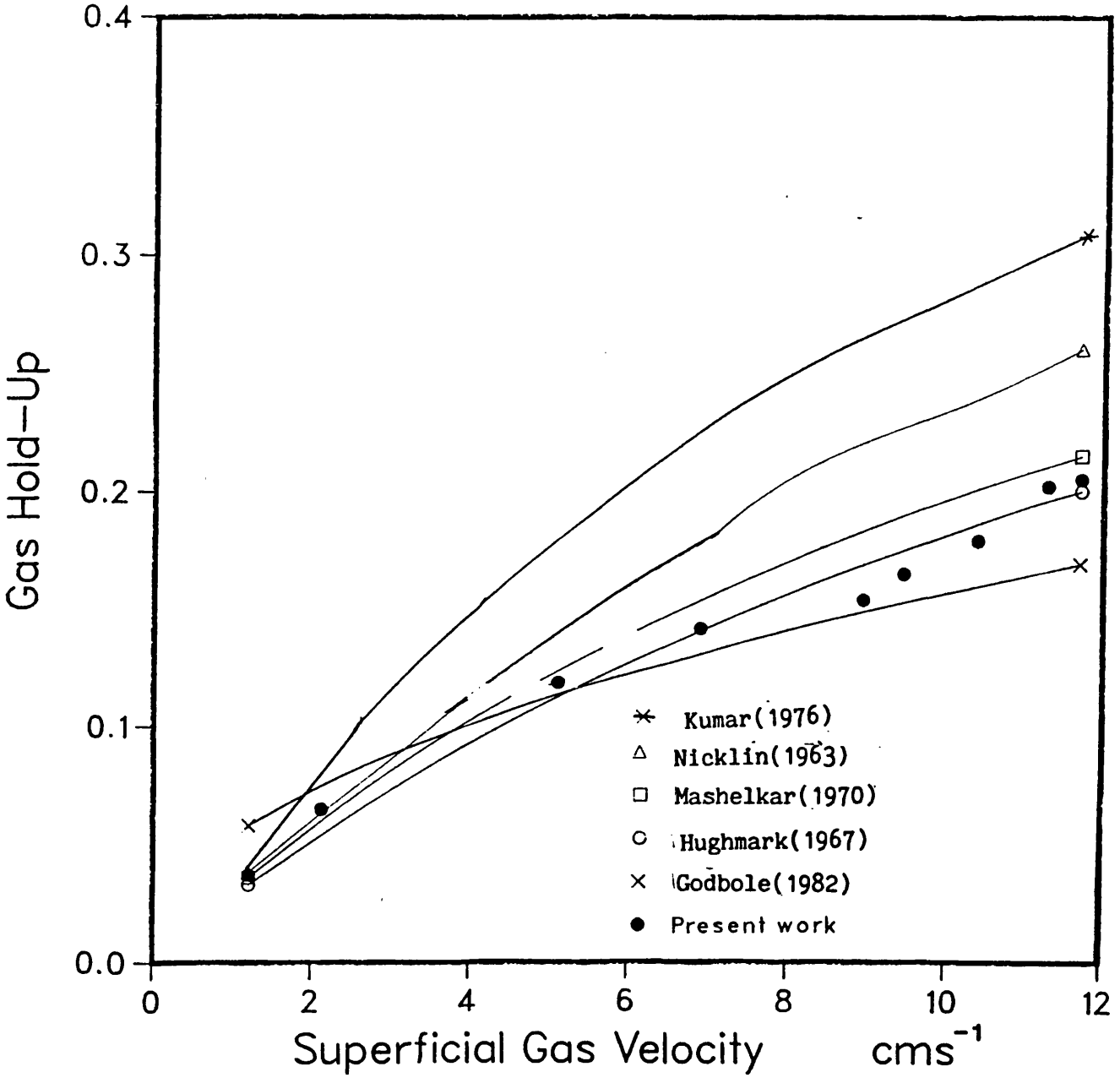

Figure 4.10.- Comparison of the predicted values of gas hold-up from several correlations with the experimental values. H= 60 cm. t_b=18 ^{o}C. Distributor used 57a.

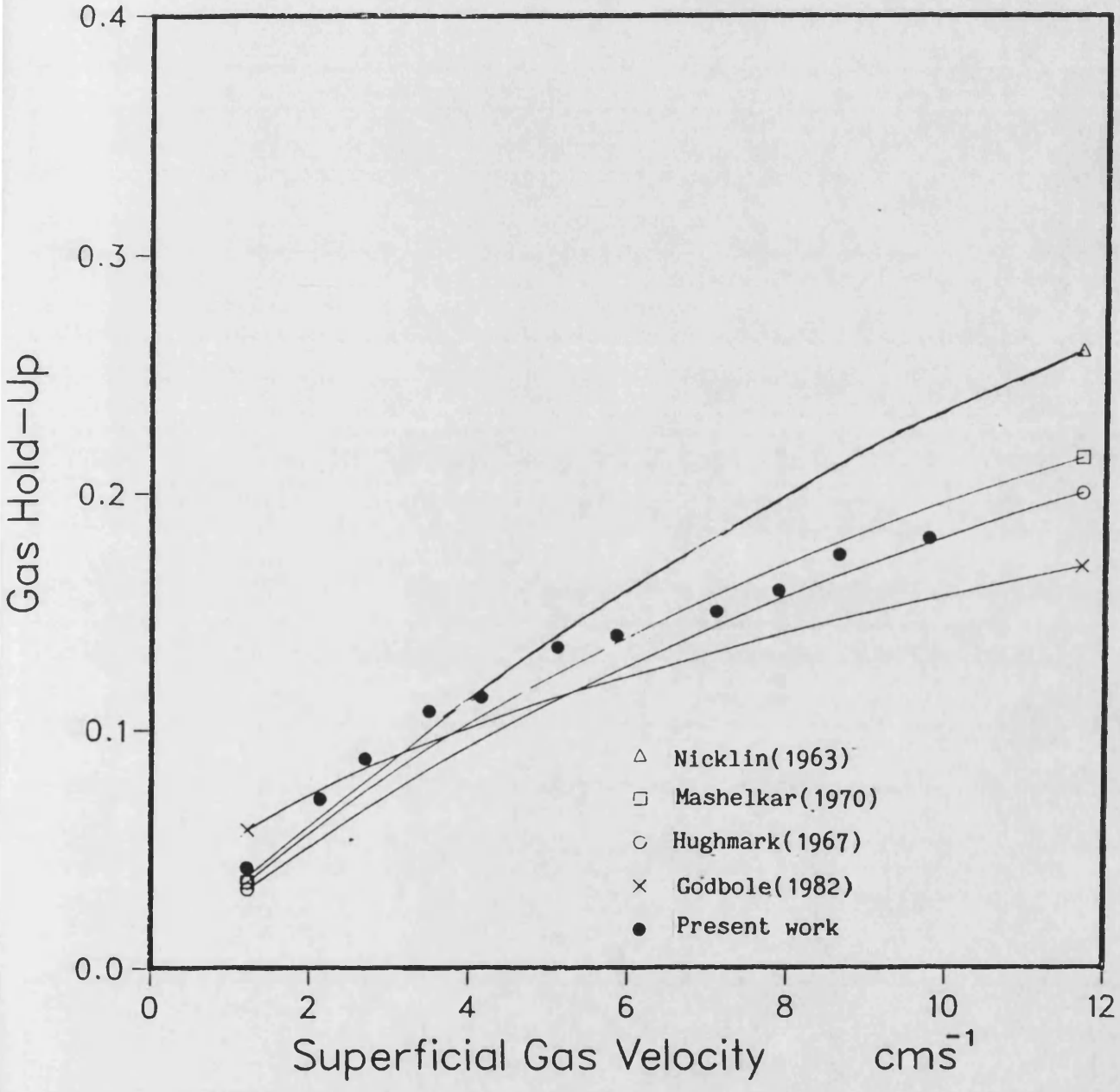

Figure 4.11. Comparison of the predicted values of gas hold-up from several correlations with the experimtntal values. H= 90 cm. t_b=18 ^{o}C. Distributor used 57c.

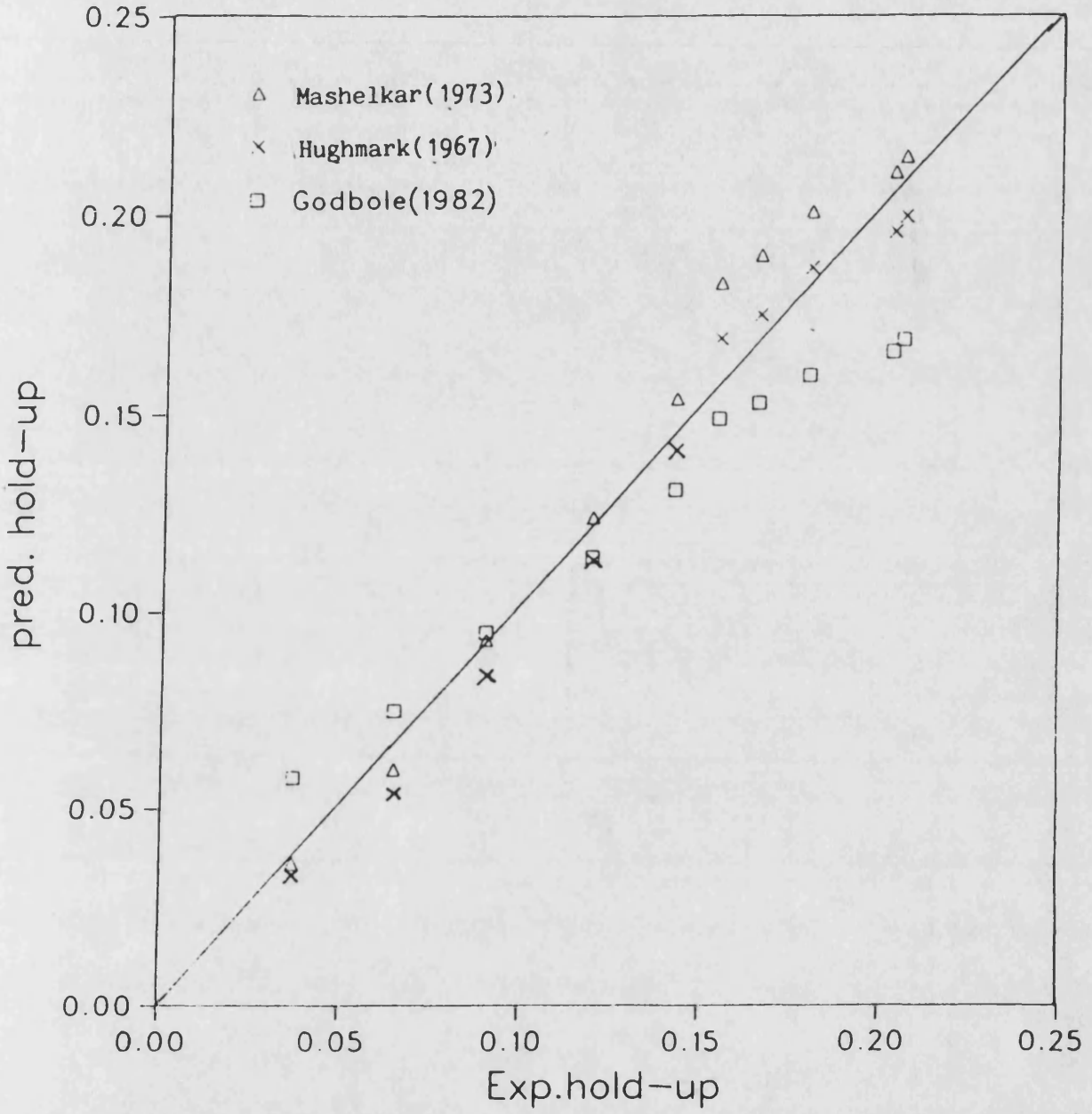

Figure 4.12.- Comparison of the predicted values of gas hold-up with the experimental values. H= 60 cm. t_b=18 ºC. Distributor 57a used.

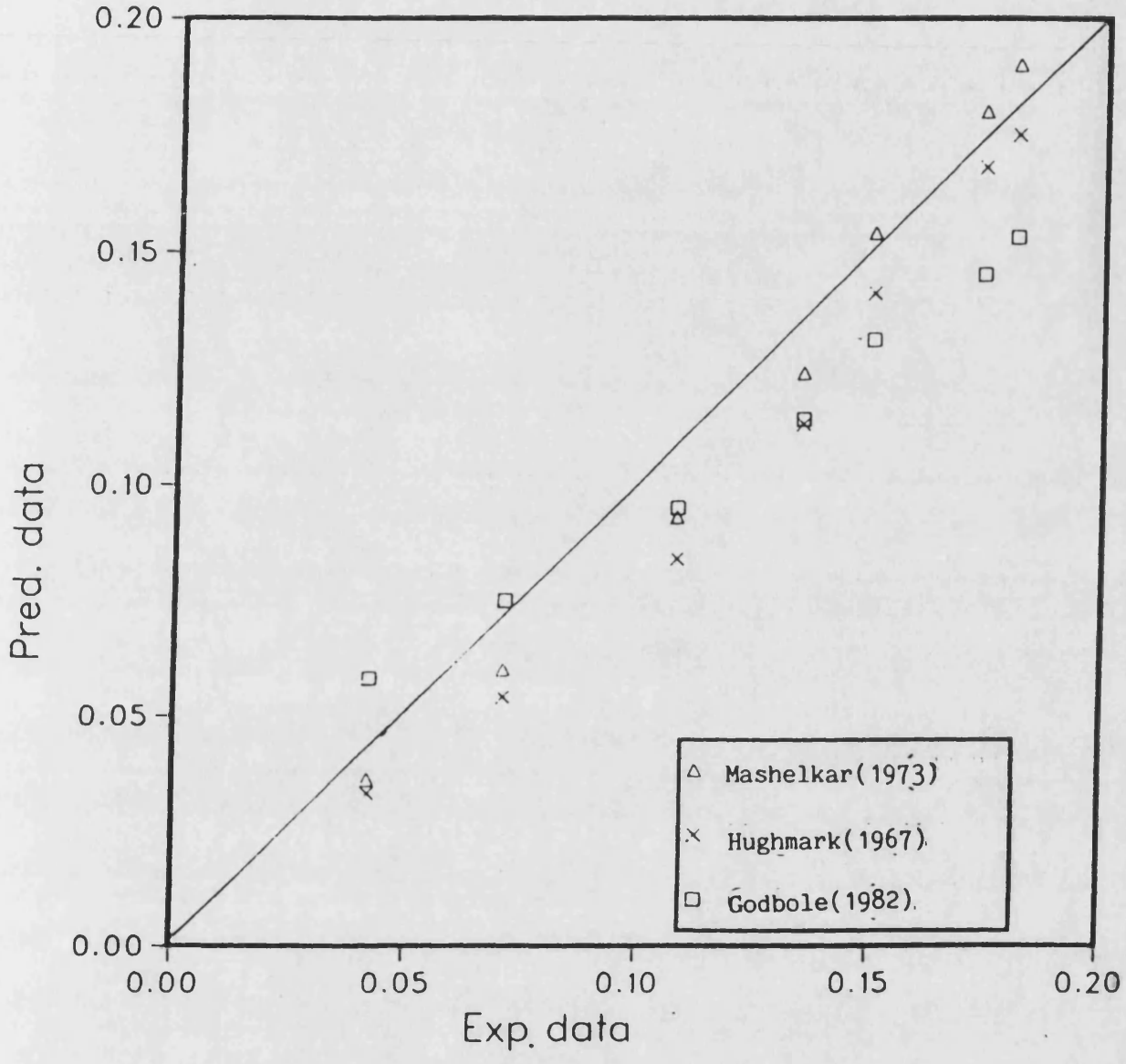

Figure 4.13.- Comparison of the predicted values of gas hold-up with the experimental values. H=90 cm. t_b= 18 ^{o}C. Distributor used 57c.

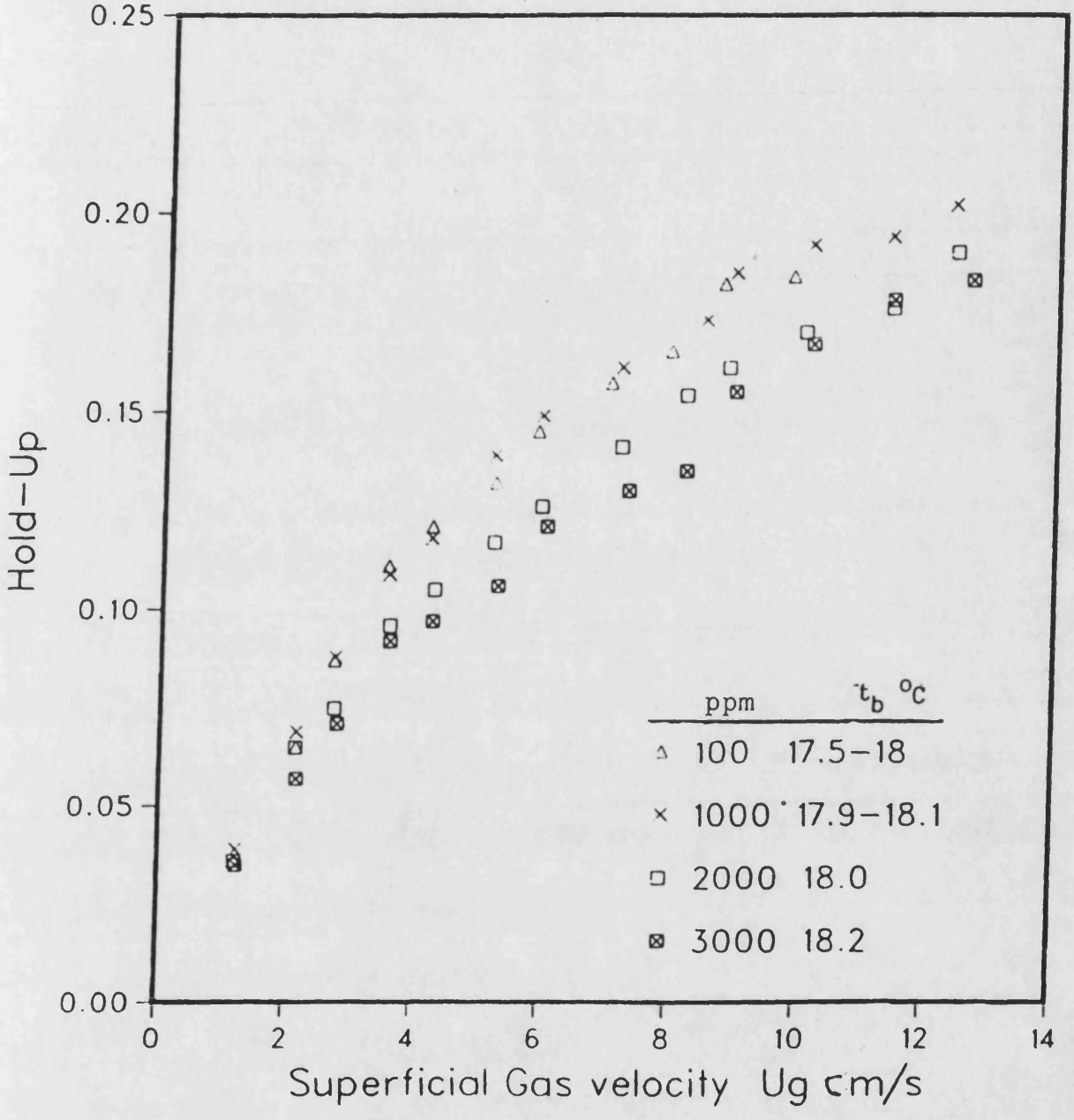

Figure 4.14.- Effect of concentration of CMC solutions upon gas hold-up. Variation of gas hold-up with superficial gas velocity for a water height of 90 cm, temprature 18 °C. Distributor used 57c.

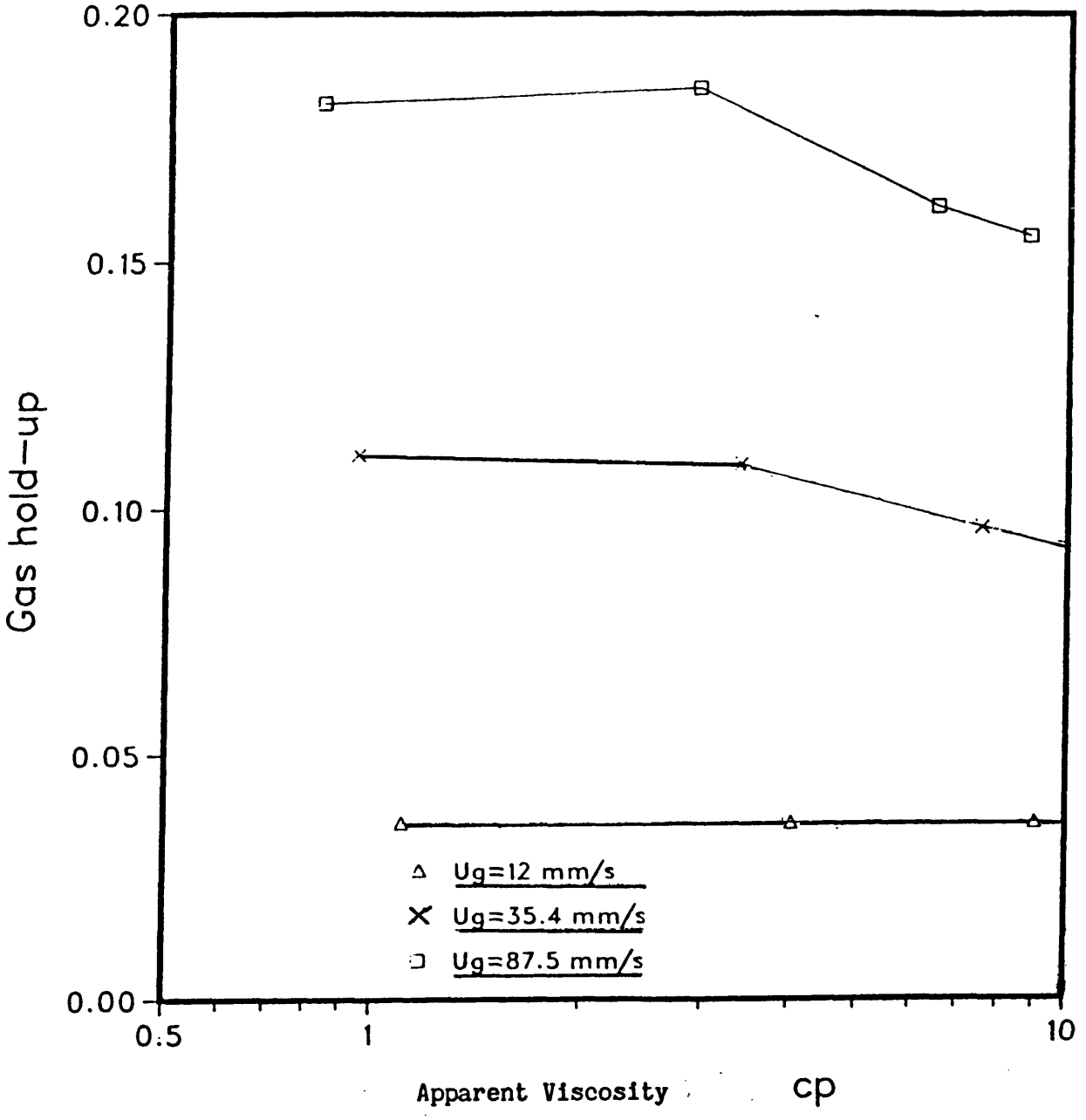

Figure 4.15.- Effect of viscosity on gas hold-up for CMC solutions Height of 90 cm, temperature 18 °C. Distributor used 57c.

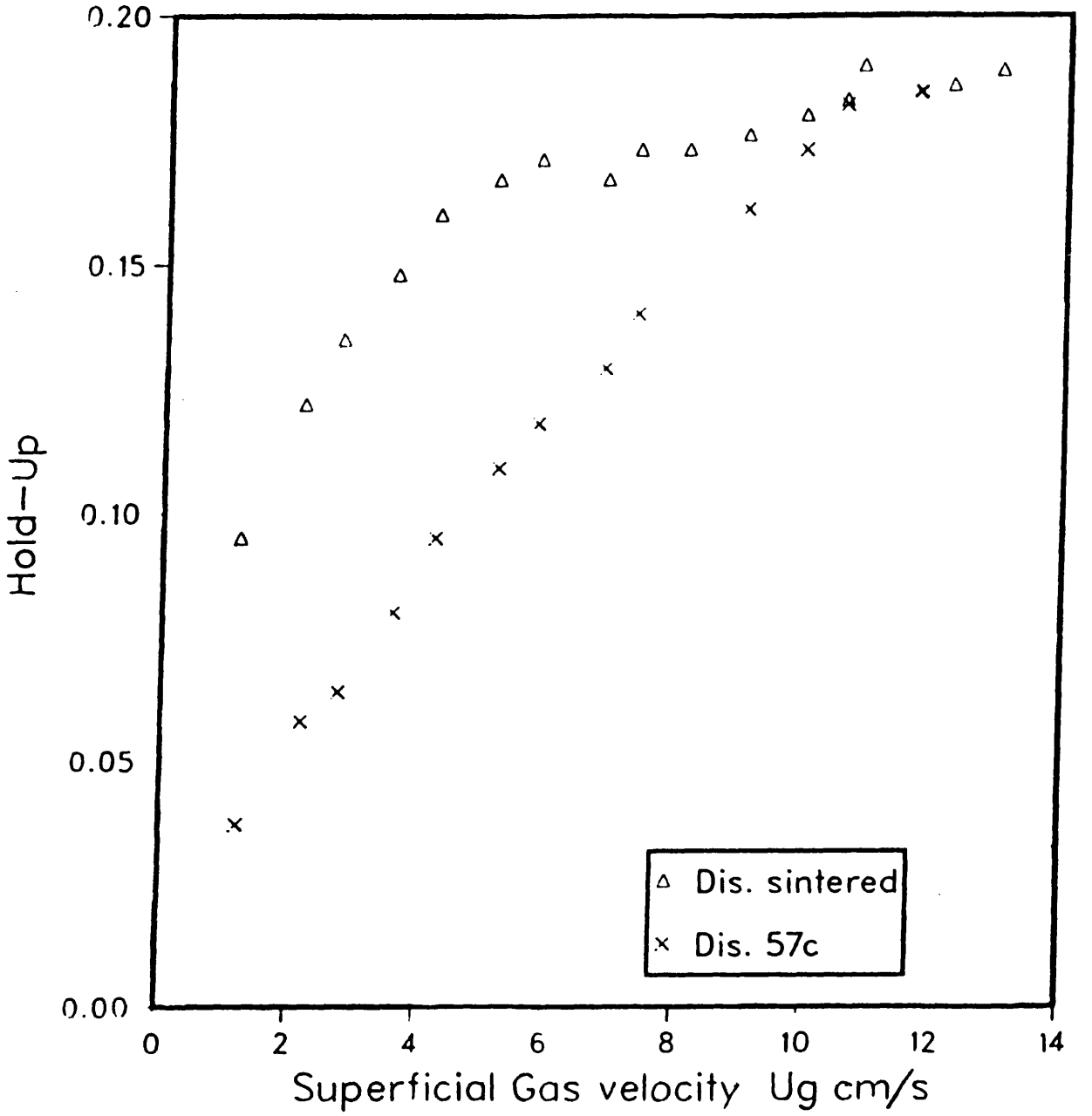

Figure 4.16.- Effect of gas distributor on gas hold-up. Variation of gas hold-up with superficial gas velocity for a 3000 ppm CMC solution height 90 cm, temperature 18 °C.

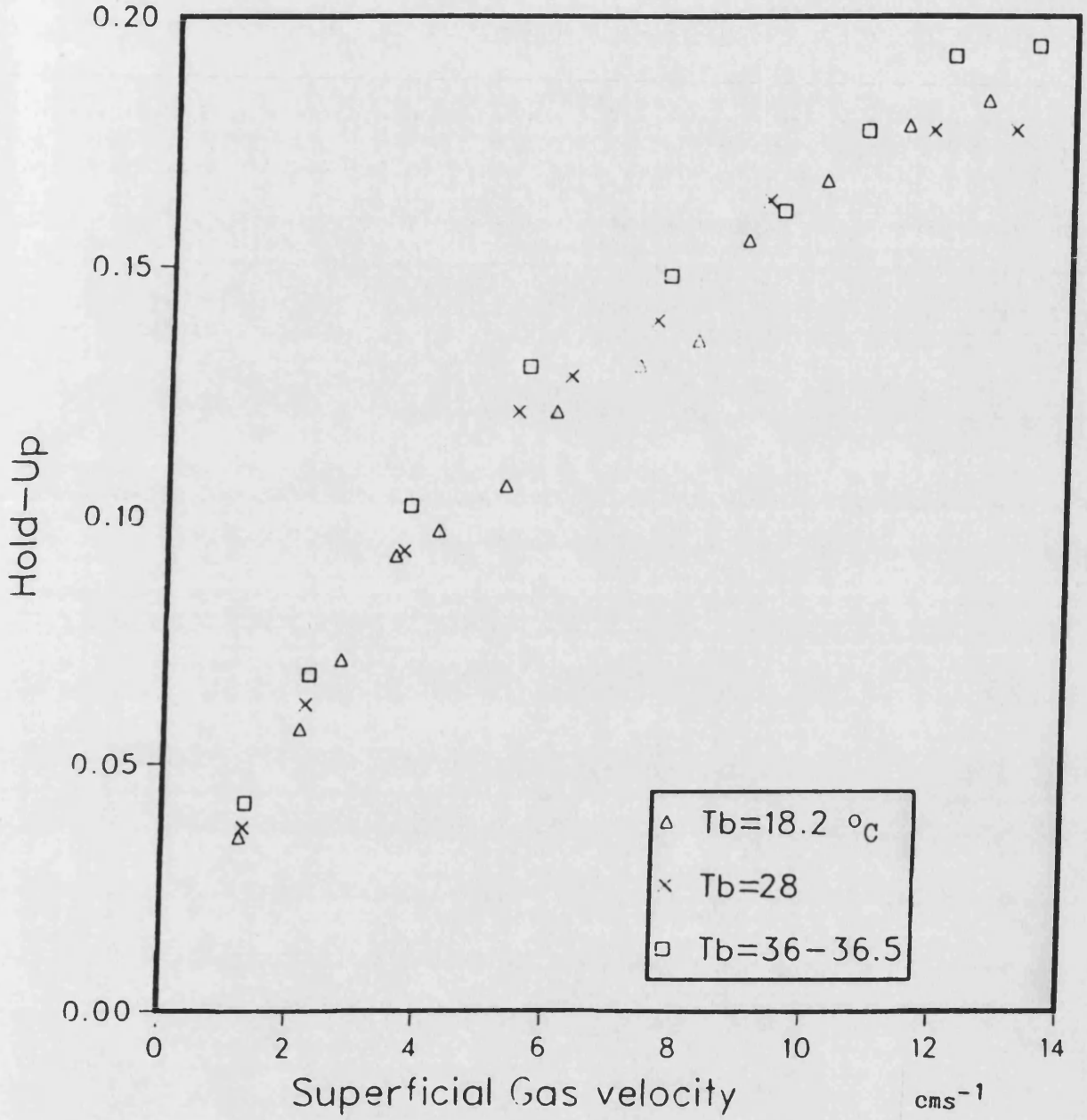

Figure 4.17.- Effect of bulk liquid temperature on gas hold-up. Variation of gas hold-up with superficial gas velocity for a 3000 ppm CMC solution height of 90 cm. Distributor used 57c.

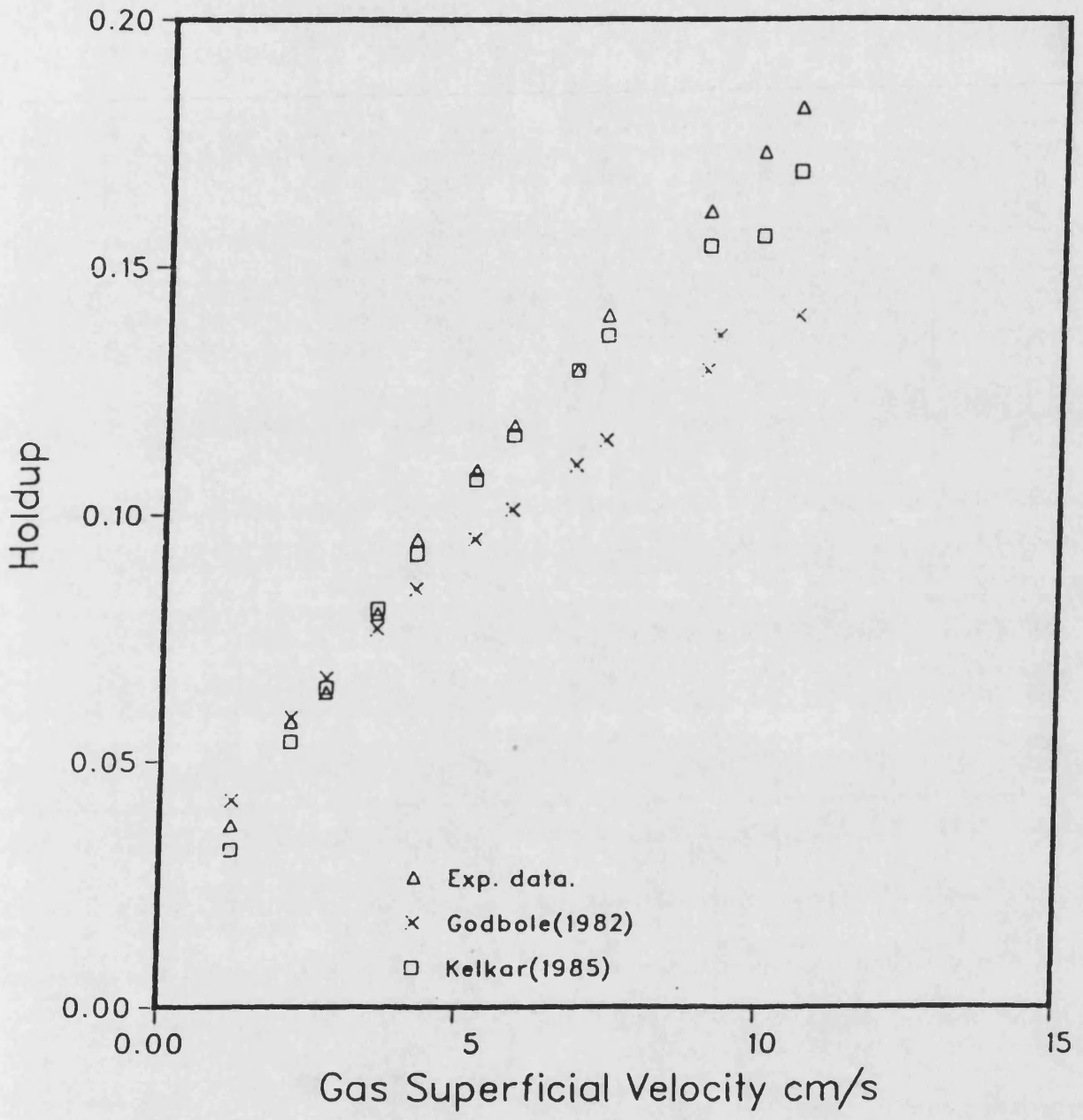

Figure 4.18.- Comparison of the predicted values of average gas hold-up from several correlations with the experimental values. Variation of gas hold-up with the superficial gas velocity for a 3000 ppm CMC solution height og 90 cm, temperature 18 ^{oC}. Distributor used 57c.

CHAPTER 5

HEAT TRANSFER FROM A SINGLE CYLINDRICAL HEATER

5.- Introduction.

The different parameters that have a direct effect on the value of the heat transfer coefficient in a bubble column can be classified as: gas throughput to the column, liquid height, distributor type, heater position in the column, heater dimensions and orientation, power input to the heater and liquid physical properties.

The results of the experimental investigations of the effect of those parameters on the heat transfer between a single cylindrical heater in a simple batch bubble column are presented below together with the relevant discussion and conclusion at the end of each section. However, the suitability of the theoretical heat trnasfer model developed in chapter 2 will be

tested for Newtonian and non-Newtonian fluid in chapter 7.

5.1.- EFFECT OF SUPERFICIAL GAS VELOCITY ON THE HEAT TRANSFER COEFFICIENT.

The variation of heat transfer coefficient and gas hold-up with the superficial gas velocity in the practical range of 10 to 100 mms^{-1} for both water and CMC solutions of 100 ppm to 10,000 ppm concentration are given in Tables 5.1 to 5.10. These data were obtained with a 30 by 60 mm heater being mounted at about 0.75 m from the 57c gas distributor plate on the column axis. The unareated liquid level was 0.9 m with the bulk liquid temperature 18 to 20 ^{o}C. Power input was 90 W.

The dependency of heat transfer coefficient, h, upon superficial gas velocity, U_g, in a power law form for water and CMC solutions are presented in Table 5.11. The water data shows that a lower index is applicable at gas superficial velocity above 50 mms^{-1}. This correspond to the transition from the bubbly flow regime to the churn-turbulent regime. The index value of 0.19 was also reported by Lewis et al (1982). It remains constant for all but one of the different type of gas distributor plate used as indicated in Figure 5.1(a) which is a log-log plot of heat transfer coefficient against superficial gas velocity. The exception is distributor 129b which was designed to produce an asymmetric bubble cloud. Further discussion on the

effect of the gas distributor plate on the heat transfer coefficient will be given in section 5.3, but it is noted at this point that there is only a minor influence of the distributor type on the heat transfer coefficient when the distribution of gas at the base of the column is even. Kubie (1974) and Lewis et al (1982) also reported that the distributor effect was negligible.

The index of superficial gas velocity in the range of 10 to 100 mms^{-1} for water data were found to be 0.24 which is close to 0.25 as repoted by Fair(1962), Hart(1976), Kolbel(1960), Nagata et al(1975) and Deckwer(1980).

Data for CMC solutions for Ug in the range of 10 to 100 mms^{-1} shows that the increase of CMC concentration, in general, have resulted in an increase of the U_g index from 0.24 to an average of 0.27.

For CMC solutions the apparent viscosity is a function of shear rate which in turn depends on the gas flow rate. Higher gas flow rate will give higher shear rates and hence a lower apparent viscosity. This will also result in a higher heat transfer coefficients. This effect is apparent from the closeness of the index of Ug in the gas superficial velocity range of 10 to 50 mms^{-1} and the 50 to 100 mms^{-1}. The index on Ug for CMC solutions given by Nishikawa et al (1977) was 0.25.

The variation in the index on superficial gas velocity due

to change in the flow pattern suggests that a simple power law relationship between heat transfer coefficient and superficial gas velocity is not appropriate and that a more complex model should be envisaged. This will be tried in chapter 7.

5.2.- EFFECT OF LIQUID HEIGHT ON THE HEAT TRANSFER COEFFICIENT.

Whilst Kubie (1974) reported that the heat tranfser coefficient in bubble column is independent of liquid height, Mersmann (1977) in a comparison of the heat transfer data of several investigators proposed that the difference in data were due to the different Heater Length employed by the investigators. Also, the theoretical model developed by Lewis et al (1982) required that the heat transfer coefficient to be a function of liquid height. However, this was not tested. In view of these conflicting results heat transfer data were obtained for aspects ratios of 2, 3 and 4.

Figures 5.2 to 5.5 shows that the variations of heat transfer coefficient with superficial gas velocity at water height of 0.60, 0.90 and 1.20 m. The relative position of the heater is roughly constant at 75% of the unareated water height, except for Figure 5.5(b) where the heater positin was constant at 0.75 m above the distributor plate. The result that are shown in Figures 5.2 and 5.3 are for a vertical heater 120 mm long, whilst results of Figures 5.4 and 5.5 are for vertical heaters 60mm and 30 mm long, respectively. In all cases heater diameter

was kept constant at 30 mm. Distributors were type 57a for data of Figure 5.2 and Figure 5.7, type 129a for data of Figure 5.3 and type 57c for data of Figure 5.4.

Figure 5.2 and Figure 5.3 shows that heat transfer coefficient for a liquid depth of 0.60 m is lower than that for water heights of 0.90 and 1.20 m at a constant superficial gas velocity. At a gas superficial velocity of 12 mms^{-1} the heat transfer coefficient for a water height of 0.60 m is about 6% lower than of both a 0.90 m and a 1.20 m water height. The heat transfer coefficient for 0.90 and 1.20 m water heights are about the same. As the superficial gas velocity was increased this pattern remained virtually constant, until a superficial gas velocity of 80 mms^{-1} above which the difference in the heat transfer coefficient for a 0.60 and 0.90 m water heights increased to about 10%.

Figure 5.4 which gives heat transfer coefficient (obtained with a 30 by 60 mm heater) for water heights of 0.9 and 1.20 m is consistant with the 30 by 120 mm heater and there is no noticeable height effect.

The results in Figures 5.5(a) and 5.5(b) are somewhat anomalous and under certain conditions the effect of liquid depth can be noticed at the aspect ratio of up to 4.

The data of Figure 5.5(b) which were obtained with the 30 by 30 mm heater and the 57a distributor clearly shows that heat

transfer coefficient is about 15% higher for a water height of 1.20 m when compared with a water height of 0.90 m. These data are for the heater position of 0.75 m from the distributor plate.

Similar results were obtained, as shown in Figure 5.5(a) for the heater position at 75% of the unaerated water height of 1.20 m, that is 0.90 m. Comparison of Figure 5.5(a) and 5.5(b) thus shows that an increase of HEATER HEIGHT from 0.75 to 0.90 m from the distributor plate, for water of height 1.20 m does not show a noticeable effect on the heat transfer coefficient. (See section 5.4 on the effect of heater position in the column).

Although no satisfactory explaination for this anomalogy has been found it is clear that bulk of data (Figures 5.2 to 5.4) suggest that the heat transfer coefficient is independent of the liquid height once the liquid level is above 0.90 m. This corresponds to an aspect ratio of 3. These figures also shows a modest increase in the heat transfer coefficient of about 5% as the aspect ratio is increased from 2 to 3 or 4.

Both of these observations could be explained by the hydrodynamic models of Field and Davidson (1980) and Joshi and Sharma (1979). Field and Davidson's model which is generally only important at low aspect ratio (Chapter 2,section 2.1.2.1) indicate that the average liquid circulation velocity is proportional to $H^{1/3}$ and hence from equation 2.23 or 2.25 in combination with the heat transfer model, equation 2.39, the heat transfer coefficient is approximately proportional to $H^{0.167}$

This gives an increase of 7 and 12% in the heat transfer coefficient as the liquid level is increased from 0.60 to 0.90 and 1.20 m, respectively. However, the relatively constant observed variation of heat transfer coefficient with the height of liquid for liquid levels of 0.90 and 1.20 m could be explained by Joshi and Sharma multistage circulation cell model (represented by equation 2.24.) which is independent of liquid height. The corollary is that the heat transfer coefficient is predicted to be independent of liquid height.

Thus overall, taking in to account the work of others it is concluded (a) that the effect of liquid depth on the heat transfer coefficient is a modest one that for practical purposes can be neglected particularly when the aspect ratio is greater than 3 and (b) that the circulation cell model of Joshi and Sharma is probably a better representation of the hydrodynamics when the aspect ratio is greater than 3.

5.3.- EFFECT OF GAS DISTRIBUTOR TYPE AND GAS HOLD-UP.

5.3.1.- Effect of Gas Distributor Type.

Experiments were conducted to measure heat transfer coefficient as function of superficial gas velocity with a number of distributor plates. This effect have been investigated by many workers such as Kast (1963) and Kubie (1974) but the reported conclusions were for a Newtonian fluids, whereas in

this work the effect of sieve plates and a sintered plate on the heat transfer coefficient for aerated 3000 ppm CMC solution is also reported.

Table 3.2 detailed the characteristics of the distributors. Experimental data were obtained for water and a CMC solution of approximately 3000 ppm, with an unaerated height of 0.90 m. The heaters were mounted vertically on the columns axis 0.75 m above the distributor plate.

Experimental results which are ploted in Figure 5.1(a, b) and Figure 5.6, shows variations of heat transfer coefficient against superficial gas velocity for water and CMC solutions with the employed distributor plates as the third parameter.

It is apparent from Figure 5.1 (a, b) that the heat transfer coefficient for water obtained from employing distributor type 129a, 57a, 57c and the sintered plate are on average only 10% different from each other at any constant gas superficial velocity.

Heat transfer coefficient with the 129b distributor (which was designed to give uneven aeration) are higher than that obtained with the other distributor, whilst at the same time it gives lowest gas hold-up (See Figure 4.6).

The effect of 129b distributor on heat transfer is more

enhanced at the lowest gas superficial velocities. At low gas superficial velocity mal-distribution of gas causes the lateral variation of gas hold-up to be significant and hence a higher circulation of liquid is generated. However, due to the greater agitation at higher gas velocities the lateral variation of gas hold-up diminishes and therefore the average liquid circulation veloctity approaches that obtained with an even distribution of gas at the distributor plate.

Figure 5.6 presents data of heat transfer coefficient for the CMC solutions against superficial gas veloctiy for both the sintered and the 57c distributor. Both of these distributors gave an even distribution of gas at the base. It is apparent that at superficial gas velocities less than 40 mms^{-1} the heat transfer coefficient for the sintered plate is about 15% lower than that of sieve plate. This is attributed to the smaller bubble size that was observed whilst the sintered plate distributor was in the region of bubbly flow. As the gas velocity was increased above 40 mms^{-1} heat transfer coefficients for the sieve and sintered plate approach each other.

5.3.2.- Effect of Average Gas Hold-Up.

As both gas hold-up and heat transfer are function of several variables (such as physical properties, flow rates and to a certain extent the distributor type) the experimental investigation of the effect of gas hold-up is a cumbersome task, because one does not have direct control over the gas hold-up. It

is anticipated that the influence of gas hold-up on the heat transfer coefficient be small. Therefore to see the effect of gas hold-up on the heat transfer coefficient high gas hold-up was produced by using a sintered plate distributor. This distributor plate produced 50% higher gas hold-up values compared with the sieve plate distributors. This is evident from Figures 4.6 and 4.13 which are plots of gas hold-up against superficial gas velocity for water and CMC solutions. One of the principal aims of this section of the work, however, was to establish the limitations of the approach of Ruckenstein and Smigelschi (1965) and Chen (1987) who suggested that any increase in gas hold-up will lead to an increase in heat transfer coefficient.

It is clear from Figure 5.1 (a) that the heat transfer coefficients obtained for water with the sintered plate distributor are higher than the heat transfer coefficients obtained with the 57c distributor plate at gas velocities higher than 50 mms^{-1}. These in turn are higher than those obtained with the 57a distributor plate. This ordering is not, however, mirrored by the hold-up variation. Whereas Figure 4.7 shows that gas hold-up obtained with the sintered plate is higher than both that of 57a and the 57c distributors, the gas hold-up data of those distributors are almost equal.

Also a comparison of Figures 4.16 and 5.6 for 3000 ppm CMC solutions shows that whilst at low gas velocity the sintered plate gives a higher gas hold-up than the 57c, the heat transfer coefficient is actually lower than that obtained with the 57c

distributor.

The effect of gas hold-up on heat transfer coefficient ,however ,can partly be explained by the energy balance model for liquid circulation in bubble column (see section 2.1.2.). Since higher gas hold-up means higher energy dissipation in gas-liquid interficial area ,therfore less energy will be available for liquid circulation . This in turn will cause less heat transfer.

The liquid circulation velocity that was given in section 2.1.2.1,equations 2.25 and 2.26, shows that the liquid circulation increases with the increase of gas hold-up. Therefore , it is apporopriate to suggest that the constants involved, 1.36, 1.31 and n, are functions of the dimension of the column and the liquid circulation intensity , respectively. The latter in turn is a function of gas distribution.

Ruckenstein and Smigelschi (1965), Kubie (1974) and Lewis et al (1982) used the gas hold-up in their correlations whilst almost all others investigators did not consider the direct effect of gas hold-up on the heat transfer coefficient.

Kubie's relationship which was obtained from dimensional analysis consideration suggested that the heat transfer coefficients is proportional to $(1- \epsilon)$. Whilst in general it is inappropriate to propose a single relationship between heat

transfer and gas hold-up, under those conditions where the circulation intensity constant, n, is fixed a simple relationship may well exist. This was investigated through a development of the equation given by Ruckenstein and Smegilschi, equation 1.29.

Field and Rahimi (1987) have shown that it can in dimensionless form be written as

$$St = A\epsilon^{0.33} (Re\ Fr\ Pr^2)^{0.33} \qquad \ldots 1.30$$

This suggest that the heat transfer coefficient is porportional to. $\epsilon^{0.33}$ and independent of any other term which is dependent on the superficial gas velocity, U_g. This was tested for a number of heat transfer data for water at ambient temperature by Field and Rahimi(1987) as presented in Figure 5.7. Figure 5.7 which is a plot of $h.\epsilon^{-0.33}$ against ϵ for water at ambient temperature, shows that with the exception of the data of Ruckenstein and Smigelschi the resuls are in good agreement. Further test of the relationship was carried out with data for aerated water at high temperature good agreement as shown in Figure 5.8 was found.

To see if the $h \alpha \epsilon^{0.33}$ was applicable for the CMC solutions the data were analyzed. The results are presented in Figure 5.9 and Table 5.12. Figure 5.9 is a plot of $St(ReFrPr^2)^{0.33}$ against ϵ on a logarithmic scale using apparent viscosity to calculate Reynolds, Re, and Prandtl, Pr,

numbers. Whilst Table 5.12 gives coefficient and index of gas hold-up for CMC solutions.

It is apparent both from Figure 5.9 and Table 5.12 that in the case of CMC solutions an equation of the form $St(ReFrPr^2)^{0.33} = A\ \epsilon^{0.33}$ is inappropriate. Taking the result as a whole the dependency is approximately $h \alpha \epsilon^{0.5}$. However, both the variation in the dependency of the gas hold-up and the variation in the coefficient, A, with concentration suggest that Ruckenstein and Smigelschi modelis not applicable in the case of power law fluids.

5.4.- EFFECT OF HEATER POSITION IN COLUMN.

The influence of the height of the heater above the distributor plate and its radial position were investigated for water. A modest amount of additional data for the CMC solution is also presented.

5.4.1.- Effect of Heater Vertical Position.

The experimental investigation of the effect of the vertical distance of the heater from the gas distributor was conducted with the heater mounted vertically on the column axis. Typical results are shown in Figures 5.10 to 5.12.

The air-water results given in Figure 5.10 and 5.11 show the variation of the heat transfer coefficient against heater

vertical distance from gas distributor at four superficial gas velocities of 12, 34, 50 and 88 mms^{-1}. The heater dimensions were 30 by 120 mm and distributor plate type 57a was employed. Data of Figure 5.10 are for a water of height 1.20 m, whilst data of Figure 5.11 are for water of height 0.90 m.

The air-3000 ppm CMC solution results presented in Figure 5.12 shows the variation of heat transfer coefficient against heater vertical position for the 30 by 60 mm heater. The liquid depth was 0.90 m and distributor 57c was used.

It is clear from Figure 5.10 and 5.11 that a difference between the heat transfer coefficients obtained at different vertical positions for any constant gas flow rates are only 7%. If the data obtained below 1.5 column diameters and near the liquid surface are excluded the difference is reduced to about 4%.

Results obtained with CMC solutions as presented in Figure 5.12, also show that in the range 0.45 m (1.5 column diameter) to 0.90 m from the gas distributor, the variation in the heat transfer coefficient is less than 5%. Some experiments carried out with a heater of size 30 by 30 mm at superficial gas velocities of 12, 35 and 93 mm gave a very similar result. In the range of heater distance 1.5 column diameters to 3 column diameters from the gas distributor, the heat transfer coefficients varied by only 4%.

During these experiments the thermo- physical properties of the gas and the liquid remained constant. The vertical local gas hold-up increased with the distance from the base. The fact that the heat transfer coefficient is independent of vertical distance from base suggest that the heat transfer coefficient is only a weak function of voidage. This also justifies the use of average gas hold-up instead of local gas hold-up in the heat trasfer model.

Shykhudinove et al (1971) reported that the heat tranfser coefficient varies with the heater height. However this does not contradict the above conclusion because their experiments were carried out in a 0.476 m long by 0.048 m diameter bubble column (aspect ratio of 10) with a number of ring heaters at the column wall. Under these conditions they have reported the establishment of a temperature gradient along the column. This in turn changes the physical properties of the liquid phase and hence heat transfer coefficient. Thus overall it is concluded that apart from the entrance effects there is no or very little effect of vertical position as such. This agrees well with others such as Kolbel et al (1958) and Kubie (1974).

5.4.2.- Effect of Heater Radial Position.

The effect of heater radial position on the heat transfer coefficient in bubble columns were investigated for water of height 0.90 and 1.20 m. The 120 mm long by 39 mm diameter heater was employed. It was mounted vertically at 0.75 m from the 57a distributor plate. The heater radial positions were the centre,

0.5R and about 0.9R or 20 mm from the column wall as indicated in Figure 3.8 by points 9, 1 and 2, respectively. At different gas flow rates and the 3 heaters radial positions heat transfer coefficients were measured. The results are shown in Figures 5.13 (a, b) and 5.14 (a, b) for water height of 0.90 and 1.20m, respectively.

Figures 5.13 (a) and 5.14 (a) shows the variation of heat transfer coefficients against gas superficial velocity with heater radial position as the third parameter, whilst Figures 5.13 (b) and Figure 5.14 (b) show the variation of heat transfer coefficient against heater position at superficial gas velocities of 12, 34.9, 50 and 87.9 mms^{-1}.

It is evident from Figure 5.13 and 5.14 that the heat transfer coefficient is lower with the heater mounted near the wall. The reduction in the heat transfer coefficient was found to be about 15%. Field (1980) reported that for the heater being mounted at 0.6R the reduction in the heat transfer coefficient is about 7%.

Figure 5.13(a) shows that at low gas flow rates up to superficial gas velocities of 40 mms^{-1} heat transfer is about 14% higher for the heater at 0.5R compared with it being on the column axis. At larger values of U_g the heat transfer coefficient for the heater at 0.5R approaches that of a centrally mounted heater. Figure 5.14(a), however, exhibits a steadier trend. The heat transfer coefficient for the heater at 0.5R is

about 8% higher compared with the one on the column axis.

The modest increase in the heat transfer coefficients at 0.5R from the axis indicate that the maximum turbulance does not neccessarily lies at the column axis. In this regard it is interesting to note that the measurements of local gas hold-up, Table 4.1, showed that the gas hold-up is not at its highest value at the column axis.

Therefore provided that the heater is not near the wall region, it is concluded that at high gas flow rates, where fully churn-turbulent flow regime exists, heat transfer coefficient is independent of heater radial position and its dependency on radial position at low and moderate flow rates is not significant.

5.5.- EFFECT OF HEATER DIMENSION AND ORIENTATION.

Almost all investigators except Kubie (1974) and Lewis et al (1982) reported that the heat transfer coefficient is independent of the employed heater dimension. Kubie employed a wire size heater whilst Lewis et al used a cylindrical rod heater and found a limiting dimension above which heat transfer coefficient becomes independent of the vertical heater dimension. These observations were for low viscosity Newtonian fluids.

In the following sections, the validity of the Lewis et al

findings will be confirmed and, for the first time results for CMC solutions with an approximate concentrations of 100-3000 ppm and with apparent viscosity of 1 to 10 cP at superficial gas velocity of 50 mms^{-1} will be reported.

To investigate the effect of heater dimension and orientation on the heat transfer coefficient in a bubble column the 120, 60 and 30 mm long heaters were employed. The heater were 30 mm in diameter. The design was described in chapter 3 and is very similar to the Lewis et al heaters. Heaters were mounted at 0.75 m from the column base. The vertical heaters were on the column axis whilst the horizontal heaters were centrally placed along the column diameter. Unaerated heights of both water and CMC solutions were kept constant at 0.90 m and distributor types 57a and 57c were used.

For a specific heater length the variation of heat transfer coefficient with gas superficial velocity was measured. The results are shown in Figures 5.15 to 5.22. Table 5.13 shows the average difference between heat transfercoefficient for 30, 60 and 120 mm long heater.

5.5.1.- Effect of Heater Vertical Length.

Figure 5.15 and 5.16 show the variation of heat transfer coefficient with gas superficial velocity and heater vertical length for water. Data of Figure 5.15 and 5.16 were obtained with the distributor 57c and 57a, respectively. Both figures

show that the heat transfer coefficient for 30 mm long heater is higher than that of 60 or 120 mm long heaters, but from Table 5.13it can be seen that the average difference in the heat transfer coefficients is about 4% for data with 57a distributor (Figure 5.16) and it is about 15% for data with distributor 57c (Figures 5.15). Figure 5.15 and 5.16 also show that at low gas superficial velocities the heat transfer coefficients for the 120mm long heater are higher than for the 60 mm long heater, whereas at high gas flow rates heat transfer coefficients with 60mm long heater are slightly higher than 120 mm long heater. The difference in the heat tranfser coefficient between data of 60 mm and 120 mm long heaters are about 7% and 3% for data of Figures 5.15 and 5.16, respectively. Figures 5.17 to 5.21 show the variation of heat transfer coefficient against gas superficial velocity with heater vertical length as parameter for CMC solutions of approximately 100, 500, 1000, 2000 and 3000 ppm with the 57c distributor plate. These figures show that heat transfer coefficient increases with the reduction in heater length from 120 to 30 mm.

Figure 5.17 show that the heat transfer coefficient for 100ppm CMC solution with 120 and 60 mm long heaters are about the same, whilst in Figure 5.18 for 500 ppm CMC solution, and above

→

a superficial gas velocity of 40 mms^{-1}, the heat transfer coefficient for 60 mm long heater gradually approaches that of 30 mm long heater. For 1000ppm and 2000ppm CMC solutions, Figure 5.19 and Figures 5.20, the difference in the heat transfer coefficient between 30 mm and 60 mm long heaters is roughly constant at about 5%. The difference in the heat transfer coefficient between 60 mm and 120 mm long heaters is slightly more pronounced. With a 3000 ppm solution (Figure 5.21) the difference between the heat trasnfer coefficient for 60 mm long and 30 mm long heaters is equal to the difference between heat transfer coefficient for 60 and 120 mm long heaters, being about 8%.

Therefore it was deduced that up to CMC concentrations of 1000 ppm with an apparent viscosity of about 2-4 cP for superficial gas velocity in the range of 10-100 mms^{-1}, the heat transfer coefficient becomes independent of heater lengths at some point in the range of 30-60 mm. For higher CMC concentrations (2000 or 3000 ppm with apparent viscosity of 7-9 cP and 8-11 cP respectively for $1< Ug <100$ mms^{-1}) the heat transfer coefficient depends on the heater vertical length over the range investigated. Further results are needed in order to establish whether there is a limiting length for such solutions.

5.5.2.- Effect of Heater Orientation.

Two horizontal positions were considered. Position 1 correspond to the direction 6-5-9-1-2 and position 2 correspond

to direction 4-3-9-7-8 as indicated in Figure 3.8. The results are shown in Figure 5.22. The variation of heat transfer coefficient against superficial gas velocity is for a water height of 0.90 m.

It is clear from Figure 5.22 that heat transfer coefficient are virtually the same for these two positions which is an indication of a symmetrical flow pattern in the column.

Figure 5.23, 5.24 and 5.25 compare a horizontal with a vertical orientation. It is clear that the heat transfer coefficient at any specific superficial velocity is higher for the 120 mm long heater positioned horizontally. Figure 5.23 and 5.25 are for water and the 57a distributor plate, whilst Figure 5.24 is for the 3000 ppm CMC solutions. Figure 5.23 and 5.24 show an increase of about 15% and 25% in the heat transfer coefficient with the heater rotation from vertical to horizontal position. These increases are attributted to the changes in vertical dimensions .

Figure 5.25 shows data of heat transfer coefficient against superficial gas velocity with the 120 mm long heater positioned horizontally and the 30 mm long heater positioned both vertically and horizontally. It shows that heat transfer coefficients for 30 by 30 mm heater position either vertically or horizontally are the same. Although the heat transfer coefficients for the 120 mm long heater position horizontally are an average 5% lower than forthe 30 mm long heater. It is reasonable to conclude that the

vertical dimension governs the heat transfer rate whether this is length or diameter and that increasing the vertical dimensions at constant gas superficial velocity leads to a reduction in heat transfer until the limiting length is reached. It is apparent from the results presented that for low viscosity liquids the heater transfer coefficient becomes less dependent on the vertical dimension of the heater once the vertical dimension is greater than 60 mm is. The best fit value reported by Lewis et al, was, for water at ambient temperature, 45 mm. Further discussion on this matter is to be found in chapter 7.

The dependency of the characteristic heater length upon viscosity, which has not been recognized, is modest but noticeable, this will also be dealt with in Chapter 7.

It is also important to note the magnitude of the effect of the heater vertical length. Kubie (1974) found that for horizontal heater the heat transfer coefficient is proportional to $d_H^{-0.375}$ with heater diameters ranging from 0.125 to 10.5 mm. However, in this work it was found that for the water data of Figures 5.15 and 5.16 the heater coefficient is proportional to $d_H^{-0.87}$ and $d_H^{-0.48}$ and for 2000 and 3000 ppm CMC solutions to $d_H^{-0.09}$ and $d_H^{-0.11}$, respectively. In deriving the indexes range of superficial gas velocity considered was 12 to 80 mms^{-1}. This shows that for practical purposses the effect of heater length on the heat transfer coefficient can be negelected. Indeed many investigators probably did not recognized the minor length effect because either the heater vertical lengths were

more than 60 mm or sufficiently close to this length for the effect to be less than the experimental error.

5.6.- EFFECT OF POWER INPUT TO THE HEATER AND HEATER SURFACE TEMPERATURE.

Kolbel et al (1958), Ruckenstein and Smigelschi (1965) are amongst the large majority of workers who reported that heat transfer coefficient is independent of the heater surface temperature. This was checked for water and CMC solutions.

Figure 5.26, 5.27 and 5.28 show variations of heat transfer coefficient against superficial gas velocity in the range of 10-110 mms^{-1} with the power input to the heater as parameter. Measurements were carried out at 45, 90 and 140 W power inputs. The 60 mm by 30 mm diameter heater was employed and it was placed vertically at 0.75 m from the column base on the column axis. Figure 5.26 shows data obtained for water of height 0.90 m at constant bulk temperature of 18 ^{o}C, whilst in Figures 5.27 and 5.28 the liquids are 2000 ppm CMC solution at 17.7 ^{o}C and 3000 ppm CMC solution at 18.1 ^{o}C, respectively.

Figure 5.26 shows that at low superficial gas velocities of less that 40 mms^{-1} the difference in the heat trasnfer coefficient for 45 W and 140 W power input are negligible, but that at gas superficial velocities higher than 40 mms^{-1} the heat transfer coefficient for 45 W power input is apparently higher

than that for 140 W power input. The difference in the heat transfer coefficient between 90 and 140 W power inputs is negligible.

It was found that the difference in heat transfer coefficients between 45 and 140 W power input is about 8% at a superficial gas velocity of 90 mms^{-1}. At this gas velocity the heat transfer coefficient for 45 W power input is 6500 $W(m^2K)^{-1}$ and the temperature difference between the surface and the bulk of liquid is 1.2 ^oC. This gives a possibe error of 8% (0.1x100/1.2) in the measured driving force for heat transfer and hence in the heat transfer coefficient. The results with a likely error greater than 7%, which roughly corresponds to a temperature difference of 1.5 ^oC, were excluded.

Therefore the conclusion that the heat transfer coefficient is a weak function of power input seems to be reasonable. This will be further confirmed through consideration of Figure 5.27 and 5.28 which are for CMC solutions. These data shows that the variation of heat transfer coefficient with the power input in the experimental range considered is negligible.

As an increasse of power input at constant bulk temperature results in an increase in the heater surface temperature of the heater it appears that the heat transfer coefficient is independent of heater surface temperature at low temperature differences. The surface temperature has been ignored in the further analysis of results obtained herein.

This result is apparently contradicted by Lewis et al (1982) who reported an almost linear increase of heat transfer coefficient with the increase of heater surface temperature for the Nitrogen-Glycol system. However, for this system the driving force, ΔT, was as high as 50 ^{o}C and the increase of heat transfer coefficient is considered to be due to changes in the physical properties of the system (see section 5.7) rather than being due to the contribution of heat transfer by natural convection which is a function of $\Delta T^{0.25}$. However it was noted that under conditions of the present study ($\Delta T < 10$ ^{o}C and bulk temperaure of 19 ^{o}C) the reported increase in heat transfer coefficient due to an increase of ΔT from 2.5 to 10 ^{o}C was less than 5%.

5.7.- EFFECT OF LIQUID PHASE VISCOSITY.

The heat transfer coefficient is a function of the physical properties of the liquid phase. This dependency was examined using water at temperatures of 10, 20, 30 and 50 ^{o}C and CMC solutions with apparent viscosies in the range of 0.5 to 180 cP at ambient temperature. This range is much wider than that of many other workers.

Figure 5.29 shows the variation of heat transfer coefficient against superficial gas velocity with the bulk temperatures of 10, 20, 32 and 50 ^{o}C as the parameter. At these temperatures the Prandtl number for water are 9.55, 7.0, 5.0 and 3.33,

respectively. It is evident from Figure 5.29 that the increase of the bulk water temperature from 10 to 50 ^{o}C leads to the significant increase of about 35% in the heat transfer coefficient. It is also interesting to note that at low temperatures of 10 and 20 ^{o}C the heat tranfer coefficient is proportional to about $U_g^{0.25}$ and at higher temperature the index is 0.28. This indicate that the index is not only a function of flow regime (see section 5.1) but it is also a function of the physical properties of the system. Similar experimental results were also given by Lewis et al (1982).

Since the variation of density and heat capacity of water with temperature in the temperature range of 10 to 50 ^{o}C are negligible, the increase of heat transfer coefficient at any constant superficial gas velocity is mainly due to the reduction of the viscosity of the water.

Figure 5.30 shows the variation of heat transfer coefficient with the viscosity of water at superficial gas velocities of 12, 34 and 76 mms^{-1}. An increase in the viscosity, at a constant superficial gas velocity, reduces the heat transfer coefficient. Assuming that. $h \alpha \mu^{-\alpha}$ the values of α are -0.36, -0.48, -0.59 at superficial gas velocities of 12, 34 and 76 mms^{-1}, respectively. Calculations also shows that at the same gas flow rates $h \alpha (\frac{\mu}{k})^{\beta}$ where. β is -0.33, -0.36 and -0.53. The variations in the index are due to the fact that conditions of the systems presented by the curves in Figure 5.29 or 5.30 are not entirely similar.

Experimental results obtained with the CMC solutions of different concentrations (Figure 5.31 and 5.32) also confirmed that increasing viscosity leads to a decrease in the heat transfer coefficient for a given gas flow rate.

Figure 5.31 shows the variation of heat transfer coefficient with superficial gas velocities in the range of 12 to 90 mms^{-1}. The CMC concentration of 100 to 10,000 ppm covers an apparent viscosity range of 0.9 to 180 cP. It can be seen that the slopes of the lines are almost equal and an average value is about 0.28 (see Table 5.15). Density, heat capacity and thermal conductivity remanined constant and are that of water. However, the only other parameter of possible importance that changes apart from viscosity is the gas hold-up which decreases considerably from 0.128 for 100 ppm CMC solution to 0.075 for 10,000 ppm CMC solution at a superficial gas velocities of $52mms^{-1}$.The weak influence of the average gas hold-up compared with the other system parameters was examined in section 5.3.2.

The variation of the heat transfer coefficient against apparent viscosity of CMC solutions at a number of superficial gas velocities are presented in Figure 5.32. It is interesting to note that the data almost lie on one curve which emphasizes the importance of this parameter. Calculation shows that $h \propto \mu^{-0.33}$ This value was also given by Nishikawa et al (1977) who has proposed the use of apparent viscosity to correlate heat transfer data of power law fluid with that of Newtonian fluids.

5.7.1.- Correlation of Experimental Data Based on Deckwer Model.

Following the semi-theoretical model of Deckwer (1980) it was assumed that

$$St = A(Re\ Fr\ Pr^2)^B \qquad ...5.1$$

Experimental data of A and B for water and CMC solutions are given in Table 5.14. The experimental value of B for water were found to be -0.254 whilst the average value of B for CMC solutions is also -0.254 with a standard deviation of 2%. These values are in good agreement with the theoretical value of 0.25 given by Deckwer.

A further test on the effect of gas hold-up was also carried out. It was found that the equation 5.1 for water can be presented as

$$St \ \alpha \ \epsilon^{0.04}(Re\ Fr\ Pr^2)-0.262$$

The superficial gas velocity range was 10 to 1000 mms^{-1} and gas hold-up range was 0.08 to 0.19.

The low index of 0.04 for gas hold-up showed that the effect of gas hold-up can be ignored and that a Deckwer type correlation is justifiable.

5.8.- SUMMARY.

Experimental investigations were conducted to consider the effect of several parameters of interest on the heat transfer coefficient in the bubble column. It was found that,

1.- For water at superficial gas velocities in the range of 10 to 50 mms^{-1}, $h \propto U_g^{0.25}$ and in the range of 50 to 100 mms^{-1} the index reduces to 0.19. The index for CMC solutions in the above range, however, remains almost constant at about 0.25.

2.- For aspect ratios of 2, 3, 4, heat tranfer coefficient is almost independent of liquid height. But a slight dependency in the aspect ratio range of 2 to 3 was observed.

3.- When heaters are positioned more than 1.5 column diameter from the distributor, the heat transfer coefficient is independent of the vertical position of the heater from the distributor plate.

4.- To a minor extent the heat transfer coefficient depends on the radial position of the heater and decreases close to the column wall. Also the maximum heat transfer coefficient is not always obtained on the column axis.

5.- For an even distribution of gas the heat transfer coefficient is independent of distributor type. Mal-distribution of gas enhances heat transfer coefficient to an extent which is

dependent upon gas hold-up and the prevailing flow regime.

6.- For aerated water the heat transfer coefficient becomes independent of the heater vertical length in the range of 30 to 60 mm. However, CMC data shows that by increasing viscosity the dependency of heat transfer coefficient on the heater length increases and heat transfer is a strong function of physical properties of the system and increasing viscosity reduces the heat transfer coefficient. The dependency of heat transfer coefficient upon viscosity is roughly proportional to $\mu^{-0.3}$ in case of CMC solutions.

8.- Finally, at low temperatures differences the heat transfer coefficient is independent of heater surface temperature and therefore physical properties could be referred to the bulk temperature.

*****

U_g mms^{-1}	hold-up	h $kW(m^2K)^{-1}$
12.1	0.038	3.65
21.2	0.075	4.20
27.0	0.092	4.44
35.0	0.112	4.84
41.0	0.124	4.92
51.5	0.129	5.26
58.0	0.134	5.38
69.0	0.159	5.77
77.5	0.163	5.78
84.5	0.172	5.91
95.0	0.178	5.98
105.0	0.186	5.98

Table 5.1.- Experimental heat transfer coefficient obtained for water with a 30 x 60 mm heater mounted vertically on the column axis. Distributor used 57c. Q=90W t_b= 19°C

U_g mms^{-1}	hold-up	h $kW(m^2K)^{-1}$
12.1	0.036	3.16
21.2	0.065	3.47
27.0	0.079	3.70
35.5	0.105	4.05
42.2	0.117	4.34
52.0	0.128	4.65
58.7	0.143	4.88
70.2	0.152	5.26
79.5	0.165	5.33
87.5	0.183	5.77
98.3	0.182	5.82
109.2	0.184	6.08

Table 5.2.-Experimental heat transfer coefficient for an approximately 100 ppm CMC solution with a 30 x 60 mm heater mounted vertically on the column axis. Distributor 57c. Q=92 W t_b=18 °C.

U_g mms^{-1}	hold-up	h kW(m^{2}K)$^{-1}$
12.0	0.038	2.5
21.4	0.064	2.8
27.3	0.085	2.92
35.7	0.111	3.25
42.5	0.125	3.41
51.7	0.143	3.70
59.1	0.150	3.86
71.5	0.165	4.27
80.0	0.178	4.40
90.0	0.183	4.55
101.0	0.197	4.66
116.0	0.204	4.66

Table 5.3.- Experimental heat transfer coefficient obtained for an approximately 500 ppm CMC solution with a 30 x 60 mm heater mounted vertically on the column axis. Distributor 57c. Q=92 W , t_b = 18 ^oC.

U_g mms^{-1}	hold-up	h kW(m^{2}K)$^{-1}$
12.1	0.039	2.15
21.4	0.069	2.39
27.3	0.088	2.57
35.5	0.109	2.70
42.1	0.118	2.76
51.0	0.139	2.98
59.3	0.149	3.08
71.5	0.161	3.19
85.0	0.173	3.34
89.0	0.185	3.38
101.0	0.192	3.42
116.0	0.194	3.47

Table 5.4.- Experimental heat transfer coefficient obtained for an approximately 1000 ppm CMC solution with 30 x 60 mm heater mounted vertically on the column axis. Distributor 57c. Q=92 W t_b=18 ^oC

U_g mms^{-1}	holdup	h kW(m^2)$^{-1}$
12.1	0.038	2.07
21.5	.036	2.30
27.8	0.081	2.39
35.9	0.105	2.53
42.8	0.118	2.66
52.8	0.128	2.85
59.9	0.144	3.06
73.0	0.158	3.10
84.0	0.158	3.25
90.0	0.174	3.37
101.0	0.187	3.42
116	0.187	3.49

Table 5.5.-Experimental heat transfer coefficient obtained for an approximately 1500 ppm CMC solution with a 30 x 60 mm heater mounted vertically on the column axis. Distributor 57c Q=92 W t_b= 18 ^oC

U_g mms^{-1}	hold-up	h kW(m^{2}K)$^{-1}$
12.1	0.037	1.72
21.4	0.066	1.95
27.4	0.076	2.012
35.9	0.095	2.14
42.8	0.106	2.3
52.1	0.118	2.40
59.5	0.127	2.60
72.0	0.139	2.67
81.0	0.157	2.70
88.6	0.159	2.87
105.0	0.167	2.87
114.0	0.174	3.03

Table 5.6.-Experimental heat transfer coefficient obtained for an approximately 2000 ppm CMC solution with a 30 x 60 mm axis. Distributor 57c Q=92 W $t_{b=}$18 ^oC.

U_g mms^{-1}	hold-up	h kW(m^{2}K)$^{-1}$
12.1	0.037	1.70
21.4	0.066	1.94
27.4	0.076	2.09
35.9	0.09	2.23
42.8	0.103	2.35
52.1	0.123	2.49
59.5	0.125	2.59
72.0	0.135	2.68
84.0	0.147	2.70
88.6	0.161	2.85
100.0	0.173	2.62
114.0	0.191	3.01

Table 5.7.- Experimental heat transfer coefficient obtained for an approximately 2500 ppm CMC solution with a 30 x 60 mm heater mounted vertically on the column axis. Distributor 57c Q=92 W t_b = 18 ^oC.

U_g mms^{-1}	hold-up	h kW(m^{2}K)$^{-1}$
12.0	0.035	1.46
21.5	0.057	1.64
27.8	0.071	1.76
35.9	0.092	1.86
42.5	0.097	1.99
52.7	0.106	2.09
60.3	0.121	2.22
73.1	0.130	2.31
88.1	0.135	2.39
89.6	0.155	2.52
101.5	0.167	2.52
114.1	0.178	2.54

Table 5.8.- Experimental heat transfer coefficient obtained for an approximately 3000 ppm CMC solution with a 30 x 60 mm heater mounted vertically on the column axis. Distributor 57c Q=92 W t_b= 18 ^oC

U_g mms^{-1}	hold-up	h kW(m^{2}K)$^{-1}$
12.5	0.034	0.99
21.7	0.05	1.25
27.4	0.06	1.39
35.9	0.064	1.57
54.4	0.088	1.76
61.3	0.088	1.82
75.2	0.095	1.90
86.0	0.102	1.96
96.5	0.116	2.06
111.0	0.130	2.15
114.0	0.131	2.22

Table 5.9.- Experimental heat transfer coefficient obtained for an approximately 5000 ppm CMC solution with a 30 x 60 mm heater mounted vertically on the column axis. Distributor 57c Q=90 W t_b= 18 ^oC

U_g mms^{-1}	hold-up	h kW(m^{2}K)$^{-1}$
12.5	0.034	0.85
21.7	0.05	0.95
27.4	0.06	1.07
35.9	0.068	1.08
54.4	0.079	1.30
61.3	0.076	1.45
75.2	0.079	1.36
86.0	0.087	1.45
96.5	0.091	1.53
111.0	0.098	1.56

Table 5.10 .-Experimental value of heat transfer coefficient obtained for an approximately 10,000 ppm CMC solution with a 30 x 60 mm heater mounted verticall on the column axis. Q=90 W Distributor 57c. t_b = 18 ^oC.

Liquid	$1<U_g<5 \times 10^{-2}$		$5<U_g<10 \times 10^{-2}$		$1<U_g<10 \times 10^{-2}$	
	A	B	A	B	A	B
Water	1.15	0.25	9.3	0.188	10.6	0.24
CMC ~ ppm						
100	9.36	0.25	13.7	0.36	11.96	0.30
500	7.26	0.25	10.8	0.36	9.30	0.30
1000	7.3	0.30	5.64	0.21	7.0	0.22
1500	6.64	0.28	5.9	0.24	6.5	0.29
2000	4.40	0.21	5.27	0.25	5.3	0.26
2500	7.74	0.37	3.56	0.11	5.4	0.27
3000	4.23	0.24	4.88	0.28	4.69	0.27
5000	5.70	0.39	3.90	0.27	4.95	0.30
10000	2.71	0.26	2.87	0.21	2.95	0.28
Average value of B		0.28		0.25		0.27

Table 5.11- Simple power law correlations for data of Tables 5.1 to 5.10. Equation of form $h = AU_g^B$ where heat transfer coefficient, h, is in $kW(m^2K)^{-1}$ and superficial gas velocity, U_g in ms^{-1}.

liquid	A	B
water	0.36	0.235
CMC ~ppm		
100	0.57	0.57
500	0.51	0.55
2000	0.43	0.40
3000	0.35	0.31
5000	0.51	0.34
10000	1.37	0.77
Average		0.52

Table 5.12.- Experimental values of A and B in Equation of form

$$St\ (ReFrPr^2)^{0.33} = A.\ \epsilon^{B}$$

Reference Figure	liquid	distributor	* percentage decrease 30 and 60	60 and 120
5.15	water	57c	15	7
5.16	water	57a	4	3**
	CMC ~ppm			
5.17	100	57c	24	8
5.18	500	57c	11***	10**
5.19	1000	57c	5	11
5.20	2000	57c	5	6
5.21	3000	57c	9	8
		average	10.4%	7.6%

* Precentage decrease in heat transfer coefficient with increase in heater length.
** $U_g < 50\ mms^{-1}$ the difference is 2%.
*** $U_g > 50\ mms^{-1}$ the difference is 16%.

Table 5.13.- Variation of heat transfer coefficient with heater length.

liquid		A	B
water		0.14	-.254
CMC ~ ppm			
100		0.09	-0.224
500		0.09	-0.235
2000		0.10	-0.256
3000		0.10	-0.262
5000		0.10	-0.262
10000		0.07	-0.239
	average	0.09	-0.254

Table 5.14.- Experimental values of A and B in

$$St = A(Re\ Fr\ Pr^2)^B \qquad U_g < 0.1\ ms^{-1}$$

U_g mms^{-1}	α
12	-0.31
34	-0.31
50	-0.33
76	-0.33
87.5	-0.33
average	-0.3

Table 5.15 .-dependency of heat transfer coefficient on the viscosity in the form of $h \propto \mu^{\alpha}$. The indexes are the slopes of lines in Figure 5.31.

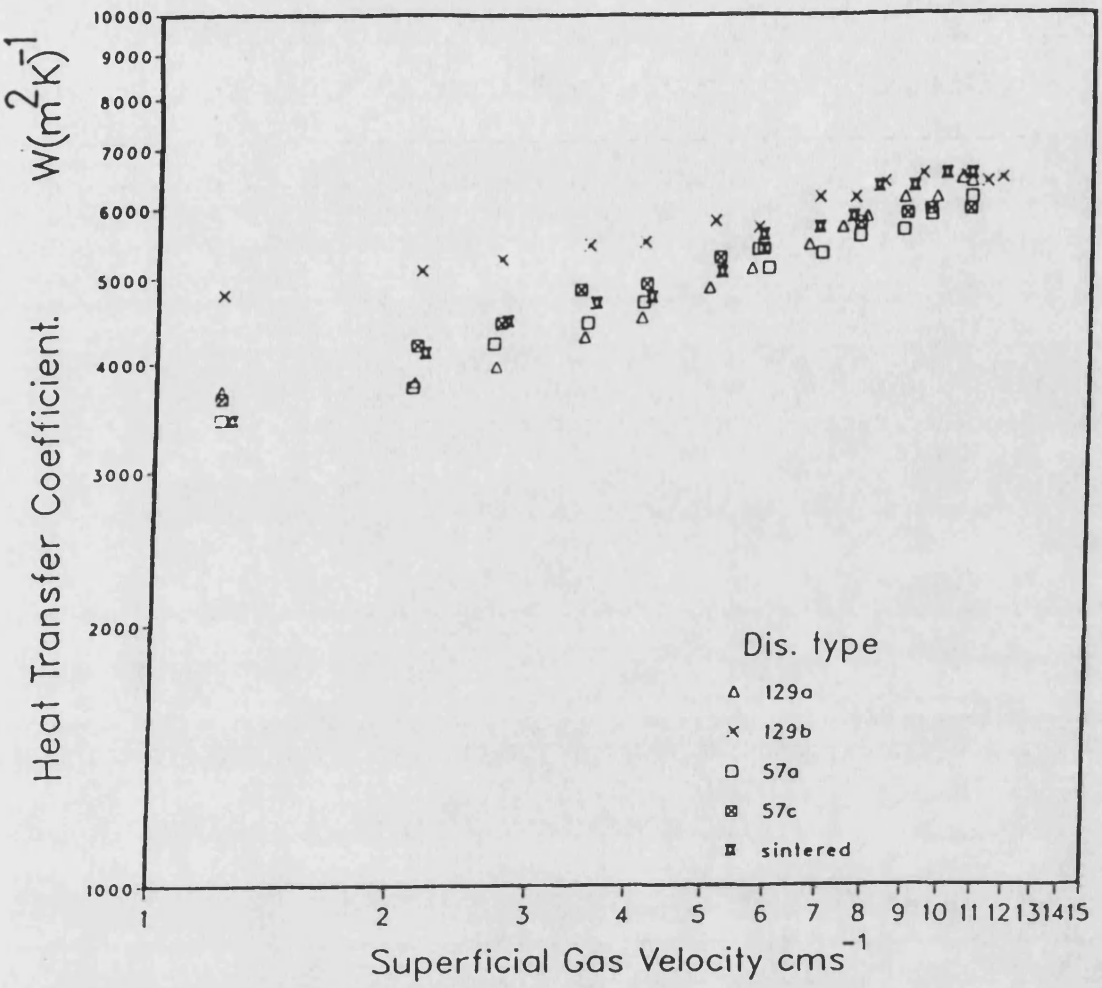

Figure 5.1(a).-Effect of Distributor Type on the Heat Transfer Coefficient.
Variation of heat transfer coefficient with superficial gas velocity for a water height of 0.90 m with a 30 x 60 mm heater mounted vertically on the column axis.

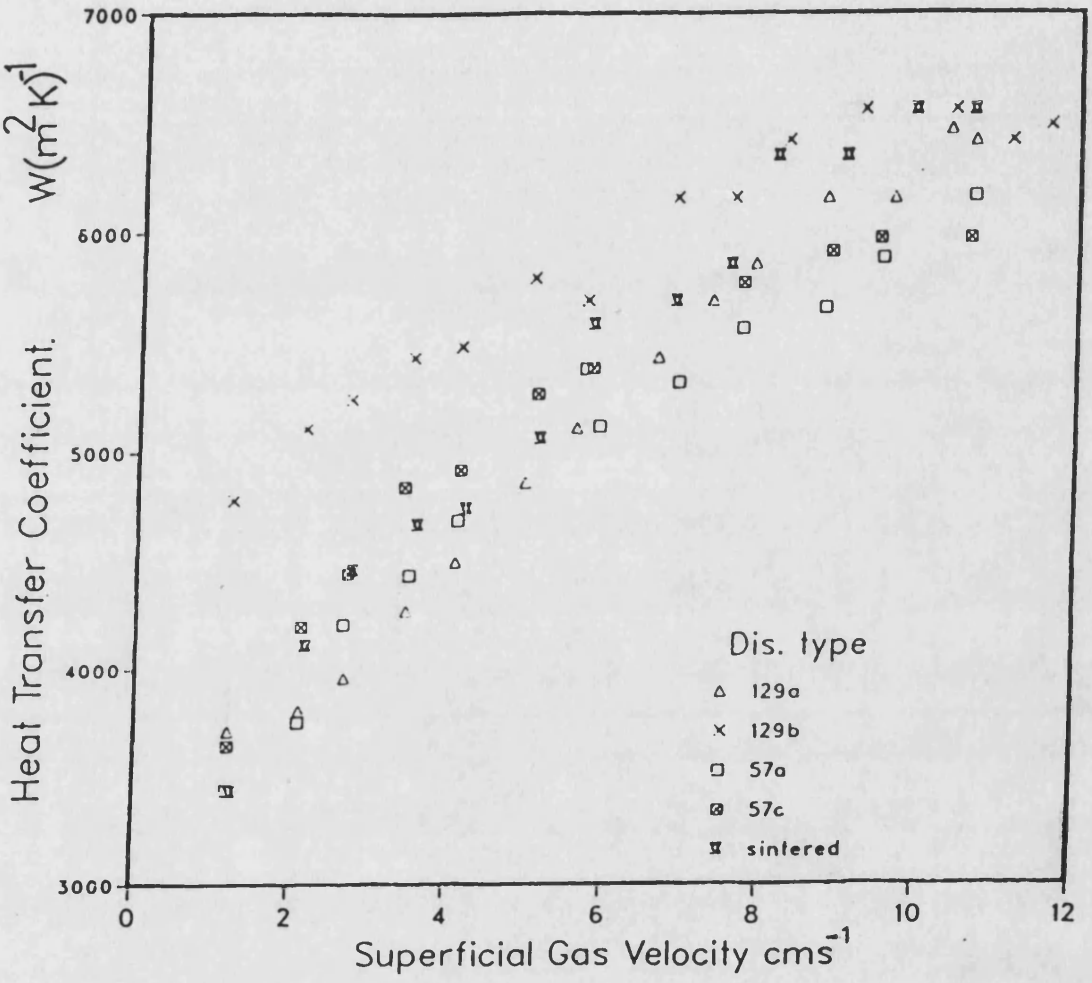

Figure 5.1 (b).- Effect of Distributor Type on the Heat Transfer Coefficient.
Variation of heat transfer coefficient with superficial gas velocity for a water height of 0.90 m with a 30 x 60 mm heater mounted vertically on the column axis.

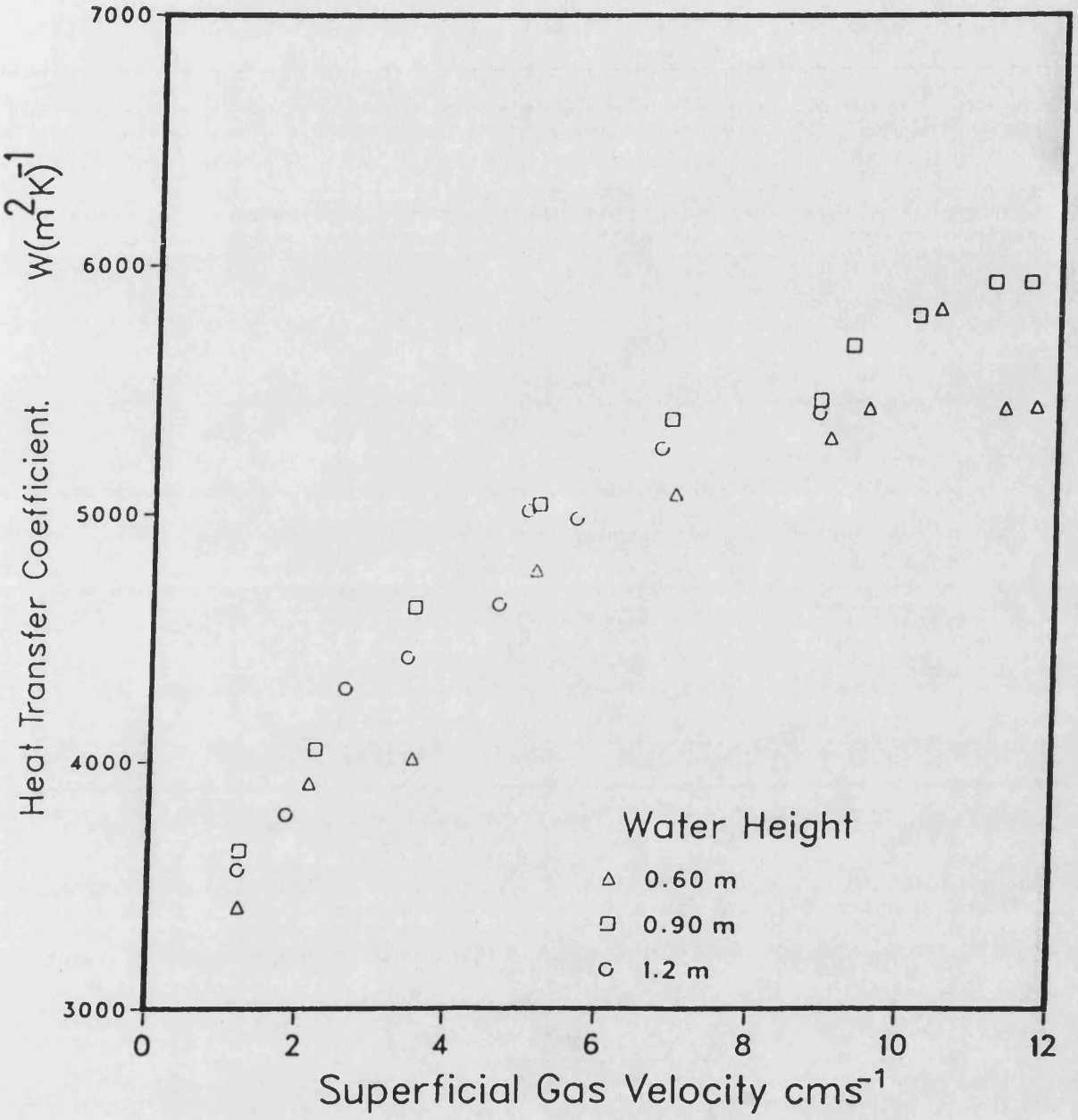

Figure 5.2.- Effect of Water Height.
Variation of heat transfer coefficient with superficial gas velocity obtained with a 30 x 120 mm heater mounted vertically on the column axis at 0.45 m, 0.75 m and 1.20 m from base. Distributor used 57a. t_b= 18 °C.

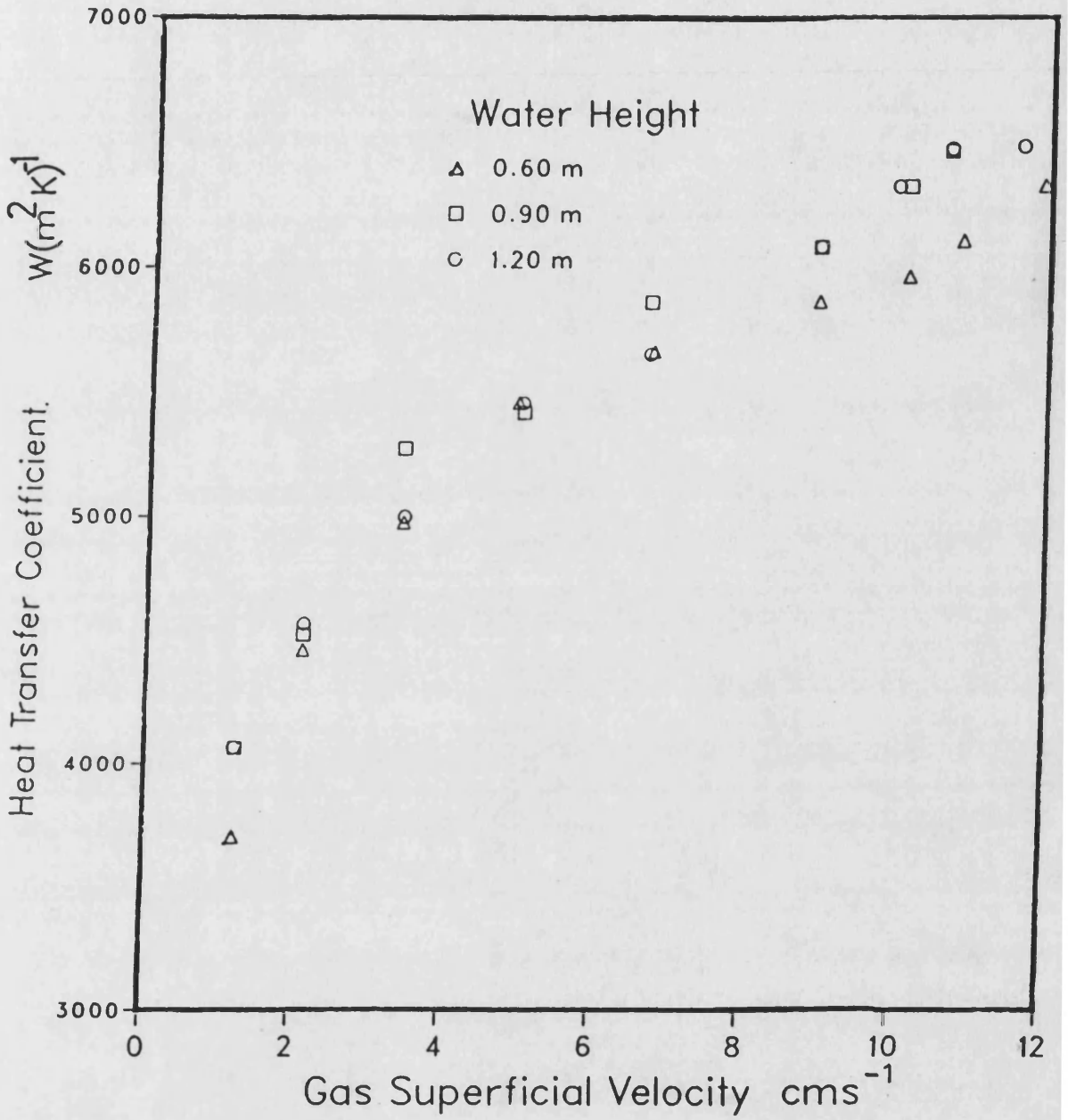

Figure 5.3.-Effect of Water(Tap Water) Height. Variation of heat transfer coefficient with superficial gas velocity. Data obtained with a 30 x 120 mm heater mounted vertically on the column axis at 0.45 m, 0.75 m and 1.20m from base. Distributor type 129a. t_b = 18 ^{o}C.

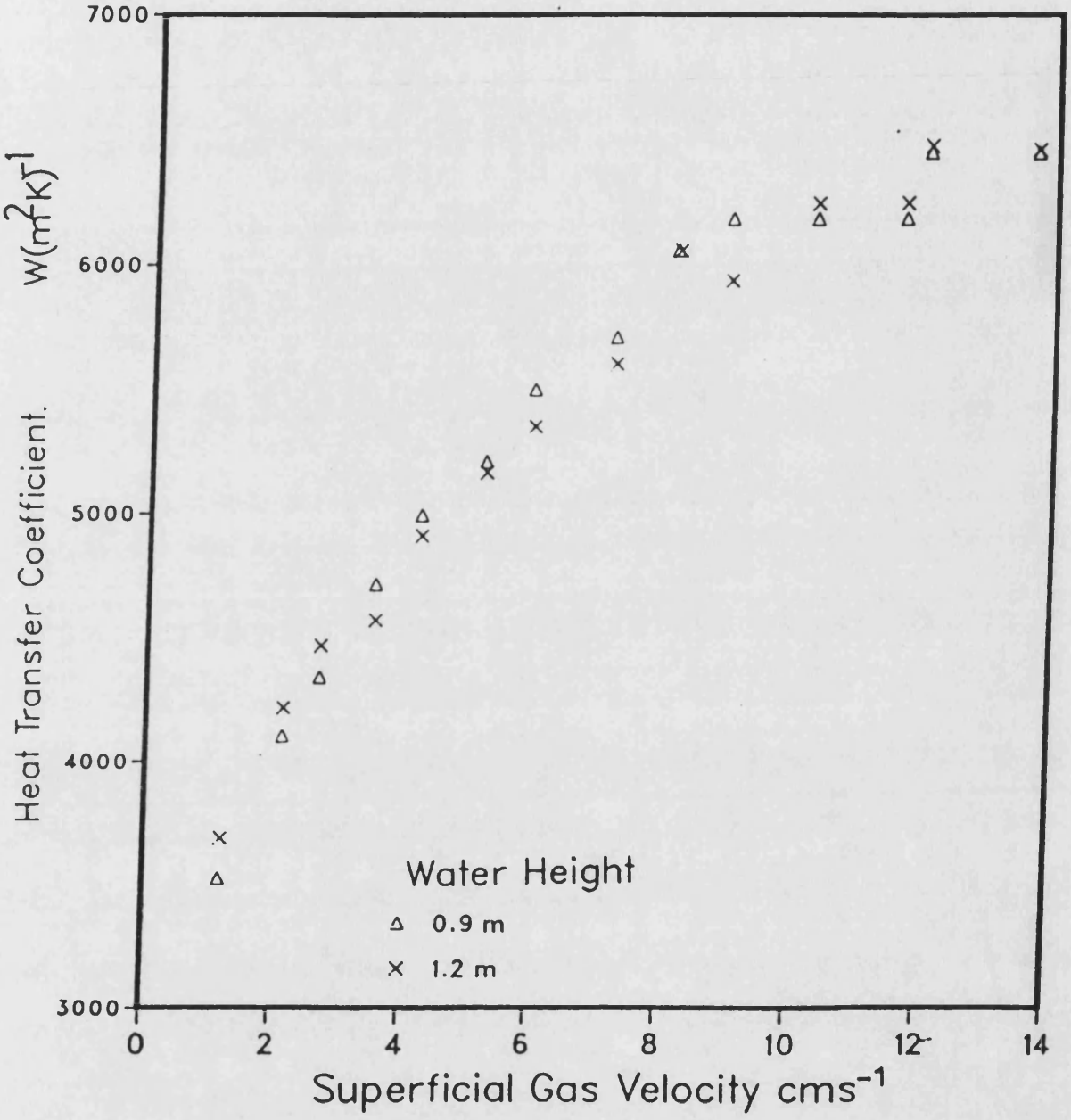

Figure 5.4.- Effect of Water Height.
Variation of heat transfer coefficient with superficial gas velocity obtained with a 60 x 30 mm heater mounted vertically at 0.75 m from base. Distributor used 57c. t_b = 18 °C.

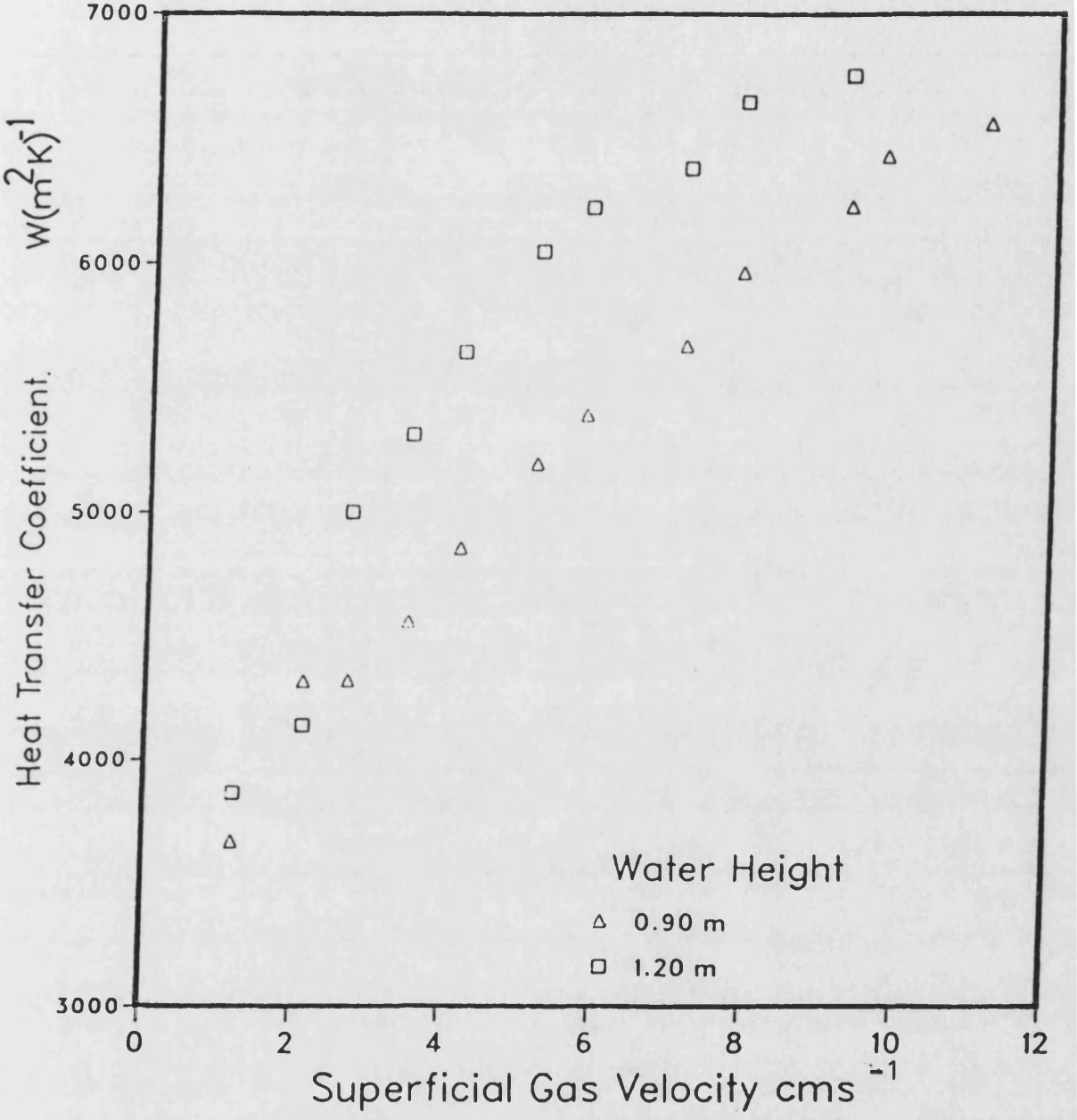

Figure 5.5(a).- Effect of Water Height.
Variation of heat transfer coefficient with superficial gas velocity obtained with a 30 x 30 mm heater mounted vertically at 0.75 m and 0.90 m from base. Distributor used 57a. t_b = 18 °C.

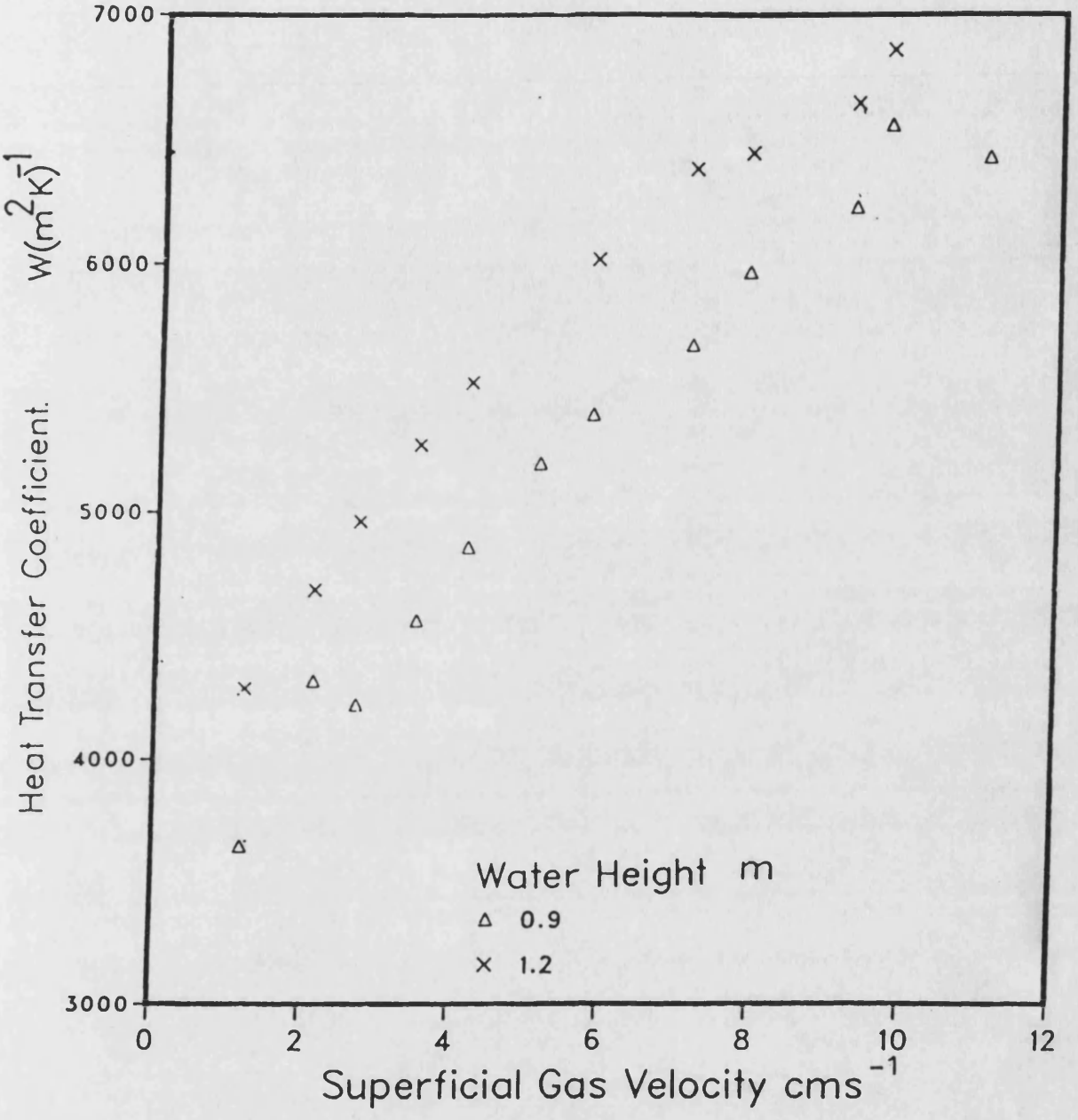

Figure 5.5(b).- Effect of Water Height.
Variation of heat transfer coefficient with superficial gas velocity obtained with a 30 x 30 mm heater mounted vertically on the column axis at 0.75 m from the base. Distributor used 57a. t_b = 18 °C.

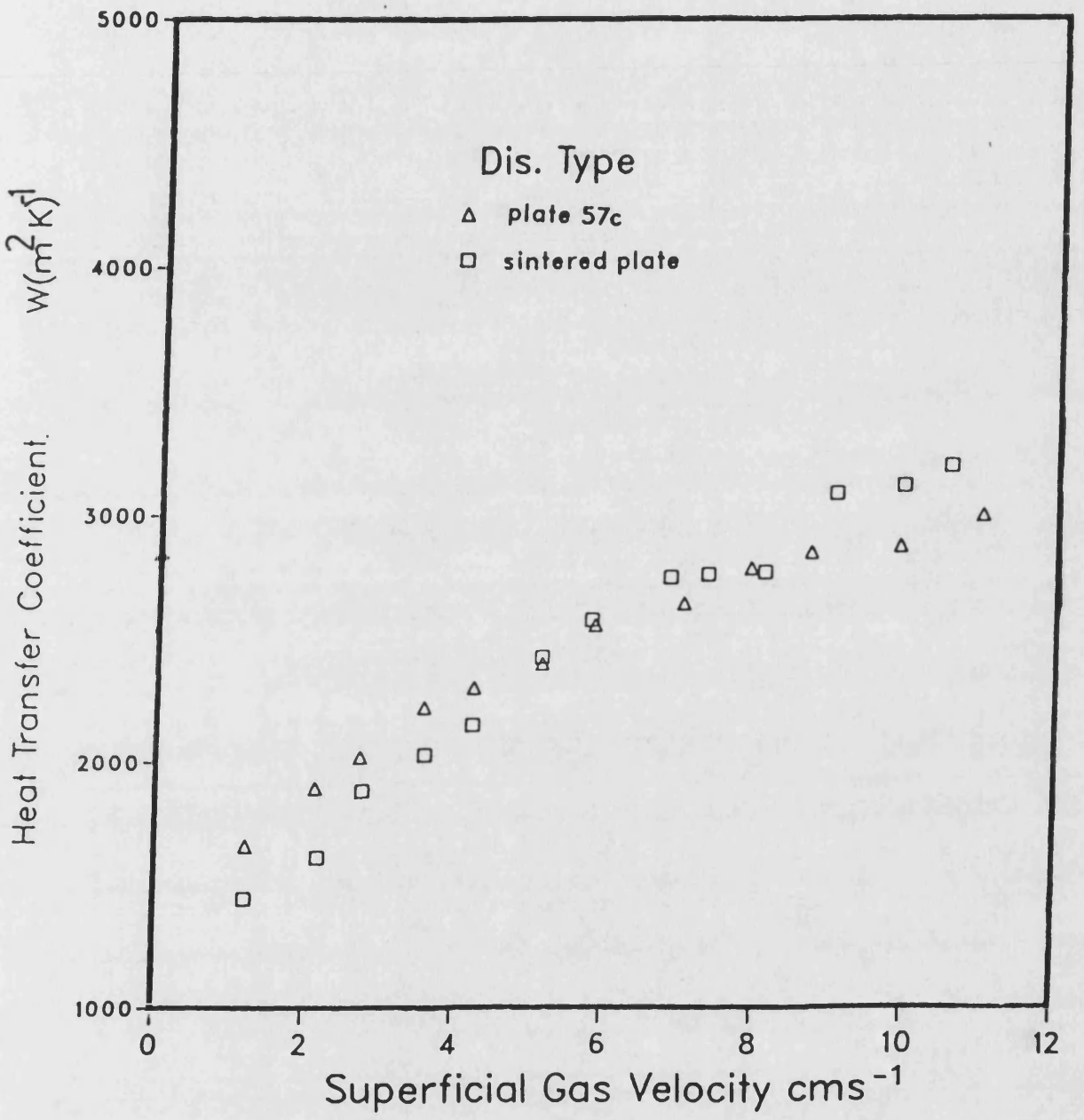

Figure 5.6.-Effect of Gas Distributor on Heat Transfer coefficient.
Variation of heat transfer coefficient with superficial gas velocity obtained for a 3000 ppm CMC solution with a 30 x 120 mm heater mounted vertically on the column axis at 0.75 m from base. t_b= 18 °C.

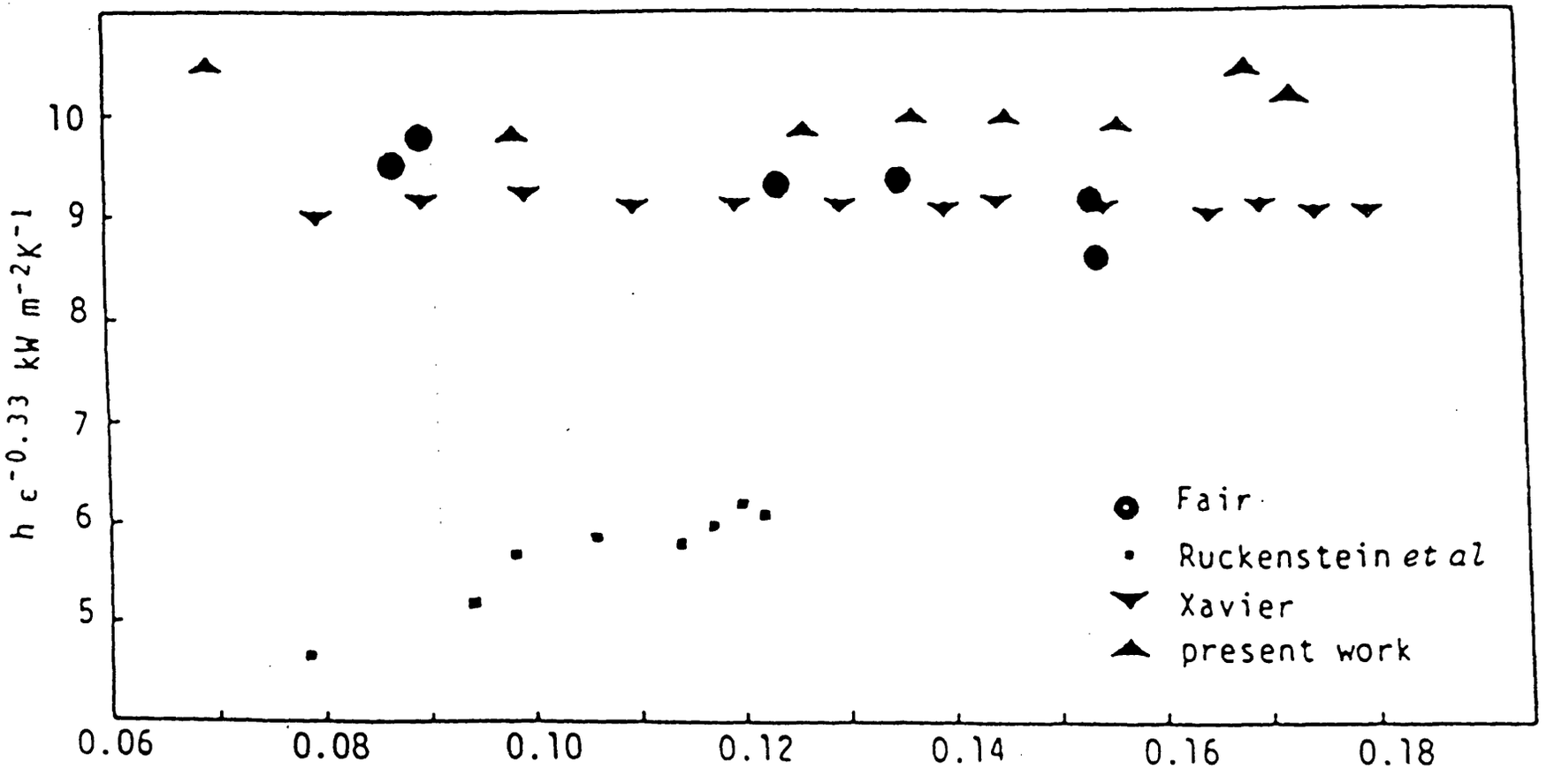

Figure 5.7.- Variation of $h\epsilon^{-0.33}$ with gas hold-up for ambient air- water data.

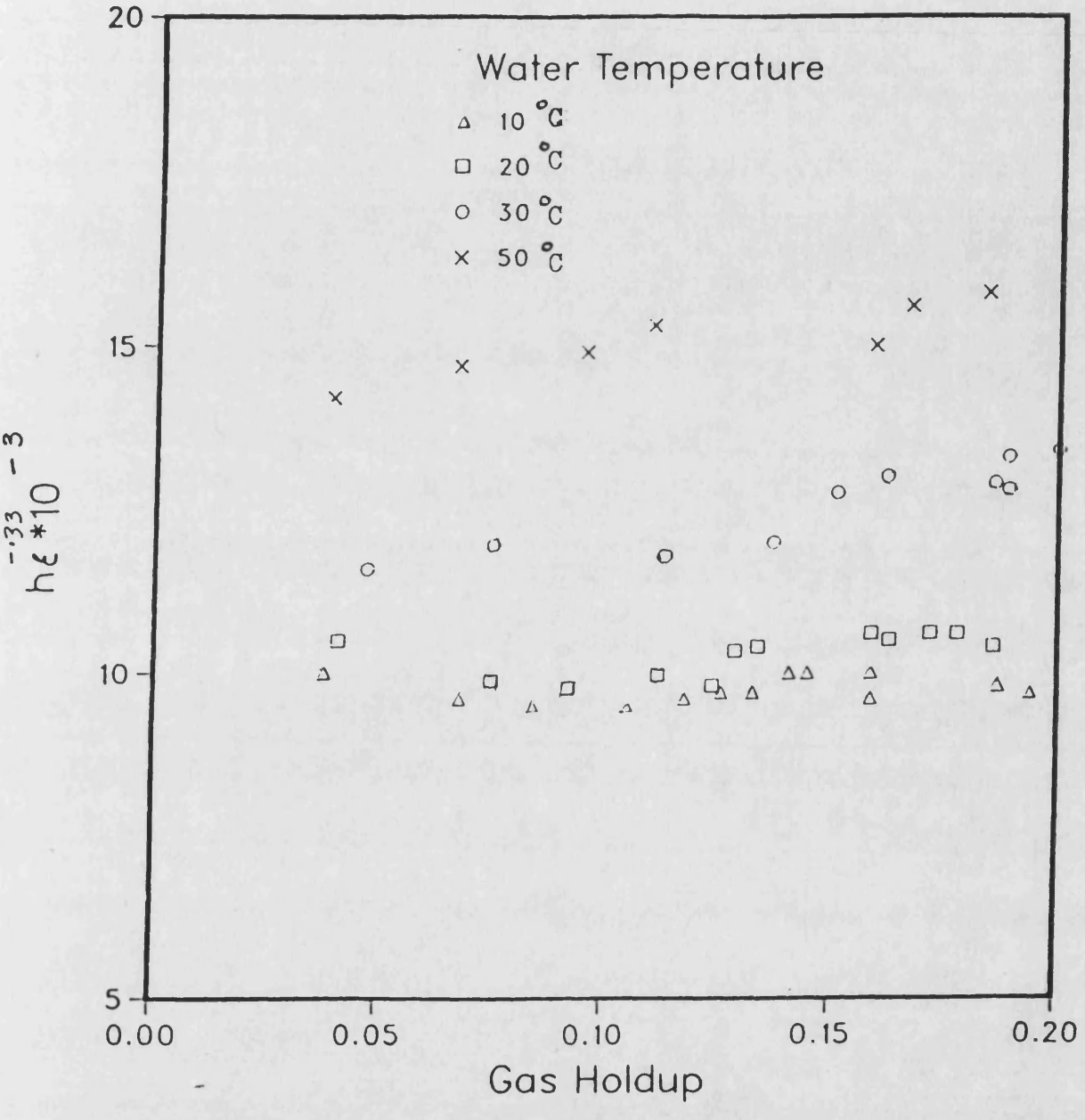

Figure 5.8.- Variation of $h\,\epsilon^{-0.33}$ with gas hold-up for air-water at various temperatures.

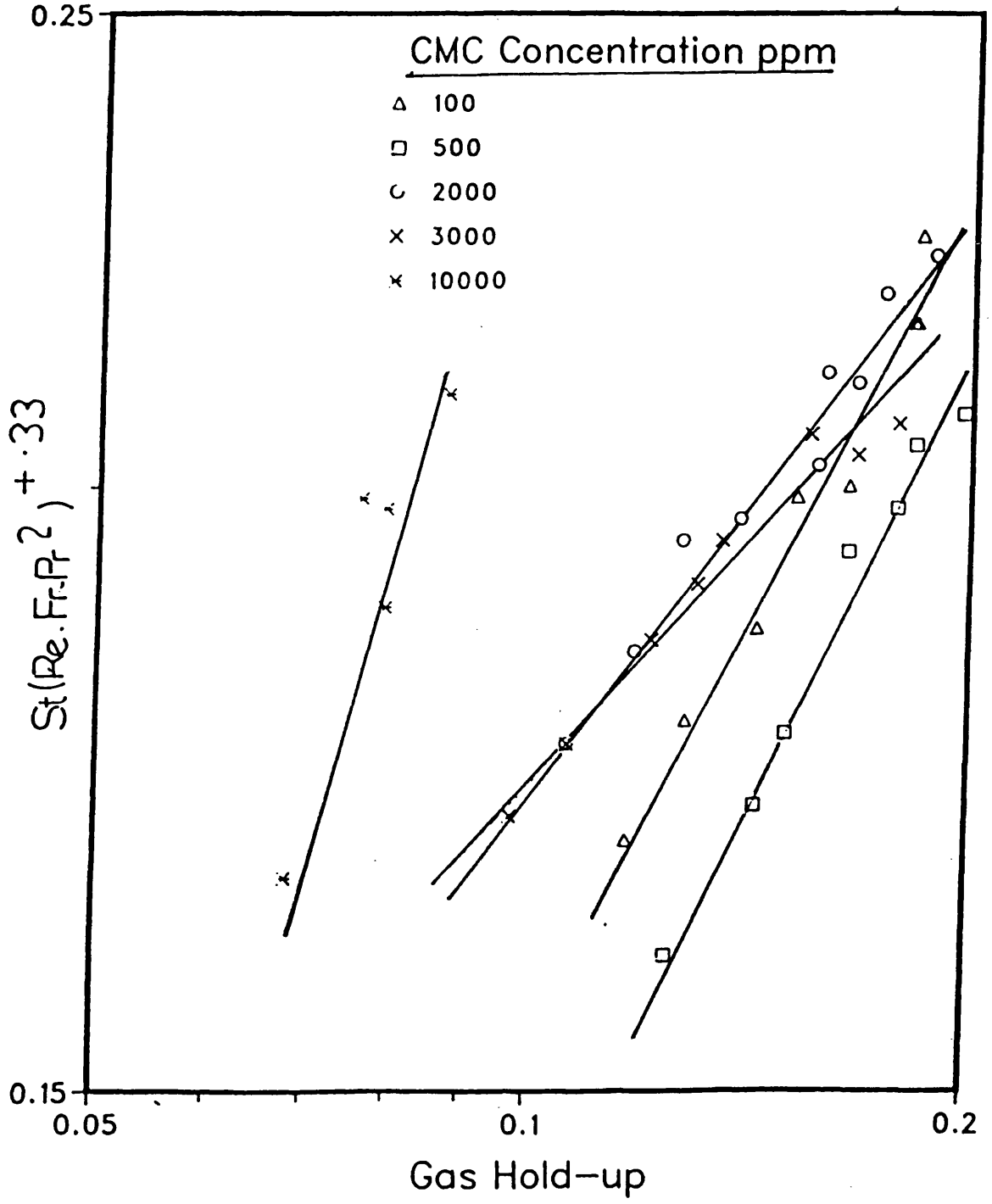

Figure 5.9.- Variation of $St(Re\ FrPr^2)^{0.33}$ with gas hold-up for CMC solutions of different concentrations.

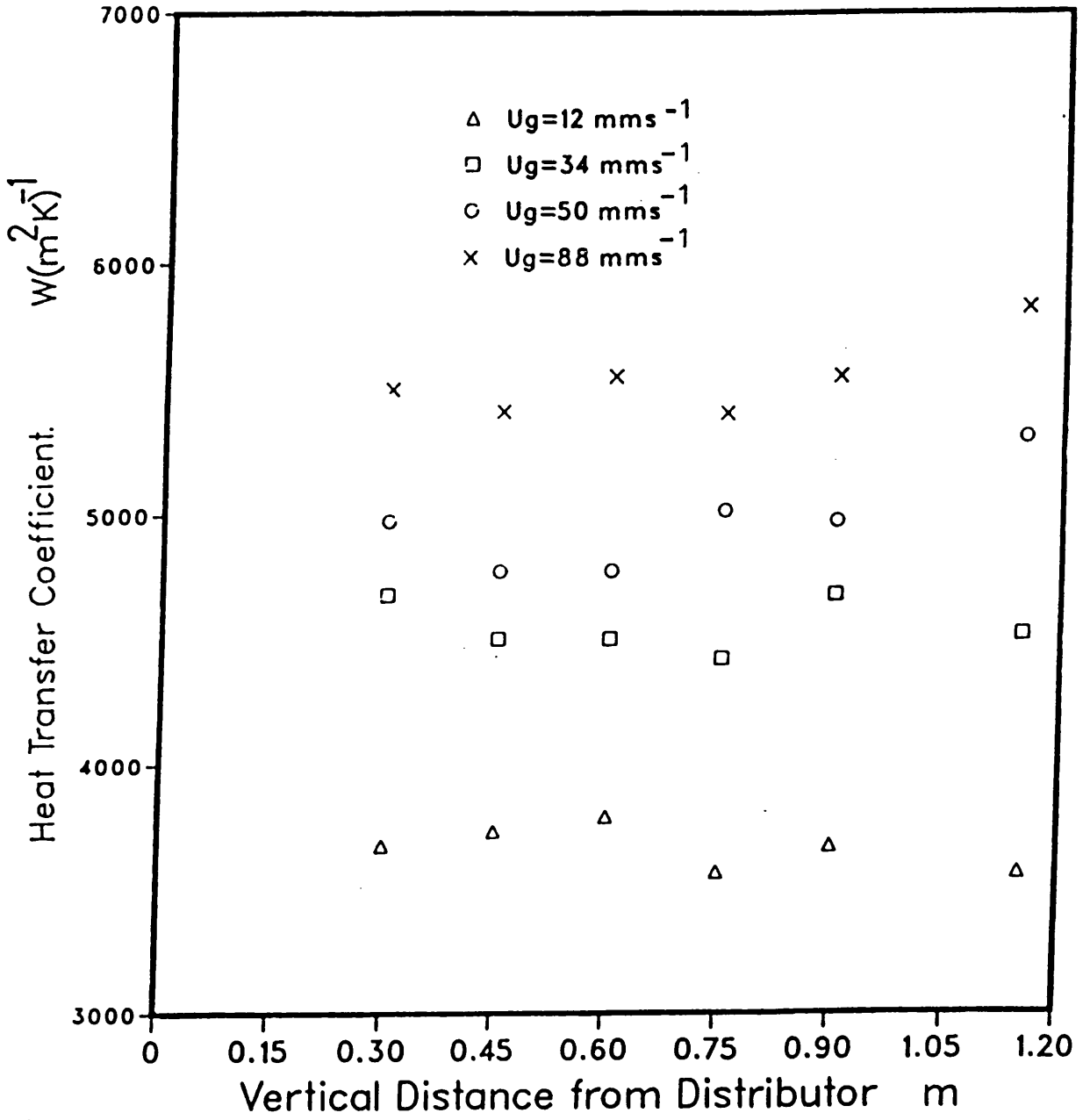

Figure 5.10.- Effect of Heater Vertical Distance from Distributor.
Variation of heat transfer coefficient with heater distance from base for a water height of 1.20 m obtained with a 30 x 120 mm heater mounted vertically on the column axis. t_b = 18 °C

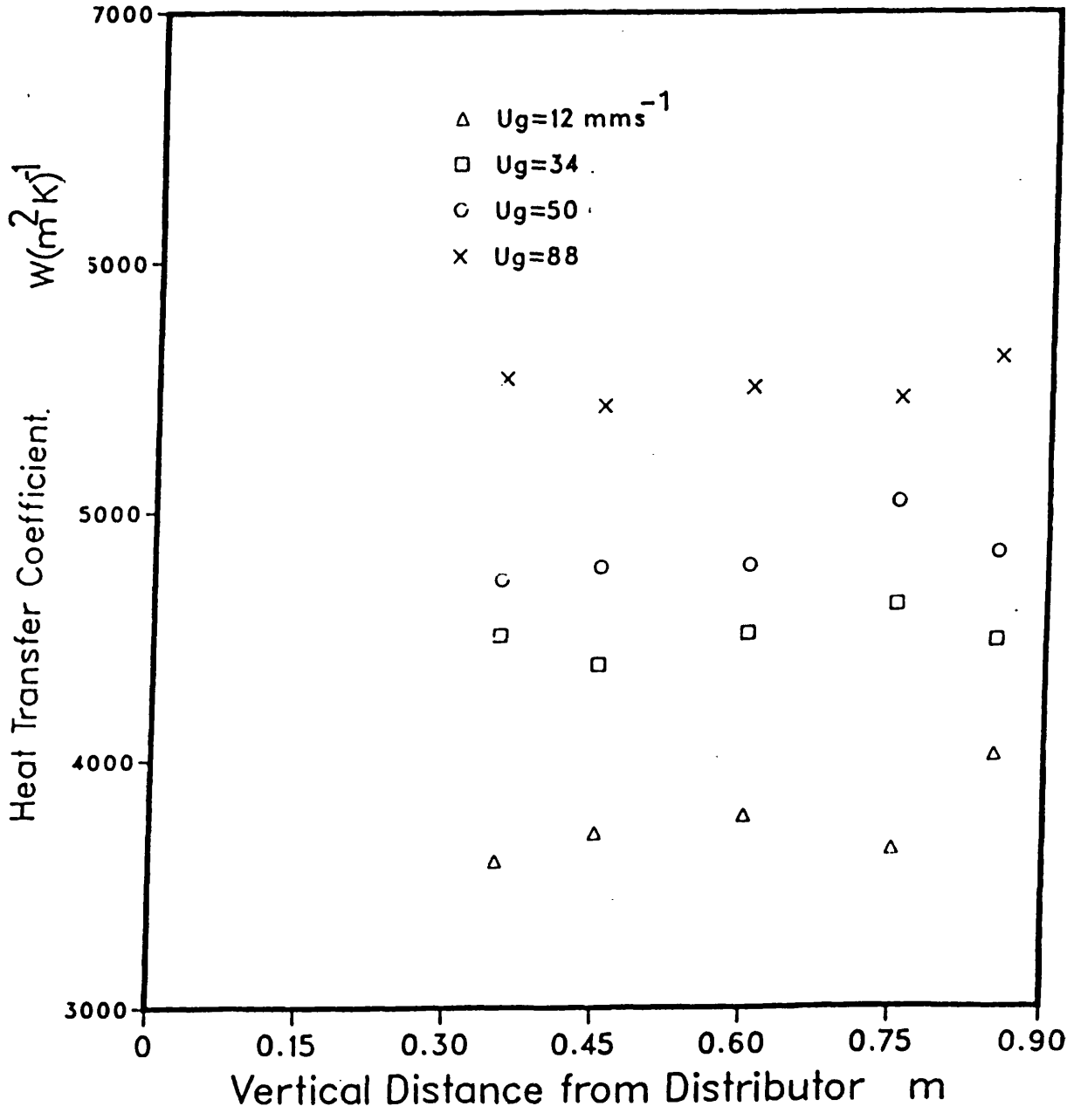

Figure 5.11.- Effect of Heater Position.
Variation of heat transfer coefficient with the heater vertical distance obtained for a water of height 0.90 m with a 30 x 120 mm heater. Distributor 57a. t_b=18 °C.

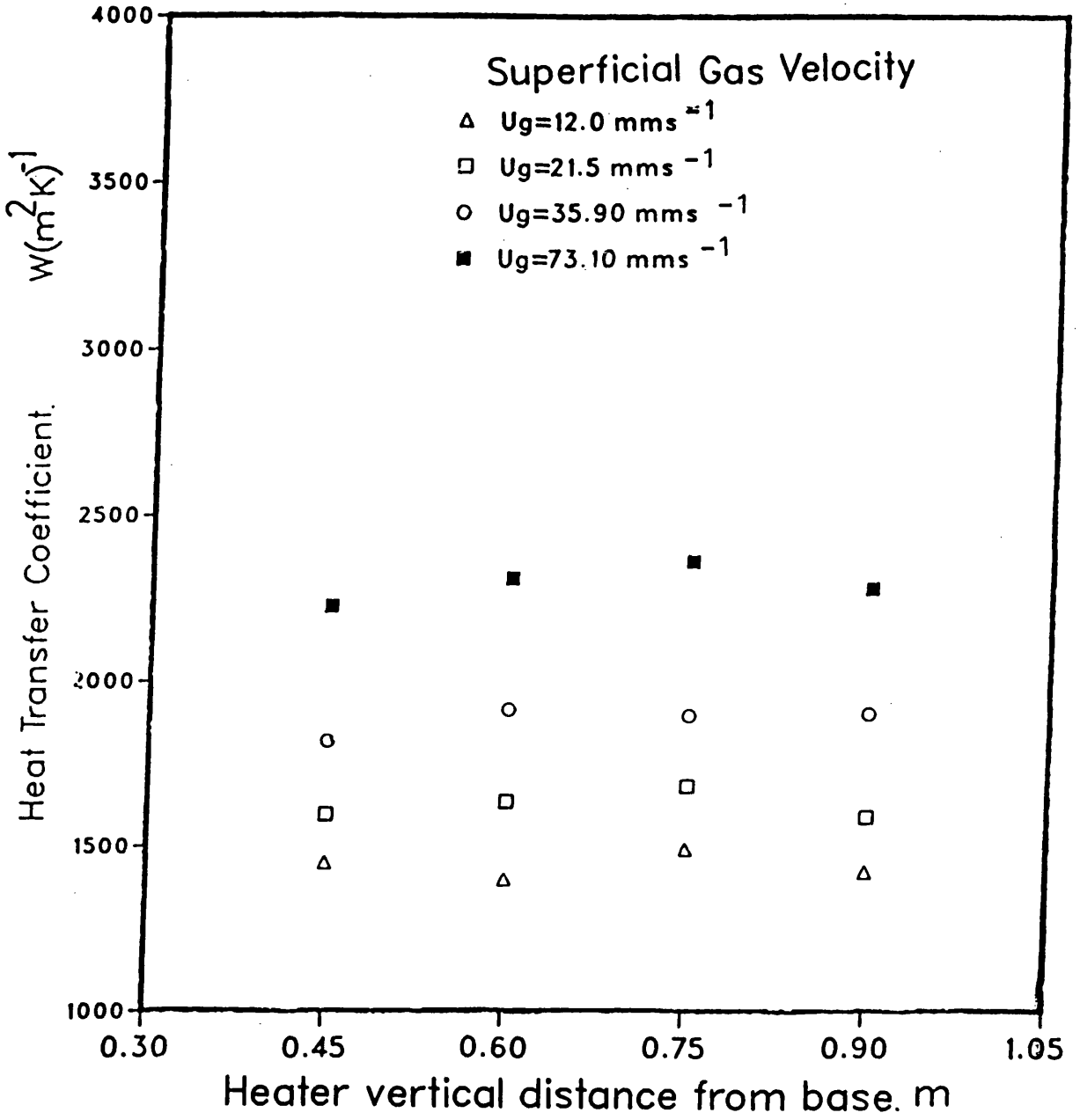

Figure 5.12.- Effect of Heater Vertical Distance from Distribtor.
Varation of heat transfer coefficient with heater vertical distance from distributor obtained for a 3000 ppm CMC solution of height 0.90m with a 30 x 60 mm heater. Distributor used 57c. t_b=18.3 ^{o}C

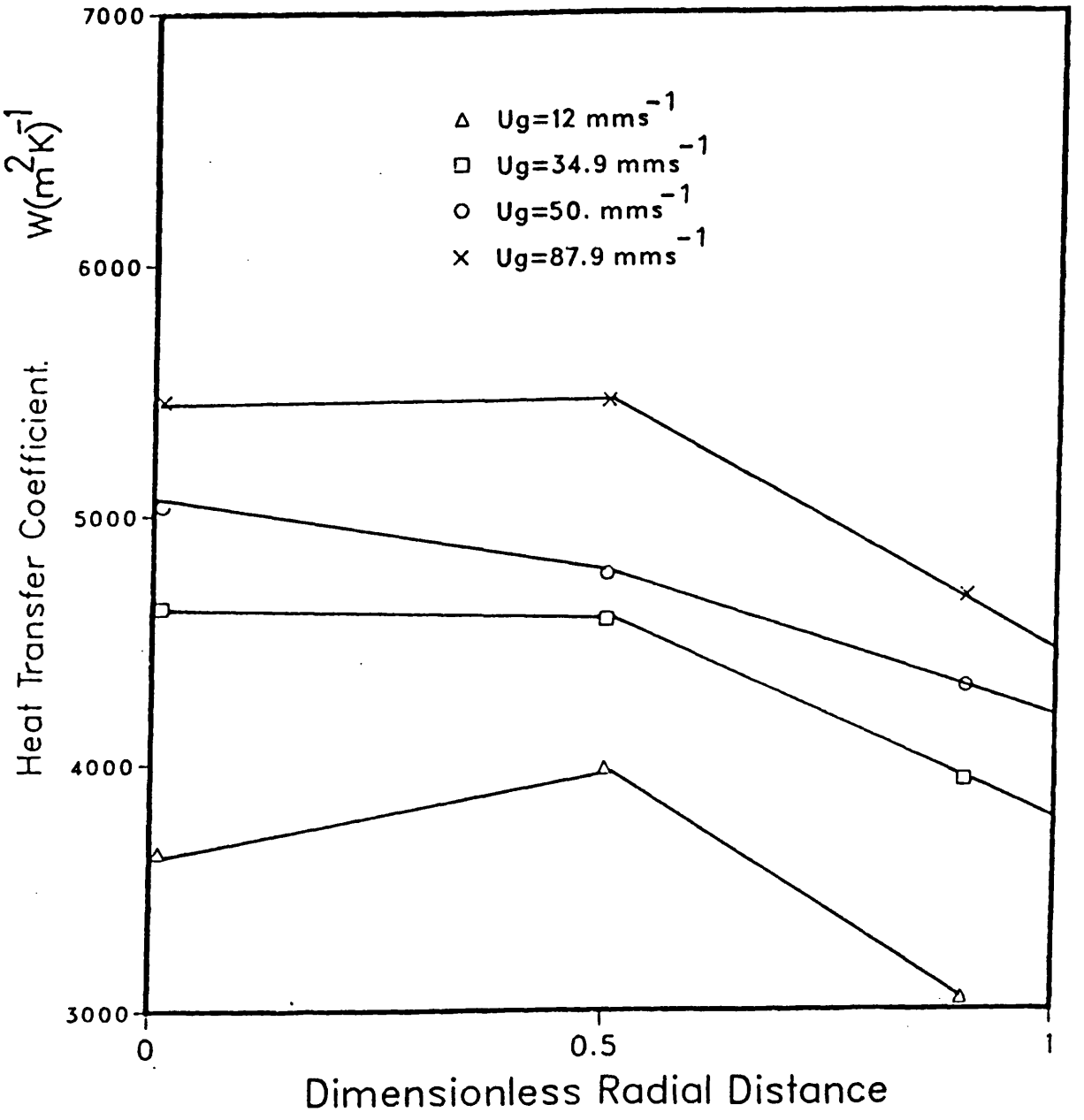

Figure 5.13(a).- Effect of Heater Radial Position. Variation of heat transfer coefficient with superficial gas velocity obtained for a water of height 0.90m with a 30 x 120 mm heatermounted verically at 0.75 m from distributor. Distributor used 57a. t_b=18 °C.

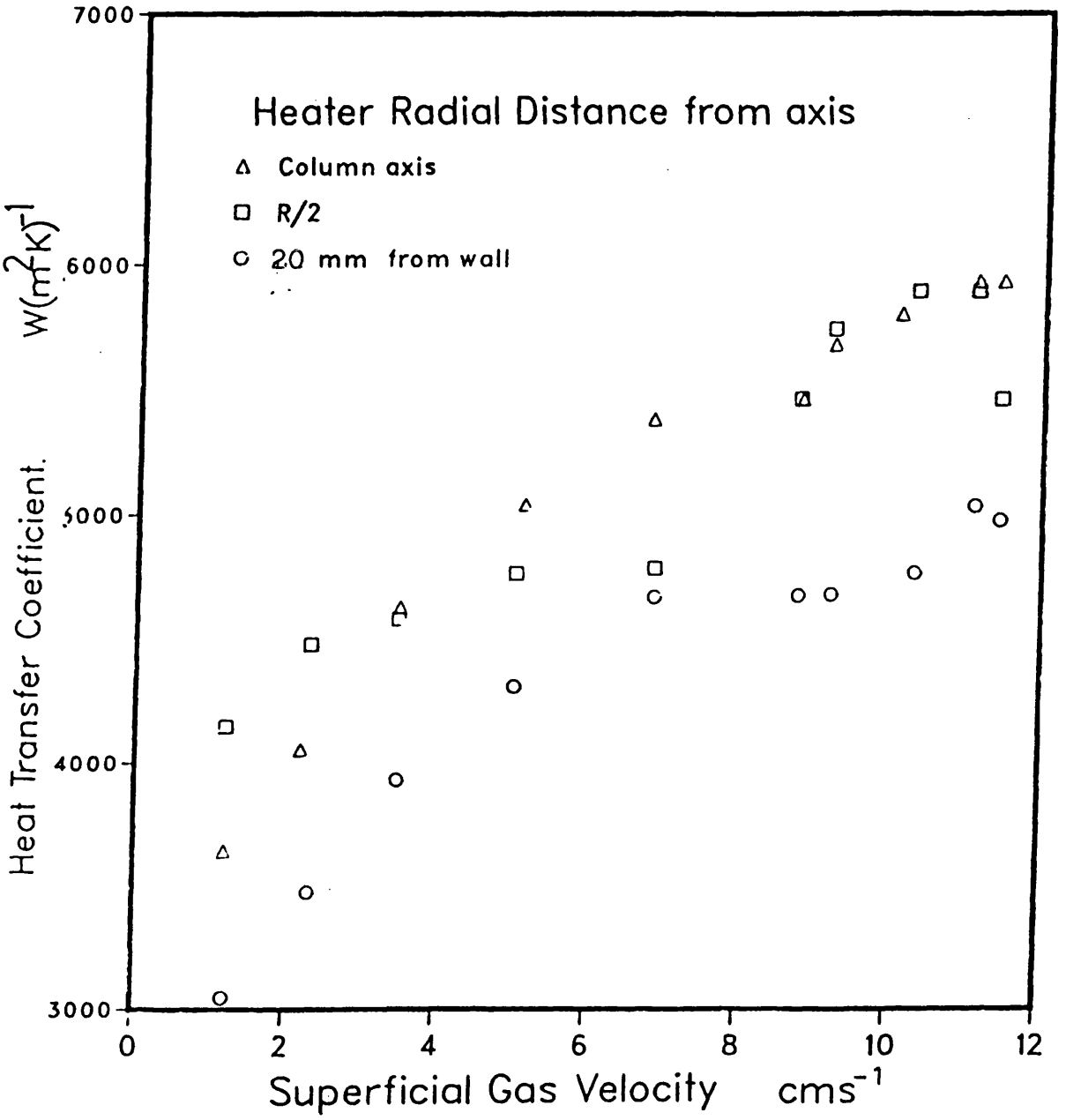

Figure 5.13(b).- Effect of Heater Radial Position. Variation of heat transfer coefficient with heater radial distance for a water of height 0.90 m obtained with a 30 x 120 mm heater mounted vertically at 0.75 m from base. Distributor used 57a. t_b =18 °C.

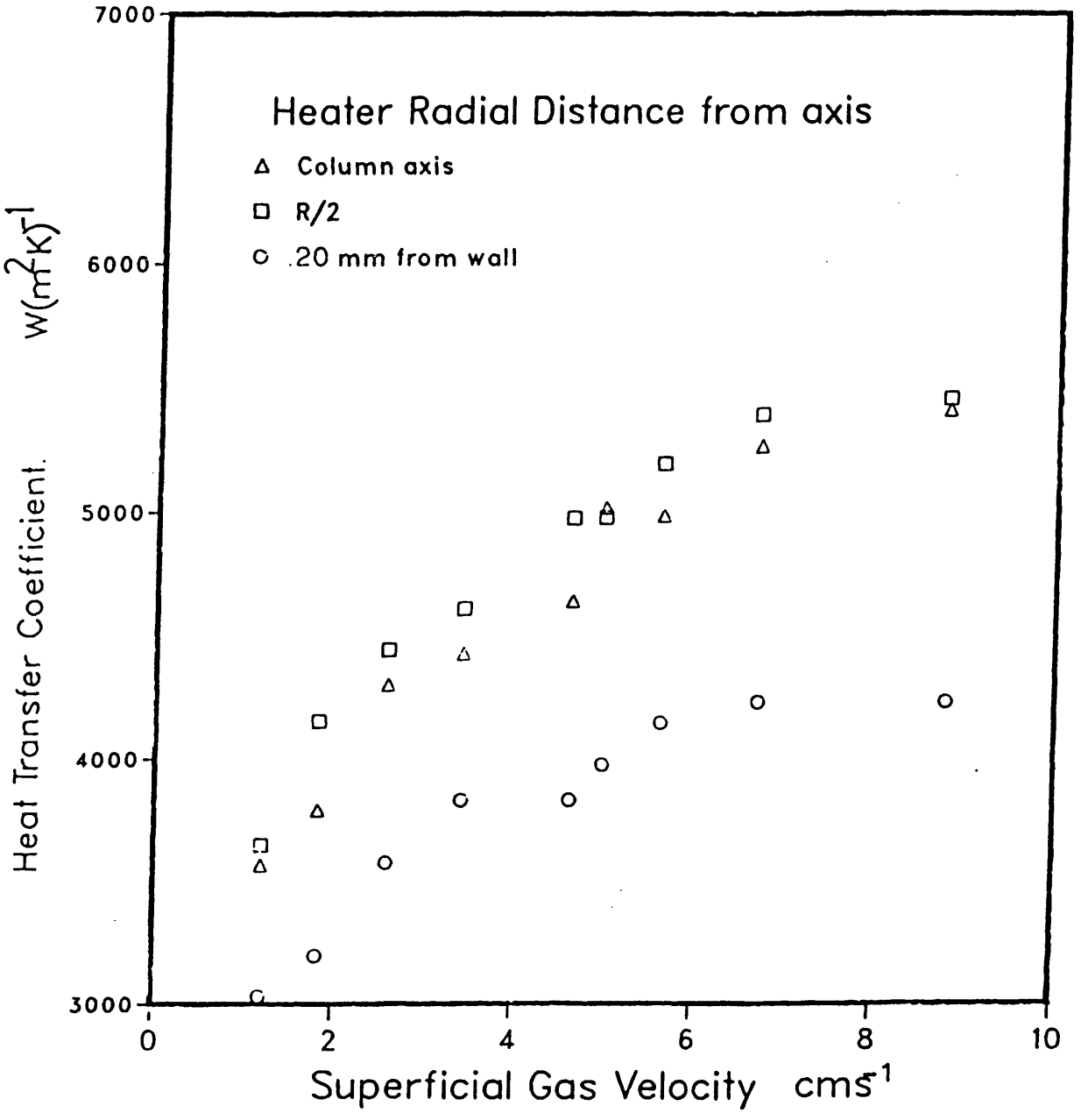

Figure 5.14(a).-Effect of Heater Radial Position. Variation of heat transfer coefficient with superficial gas velocity obtained for a water of height 1.20 m with 30 x 120 mm heater mounted vertically at 0.75 m from distributor. Distributor used 57a. t_b=18 °C.

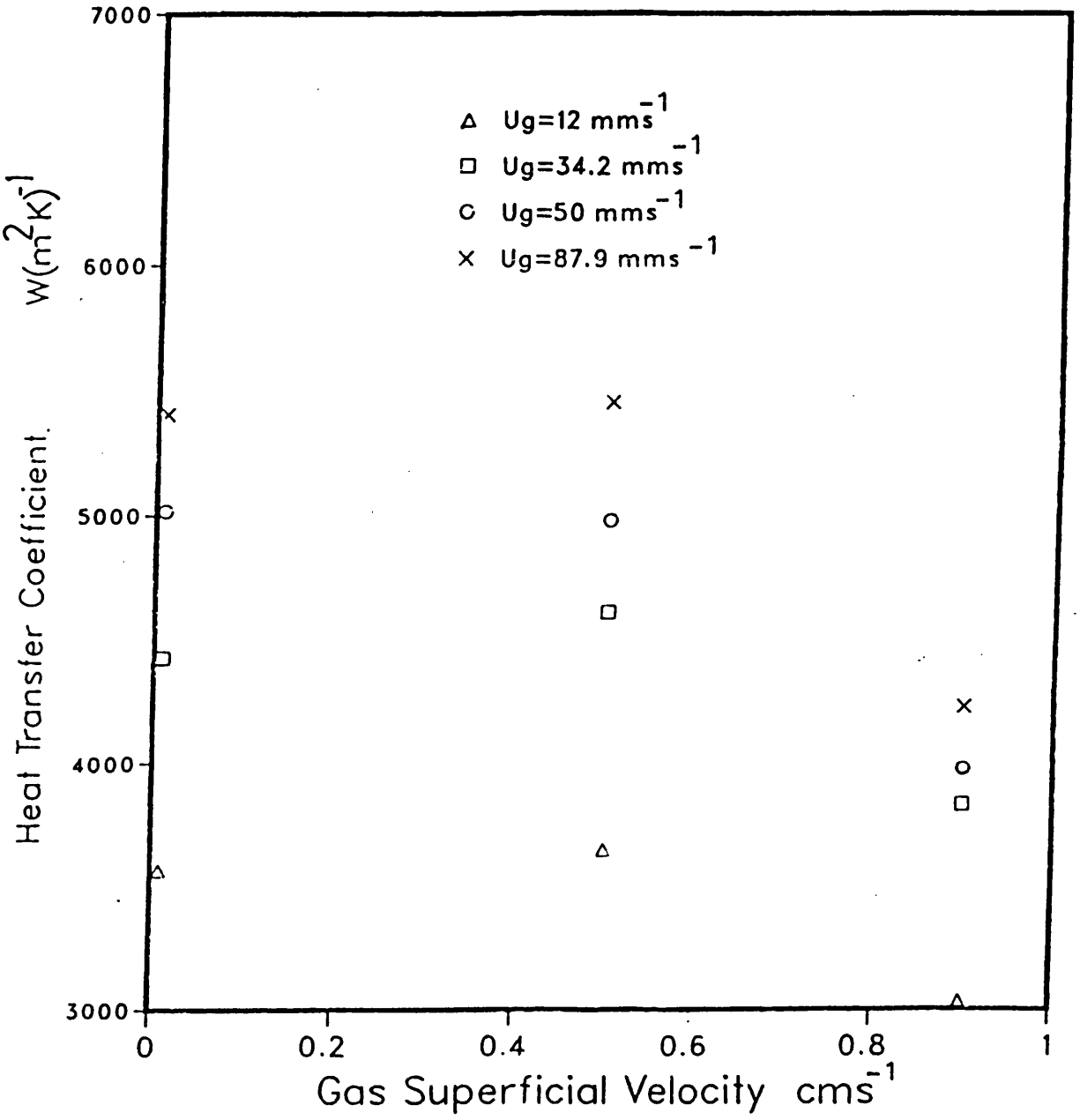

Figure 5.14(b).-Effect of Heater Radial Position. Variation of heat transfer coefficient with heater radial distance obtained for a water of height 1.20 m with 30 x 120 m heater monted vertically at 0.75 m from distributor. Distributor uesd 57a. t_b=18 °C.

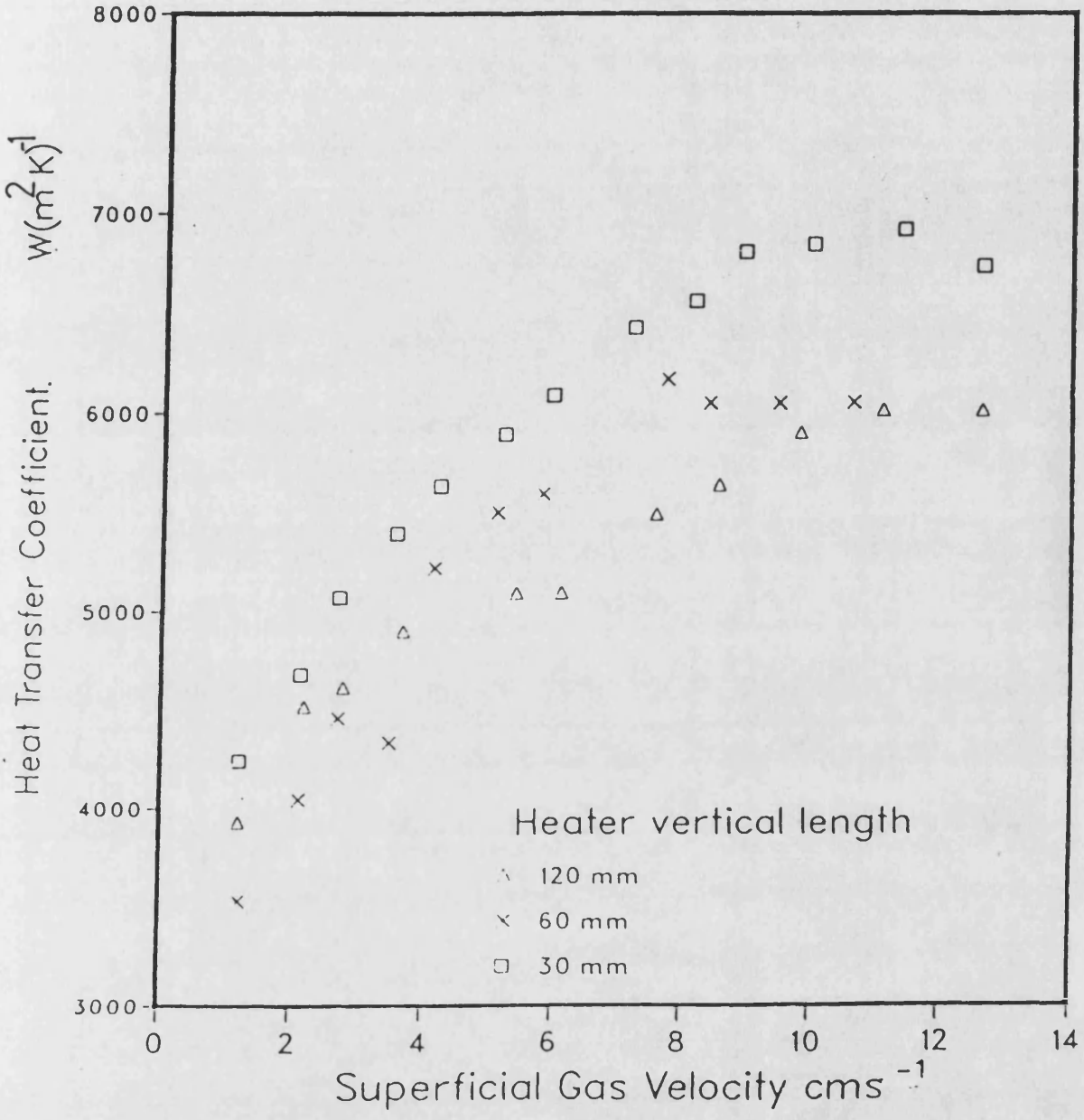

Figure 5.15.- Effect of Heater Vertical Length. Variation of heat transfer coefficient with superficial gas velocity obtained for a water height of 0.90m with heaters of 30 mm in diameter and 30, 60 and 120 mm in length. Distributor used 57c. t_b= 18 °C.

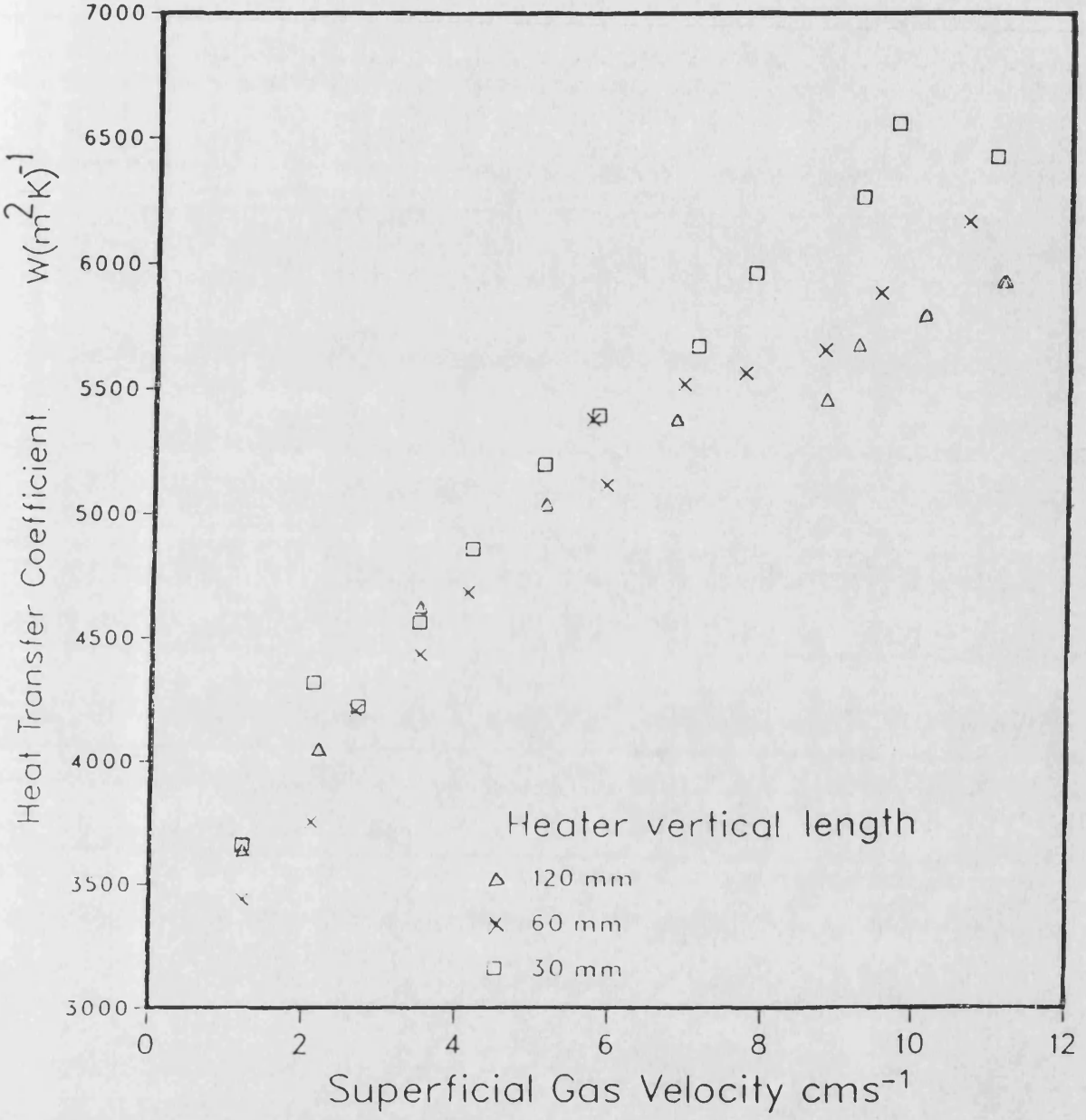

Figure 5.16.-Effect of Heater Vertical Length. Variation of heat transfer coefficient with superficial gas velocity obtained for a water height of 0.90m with heaters of 30 mm in diameter and 30, 60 and 120 mm in length. Distributor used 57a. t_b=18 °C.

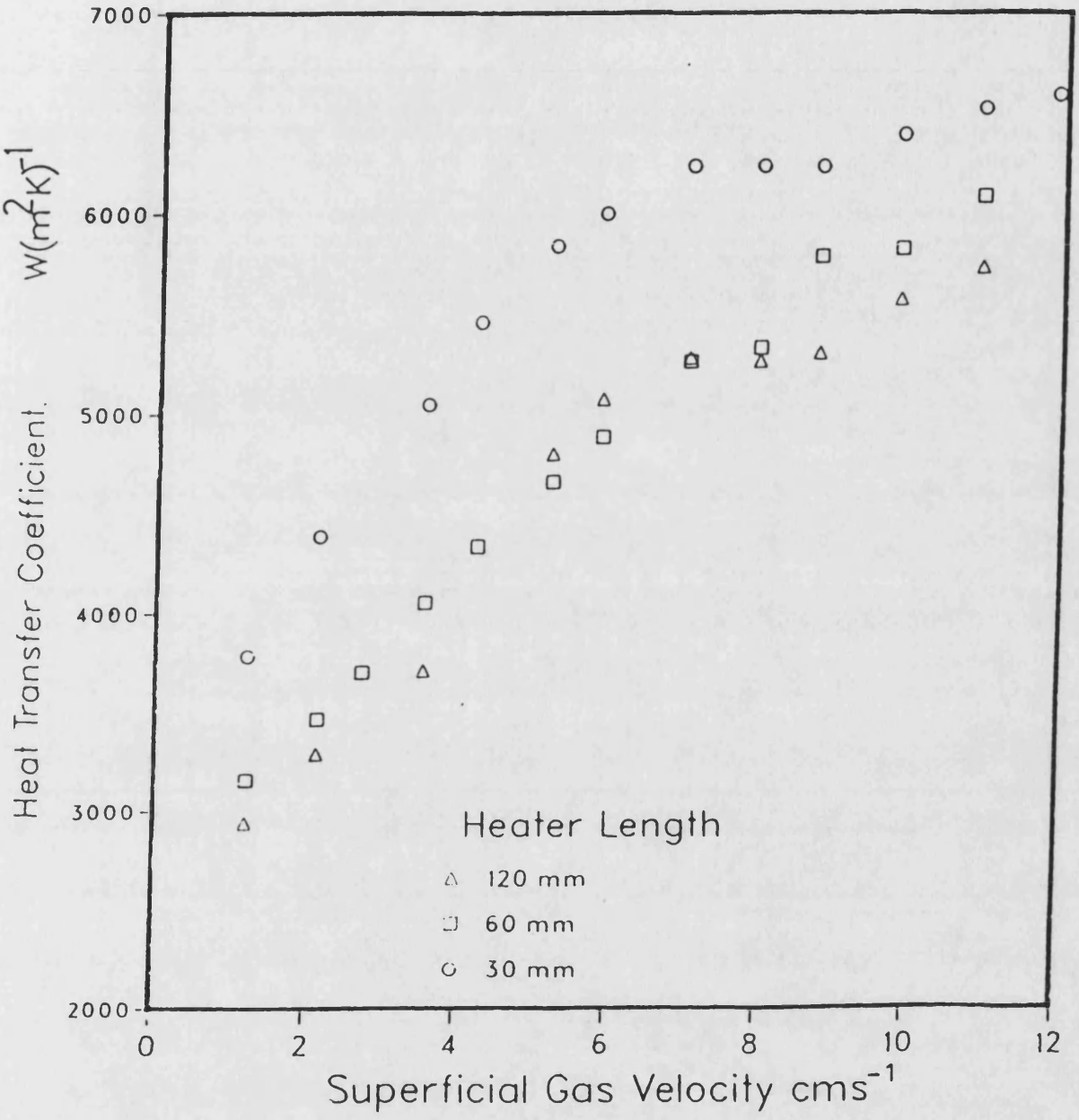

Figure 5.17. Effect of Heater Vertical Length. Variation of heat transfer coefficient with superficial gas velocity obtained for a 100 ppm CMC solution of height 0.90 m with heaters of 30mm in diameter and 30, 60 and 120 mm in length. Distributor 57c. t_b= 18 ^{o}C.

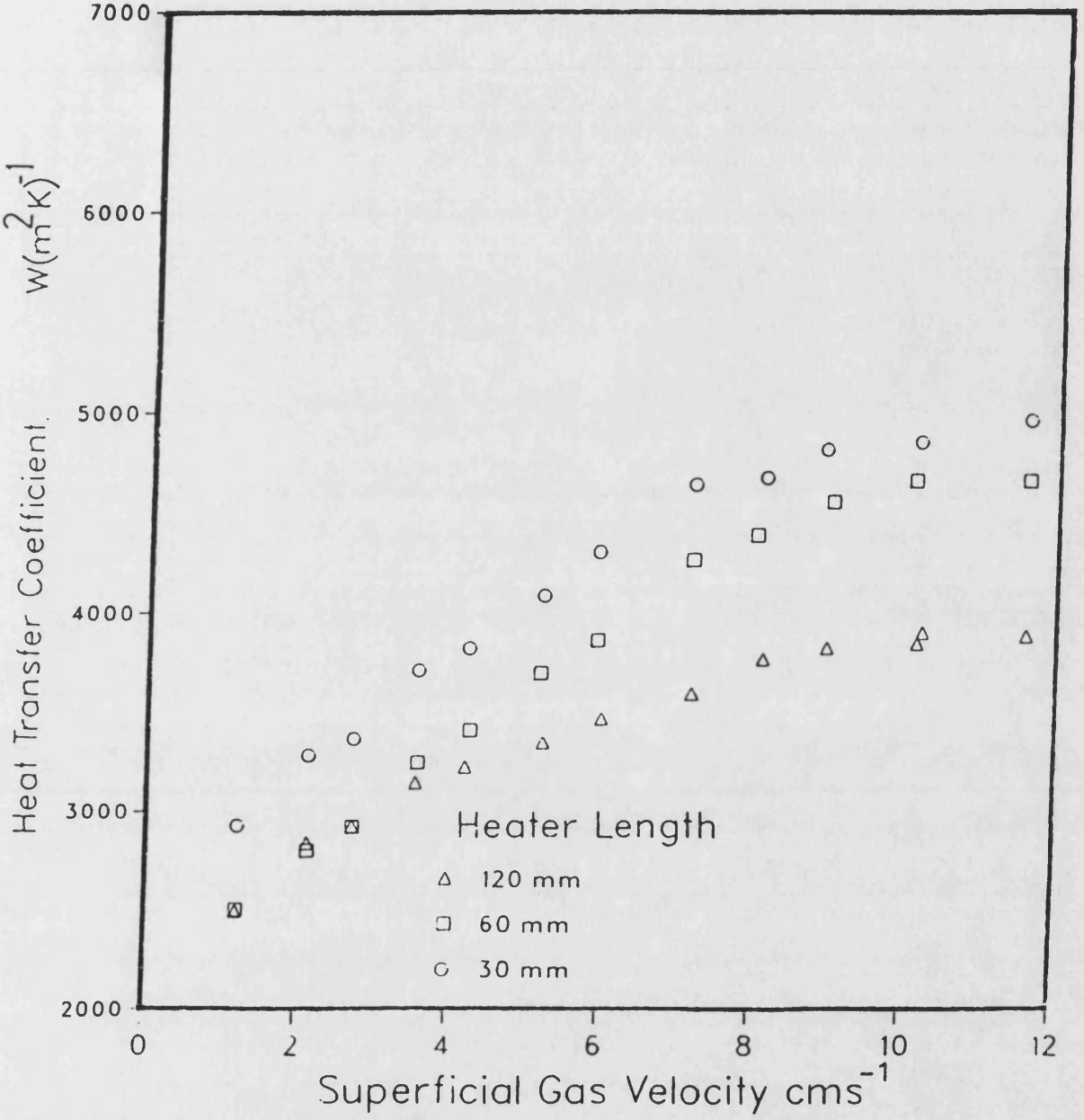

Figure 5.18.- Effect of Heater Vertical Length. Variation of heat transfer coefficient with superficial gas velocity obtained for a 500 ppm CMC solution of height 0.90 m with heaters of 30mm in diameter and 30, 60 and 120 mm in length. Distributor used 57c. t_b= 18 ^{o}C.

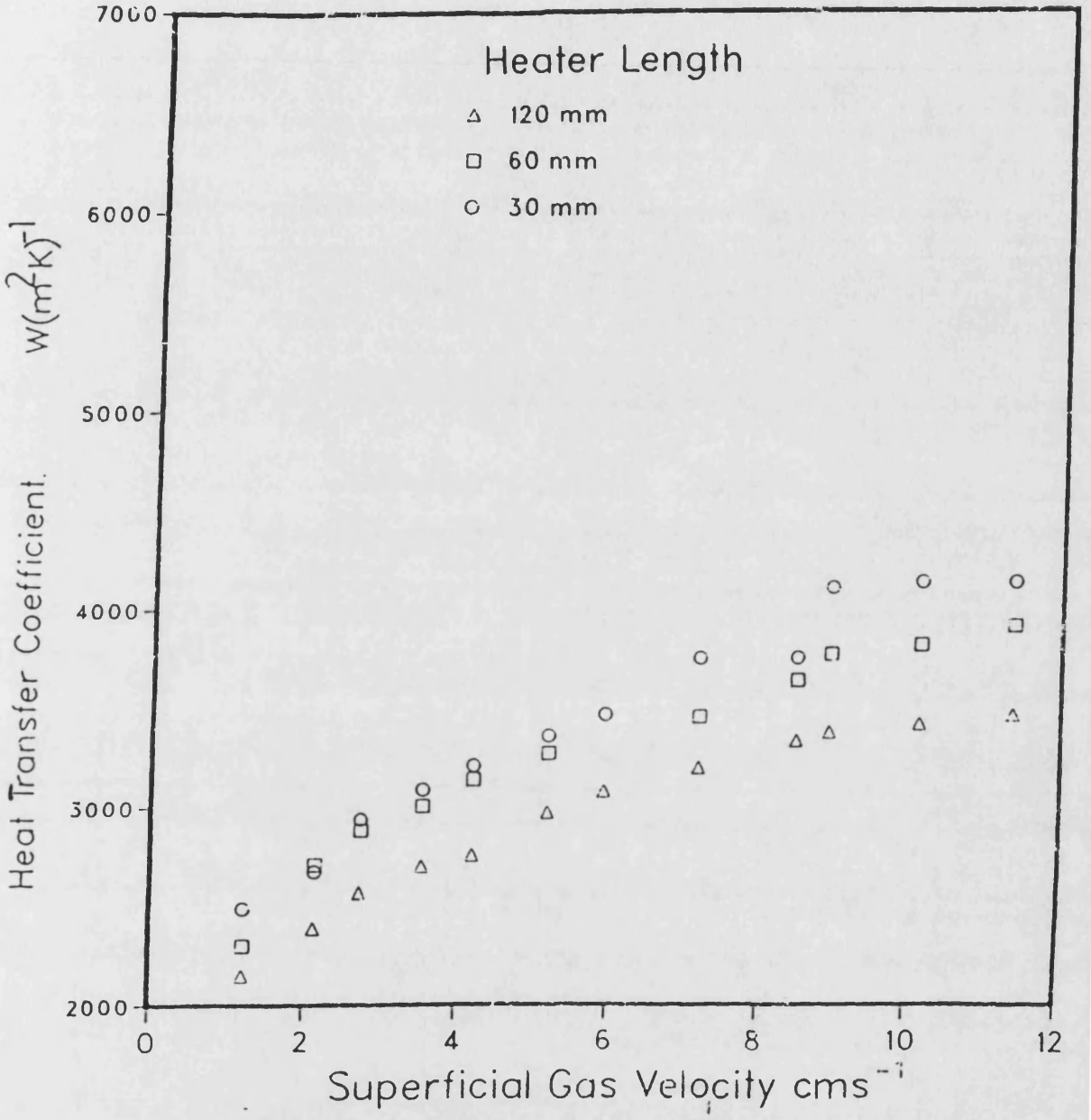

Figure 5.19.- Effect of Heater Vertical Length. Variation of heat transfer coefficient with superficial gas velocity obtained for a 1000 ppm CMC solution of height 0.90m with heaters of 30mm in diameter and 30, 60 and 120 mm in length. Distributor used 57c. t_b=18.3 °C.

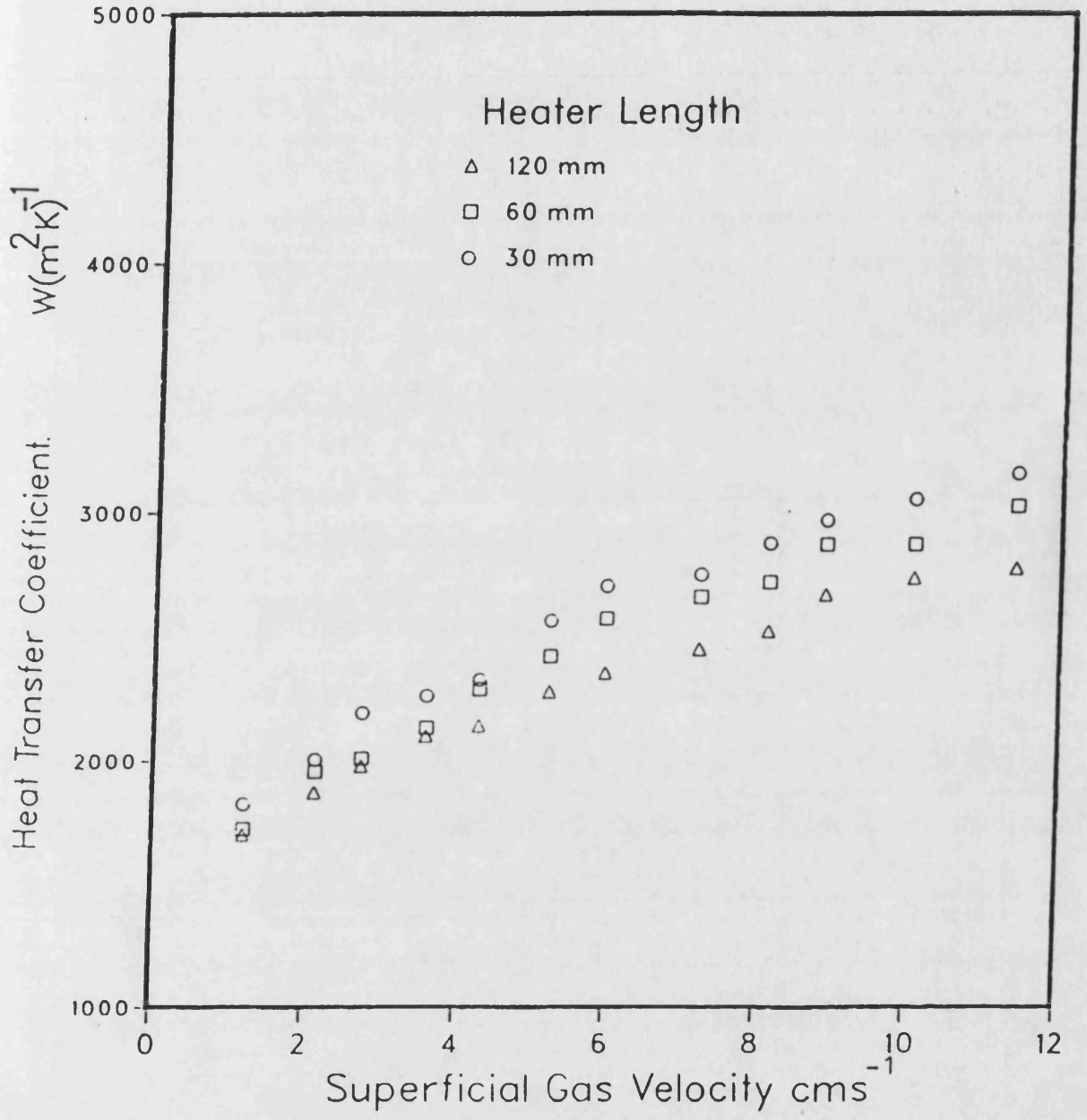

Figure 5.20.- Effect of Heater Vertical Length for 2000 ppm CMC solution.

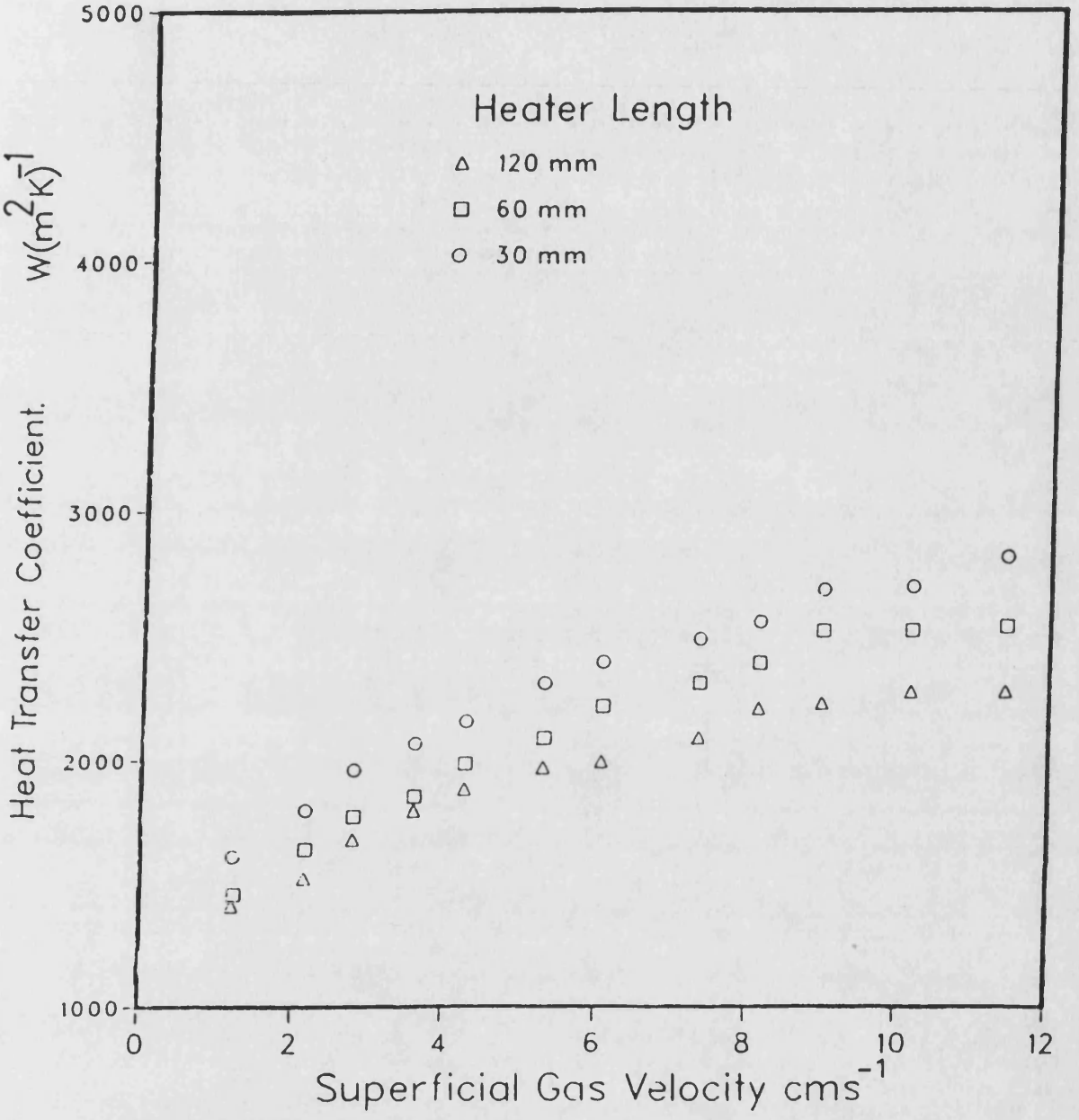

Figure 5.21.- Effect of Heater Vertical Length for 3000 ppm CMC solution.

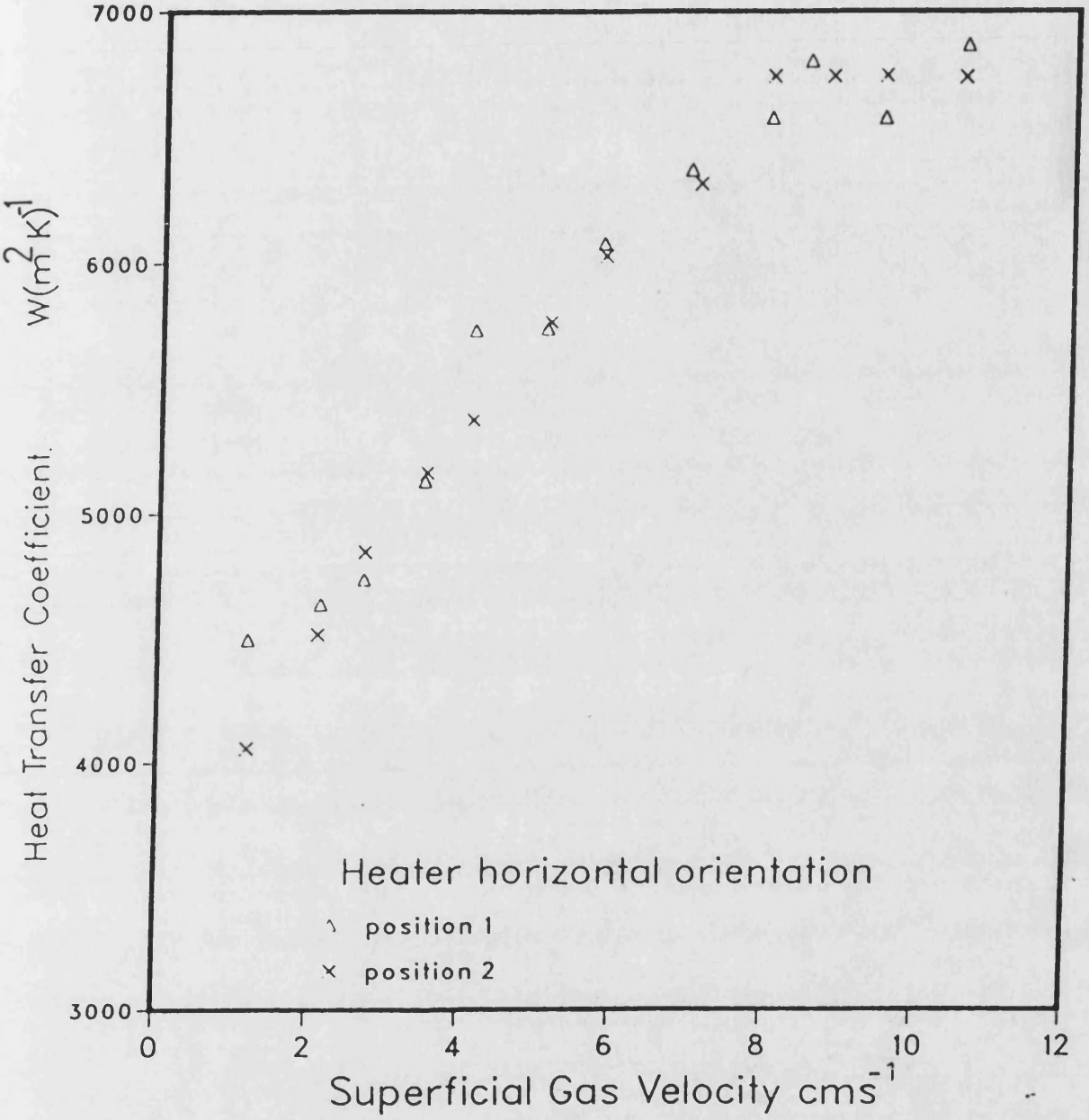

Figure 5.22.- Effect of Horizontal Heater Rotation. Varation of heat transfer coefficient with superficial gas velocity obtained for a water of height 0.90 m with 30 x 120 mm heater mounted horizontally at 0.75 m from 57c distributor.

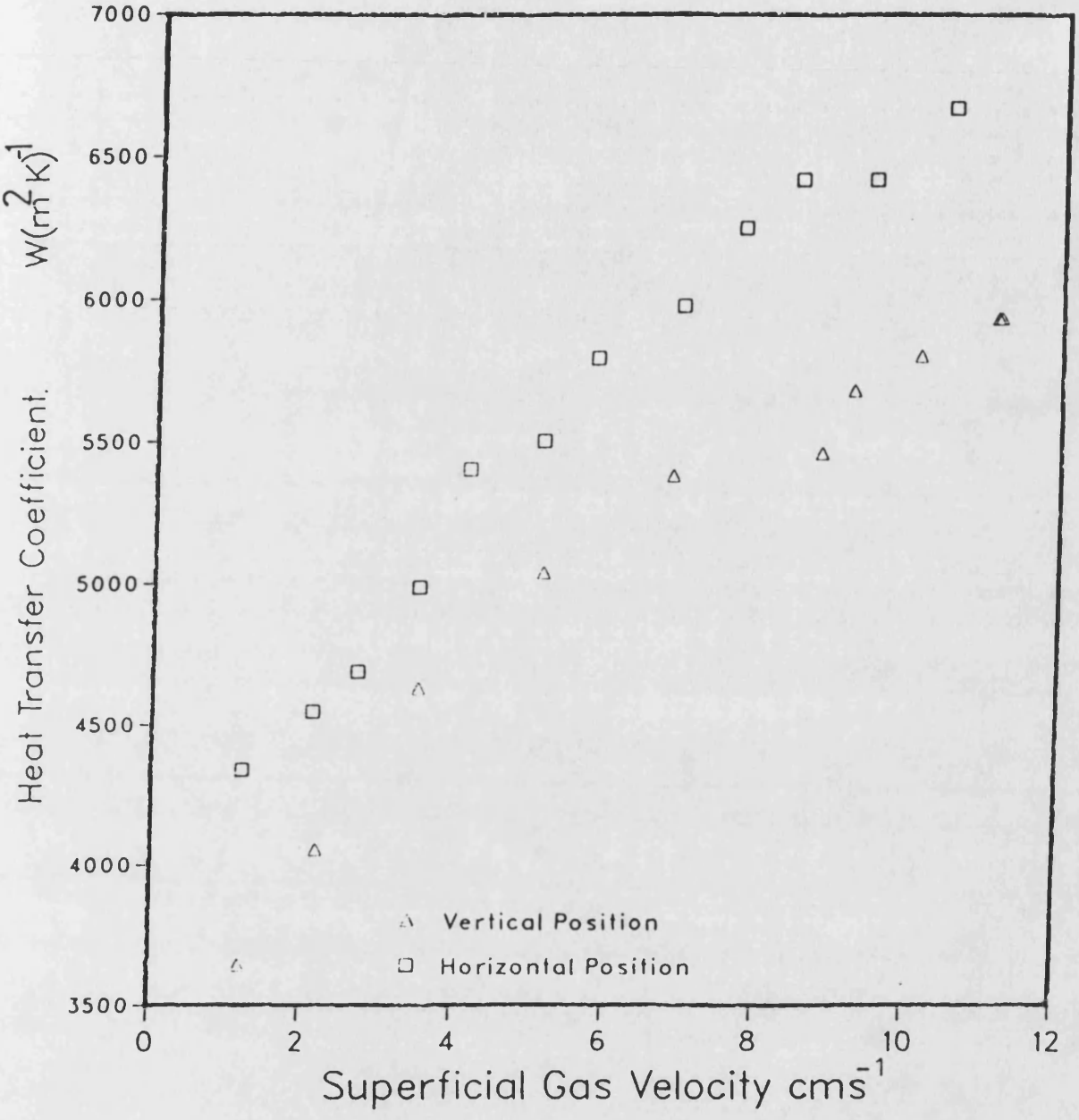

Figure 5.23.- Effect of Heater Orientation.
Variation of heat transfer coefficient with superficial gas velocity obtained for water of height 0.90 m with 30 x120 mm heater mounted vertically at 0.75 m from 57a distributor.

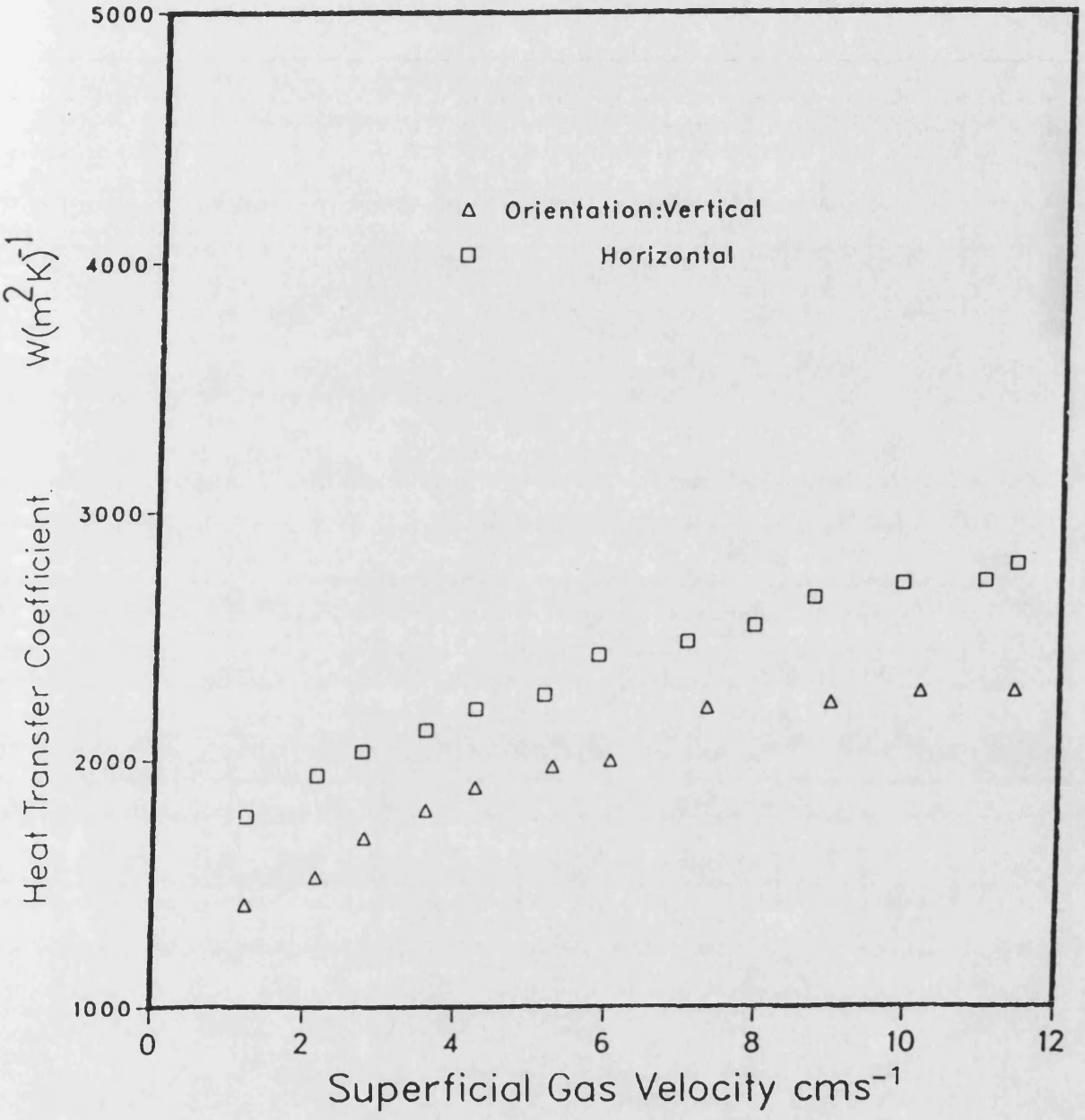

Figure 5.24.- Effect of Heater Orientation. Variation of heat transfer coefficient with superficial gas velocity obtained for a 3000 ppm CMC solution of height 0.90 m with 30 x 120 mm heater. Distributor used 57c. t_b= 18 °C.

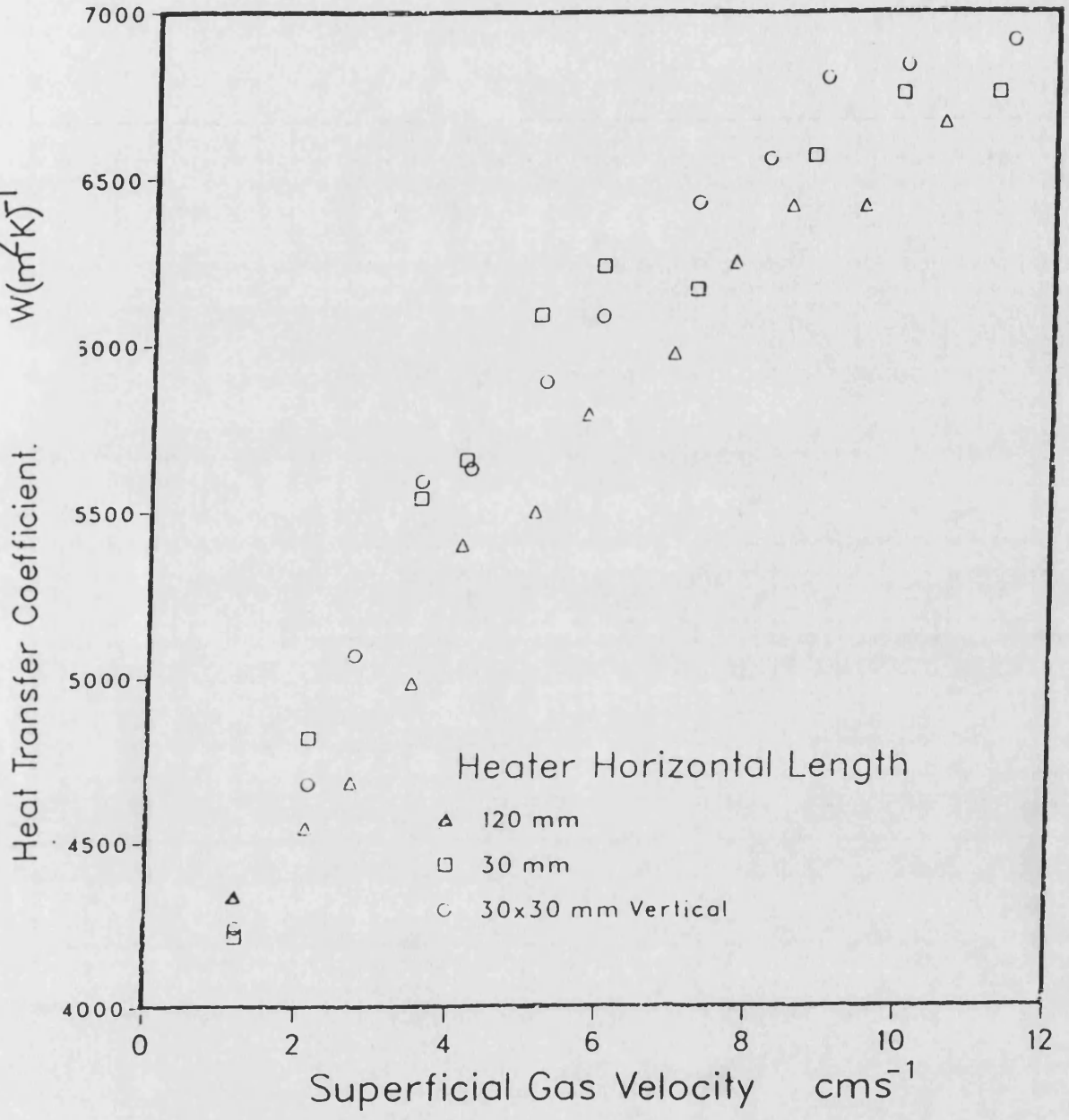

Figure 5.25.-Effect of Heater Horizontal Length. Variation of heat transfer coefficient with superficial gas velocity obtained for a water of height 0.90m with with heaters of 30mm in diameter. Distributor used 57a.

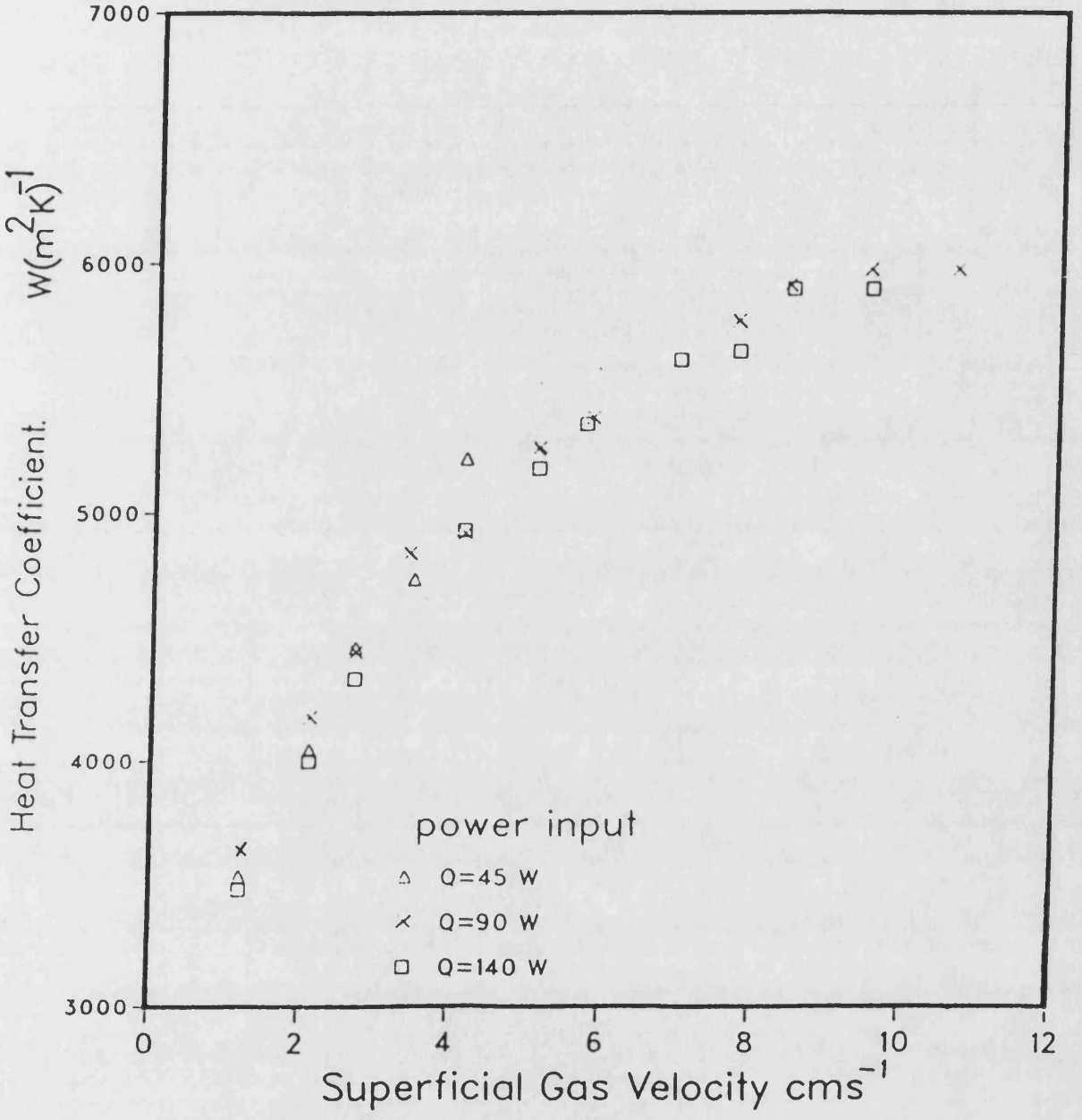

Figure 5.26.- Effect of Power Input.
Variation heat transfer coefficient with superficial gas velocity obtained for a water height of 0.90 m with 30 x 60 mm heater mounted vertically on the column axis at 0.75 m from disteributor. Distributor used 57c.

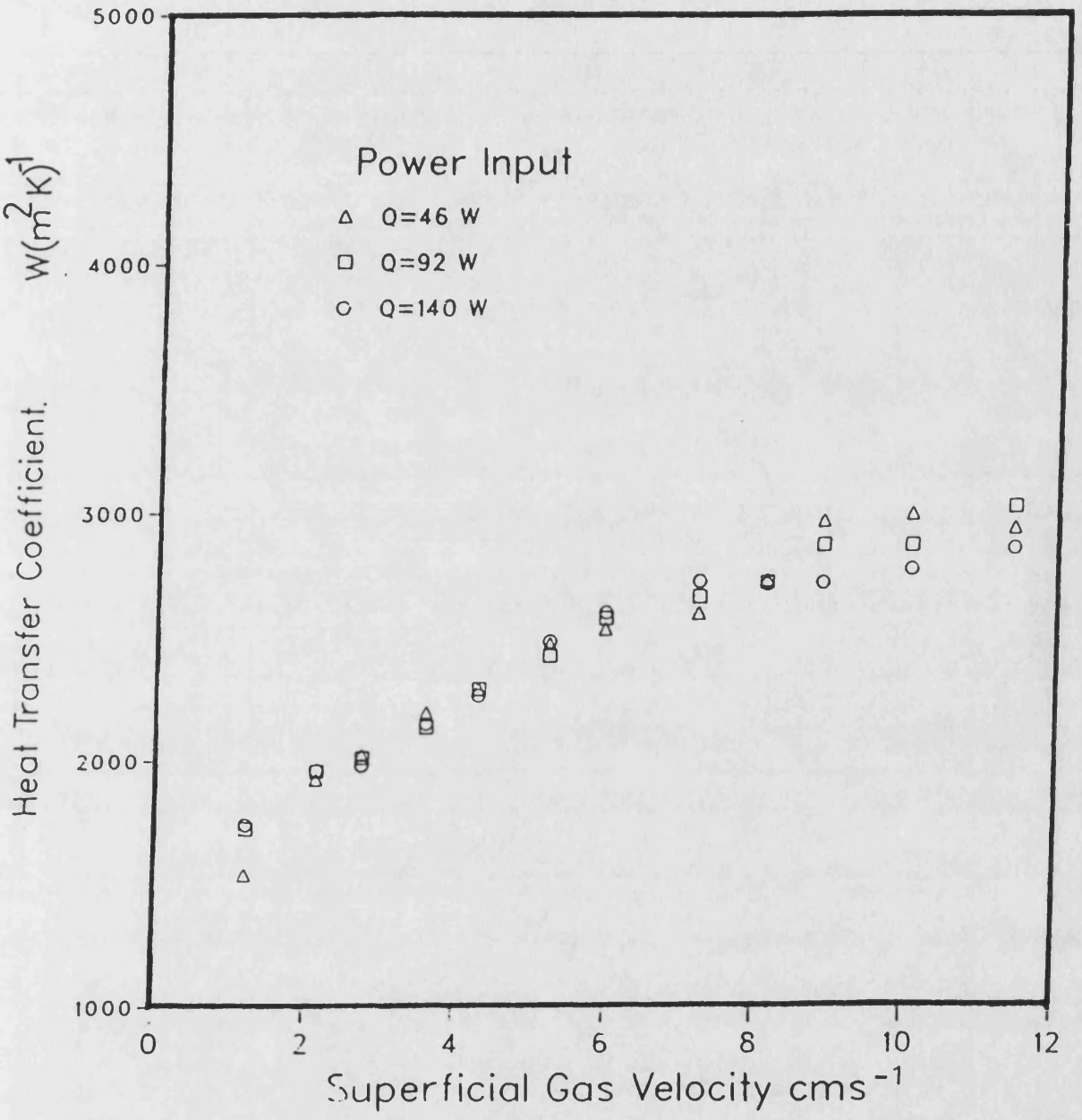

Figure 5.27.- Effect of Power Input.
Variation of heat transfer coefficient with superficial gas velocity obtained for a 2000ppm CMC solution of height 0.90 m with a 30 x60 mm heater mounted vertically at 0.75 m from the distributor. Distributor used 57c. t_b= 17.7 ^{o}C.

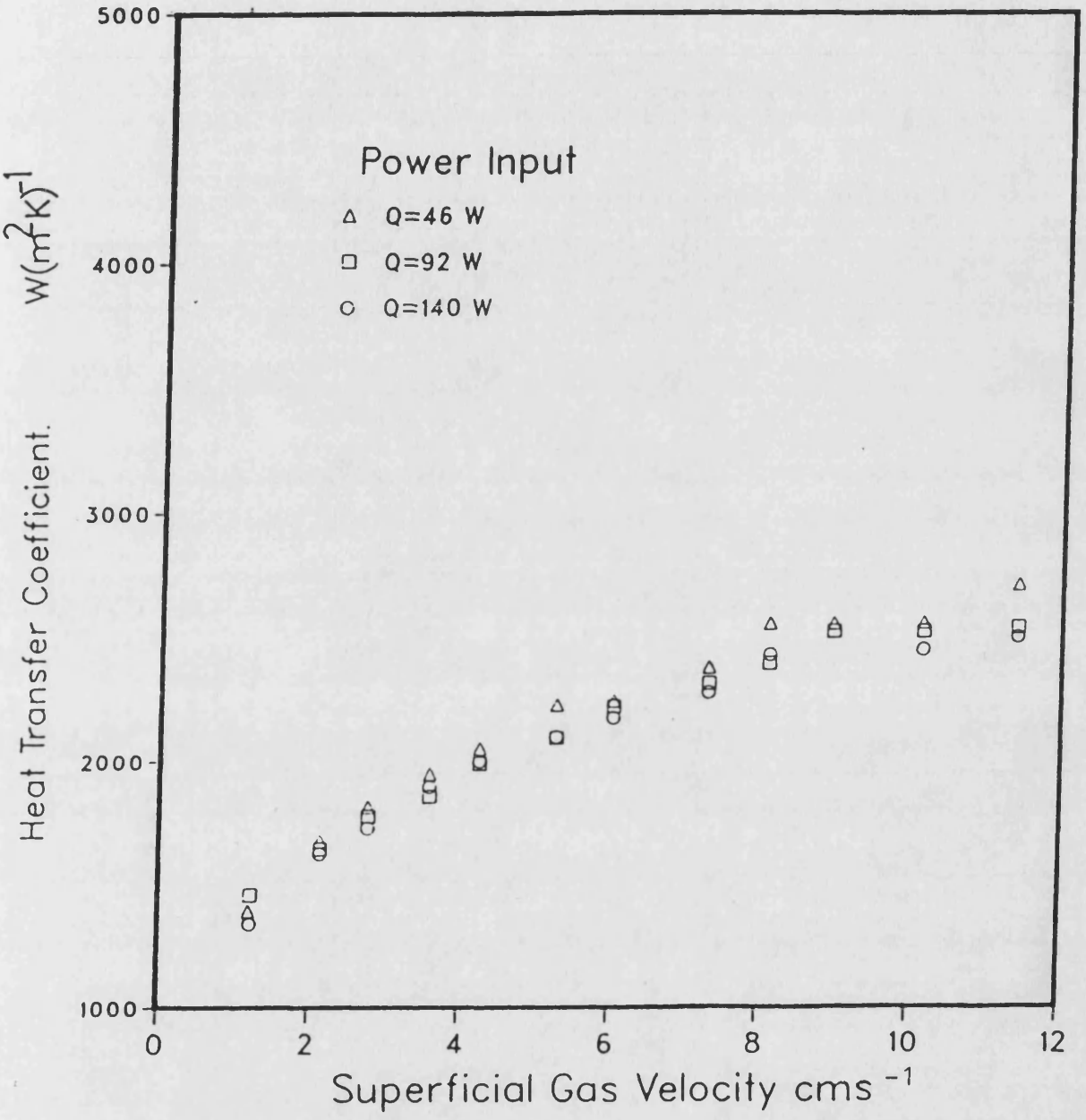

Figure 5.28.- Effect of Power Input.
Variation of heat transfer coefficient with superficial gas velocity obtained for a 3000ppm CMC solution height of 0.90 m with a 30 x 60 mm heater mounted vertically at 0.75 m from the distributor. Distributor used 57c. t_b= 18.1 °C.

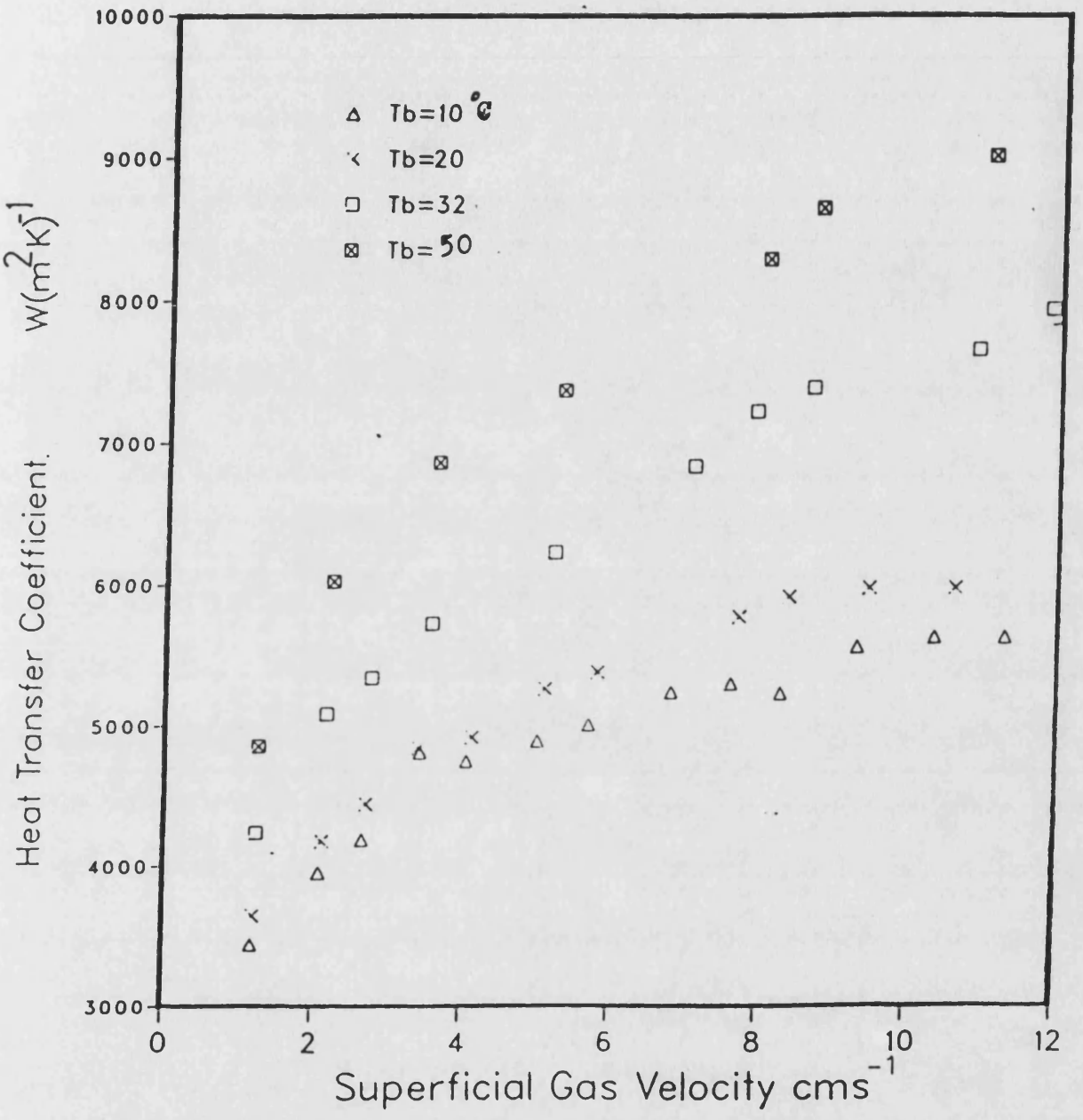

Figure 5.29.- Effect of Bulk Temperature.
Water height 0.90m. Heater 30 x 60 mm Distributor 57c.

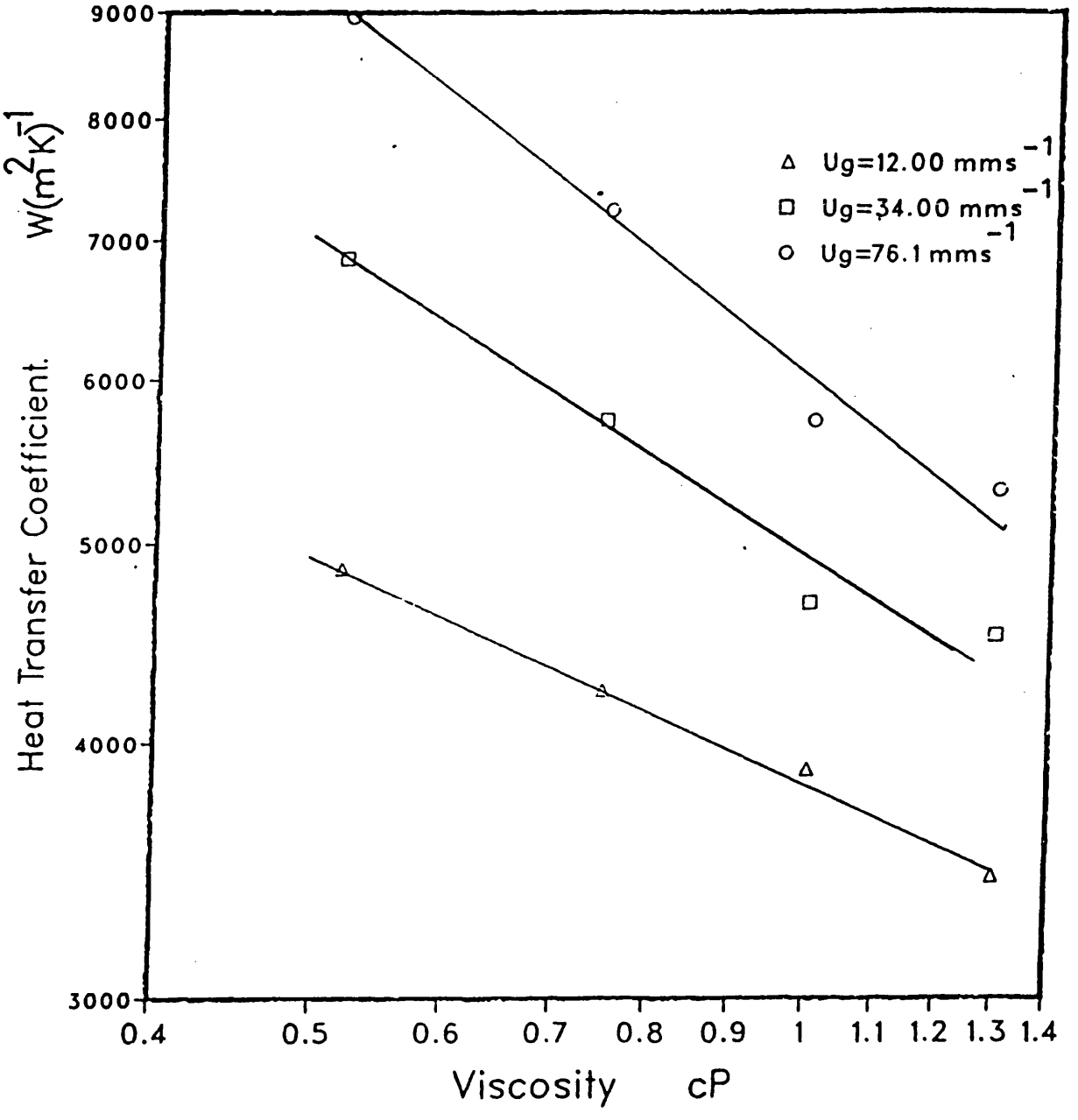

Figure 5.30.- Variation of heat transfer coefficient with viscosity obtained for a water of height 0.90 m with a 30 x60 mm heater mounted vertically.

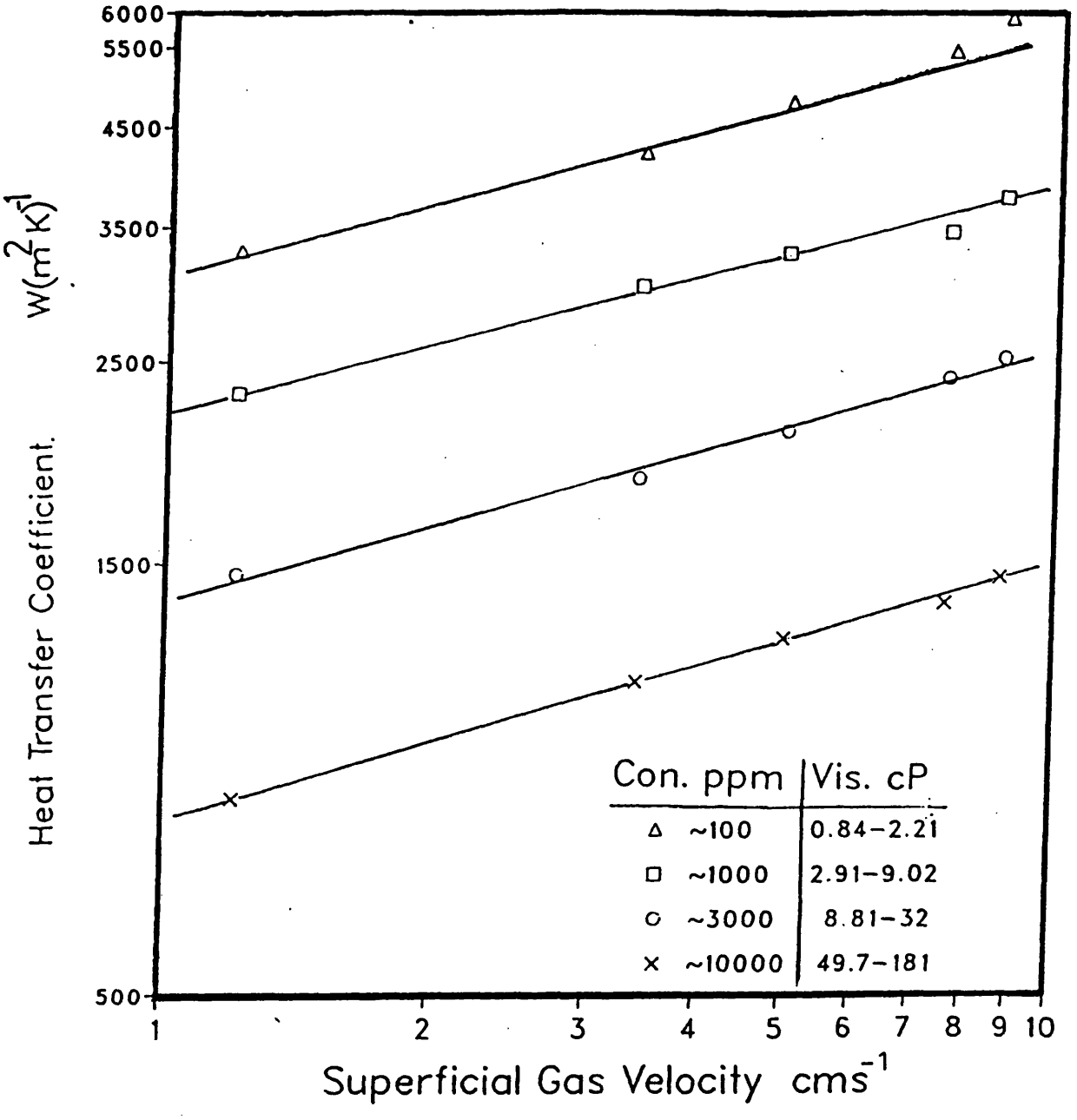

Figure 5.31.- Effect of Concentration of CMC solutions.
CMC solutions height were 0.90 m. 30 x 60 mm heater used. Distributor used 57c.

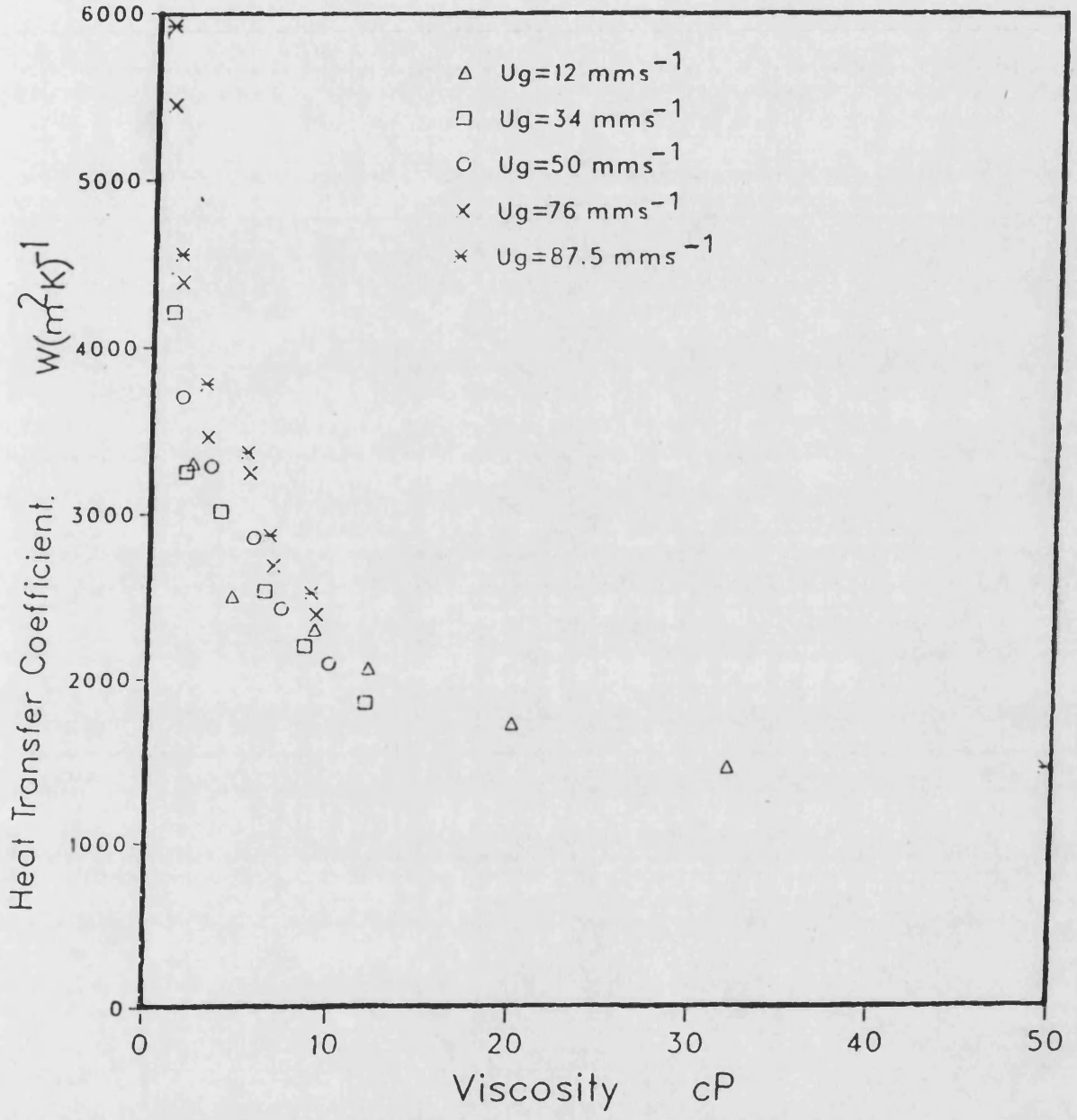

Figure 5.32.- Variation of heat transfer coefficient with viscosity of CMC solutions obtained with solutions height of 0.90 m with 30 x60 mm heater positioned vertically on the column axis at 0.75 m from distributor. Distributor used 57c. Q= 90 W, t_b = 18 ^{o}C.

CHAPTER 6

HEAT TRANSFER FROM A BUNDLE OF HEATERS

6.-INTRODUCTION

Many modifications of bubble columns, such as bubble columns with downcomers, packed bubble columns and sectionalized bubble columns (eg. columns that have horizontal baffles) have been suggested in recent years to suit certain specific processes. For example, sectionalized bubble columns have been suggested to reduce backmixing. Furthermore sectionalized bubble columns provide high values of the gas holdup, as well as high values of heat and mass transfer coefficient. This was reported by Patil et al (1984). However information on the effect of different obstacles, such as heat exchanger tubes or vertical baffles, inside bubble columns on the hydrodynamics and transport properties are scarce.

Patil et al (1984) reported that for a sectionalized bubble column the gas hold-up is higher compared with that of a normal bubble column. Yamashita (1987 a) reported that gas hold-up does not depend on the cross-sectional shape of the baffles plates, but rather on their cross-sectional area. Yamashita (1987 b) reported that insertion of vertical pipes and rods reduced the

effective column cross-sectional area and hence increased the actual gas superficial velocity and therefore it appeared that the existance of vertical rods increases gas hold-up. He also reported that the gas hold-up does not depend on the arrangements of the rods. This is consistant with his earlier investigation (1985) that the gas hold-up is independent of cross-sectional shape of the column.

No information on the effect of column internals on the liquid circulation in bubble columns was found in the literature in course of the present study. However Patil et al (1984) explained the increase of the average mass transfer or heat transfer coefficients in sectionalized bubble columns with qualitative reference to energy balance liquid circulation model.

It was said that one expects that when gas hold-up is high (as is the case with sectionalized bubble column) more energy will be dissipated at the gas liquid interface and less energy will be dissipated in the bulk of liquid therefore, the liquid circulation velocity is expected to be low. This is only true of simple bubble columns where energy is dissipated uniformally in the column. However, in the case of sectionalized bubble column the horizonatal baffles limit liquid flow and most of the energy dissipation occurs in the wall region which results in high values of the wall mass transfer coefficient and by analogy the high heat transfer coefficient.

Wendt et al (1984) work on the heat transfer to horizontal

tube bundles in bubble columns is the only known work directly relevant to the present study. It was reported that in common with fluidized beds, an increase in the number of rods in the tube bundles decreased the heat transfer coefficient. Also a decrease in the distance between the tube within a bundles reduced the heat transfer coefficient.

It was also reported that the tube arrangements (square pitch or triangle pitch) had a little effect on the heat transfer coefficients. Their proposed equation for co-current bubble column was given as;

$$St = (0.18 + 7.2\times10^{-7})\left[(ReFrPr_L^2)^{1/3}\right]^{-0.87}\times F(N)\times F(P)$$

$$F(N) = N_{row}^{(-0.13 + 1.5\times10^{-6}Re_L)}$$

$$F(P) = \left[\frac{t_R}{H_d}\right]^{(0.22 - 5.2\times10^{-6}Re_L)}$$

t_R= distance between tubes.

H_{dl}= heater diameter.

Re_L= Reynolds number based on the liquid flow rate.

Re = Reynold number based on the gas flow rate.

Given the above background , a decision to conduct an experimental investigation of heat transfer from a horizontal heater bundel was made.

6.1.- EXPERIMENTS.

In these experiments the 57c distributor plate was employed and no noticeable change in gas hold-up compared with the single

heater were observed. The liquid height was kept constant at 0.90 m for most runs and the experiments were carried out at room bulk temperature.

The experimental investigation will be described under the following sub-headings;

1.- Effect of the tube bundle end plate support.
2.- Effect of liquid height.
3.- Effect of vertical position of the heater.
4.- Effect of bundle horizontal rotation.
5.- Effect of number of rows and columns within the bundle.
6.- Effect of tube spacing.

6.1.1.- Effect of the Tube Bundle End Plates.

Experiments were carried out to investigate the effect of the two end plates on the heat transfer coefficient. The heater support plates described in chapter 3 are 165 mm by 165 mm long. The distance between them was 165 mm. The single horizontal heater 30 x 120 mm alone was supported by the end plates and was placed at 0.75 m from the column base.

The variation of heat transfer coefficient with superficial gas velocity for this arrangements is shown in Figure 6.1 together with the variation for a single horizontal heater without the end plates. It shows that the reduction in heat transfer coefficients when the heater suppport was employed is

about 30%.

6.1.2.- Effect of the Liquid Height.

The heater bundle which consisted of 3 rows and 3 columns with a pitch to diameter ratio of 2.25 was used to investigate the effect of water height. Two water heights of 0.90 m and 1.20 m were investigated.

The results of variations of heat transfer coefficients against superficial gas velocity are shown in Figure 6.2. It shows that practically there is no effect of liquid height on the heat transfer coefficient.

6.1.3.- Effect of Vertical Position of the Heater Bundle.

To investigate the effect of heater vertical position, the column was filled with water to height of 0.90 m. The same 3 by 3 heater bundle as used above was positioned at two points, 0.45m and 0.75 m above the column base. The variation of heat transfer coefficient against superficial gas velocity was noted. The results are shown in Figure 6.3. It shows that for the two distances of 0.45 m (50% of the initial column height) and 0.75 m from column base the heat transfer coefficients are approximately equal with the average difference being 3%.

6.1.4.- Effect of Horizontal Rotation of Bundle.

The heater bundle was positioned in two directions. Direction 1 corresponds to direction 6-5-9-1-2 and direction 2 correspond to direction 8-7-9-3-4 as shown in figure 3.8.

The variation of heat transfer coefficient with superficial gas velocity for the two directions are shown in Figure 6.4. It shows that at low gas superficial velocity less than 40 mms^{-1} heat transfer coefficient for direction 2 is about 3% higher than direction 1. Whilst above gas superficial velocity of 40 mms^{-1} the effect of horizontal position of the heater bundle disappears.

6.1.5.- Effect of Number of Rows and Column within the Bundle.

This effect was investigated keeping the pitch to tube diameter ratio approximately constant at 1.25 and 1.23 for the 3 by 3 and 5 by 5 bundles, respectively. Water and 3000 ppm CMC solution were used. The heaters were positioned in direction 2 at 0.75 m from the column base. The results are shown in Figures 6.5(a) and 6.5(b) for water and CMC solutions, respectively. They show that the increase in the number of rows at a specific superficial gas velocity reduces the heat transfer coefficient slightly. The average difference is less than 3.5% for water and CMC data. The values of heat transfer coefficient obtained with the CMC solutions is lower compared with that of water. The viscosity effect on the heat transfer coefficent was discussed in

section 5.7.

6.1.6.- Effect of Tube Spacing.

The effect of tube spacing and the heat transfer coefficient was investigated using the heater bundle of which consisted of 3 rows and 3 columns. The pitch to tube diameter ratios used was 1.25, 1.50, 2.25 and 2.46. The bundles were positioned at 0.75 m from column base in direction 2. Water and 3000 ppm CMC solutions with an unaerated depth of 0.90 m were used. The results are shown as variation of heat transfer coefficient with superficial gas velocity with the employed tube pitches to diameter ratios as parameter in Figure 6.6(a) and Figure 6.6(b). The former results are for CMC solution whilst the latter results are for water on a logarithmic scale.

It is clear from Figure 6.6(a) that increasing the pitch to diameter ratio from 1.25 to 2.46 causes an increase in heat transfer coefficient. However,it appears that in the case of water data (Figure 6.6(b)) further reduction of pitch to diameter ratio from 1.5 to 1.25 has caused an increase of heat transfer coefficient at low gas velocity of less than 50 mms^{-1}. This effect has not been seen in case of CMC data.

6.2.- DISCUSSION OF THE RESULTS.

6.2.1.- Effect of the tube bundle end plate.

Variation of the heat transfer coefficient with superficial gas velocity for the heater with and without the end plates were given in Figure 6.1. It is apparent that the effects of the end plates have been to reduce the heat transfer coefficient by a significant amount of 29%. This effect is very interesting since the effect of vertical baffles on the heat transfer coefficients has not been reported elsewhere. It seems that in contrast to the horizontal baffles of Patil (1984) vertical baffles reduces the heat transfer coefficient. The end plates have separated the local upflow and downflow of the liquid in the vicinity of the heater surface and by so doing the radial movement of the liquid mixture, and hence enhancement of heat transfer coefficient has been reduced.

6.2.2.- Effects of Water Height and Heater Bundle Position.

Figure 6.2 and 6.3 shows the variation of heat transfer coefficient with the superficial gas velocity together with the effects of water height and distance of the heater bundle from the distributor plate, respectively. It appears that neither the vertical position of the heater bundle nor the initial liquid height have a significant effect on the heat transfer coefficient in the experimental range studied. This is similar to the results obtained with a single heater (Chapter 5). However

Figure 6.4 shows that at superficial gas velocity of less than 50 mms^{-1} the rotation of heater has a slight effect on the heat transfer coefficient. A similar effect was not observed with a single horizontal heater. This shows that at low gas flow rates a bundle was caused a slight change in the uniformity of the liquid mixture circulation pattern.

6.2.3.- Effect of Bundle Layout.

As expected an increase in the number of rows and columns from 3 to 5 at a constant pitch of 1.25 caused a reduction in the heat transfer coefficient. Figure 6.5(a) and 6.5(b) shows the effect to be noticeable.The effect is attributed to a reduction in local turbulence caused by the wooden rods acting like vertical baffles .

A decrease of the heat transfer coefficient with a decrease in the distance between the tubes was also expected. This expectation was due to the fact that by narrowing the distance between the tubes the quantity of liquid passing through the tube bundle would decrease. However, by decreasing the clearance the velocity of the liquid passing through the available passage might increase and an optimum condition may be reached so that at that condition the heat transfer coefficient is at its highest value. This effect has been shown by the air-water data in Figure 6.6(b). In general decreasing the pitch to diameter ratio from 2.46 to 2.25 or 1.5 has caused a decrease in the heat transfer coefficient, at a constant gas superficial velocity.

However, for superficial gas velocity of less than 50 mms^{-1} the lowest pitch to diameter ratio of 1.25 has given higher heat transfer coefficient. This effect is not observable for higher viscosity liquid used.

However, for practical reasons a very low pitch to tube diameter ratio is not advisable because first it could cause a higher pressure drop inside the column. Secondly too small a width of metal between the adjacent tubes structurally weakens the tube sheet. However, a pitch to diameter ratio of 1.25 may be attractive.

6.3.- CONCLUSIONS.

1.- Vertical baffles, in contast to horizontal baffles, can cause a local reduction in heat transfer coefficient.

2.- As with single heaters,the heat transfer coefficient for tube bundles is independent of liquid height and vertical position of the heater bundle.

3.- Horizontal rotation of the heater bundle can show a slight difference in heat transfer coefficient. In other words, rotation of the heater bundle amplifies any non-uniformity of the initial gas distribution at the column base. The effect is more profound at low gas superficial velocity where the initial non-uniformity is more profound.

4.- Increasing the number of rows and columns decreases the heat transfer coefficient slightly.

5.- In general decreasing the tube-tube clearance decreases the heat transfer coefficient. However,for low viscosity systems,small clearances can enhance the heat transfer. There may thus be an optimum pitch to diameter ratio.

******

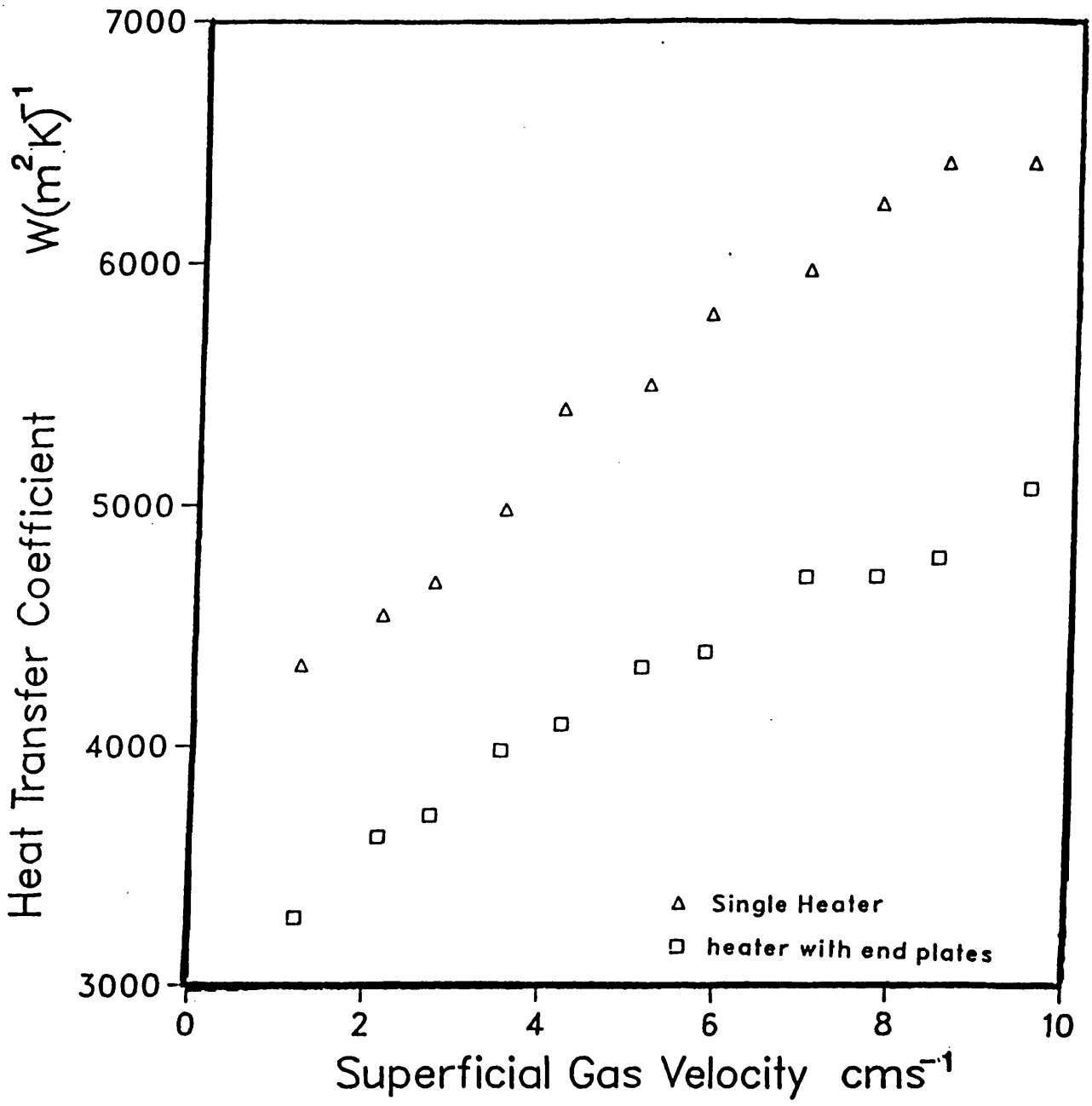

Figure 6.1.-Effect of Bundle of Heaters End Plate Support,o.75 m from base.t_b= 18 °C Heater dimension 30 x 120 mm.

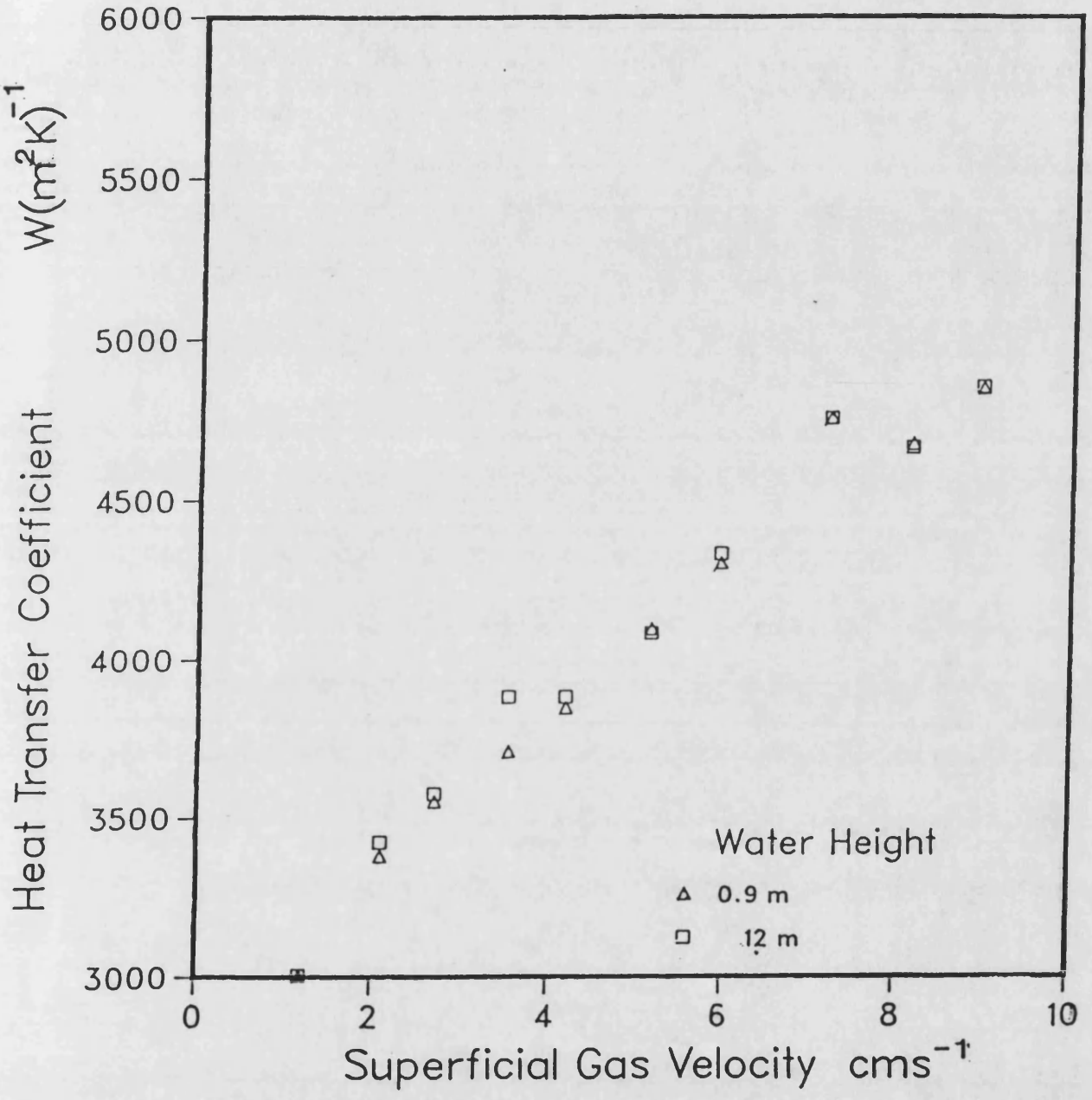

Figure 6.2.-Effect of Water Height.
Variation of heat transfer coefficient with superficial gas velocity obtained with a 3 x 3 bundle with a pitch to diameter ratio of 2.25. t_b= 18 °C.

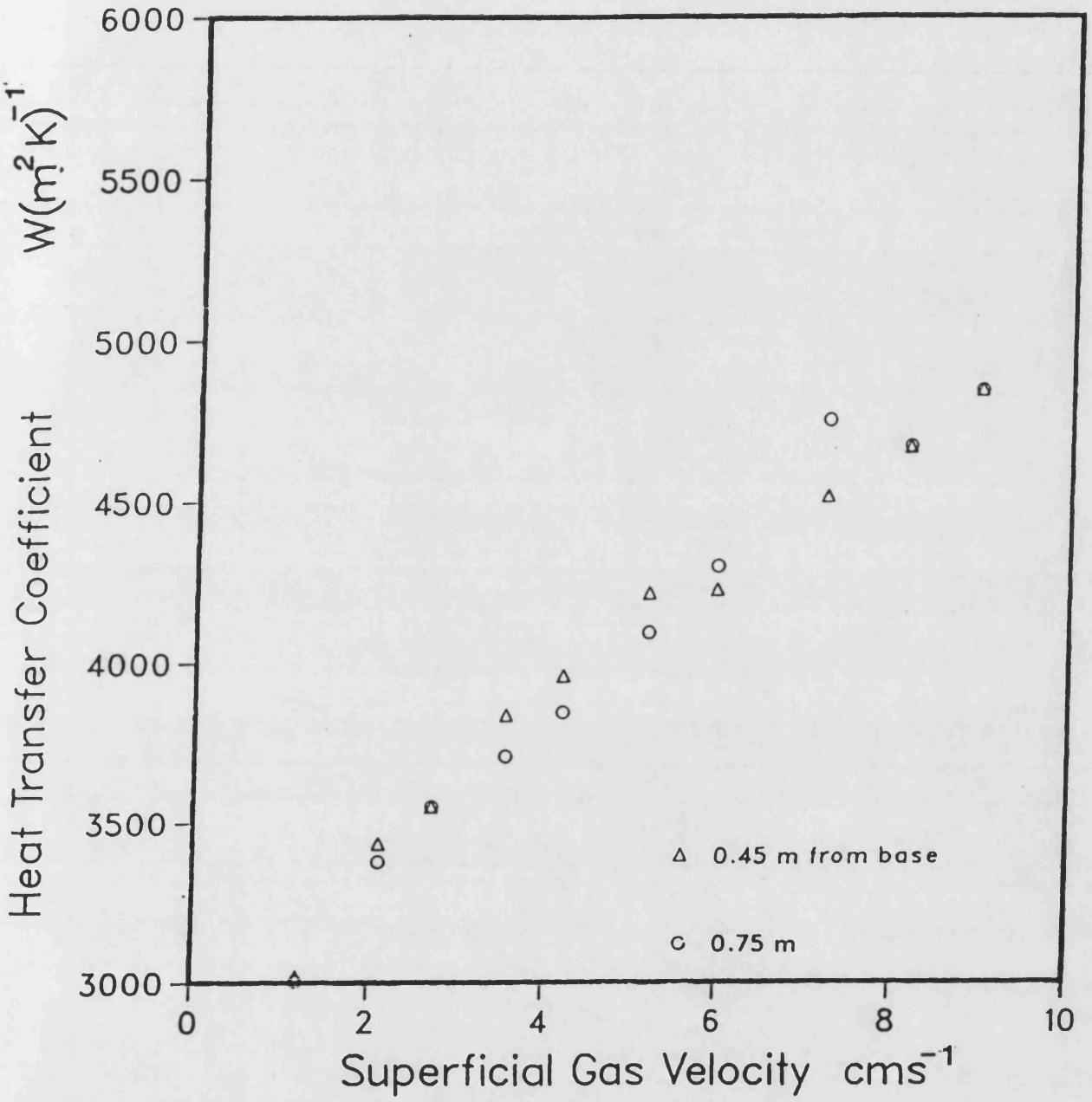

Figure 6.3.-Effect of Bundle of Heaters Distance from base.
Variation of heat transfer coefficient with superficial gas velocity obtained with a 3 x 3 bundle with a pitch to diameter ratio of 2.25. t_b= 18 ^{o}C .

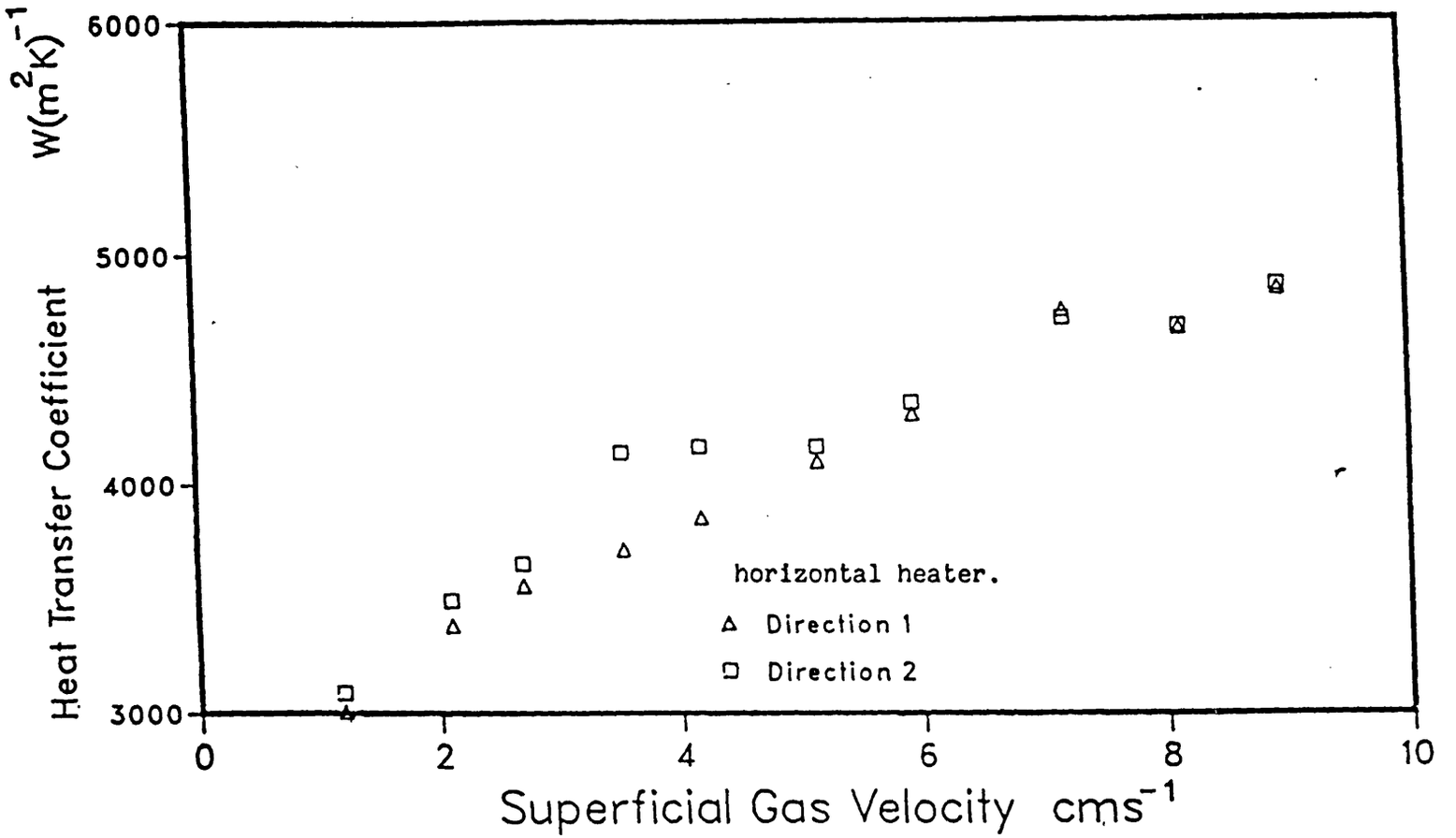

Figure 6.4.-Effect of Bundle Position
Variation of heat transfer coefficient with superficial gas velocity obtained for a water of height 0.90 m with a 3 x 3 bundle . Bundle pitch to diameter used 2.25.

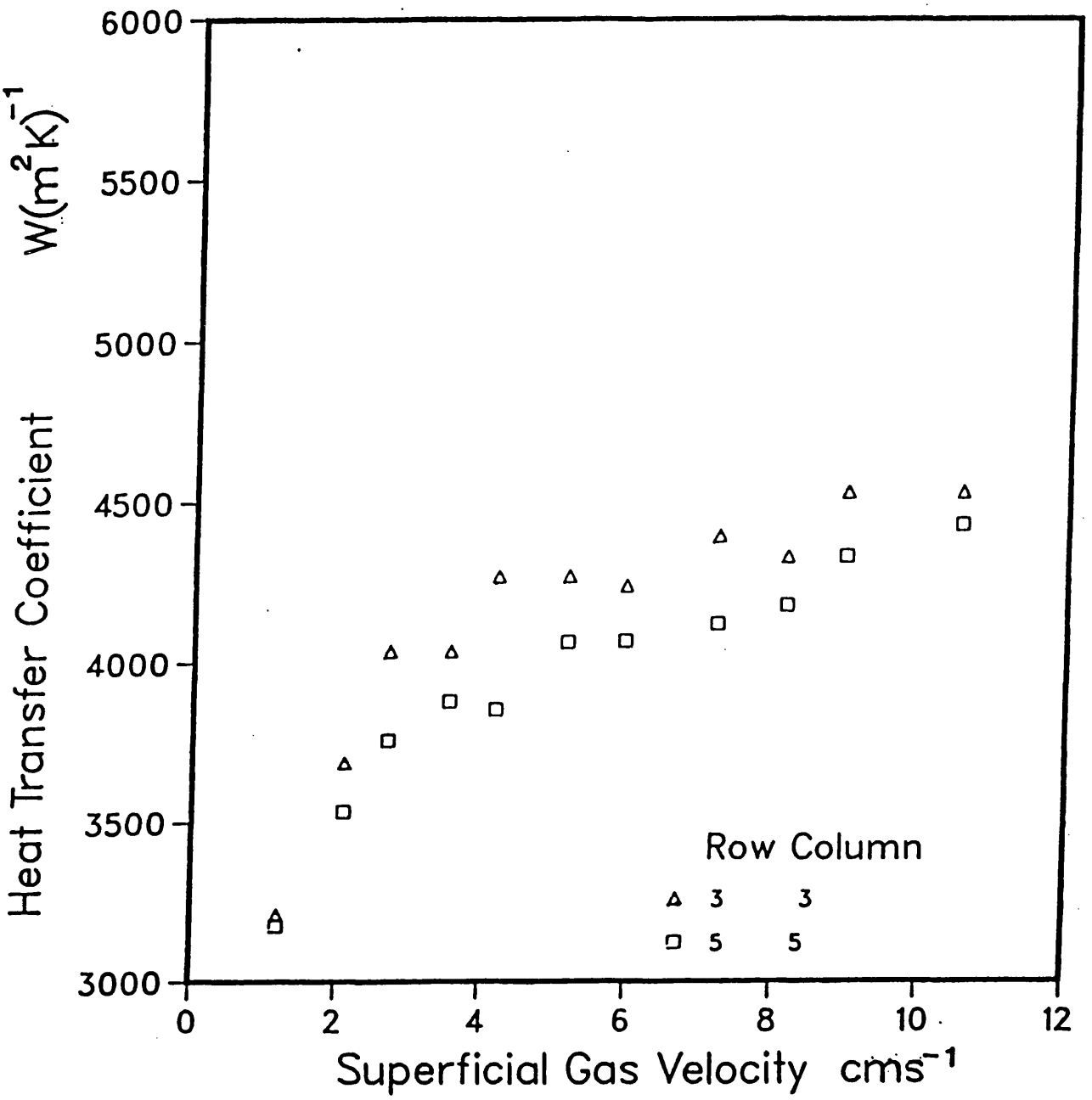

Figure 6.5.(a).- Effect of Number of Bundle Rows. Variation of heat transfer coefficient with superficial gas velocity obtained for a water of height 0.90 m with a 3 x 3 heater bundle. Bundle pitch to diameter ratio used 1.25.

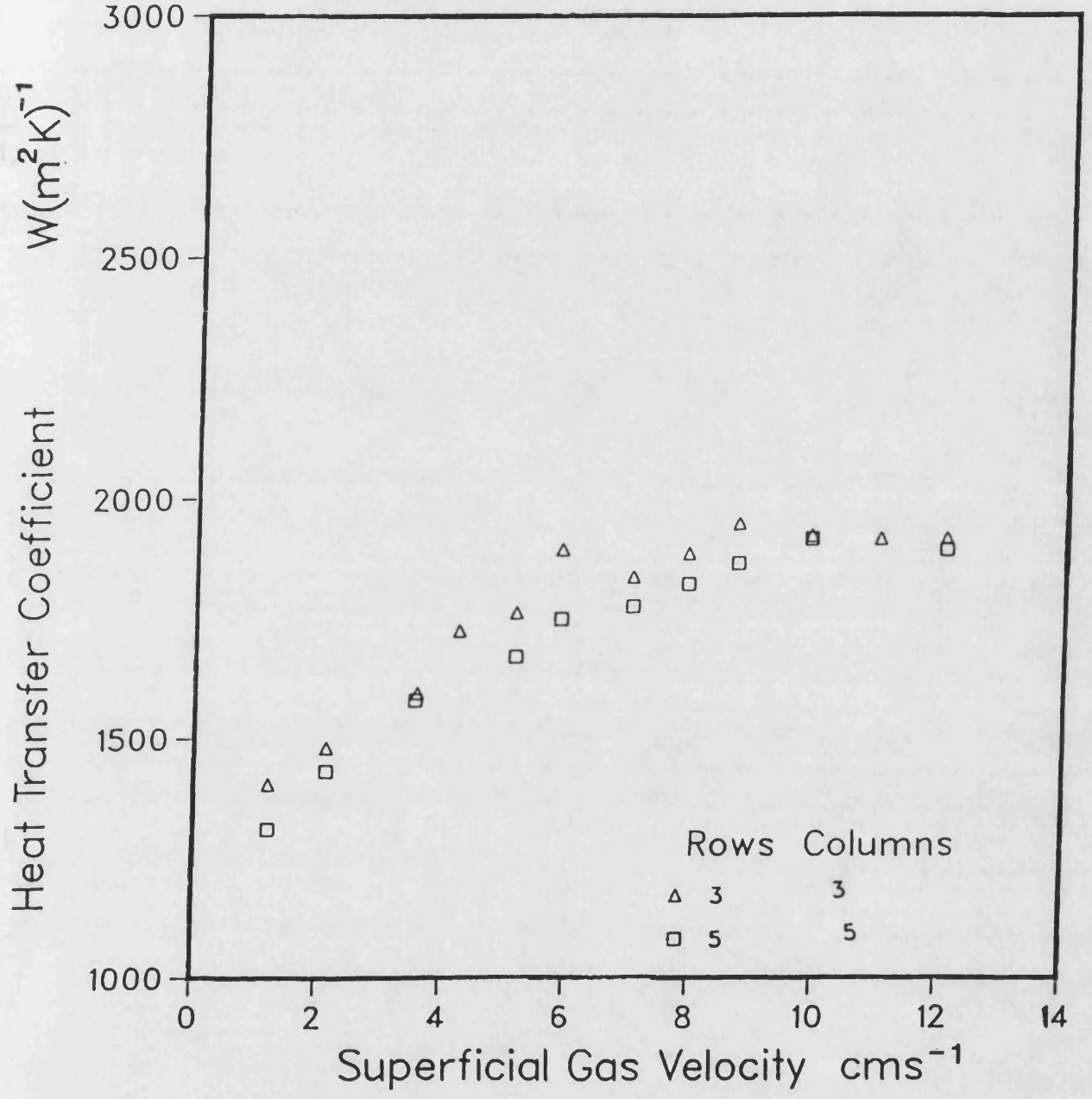

Figure 6.5(b)- Effect of Number of Bundle Rows
Variation of heat transfer coefficient with superficial gas velocity obtained for a 3000 ppm CMC solution of height 0.90 m ,temperature 18.4. Bundle position was 0.75 m from the distributor.

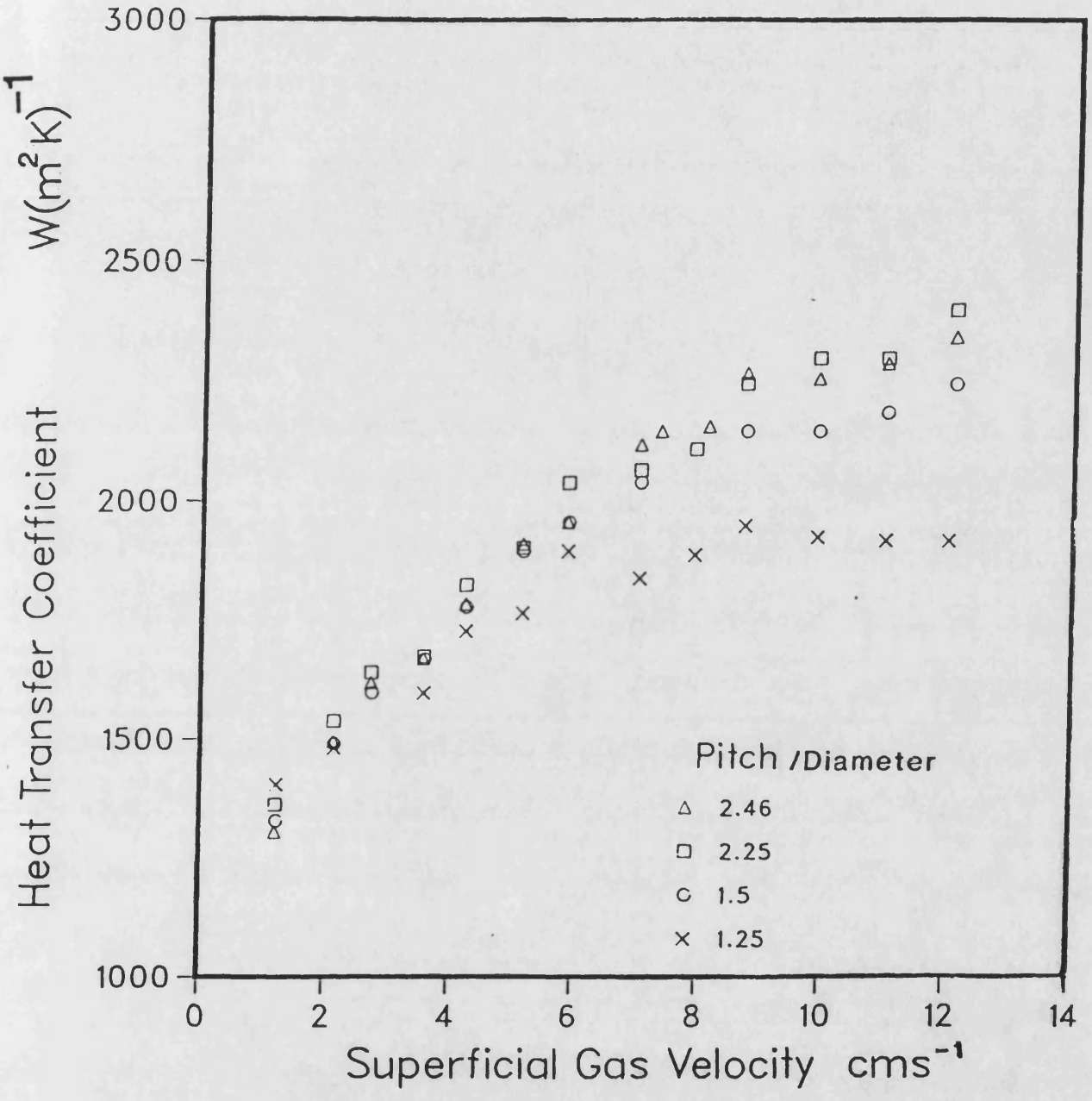

Figure 6.6(a). Effect of Pitch to Diameter Ratio
Variation of heat transfer coefficient with superficial gas velocity obtained for a 3000ppm solution of height 0.90 m, temperature 18 °C. A 3 x3 bundle used.

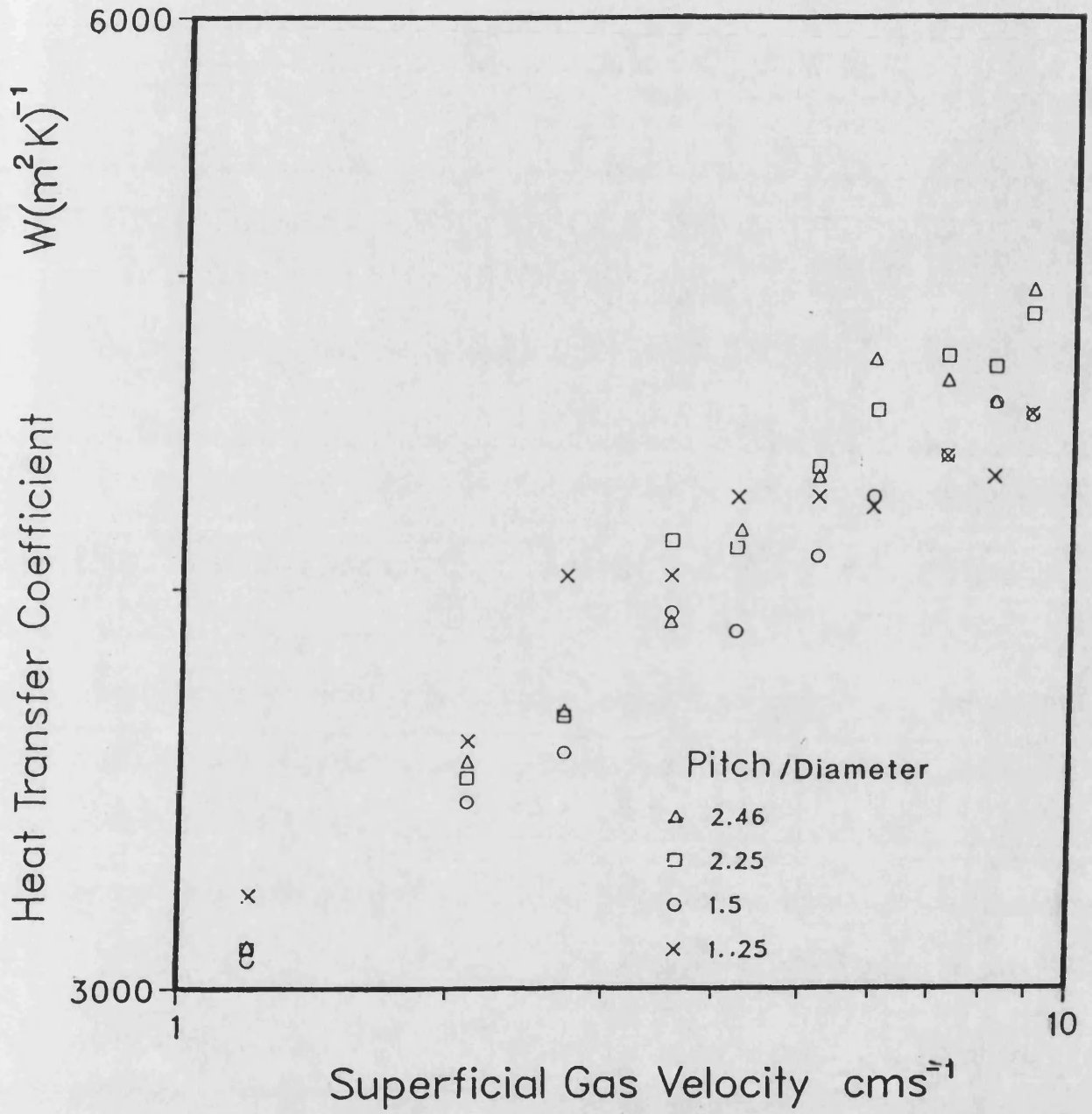

Figure 6.6(b)-. Effect of pitch to Diameter Ratio.
Variation of heat transfer coefficient with superficial gas velocity obtained for a water of height 0.90 m, temperature 18 °C.
A 3 x3 bundle used.

CHAPTER 7

FURTHER DISCUSSION OF RESULTS, THEORETICAL CONSIDERATIONS AND TEST OF THE NEW THEORETICAL MODEL.

7.1.- Introduction.

Some of the experimental features of heat transfer from a single cylindrical heater in a batch bubble column were covered in Chapter 5 and reference was made to the Ruckenstein and Smigelschi's (1965) and Deckwer's (1980) models. In this chapter, the applicability of the theoretical model that was developed in Chapter 2 will also be examined with respect to both Newtonian and non-Newtonian fluids. Finally those areas of the work requiring a further attention will be specified.

At this stage it is appropriate to compare the experimental data of several experimenters and the existing semi-theoretical correlation against each other. Purely experimental correlations will not be considered.

7-1-1.- Comparison of Experimental Heat Transfer Coefficient Data.

Figure 7.1 shows variation of heat transfer coefficient against superficial gas velocity for air/water system from the work of several investigators. Hart's data were obtained at high temperature of 71 ^{o}C, and Fair's, Ruckenstein and Smigelschi's data are at 27 ^{o}C and 30 ^{o}C respectively, whilst Xavier's data and data of the present work were obtained at room temperature.

The relatively high values of the heat transfer at low gas superficial velocity obtained by Hart are partly due to the higher temperature of the bulk of the liquid and partly due to the use of a single nozzle gas sparger in a 0.099 m diameter bubble column. The Ruckenstein and Smigelschi's data on the other hand are very low. This is because firstly the data were collected from a heated wall rather than an immersed heater and secondly the geometrical arrangement was a column with a square cross sectional area of 51 cm^2 and side wall of 104 cm^2. Data of Fair, Xavier and the present work are comparable except that the data of the present work are about 12% higher than the Xavier's data. Comparison of the gas hold-up data of Xavier and the present work also shows that the gas hold-up data of the present work is higher than the gas hold-up data obtained by Xavier. The higher values of gas hold up suggest that there would have been higher liquid circulation and hence higher heat transfer coefficient.

It is therefore evident that the heat transfer coefficient is not uniquely determined by the physical properties of the liquid phase and the parameter U_g, particularly at low values of superficial gas velocity.

Some experimental heat transfer coefficients for CMC solutions were given by Nishikawa et al (1977). The data were obtained in a column with diameter of 0.15 m, and the rheological properties of the CMC solution was specified as n=0.72, K=0.006 Pa.s ^{n}. This together with the heat transfer coefficients for the approximately 1000 ppm CMC solution (n=0.834, K=0.008 Pa.s ^{n}) obtained in the present work are given in Figure 7.2. The magnitude of the heat transfer coefficient are similar.

7-1-2.- Comparison of the Existing Correlations with the Experimental Data.

Although, there are many experimental correlations for the predictions of heat heat transfer coefficients in bubble columns, only a few correlations are based on the theoretical considerations and are mainly for Newtonian low viscosity liquids (Chapter 1).

The prediction of heat transfer coefficient for air- water

system from the models of Ruckenstein and Smigelschi (1965), Deckwer (1980) and Lewis et al (1982) as well as that of Chen (1987) which is an improvement of the Ruckeinstein and Smigelschi's model are presented as a function of superficial gas velocity in the Figure 7.3. Prediction of heat transfer coefficient from the Lewis et al model are for water of height 0.9 m. The bubble rise velocity and the gas hold-up were estimated by equations 2.4 and 2.8 respectively. Figure 7.3 also includes the experimental data of Xavier (1979) and the present work.

It is evident from Figure 7.3 that the prediction of heat transfer coefficient from Deckwer's equation is lower than that of the other equations at superficial gas velocities greater than 40 mms^{-1}. Whilst at superficial gas velocities of less than 40 mms^{-1} Ruckenstein and Smigelschi's equation predicts the lowest value of heat transfer coefficients. The predictions of Chen's equation is higher than that of the other equations. Lewis et al's model predictions are in between Chen and Ruckenstein and Smigelschi's model predictions are in good agreement with the experimental data of Xavier. However, Chen's equation, which predicts about 25% higher values of the heat transfer coefficient than Lewis et al equation are in good agreement with the present data. The difference between the lowest prediction (Deckwer's prediction) and the highest prediction (Chen's predictions) are about 40% .

7-1-3.- A General Considerations of the Lewis et al Model.

The Lewis et al model, Table 1.3, containes a term depending upon $U_c^{0.5}$. This lead to the prediction of h being depending on $U_g^{0.167}$. The relationship was tested by plotting 1/h against $U_g^{-.167}$ for Xavier's and the present data in Figure 7.4. A positive interception equal to $1/h_f$ was expected. The fact that the data in the Figure 7.4 lie on a straight line indicates that the dependency on U_g is reasonable.

However, these lines gave a negative intercept. At low values of $U_g^{-.167}$ or high U_g the data shows a clear curvature. This indicates that for high gas velocity the effect of boundary layer diminishes and film resistance assumes a constant value.

Figure 7.5 shows variations of 1/h with $(\epsilon U_g)^{-0.167}$ (This is another measure of liquid circulation and is discussed in section 7.2.1). The data are for water at temperatures of 10, 20, 30 and 50 ^{o}C. Data points lie on a straight line. The best fits to the lines, that were obtained by linear regression of the data points, are given in Table 7.1.

In Figure 7.5 the intercept is a measure of film heat resistance, $1/h_f$, and the product of the slopes of the lines and $(\epsilon U_g)^{-0.167}$ is a measure of the packet heat resistance, $1/h_p$. It is clear from Table 7.1 or Figure 7.5 that both the intercepts and the slopes of the lines are function of the

physical properties of the system. As the water temperature increases the slope and intercept of the lines decreased but for practical purposes the slope of the lines could be considered relatively constant. The change in intercept is more significant.

The Lewis et al model predicts that at high gas velocities the film thickness will decrease and hence the resistance to the heat transfer coefficient will tend to the Deckwer's type equation (Chapter 2). Although, at high gas velocities Deckwer's equation and Lewis' equations are of similar form to each other, their definition of the liquid contact time with the heater are different. The results is that Deckwer's model predicts a dependency of heat transfer to superficial gas velocity of $U_g^{0.25}$ for all gas flow rates. Experimental observations of several investigators including this work has indicated that the index, for gas velocities higher than 50 mms^{-1} is about 0.19. This is close to the theoretical value of 0.167 in the h_p part of the Lewis et al model.

However, Lewis et al model is difficult to use specially in regard to the prediction of the term $(U_g - \epsilon U_s)$ which appears in the prediction of the liquid circulation velocity. Also their definition of the film thickness requires further attention. These matters are examined in the following section.

7-2.- EVALUATION OF PARAMETERS OF THE PRESENT MODEL.

Prediction of heat transfer coefficient according to the theoretical development of Chapter 2 requires calculation of circulation velocity, U_c, knowledge of the heater characteristic length, L_c, and the calculation of film thickness. These were examined further and a new procedure to calculate the heat transfer coefficient was proposed.

7-2-1.- Average Liquid Circulation Velocity.

Previous workers have calculated the average liquid circulation velocity by either equation 2.23 or 2.24,

$$U_{cF} = 1.36 \{ Hg (U_g - \epsilon U_s) \}^{1/3} \qquad ...2.23$$

$$U_{cJ} = 1.31 \{ Dg (U_g - \epsilon U_s) \}^{1/3} \qquad ...2.24$$

However, experimental observations showed that the heat transfer coefficient is almost independent of liquid height for columns with an aspects ratios of over 3. Therefore equation 2.23 is recommended only for aspect ratio of 1 to 3, whilst equation 2.24 is recommended for aspect ratio of over 3.

However, use of these equations requires knowledge of gas hold-up and slip velocity. Errors may arise in calculating the term $(U_g - \epsilon U_s)$ which is a measure of energy used in the liquid circulation of the liquid phase. To overcome this difficulty the

simplified version of equation 2.23 and 2.24 which are

$$U_{cFs} = 1.36\ (gnH.\epsilon\ )^{1/3} \qquad ...2.25$$

$$U_{cJs} = 1.31\ (gnD\ \epsilon\ )^{1/3} \qquad ...2.26$$

were used.

It was found that Mashelkar or Hugmark equations, equation 2.7 and 2.9, respectively can represent the present gas hold-up data best (See Chapter 4). Hence a value of n=2 was adopted in use with equations 2.25 and 2.26.

The bubble rise velocity was estimated to be 300 mms^{-1}. Knowing this the gas hold-up were estimated from Mashelkar's equation for different gas flow rates. The theoretical liquid circulation velocity in a column with diameter of 138 mm were then estimated using equation 2.26 and compared with the experimental average liquid circulation veloctiy reported by Hills (1974) for columns with a diameter of 138 mm and an aspect ratio of 9.8. The results that are given in Table 7.2 are in good agreement with each other suggesting that the liquid circulation can be calculated by use of equation 2.26. Prediction of equation 2.25 will be 2 times higer than that of equation 2.26 at the same conditions, which confirms that this equation is unsuitable for relatively large aspect ratios.

7-2-2.- Heater Characteristics Length.

The characteristic lengths were determined from the slope of the folllowing equation

$$1/h = A + B(\epsilon \ U_g)^{-1/6} \qquad ...2.47$$

where

$$B = \left(\frac{\pi L_c}{4 \ \rho \ C_p.k \ 1.31(2gD)^{1/3}} \right)^{1/2}$$

and

$$A = 1/h_f$$

Values of A and B that were found from the best fit of the experimental heat transfer coefficient data to equation 2.47 were given in Table 7.3. The predicted values of heat transfer coefficient are insensitive to the value of A and so in order to reduce data scatter the value of A was in subsequent calculations kept constant at a value of 0.3×10^{-4} $(m^2K)W^{-1}$.

Table 7.3 shows that for 120 and 60 mm long heaters the heater's characteristic length is about 37mm, whilst the characteristic length for a 30 mm long heater is 30mm. These values can be compared with the range of 30 to 60 mm that were found experimentally in Chapter 5.

Use of equation 2.25 rather than 2.26 would have resulted in a characteristic length of 47 mm. This is almost equal to the value of 45 mm that was reported by Lewis et al who used an

equation for liquid circulation velocity that, like equation 2.25 was based upon the height of the bubbly bed.

The characteristic lengths were found to be a weak function of temperature . Results for temperatures of 10, 20, 30 and 50. ^{o}C are presented in Table 7.1. Except for the value of L_c that was obtained at bulk temperatures of 20 ^{o}C , the rest are in the range from 33 to 26 mm, increasing slightly with increasing temperature. The average of L_c, equal to 31 mm, was used as the heater characteristic length for all further calculations involving water data.

7-2-3.- Evaluation of Thermal Boundary Layer Thickness.

The values of film resistance, A, in equation 2.47 or the intercept of the lines in Figure 7.5 together with the calculated values of the thermal boundary layer thickness are given in Table 7.1. The thermal boundary layer is the product of the film resistance and the thermal conductivity of the system. The approximate dependency of film thickness on viscosity for air-water system are found to be $\mu^{0.90}$ in the viscosity range of 0.5 to 1.3 cP.

Table 7.4 gives values of thermal boundary layer thickness δ_t that were obtained from unpublished Nitrogen-Glycol data of Lewis (1980). These data were obtained with a 30x60 mm heater mounted vertically in a 1 m long and 0.292 m in diameter column.

These conditions are similar to the present study. These data covers a wide viscosity range of 2.84 to 19.3 cP. In order to calculate δ_t it was assumed that Lc=31 mm. Uc was calculated from equation 2.26. Film resistance were obtained by substracting the packet resistance from the overall experimental resistance. It was found that for this Nitrogen- Glycol data L_c is proportional to $\mu^{0.54}$ This is closer to the theoretical index of 0.567 given in Chapter 2.

Lastly, it was decided that a relationship between μ and δ_t be calculated by assuming that the theoretical dependency held for the Newtonian fluids. The best fit to the combined water and glycol data, was founnd to be

$$\delta_t = 1.49\times10^{-3}\mu^{0.567} \qquad \ldots 7.1$$

The viscosity range was 0.5 -19 x 10^{-3} Pa.s and the goodness of fit was about 97%.

7.2.4.- Procedure for the Calculation of the Heat Transfer Coefficient for a Newtonian Fluid.

Having obtained experessions for the three parameters U_c, L_c, and δ_t a procedure for predicting the heat transfer coefficient in a bubble column was developed.

1.- Estimate gas hold-up by a suitable relationship,or

(a) obtain value of U_b, from either experiments or the following

equation

$$U_b = 1.53\left(\frac{\sigma g}{\rho}\right)^{0.25}$$

(b) assume that $U_s = U_b$ and,

(c) use the following equation to obtain gas hold-up, ϵ, for any given value of U_g.

$$\epsilon = \frac{U_s}{2U_g + U_s}$$

2.- Calculate liquid circulation velocity from the following equations,

$$U_{cFs} = 1.36(ngH\epsilon U_g)^{\frac{1}{3}} \qquad 1 < \frac{H}{D} < 3$$

$$U_{cJs} = 1.31(ngD\epsilon U_g)^{\frac{1}{3}} \qquad 1 < \frac{H}{D} < 3$$

where n=2

3.- Calculate heat transfer coefficient;

$$h = \left[\frac{\delta t}{k} + \left[\frac{\pi L_c}{4\rho C_p k U_c}\right]^{1/2}\right]^{-1}$$

where

$$\delta_t(m) = 1.49\times10^{-3}\mu^{0.567} \qquad \mu > 5\times10^{-3}$$

$$\delta t = 0 \qquad \mu < 5\times10^{-3}$$

and L_c = 0.045 m if U_{cFs} is used , or

L_c = 0.031 m if U_{cJs} is used.

L_c = vertical dimension of heater if it is less than the above values.

In the following section the prediction obtained using the above mentioned procedure are tested against some of the existing theoretical and semi-teoretical models. The numerical details are to be found in Appendix C. Also the equation is represented in dimensionless form .

7.3.- COMPARISON OF THE MODEL WITH THE EXPERIMENTAL DATA AND THE PREVIOUS MODELS.

7.3.1.- Air-Water System.

Figures 7.6, 7.7 and 7.8 show the variation of experimental and model predicted heat transfer coefficient with the superficial gas velocity for water at different temperatures.

Figure 7.6 includes experimental data of the present work at bulk temperatures of 10, 20, 30 and 50 ^{o}C. Whilst Figure 7.7 includes experimental data of Xavier (1979) at water bulk temperature of 20 ^{o}C and Ruckenstein and Smigelschi (1965) at water temperature of 27^{o}C . Harts (1976) experimental water data at 71 ^{o}C are given in Figure 7.8 together with the Lewis et al (1982) model predictions.

Both Figures 7.6 and 7.7 show that the experimental data and model prediction closely follow each other at low temperatures. At temperatures of over 30 ^{o}C, Figure 7.6 indicates that the present model under predicts the present data. A similar trend is apparent in Figure 7.8 where the degree of underestimation is seen to be somewhat less than the degree of over prediction of

the Lewis et al model.

Figure 7.9 compares heat transfer data of several investigators with the predictions of the present model. The hold-up data were used when available . Otherwise the above procedure was followed. The film resistance ($1/h_f$) was included. The computations are given in Appendix C1.

It is clear from Figure 7.9 that about 80% of the experimental data points are within the error band of $\pm$20% . However the prediction of Hart's water data with viscosity of 0.41 cP at 71^{o}C are about 32% lower than the experimental data. If the film resistance is neglected, the accuracy improved to -27%. This is shown in Figure 7.8.

7-3-2.- Other Systems.

Figure 7.10 shows the variations of heat trasnfer coefficient with the superficial gas velocity for the Lewis et al (1982) Nitrogen/Glycol system at various temperatures. The average percentage of the differences between predictions and the experimental values are only -9, -3 and +7% at temperatures of 18, 48 and 82 ^{o}C, respectively.

Model predictions for a number of organic liquids are given in the Figure 7.11(a) and 7.11(b) (see Appendix C2 for detailes). Gas hold-up values were estimated. In the Figure 7.11(a) the

film resistances were included, whilst they were excluded in the data of Figure 7.11(b).

Figure 7.11(a) shows that the largest errors of -36% are for xylen data with viscosity of 0.2 cP at 143 ^{o}C and about 70% of the data points are within the error band $\pm$25%. However by excluding film resistance about 80% of the data points laid within an error band $\pm$20%.

The comparison have shown that the predictive power of the model is reliable to $\pm$25%. This is, generally better than that of the other models as it will be shown in the next section.

7-3-3.- Comparison with Lewis et al (1982), Deckwer (1980) and Ruckenstein and Smigelschi's (1965) Models.

Prediction of Lewis et al, Deckwer and Ruckenstein and Smigelschi models against experimental data for water and a number of other liquids are shown in Figures 7.12, 7.13 and 7.14 respectively. These figures show that the prediction of the models vary considerably. The predictions are summarized in Table 7.5.

It appears from Table 7.5 and Figure 7.13 that the predictions of Deckwer's model are superior to the other models. However by neglecting the film resistance for liquids with a viscosity lower than 0.50 cP. (which was the case in Figure

7.11(b)) the prediction of the present model are as accurate as those of the Deckwer model. Therefore these two models are comparable with low viscosity fluids. With high viscosity fluids (eg Nitrogen-Glycol data with viscosity of 18 cP at 20 ^{o}C) the predective power of the present model is superior. The present model is thus of value.

7.3.4.- Test of the Model in Dimensionless form.

In Chapter 2 the heat transfer model was represented in dimensionless model as ,

$$\frac{1}{St} = \frac{1}{St_f} + \frac{1}{St_p}$$

where

$$\frac{1}{St_f} = A(Re^{0.1}Pr^{2/3}) \qquad \frac{1}{St_p} = B(RePr)^{1/2}$$

and

$$\frac{1}{St} = \frac{\rho C_p U_c}{h} \qquad Re = \frac{\rho U_c L_c}{\mu}$$

The theoretical values of A and B were given as 33 and 0.89 respectively. However, the experimental value of the film resistance coefficient, A, for water data at temperatures of 10, 20, 30 and 50 ^{o}C were found to be 7.90, 8.22, 4.05 and -1.14, respectively.These were found from the best fit to the following equation,in which the theoretical value of B=0.89 was maintained.

$$\frac{\rho C_p U_{cJs}}{h} - 0.89(RePr)^{1/2} = A(Re^{0.1}Pr^{2/3}) \qquad \ldots 7.2$$

Re was calculated assuming that L_c=31 mm and the circulation velocities were estimated using equation 2.26.

The low value of A for water data at temperatures of 10, 20 and 30°C and the negetive value of A for temperature of 50 °C suggest that the fully developed theoretical model does not represent the behaviour of the system accurately. This is more pronounced for low viscosity liquid.

Considering that ;

$$\frac{1}{St_f} = \frac{\rho C_P U_c}{h_f} \alpha \left(\frac{\rho U_c L_c}{\mu}\right)^{0.1}$$

It follows that $h_f \alpha U_c^{-0.9}$. Hence by use of equation 2.26 one obtains $h_f \alpha U_g^{-0.3}$. This index by intuitive reasoning was considered to be rather high specially at higher gas velocities and by neglecting this term the proposed simplified model (section 7.2.4) assumed a semi-theoretical nature.

7.4.- APPLICATION OF THE MODEL TO NON- NEWTONIAN LIQUIDS. CMC SOLUTIONS

Following the work of Nishikawa et al(1974) apparent viscosity were employed in correlating the CMC data in a manner similar to that of Newtonian fluids. The required values of heat transfer coefficient at different viscosities and a constant

superficial gas velocity were estimated (for details see Appendix D1) and are given in table 7.6. The best values of A and B of equation 2.47 for the apparent viscosities in the range of 1 to 180 cP are shown in Table 7.7 (detailes of the regression analysis of data are given in Appendix D2). Table 7.7 also gives the calculated value of film thickness δ_t and the heater characteristic length, L_c. The method of calculation are also presented in table 7.7.

The increases of film thickness with the increase of viscosity of the CMC solutions are shown in Figure 7.15. The dependency of film thickness on the the apparent viscosity were found to be $\mu^{0.375}$. This value is not very close to the theoretical value of 0.567, nevertheless,the latter was retained in the correlation for film thickness. The equation found was

$$\delta_t = 1.82\times10^{-0.3}\mu^{0.567} \qquad \ldots 7.3$$

where μ is meaured in Pa.s.

This is comparable with equation 7.1 for the Newtonian fluids.

It was found in chapter 4 that the gas hold-up for the CMC data can be calculated by the Kelkar et al equation,equation 4.6. Therefore,the liquid circulation velocity were estimated by equation 7.4,

$$U_{cJs} = 1.31(2.6gD\epsilon U_g)^{1/3} \qquad \ldots 7.4$$

Hence using U_{cJs} given by the equation 7.4, L_c was calculated and its values are given in the Table 7.7. The variation of heater characteristic length from 8 to about 23 mm in the viscosity range of 1 to 180 cP is shown in the Figure 7.16. The best linear fit of the data is;

$$L_c(mm) = 13.293 + 0.116\mu\,(cP) \qquad \mu < 100\ cP \qquad \ldots 7.5$$

The average value of L_c in the viscosity range of 1 to 180 cP is 16 mm. This is 1/2 of the value that was obtained for the Newtonian liquids. However, L_c=16 mm is taken as the heater characteristic length for the non- Newtonian CMC data.

Its use, together with the equations 7.3 and 7.4, enables calculation of heat transfer coefficient for the non-Newtonian liquids to be completed. Variation of experimental and predited heat transfer coefficients with superficial gas velosity for 100,and 10000 ppm solutions are given in Figures 7.17 and 7.18. They show that the model predictions and the experimental data follow a similar trend.

Figure 7.19 is a test of model predictions. It shows that the model predictions in general are about 32% higher than the experimental data. However,if the value of n=2 were used to calculate the liquid circulation velocity,the error would have been reduced to below 25%. But in line with the gas hold up data the value of n=2.6 were retained.

7.5.- SUMMARY

The predictions of existing theoretically based models vary widely; those based on Chen's(1987) model are 40% greater than those predicted from Deckwer(1980) model. Also the only previous model that can explain the change of dependency of superficial gas velocity from 0.33, at low U_g values, to about 0.19, at high U_g value, is that of Lewis et al which is only suitable for low viscosity liquids.

In this section the fully developed theoretical model of chapter 2 was tested with the experimental data of chapter 5 and compared with the prediction of other models. The parameters involved in the model, which are liquid circulation velocity, heater characteristic length and film thickness were confirmed and consequently two similar new procedures to predict heat transfer coefficient in bubble column for Newtonian and non-Newtonian systems were presented.

These procedures, although, are not fully theoretical, can explain the behaviour of the system and are applicable to viscosities of up to 180 cP. The model predictions are $\pm$25% accurate which are better than most of the current available models. These are a positive development of the Lewis et al model.

7.6-SUGGESTIONS FOR FURTHER WORK.

1.- The development of heat transfer model presented in chapter 2 is based upon single phase flow. Wallis (1969) suggested that for a two phase flow a homogeneous model should be used. Therefore, application of the homogenous model seems more realistic and should be investigated.

2.- The simplified liquid circulation model requires the constant, n, to be known. Its value at the present time depends on the choice of the gas hold up correlation. Therefore a correlation to predict its value is desirable.

3.- The hydrodynamic model of non-Newtonian fluids is yet to be fully developed. Nevertheless, attempts should be made to obtain a unified procedure for the calculation of heat transfer coefficient in bubble column for Newtonian and non-Newtonian fluids. This may be achived by considering the variation of thermal boundary layer for the non-Newtonian fluids.

4.- The experimental aspects of the work should be developed to confirm the existance of heater characteristic length for continuous columns.

5.- The model with non-Newtonian solution other than CMC should be tested. More data required in order to correlate data for tube bundles.

water temperature °C	A x 10^{-4} (SI)	B x 10^{-4} (SI)	L_c mm	δ_t mm	viscosity cP
10	0.45	0.69	33	0.025	1.3
20	0.29	0.70	37	0.017	1.0
30	0.26	0.59	26	0.016	0.8
50	negative	0.59	26	-	0.6
		average	31 mm		

Table 7.1.- Gives slope, B, and intercept, A, of the lines represented by

$$\frac{1}{h} = A + B(\epsilon U_g)^{\frac{-1}{6}}$$

for data of Figure 7.5. Heater dimensions was 30 x 60 mm.

U_g mms^{-1}	holdup *	U_{cJs} mms^{-1}	U_c Hills(1974) mms^{-1}
19	0.06	190	200
38	0.10	290	300
64	0.15	390	370
95	0.19	480	430
169	0.26	650	600

* Gas hold-up was calculated from U_g / ($2U_g$ + 300)

Table 7.2 -Comparison of the predicted and experimental values of liquid circulation velocity. Column diameter was 138 mm. H/d=9.8.

Heater dimension mm	A x 10^{-4} (SI)	B x 10^{-4} (SI)	L_c mm
30 x 120	0.30	0.70	37
30 x 60	0.30	0.70	37
30 x 30	0.30	0.61	30

Table 7.3.- The best value of intercept and slope of equation 2.47 for water at bulk temperature of 20 °C. Data of different heater length mounted vertically at the column center.

Temp. °C	μ cP	k $W(mK)^{-1}$	U_g mms^{-1}	hold-up	$h_{exp.}$ $W(m^2K)^{-1}$	U_{cJs} ms^{-1}	δ_t mm	$1/h_p$ x10^{-4} (SI)
19.4	19.30	0.255	20.9	0.057	1020	0.25	0.153	3.766
20.4	18.62	0.255	16.1	0.050	978	0.22	0.158	4.015
45.5	8.01	0.258	12.5	0.050	1180	0.20	0.111	4.211
68.0	4.20	0.261	13.3	0.050	1490	0.21	0.064	4.159
84.0	2.84	0.260	19.5	0.077	1690	0.268	0.059	3.638

Table 7.4.- N_2-Glycol data of Lewis(1985).

Experimental data	Present work	Deckwer	Lewis et al	Ruckenstein & Smigelschi
water data:				
Fair(1962) D= 0.447 m t_b= 27 °C	+15	-10	+36	-27
Fair(1962) D= 1.027 m t_b= 27 °C	+38	+7	+54	-31
Hart(1976) D= 0.09 m t_b= 71 °C	-32,-27*	-12	+40	-38
Present work D= 0.292 m t_b= 20 °C	-26,-11*	-33	-19	-45
N_2- glycol :				
Lewis et al D= 0.292 m t_b= 18 °C	-9.4	-17	-65	-50
xylen data:				
Deckwer(1982) D= 0.1 m t_b= 143 °C	-36,-24*	-22	--	--

* Film resistance excluded.

Table 7.5.-The average error in prediction of heat transfer coefficient from different models.

U_g cms^{-1}	Viscosity cP													
	1		5		10		20		50		100		180	
	ϵ	h	ϵ	h	ϵ	h	ϵ	h	ϵ	h	ϵ	h	ϵ	h
1.21	0.036	4068	0.038	2530	0.039	2062	0.037	1690	0.035	1270	0.034	1046	0.034	879
2.14	0.040	4045	0.064	2485	0.064	2015	0.062	1633	0.059	1238	0.054	1003	0.047	840
2.74	0.060	3927	0.088	2462	0.076	2014	0.074	1647	0.060	1263	0.050	1033	0.050	871
3.56	0.100	4087	0.106	2462	0.090	1979	0.070	1591	0.068	1192	0.050	958	0.050	797
5.25	0.120	4422	0.128	2681	0.106	2161	0.190	1742	0.079	1310	0.030	1056	0.030	879
7.19	0.150	4901	0.158	2905	0.130	2319	0.190	1851	0.079	1375	0.040	1097	0.030	907
8.76	0.183	5215	0.160	3060	0.135	2432	0.062	1933	0.087	1427	0.040	1134	0.030	934

Table 7.6.-The estimated values of heat transfer coefficients and gas holdup for CMC solutions. Detail s are given in Appendix D1.

Viscosity mpa.s	A x 10^{-4} (SI)	B x 10^{-4} (SI)	Film thickness* mm	Heater characteristic** length mm
1	1.44	0.32	0.086	8.32
5	2.71	0.41	0.162	13.66
10	3.41	0.48	0.204	18.73
20	4.46	0.43	0.267	15.03
50	6.24	0.53	0.374	22.83
100	7.99	0.53	0.479	22.83
180	10.50	0.32	0.630	8.32

* Film Thickness= A x k

** $U_c = 1.31(2.6 \times 0.292 \times 9.81 \times \epsilon U_g)^{\frac{1}{3}}$

$$\frac{1}{hp} = \left(\frac{3.14 \times Lc}{4 \times 998 \times 4181 \times 0.6 \times U_c}\right)^{\frac{1}{2}} = B$$

Table 7.7 - The best value of A and B in equation

$$\frac{1}{h} = A + B.(\epsilon U_g)^{-\frac{1}{6}}$$

for CMC solutions at different concentrations.

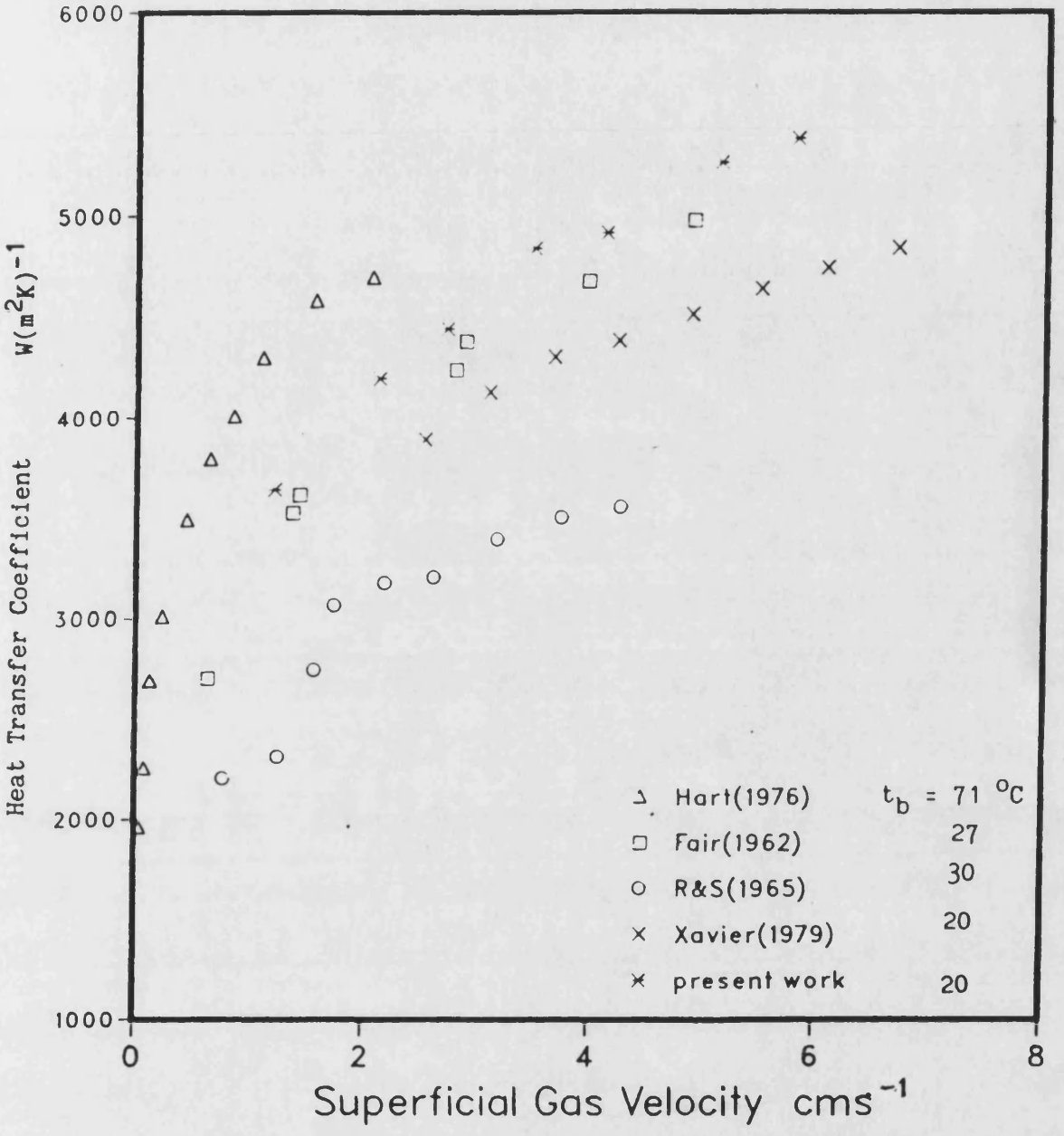

Figure 7.1.- Variation of heat transfer coefficent with superficial gas velocity for air water system obtained by several investigators.

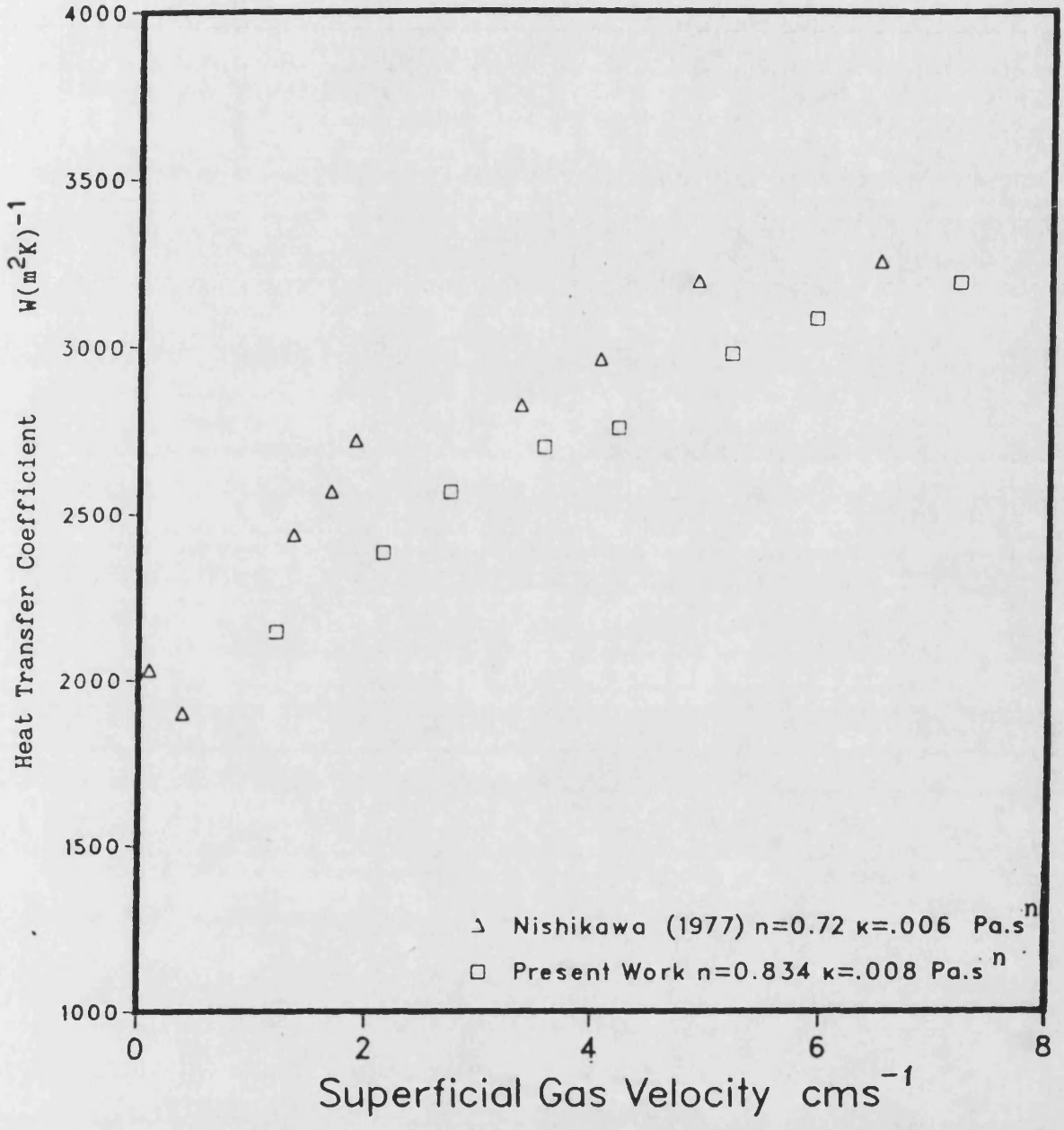

Figure 7.2.- Variation of heat transfer coefficient aginst superficial gas velocity for aerated CMC solutions .

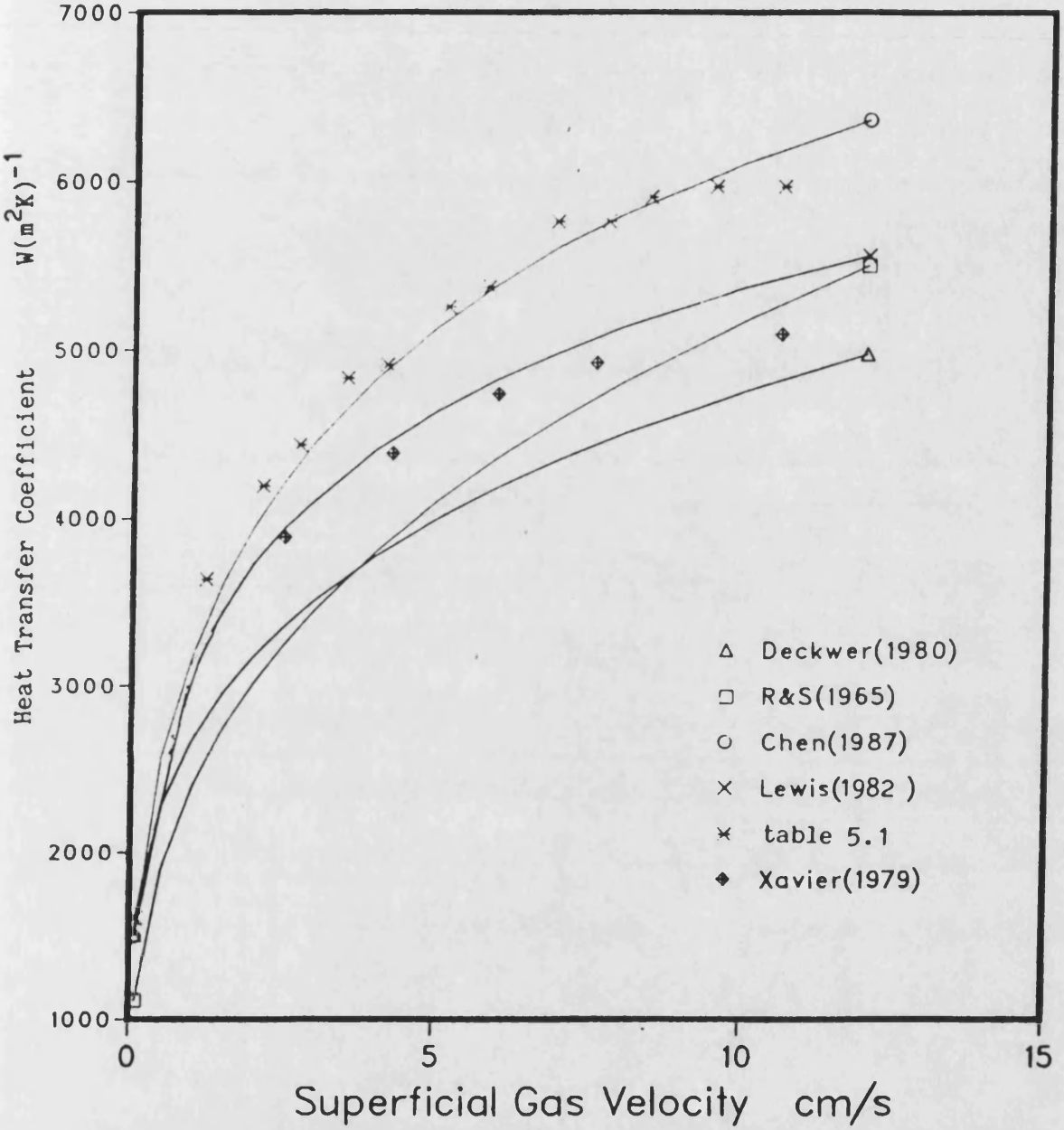

Figure 7.3.- Predicted values of heat transfer coefficient aginst superficial gas velocity calculated for water of Height 0.90 m, temperature 20 °C Comparison of models with the experimental data of Xavier and the present work.

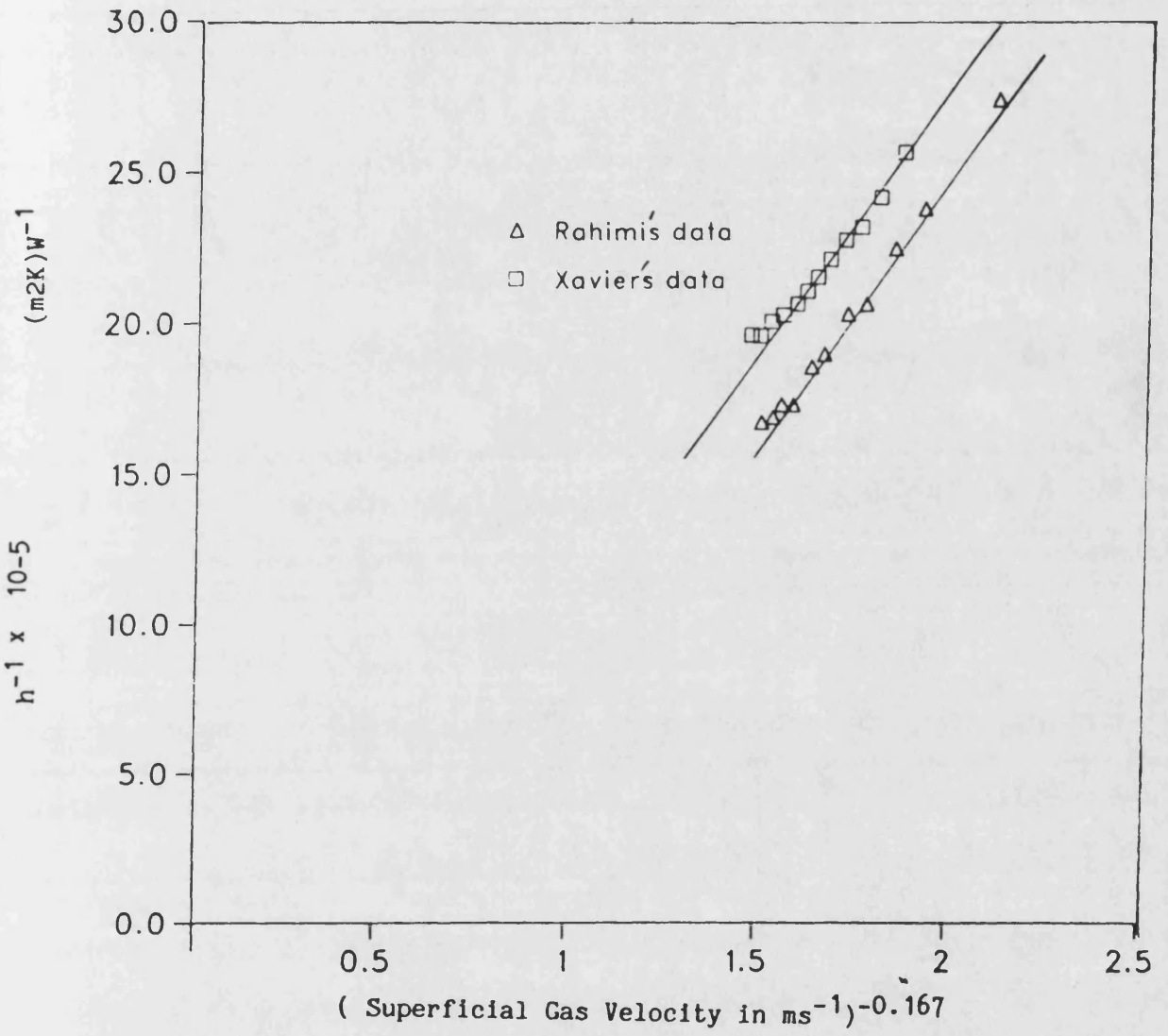

Figure 7.4.-Variation of h^{-1} with $U_g^{-0.167}$ for Xavier and present water data.

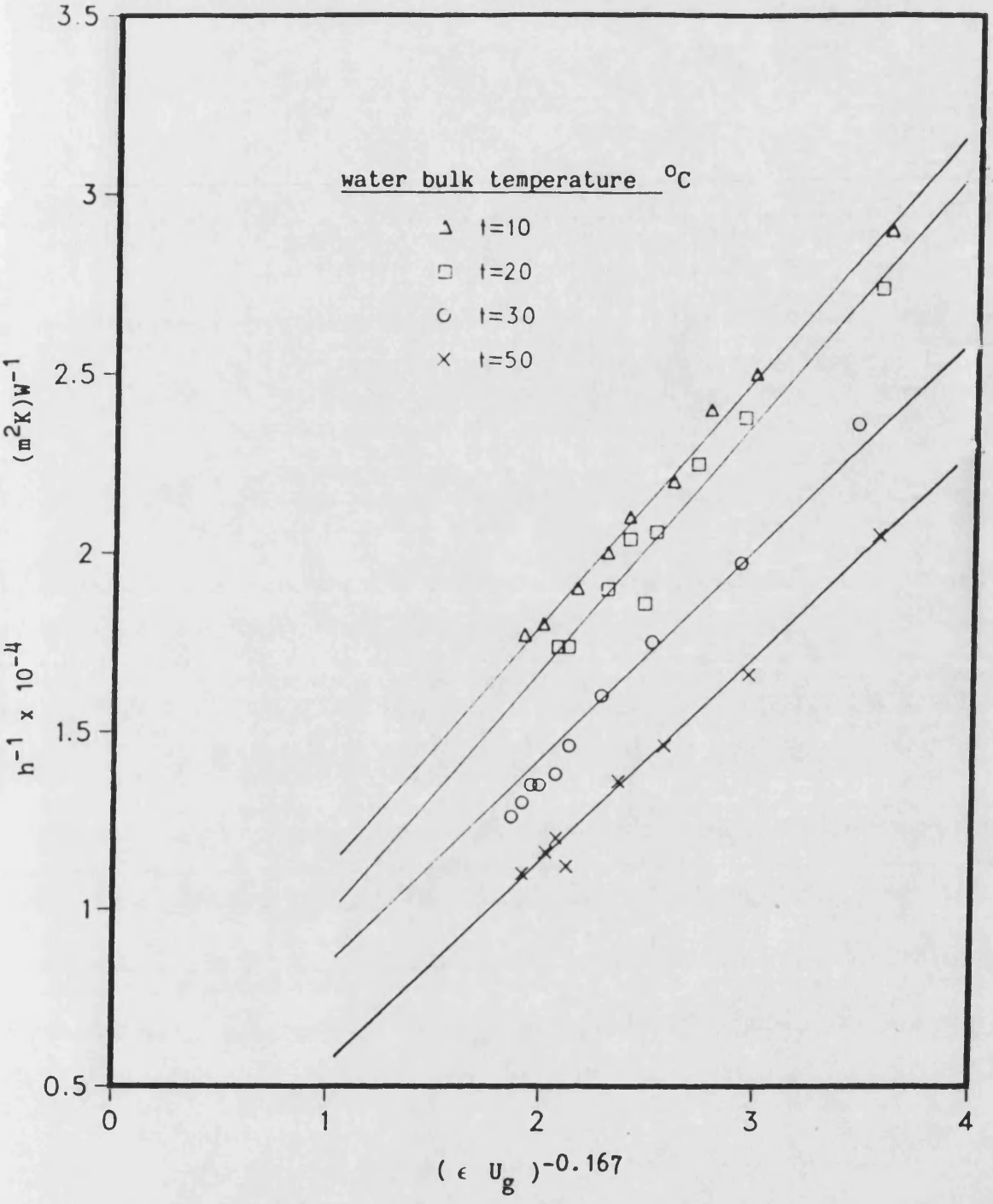

Figure 7.5.- Variation of h^{-1} with $U_g^{-0.167}$ for water data at different temperatures.

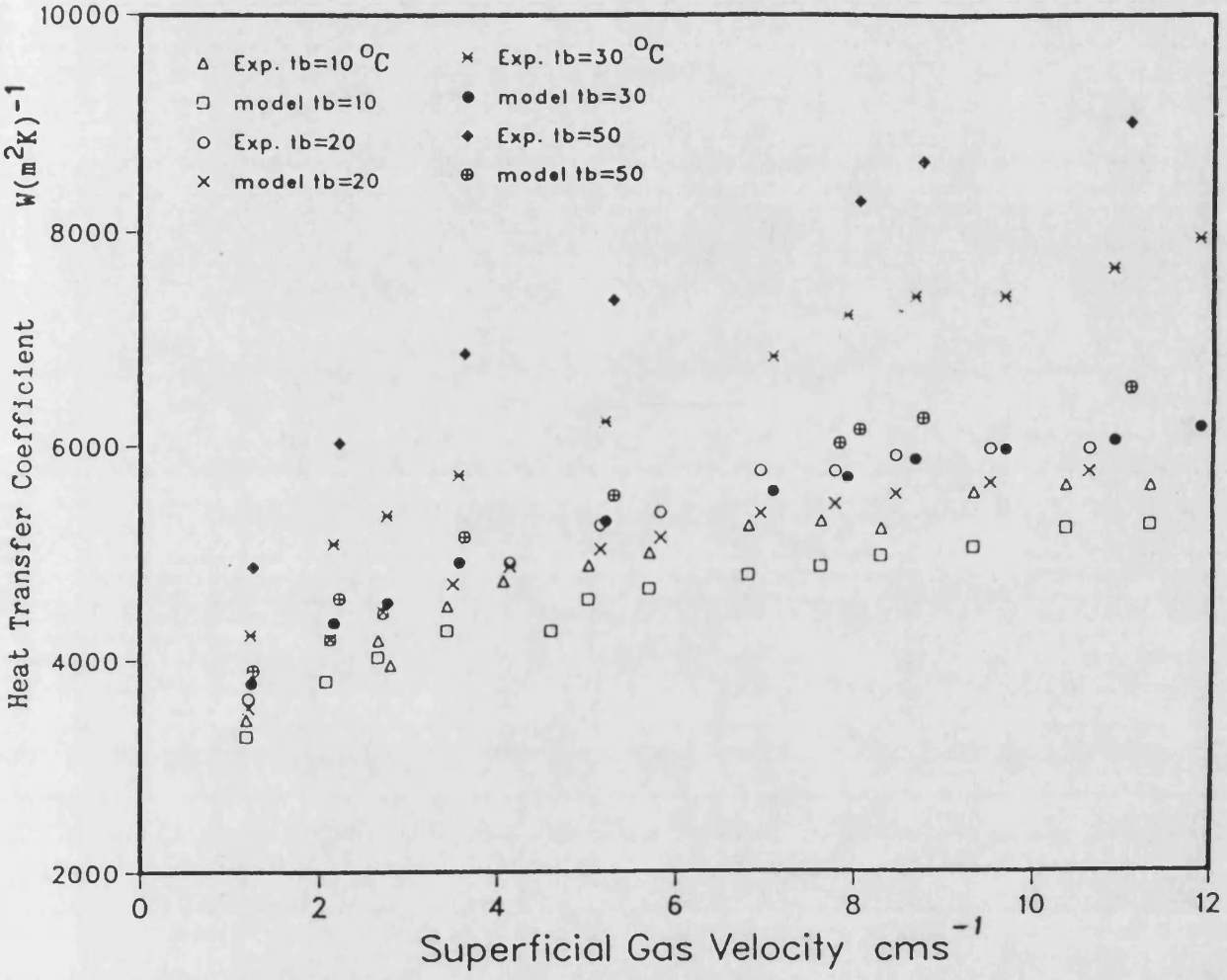

Figure 7.6.-Variation of experimental and model prediction of the heat transfer coefficient with superficial gas velocity for water at different temperatures. Heater dimensions was 30 x 60 mm. Data in tables C1-6 to C1-8. Model used with U_{cJs} as detailed in appendix C.

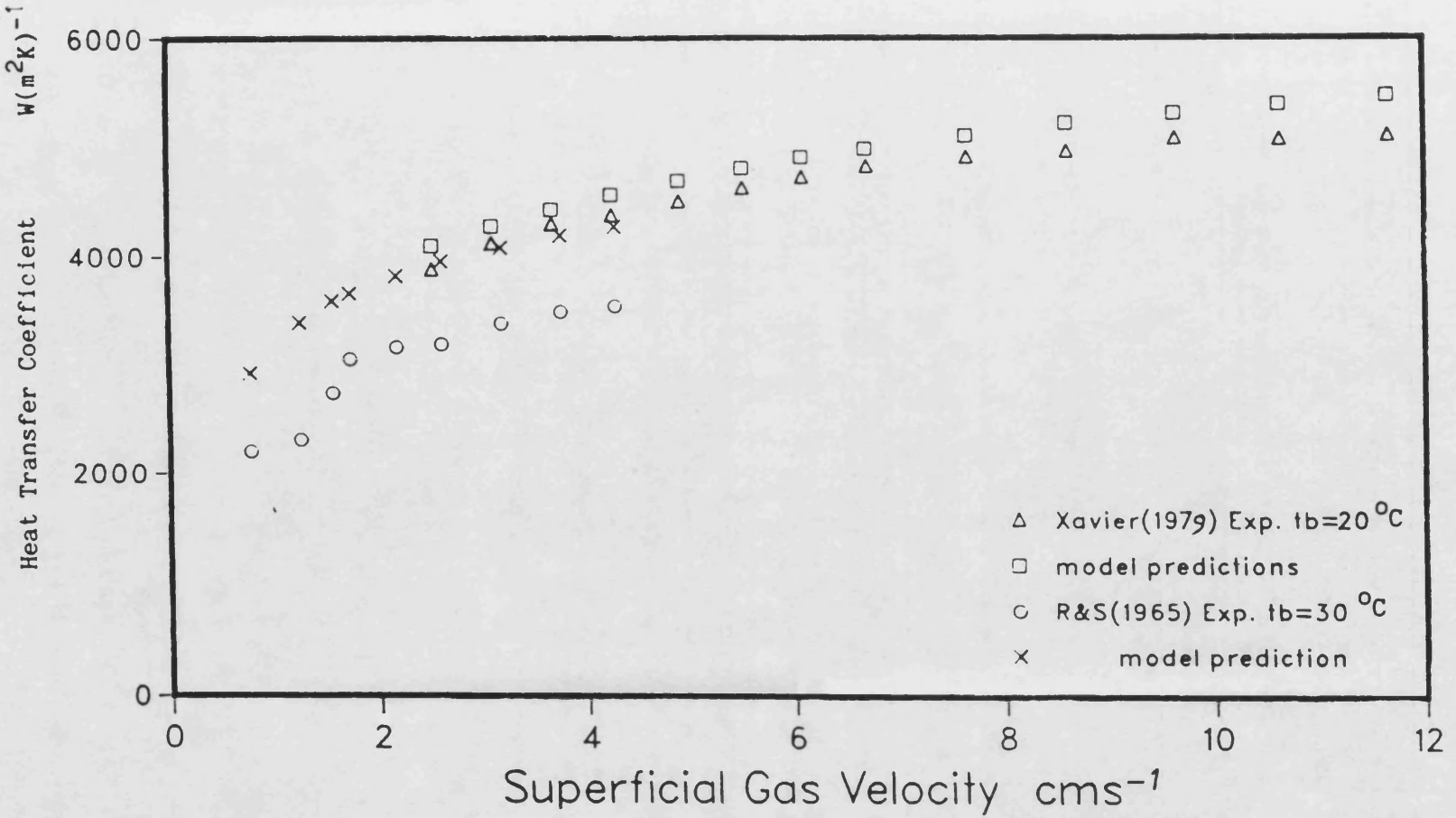

Figure 7.7.-Variation of experimental and model predicted heat transfer coefficient with superficial gas velocity for the air- water system. Data of Xavier and Smigelschi and Ruckenstein.

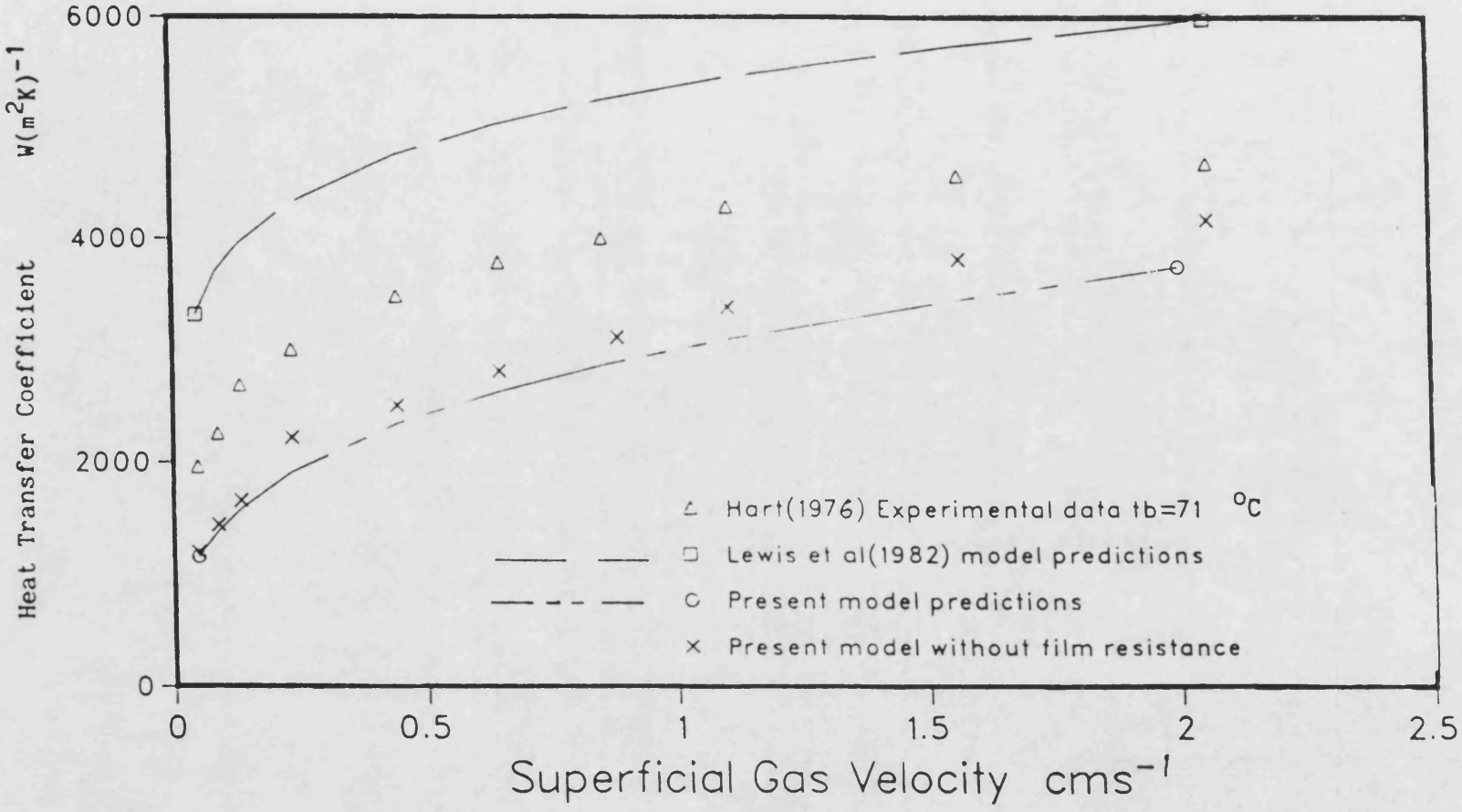

Figure 7.8.- Variation of heat transfer coefficient with superficial gas velocity for aerated water. Experimental data of Hart together with prediction of Lewis et al and present model are shown.

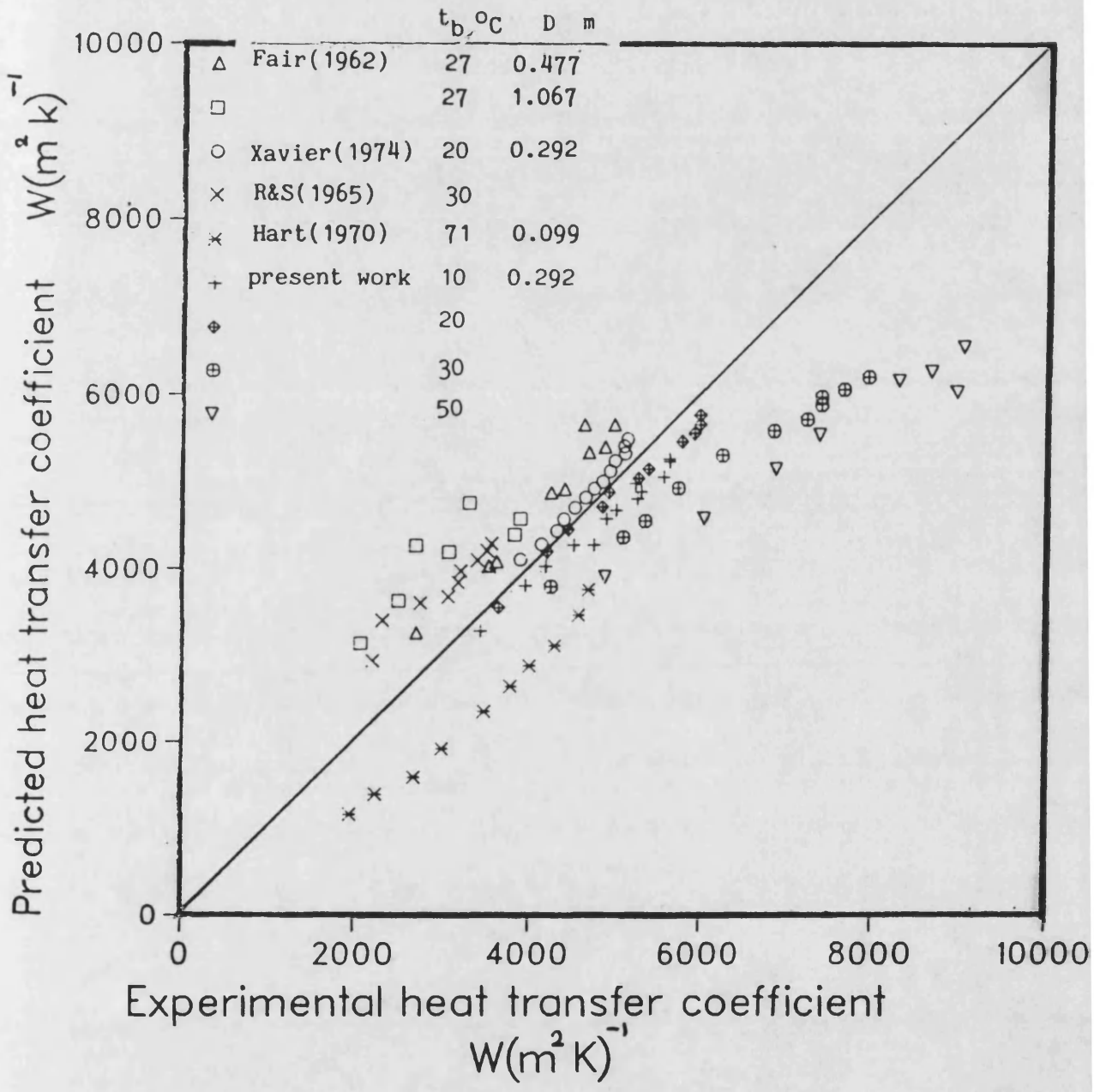

Figure 7.9.-Comparison of experimental heat transfer data for which holdup vales were available with present model. air water system.

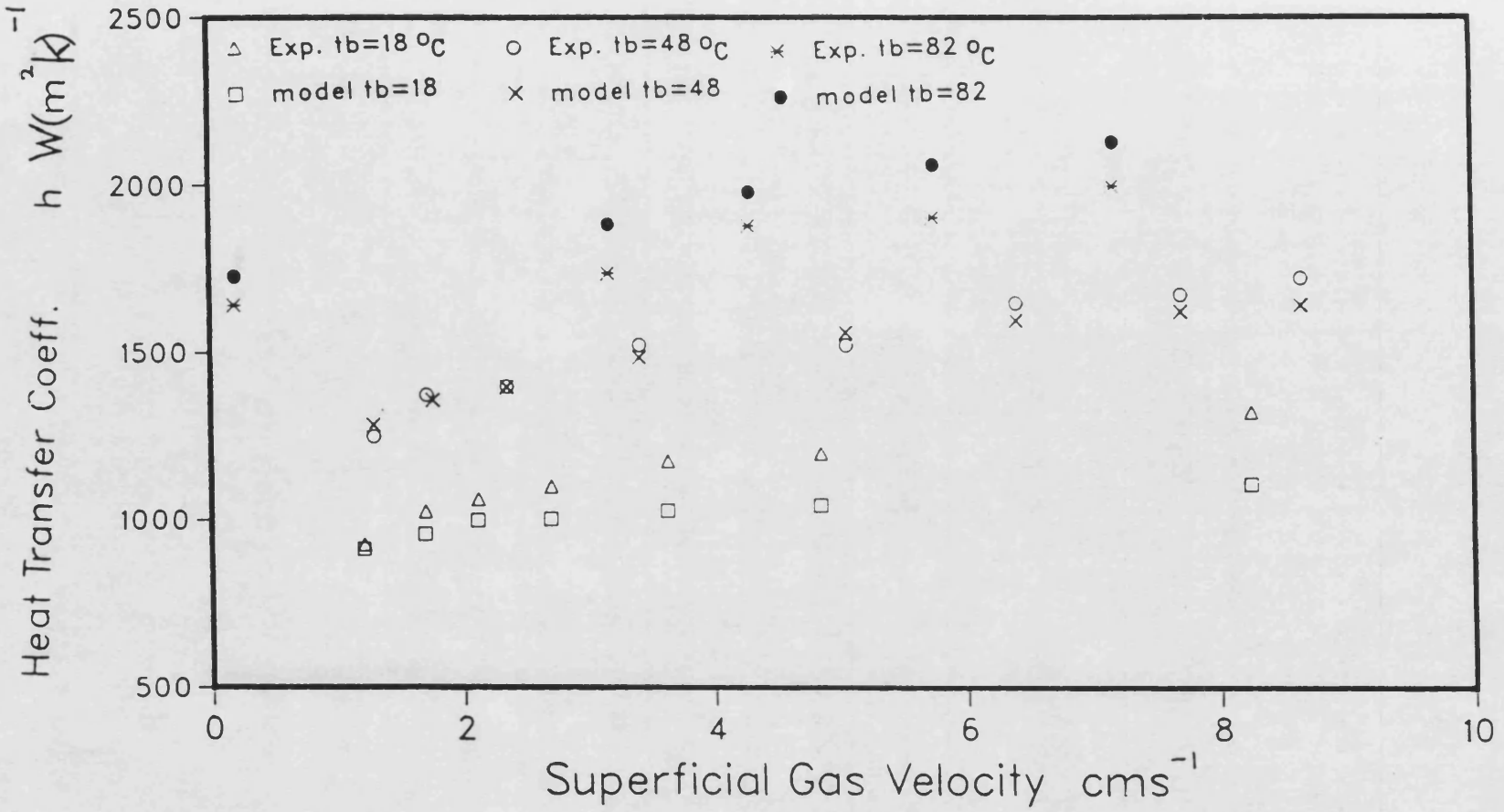

Figure 7.10.- Variation of heat transfer coefficient with superficial gas velocity for Glycol- N_2 data of Lewis et al. Comparison of the experimental data with the prediction of the present model.

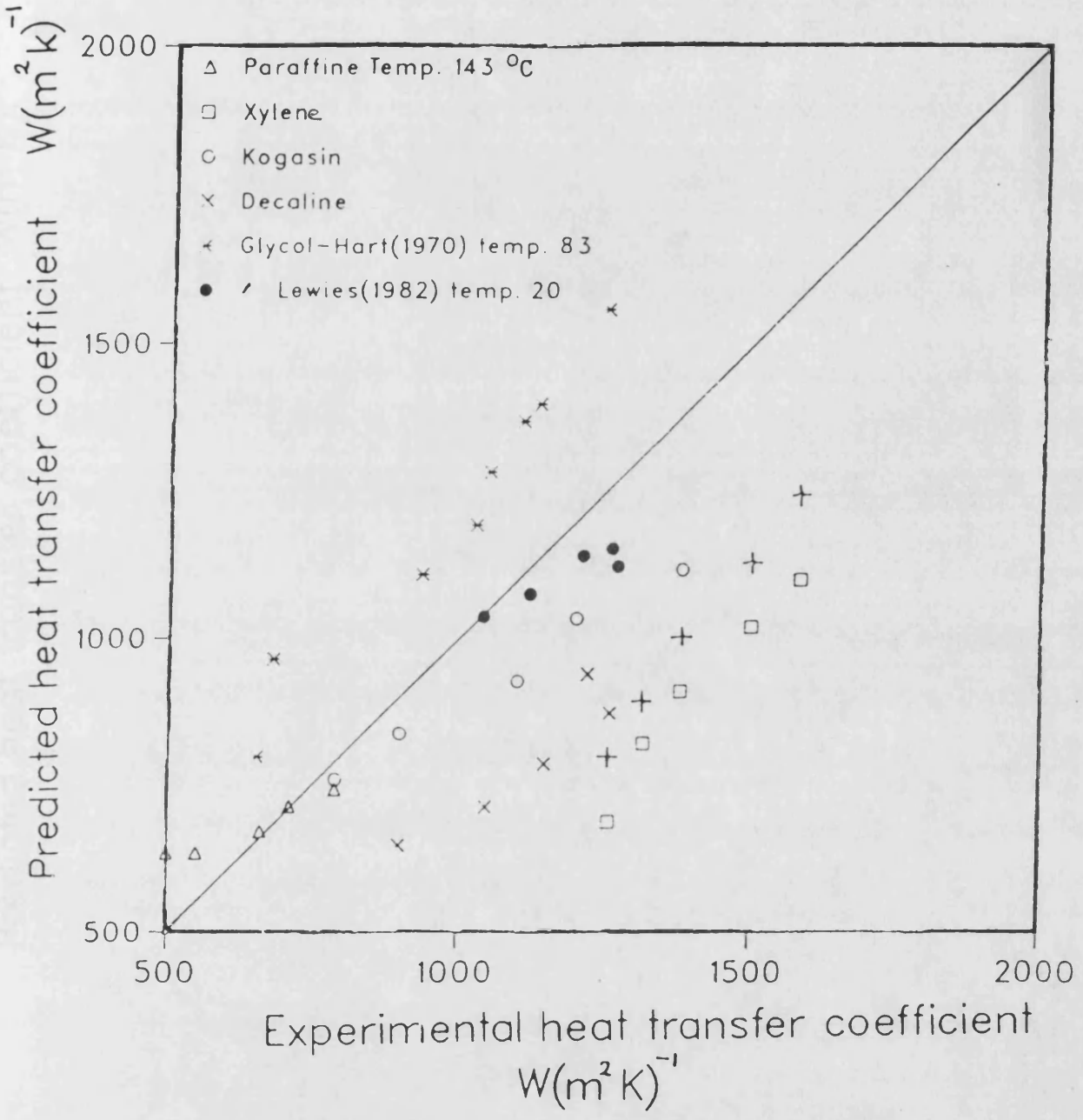

Figure 7.11.(a)- Comparison of experimental heat transfer data for which hold-up values were estimated with the present model .Film resistance was include.

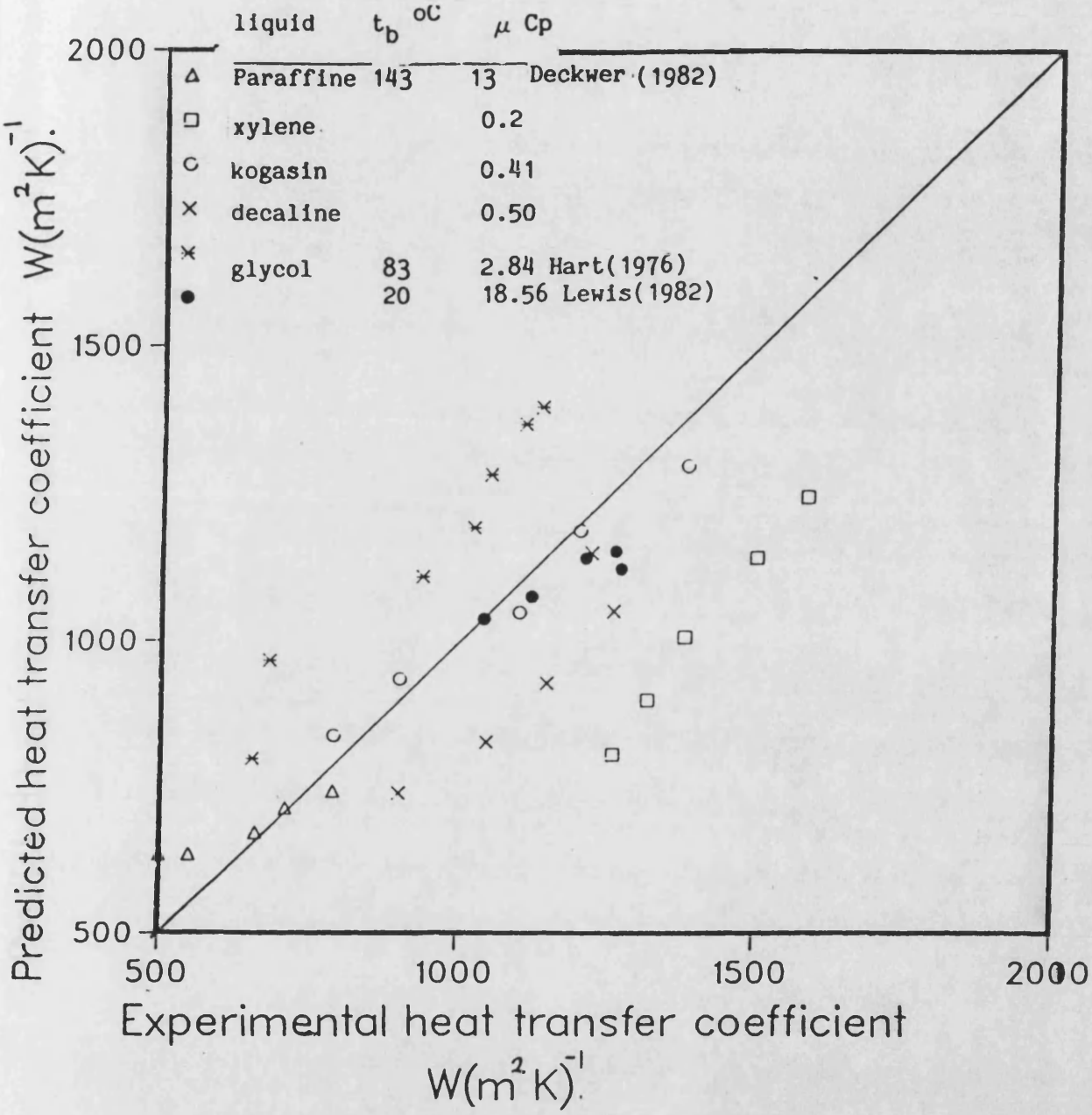

Figure 7.11.(b)- Comparison of experimental heat transfer data for which hold-up values were estimated with the present model. Film resistance was excluded.

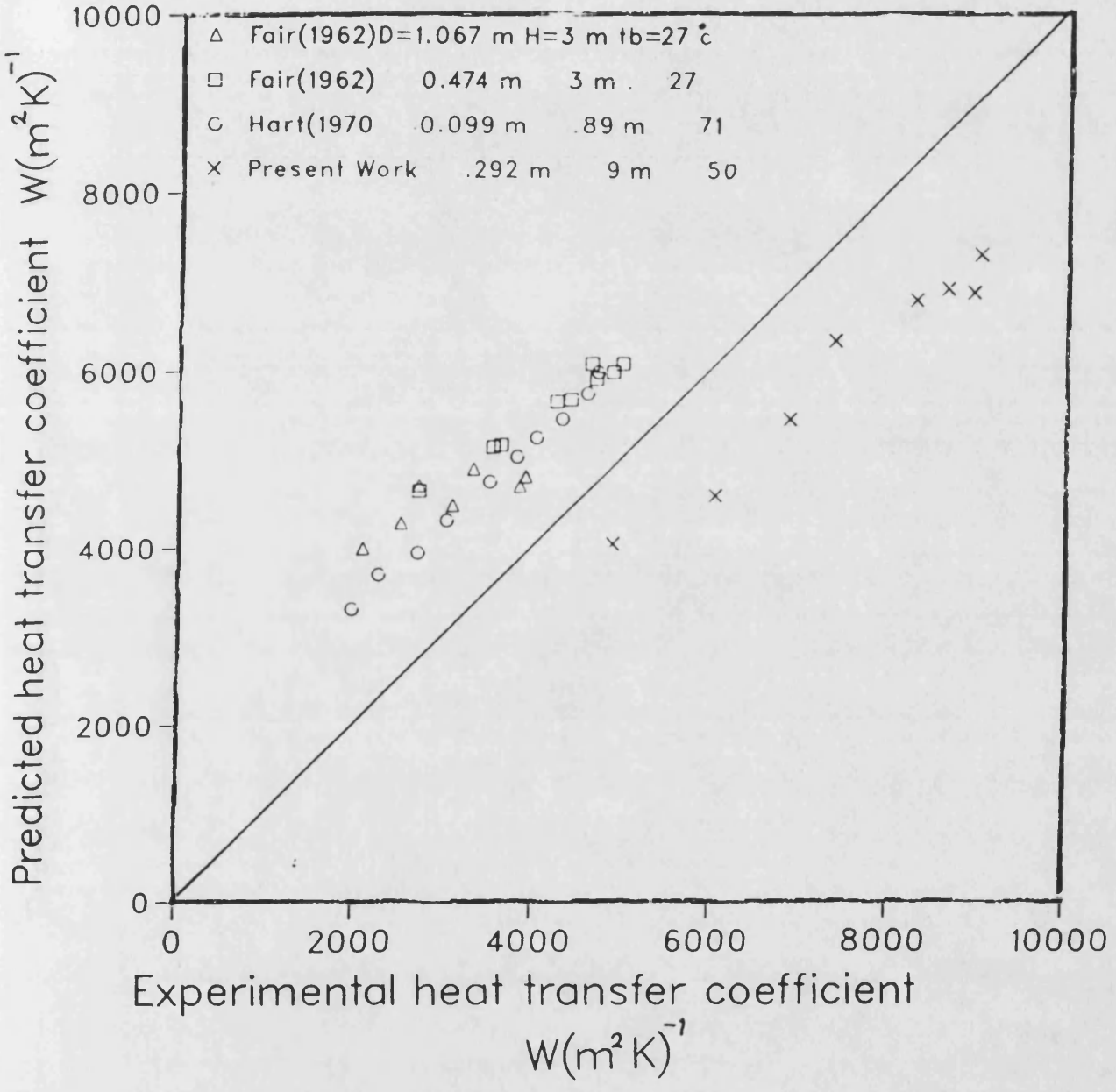

Figure 7.12.- Comparison of experimental heat transfer data with the Lewis et al model.

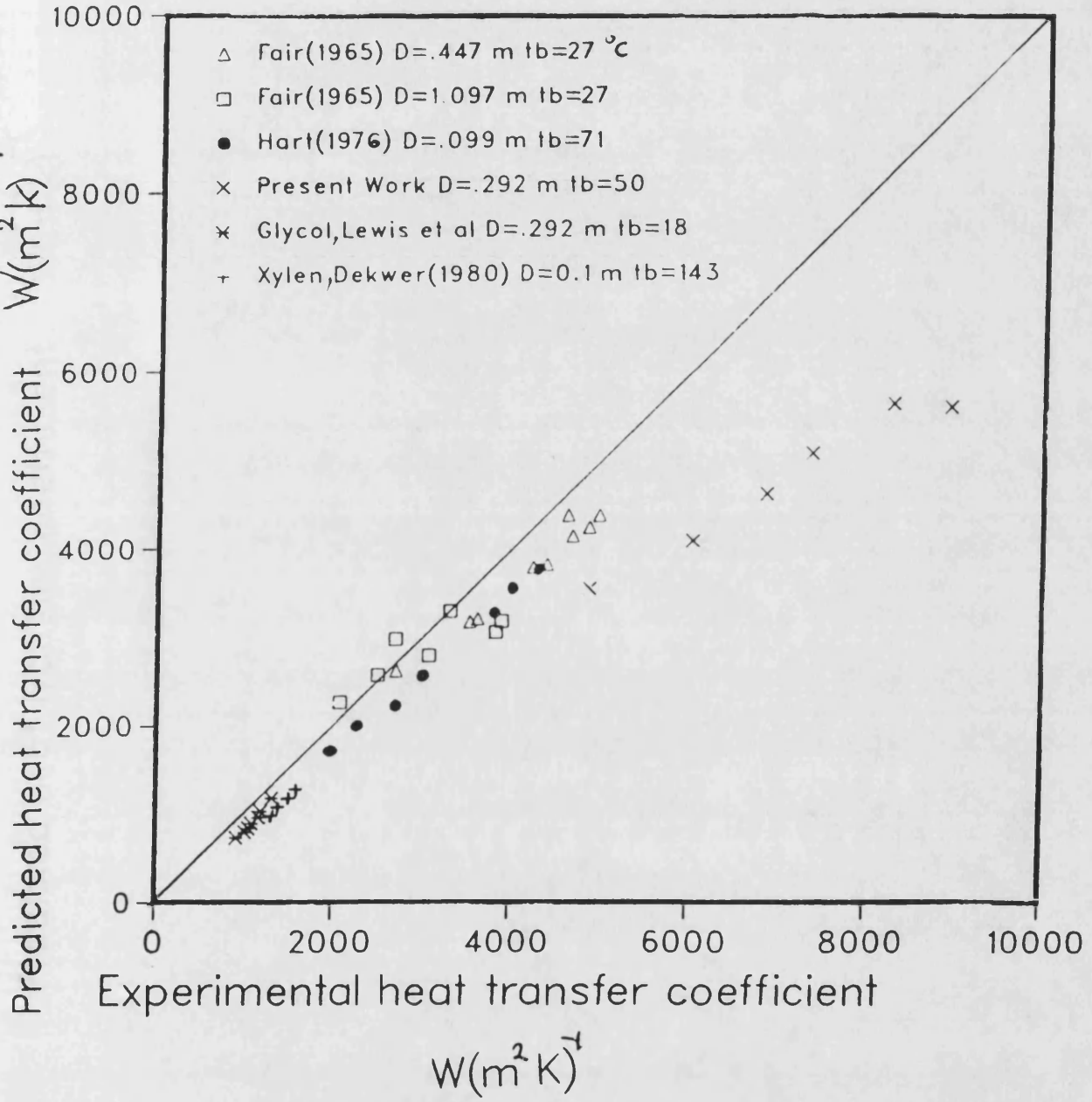

Figure 7.13.- Comparison of heat transfer data for which hold-up values were available with the present model. air- water system.

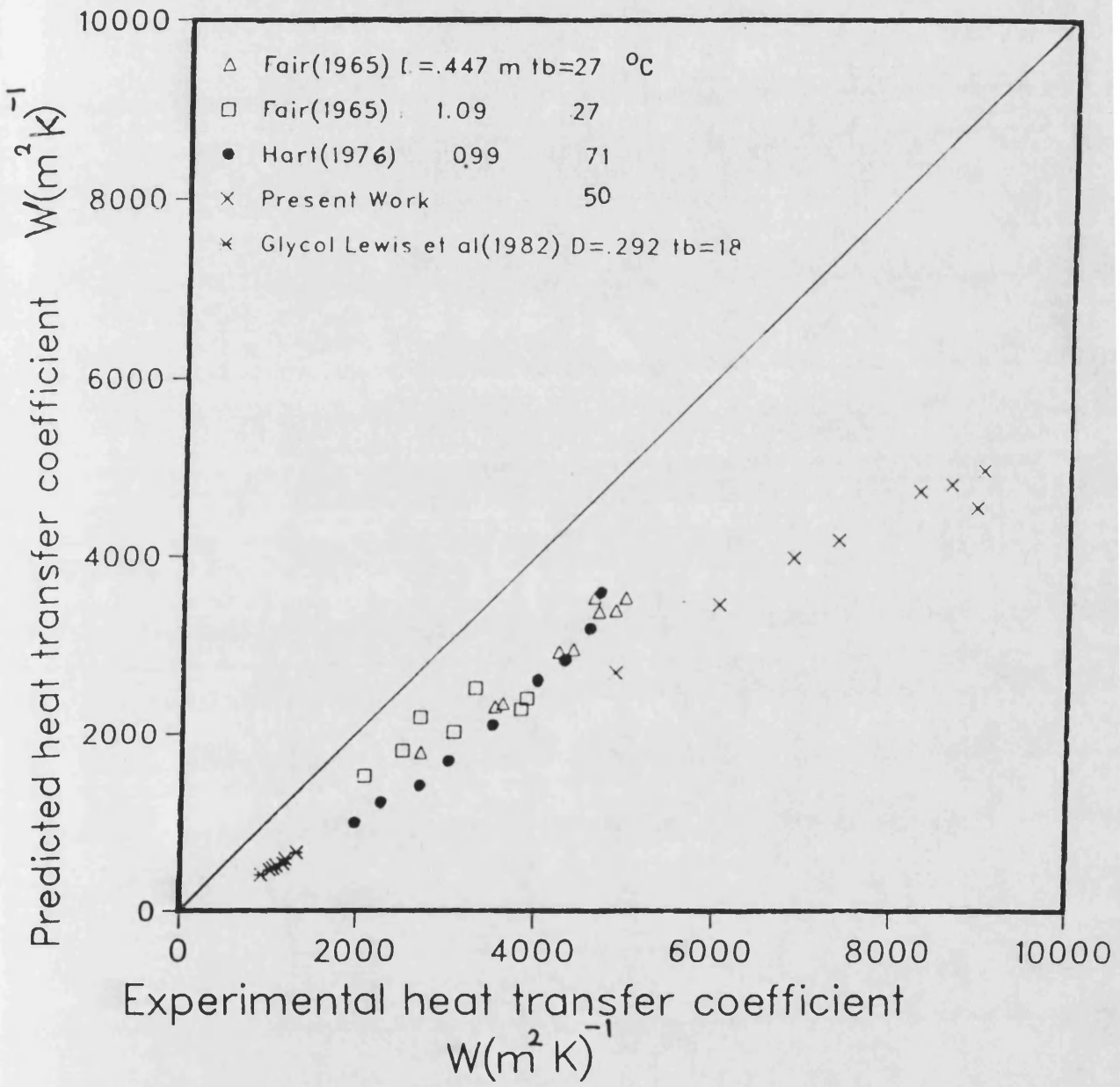

Figure 7.14.- Comparison of heat transfer data for which hold-up values were available with Ruckenstein and Smigelschi model. air water system.

Figure 7.15 Variation of the Thermal Boundary Layer Thickness with Viscosity for CMC solutions

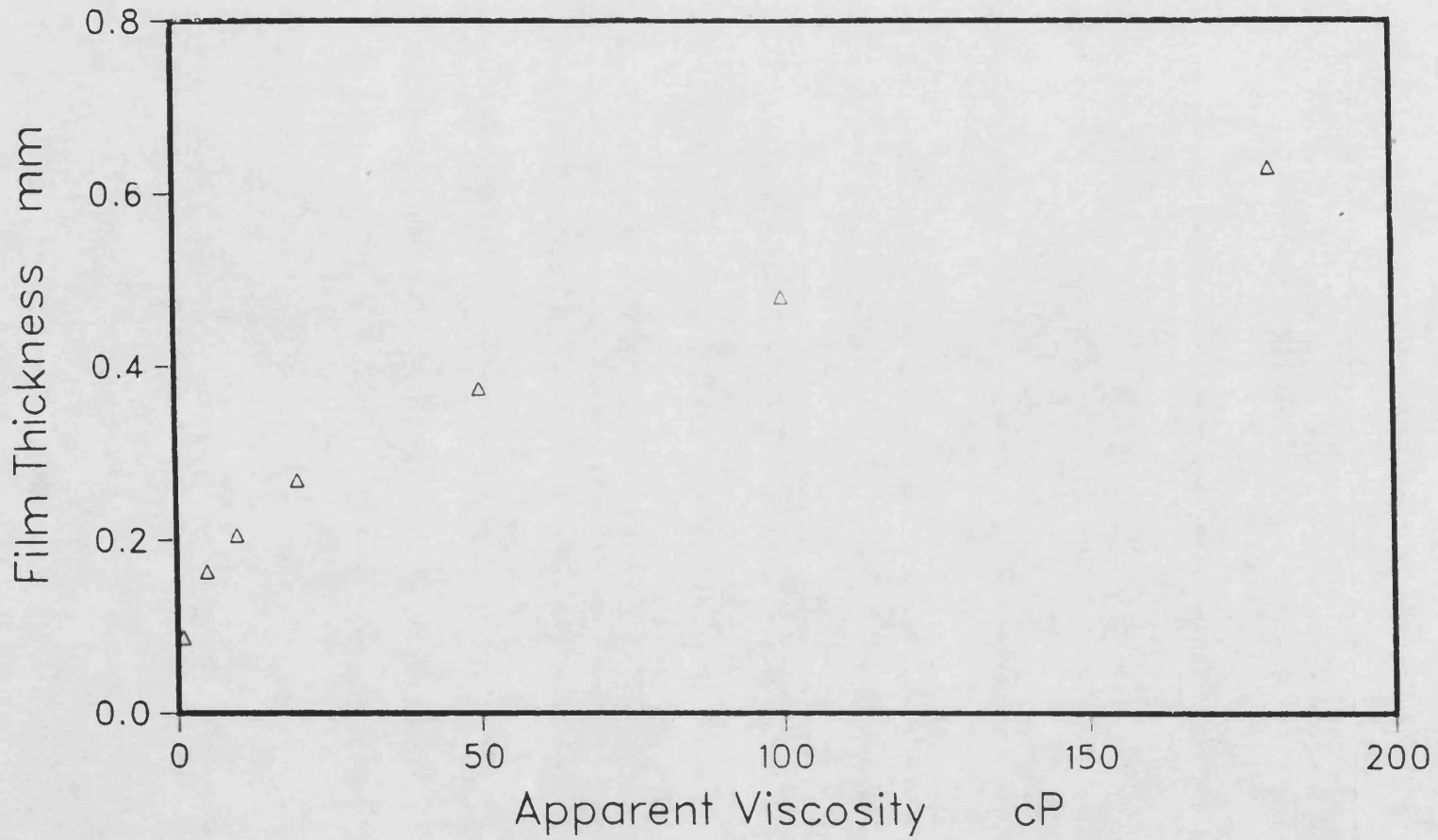

Figure 7.16.- Variation of Heater Characteristic Length with Viscosity for CMC solution

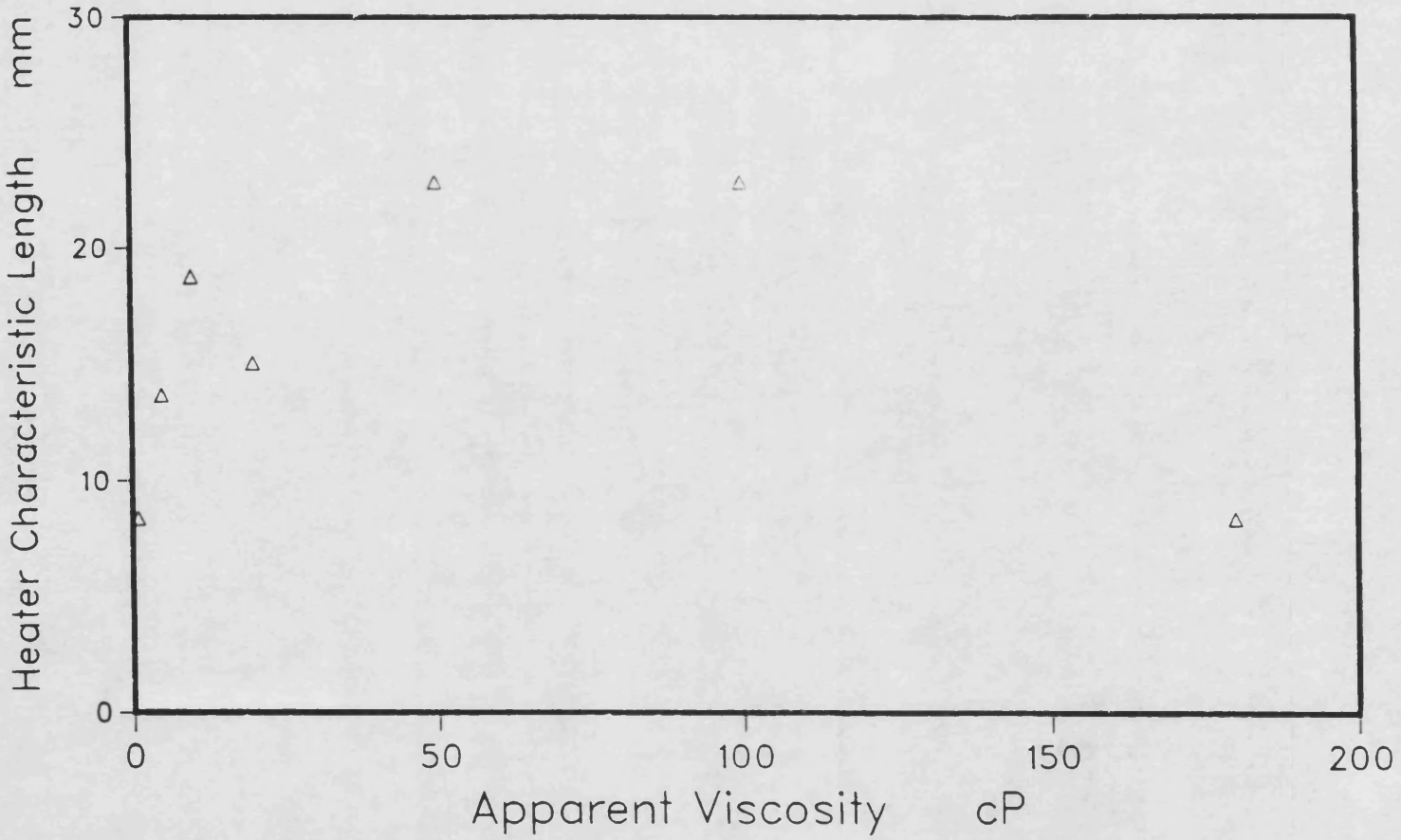

Figure 7.17.- Variation of Heat Transfer Coefficient with Superficial Gas Velocity for 100 ppm CMC solution

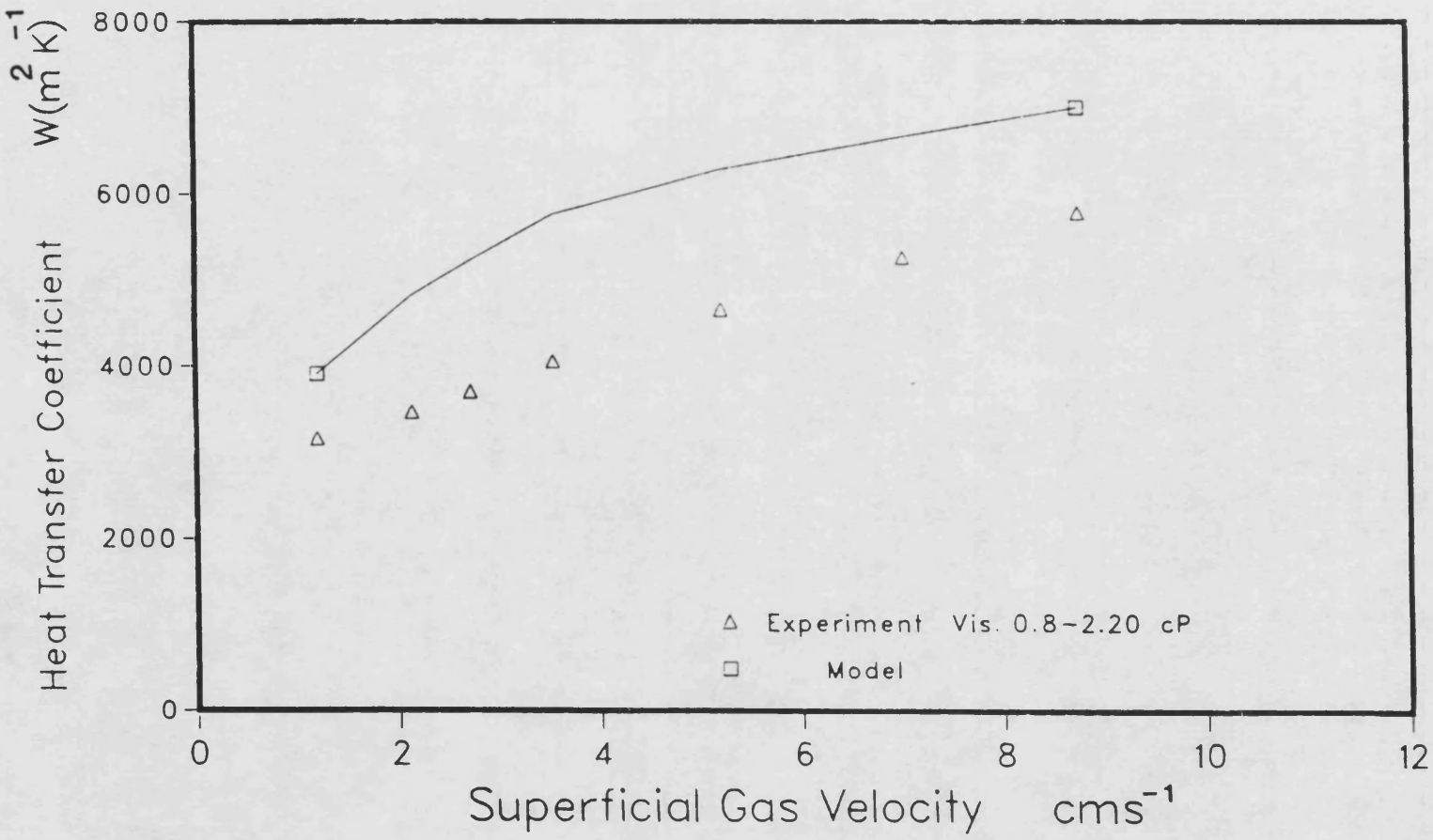

Figure 7.18.- Variation of Heat Transfer Coefficient with Superficial Gas Velocity for 10000 ppm CMC solution

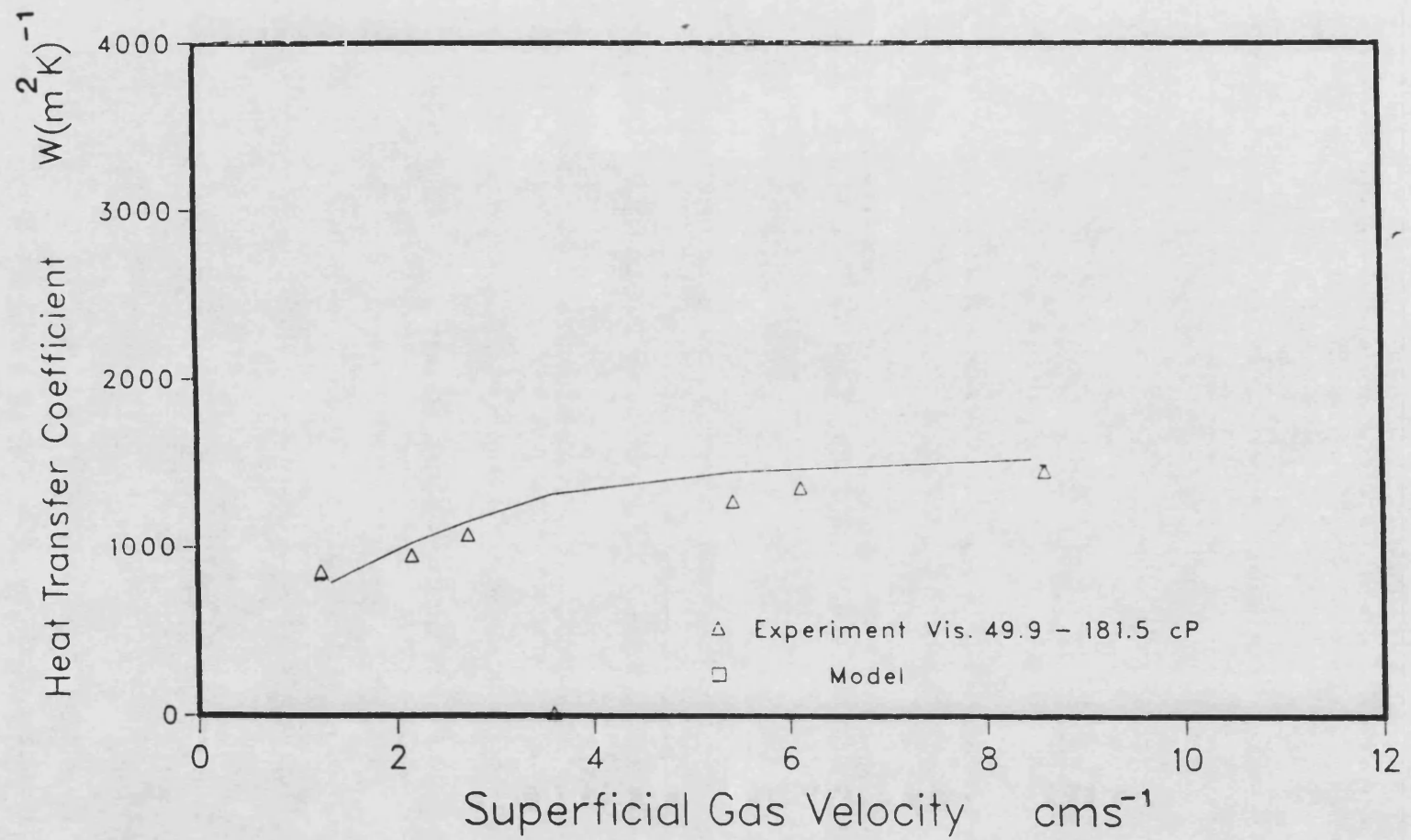

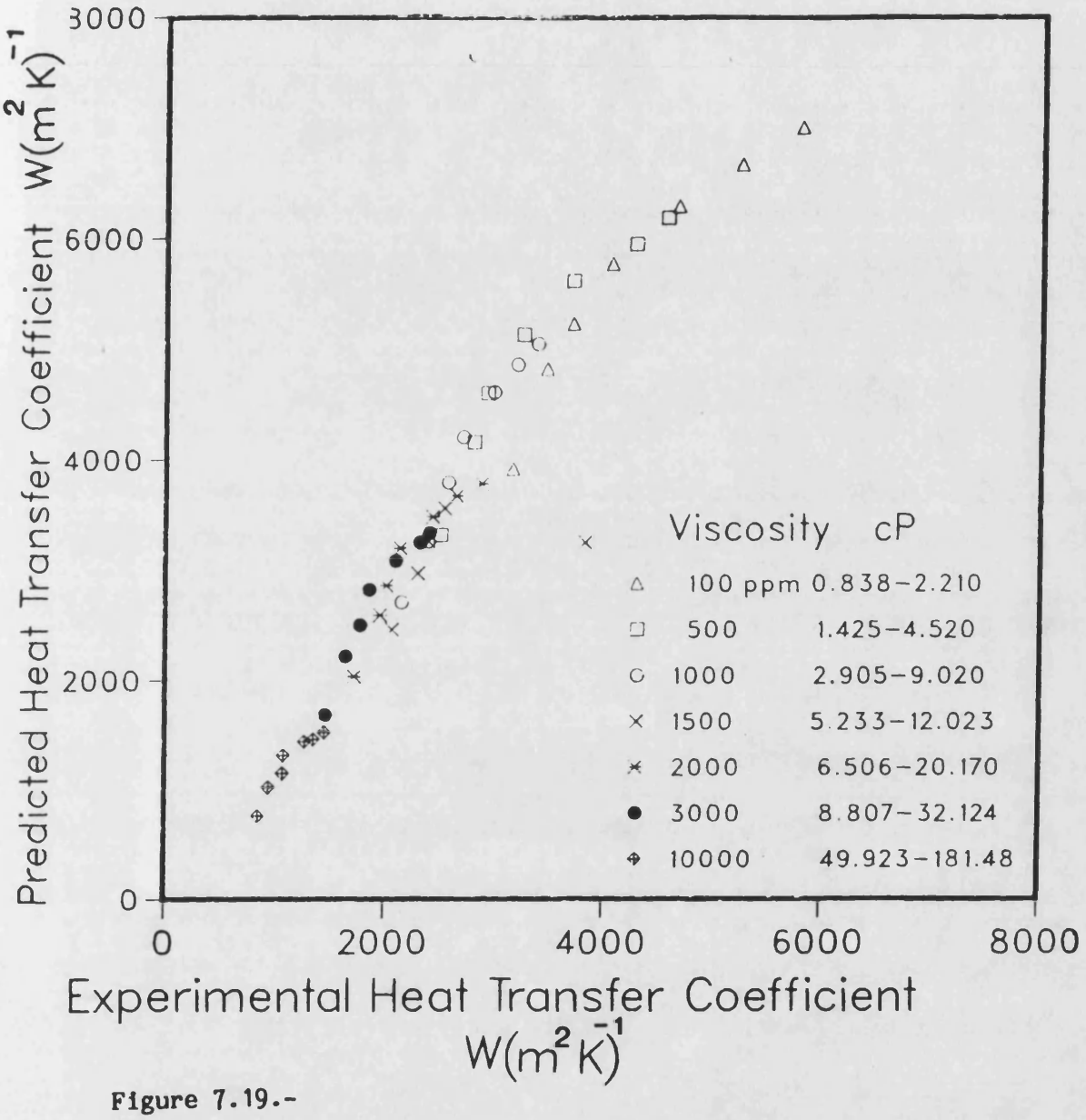

Figure 7.19.-
Comparison of Experimental and Predicted Heat Transfer Coefficients for a number of CMC solutions

APPENDIX A

A1- Calculation of Superficial Gas Velocity

The volumetric gas flow rates were measured by rotameter. The values obtained from the manufacturer's calibration chart were corrected to give the volumetric flow rate at room temperature and pressure at the column base. The following procedure was employed.

The volumetric gas flow rate measured by rotameters (See for example Coulson and Richardson Vol. 1)is given by

$$V = A_2 \left[\frac{2gv_f(\rho_f - \rho_g)}{c(Re)\rho_g A_1} \right]^{1/2} \qquad \ldots A1$$

V= Volumetric gas flow rate.

A_2 =the minimum area between the float and the heater

A_1 =the minimum cross sectional area of the float in a horizontal plane.

V_f =float volum.

ρ_f =float density

ρ_g =gas density - Air in this case

c(Re) shows that the discharge coefficient is a function of

Reynolds number,Re.

Assuming that the height of float is the same for two conditions 1 and 2, then one obtains from A1 that;

$$\frac{\rho_f - \rho_{g1}}{\rho_f - \rho_{g2}} = \frac{C_1}{C_2}\frac{\rho_{g1}}{\rho_{g2}}\left(\frac{V_1}{V_2}\right)^2 \qquad \ldots A2$$

Since the gas density $\rho_g << \rho_f$ and assuming that the discharge coefficients are also equal at the two conditions, equation A2 simplifies to equation A3

$$V_2 = V_1\sqrt{\frac{\rho_{g1}}{\rho_{g2}}} \qquad \ldots A3$$

where V_1 can be read from the calibration chart. Now , in the case of gas , ρ_{g1}, ρ_{g2}, are related to pressure and temperature (ideal gas flow) hence A3 can be written as

$$V_2 = V_1\sqrt{\frac{p_1}{p_2}\cdot\frac{T_2}{T_1}} \qquad \ldots A4$$

where P_2 is pressure just above the rotameters and T_2 is room or bulk temperature. V_1 and T_1 are conditions that have been specified by the calibration chart.

Value of V2 can further be corrected to pressure at column base.

$$V_c = \frac{P_2 V_2}{P_c} \qquad \ldots A5$$

where Vc = volumetric flow rate of gas at column base and

Pc = pressure at column base.

But

$$Pc = P_{atm} + \rho g H \qquad \ldots A6$$

where H = initial column liquid height m

ρ = liquid density Kg m^{-3}

P_{atm} = Atmospheric pressure Pa

Also superficial gas velocity can be defined as

$$U_g = \frac{V_c}{A_1} \qquad \ldots A7$$

Where $A_1 = \frac{\pi D^2}{4}$ column area

Therefore from A4 to A7 one obtains

$$U_g = \frac{4P_2 V_1 \left(\frac{P_1}{p_2} \cdot \frac{T_2}{T_1} \right)^{1/2}}{\pi (P_{atm} + \rho g H) D^2} \qquad \ldots A8$$

In this work P_1 = 14.7 psi

T_1 = 288 K

V_1 = 1000/60 V_1'

where V_1' is read from the calibration chart in $1 min^{-1}$.

P_{atm} = 1.01x105 Pa

P_2' = Measured pressure psig

hence P_2 = P_2' + 14.7 psia

$$P_2 = (P_2' + 14.7) \times 6.89 \times 103 \quad Nm^{-2}$$

therefore

$$U_g = 38.76 \frac{V_1'(T_2(P_2' + 14.7))^{1/2}}{1.01\times10^5 + \rho g H} \qquad \ldots A9$$

A2.- CALCULATION OF THE CORRECTED SURFACE TEMPERATURE OF THE HEATER.

In order to calculate an average surface temperature of the heater the measured temperature inside the heater where corrected in the following way.

Refering to Figure A1 the distance of the thermocouple from the heater sureface, CD, is given by,

$$CD = AB - DB \times \sin(\alpha) \qquad \ldots A10$$

where AB is the distance of the entrance holes for the thermocouples from the edge of the heater and BD is the thermocouple length inside the heater. These are specifiec in Figure 3.5a and their values are given in Tables A1 to A3 for heater lengths of 120, 60 and 30 mm respectively.

Assuming one dimensional heat conduction the difference between surface temperature, T_s, and the measured

temperature T_t is calculated from;

$$Q = \frac{2\pi k l(\Delta T)}{\ln \frac{r_s}{r_t}} \qquad \ldots A11$$

where

Q = Heat input to the heater W

l = Heater length mm

r_s = Heater radius mm

r_t = r_s - CD

k = Thermal conductivity of the heater. $W(mK)^{-1}$

Therefore the average value of the heater surface temperature is,

$$T_a = \frac{\sum T_t - \sum \Delta T}{4} \qquad \ldots A12$$

The calculated values of Δ T for each thermocouple and for power inputs of 45, 90 and 180 W are given in Tables A1 to A3.

Table A1 Position of the thermocouples for the 30x120 mm heater together with the values of ΔT for each thermocouple at different power inputs.

Thermo-couple	DB mm	α degree	CD mm	ΔT °C		
				45 W	90 W	180 W
1	55.5	7	0.73	0.03	0.06	0.12
2	55.5	7	0.73	0.03	0.06	0.12
3	42	7	2.38	0.10	0.21	0.41
4	55.5	7	0.73	0.03	0.06	0.12
			sum	0.19	0.38	0.76

Table A2 Position of the thermocouples for the 30x60 mm heater together with the values of ΔT for each thermocouple at different power inputs.

Thermo-couple	DB mm	α degree	CD mm	ΔT °C		
				45 W	90 W	180 W
1	32.5	12	2.24	0.19	0.39	0.78
2	32.5	12	2.24	0.19	0.39	0.78
3	31	12	2.55	0.22	0.44	0.89
4	34	12	1.93	0.16	0.33	0.66
			sum	0.76	1.55	3.11

Table A3.- Position of the thermocouples for 30x30 mm heater together with the values of ΔT for each thermocouple at different power inputs.

Thermo-couple	DB	α	CD	ΔT °C		
	mm	degree	mm	45 W	90 W	180 W
1	29	14	1.48	0.25	0.50	0.77
2	24	14	2.69	0.47	0.94	1.47
3	24	14	2.69	0.47	0.94	1.47
4	29	14	1.48	0.25	0.50	0.77
			sum	1.44	2.88	4.48

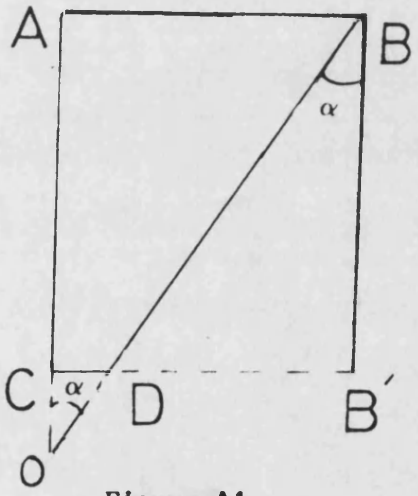

Figure A1

APPENDIX B

HOLD-UP MEASUREMENT-USE OF DIGITAL MANOMETER.

The following describes the method used to obtain equation 4.4 in order to calculate local gas hold-up .

Refering to Figure B1 one obtains

$$Z_1 = Z_2 + \Delta h - \Delta Z \qquad \ldots B1$$

Pressure at point 1 and 2 in Figure B1 can be related to static pressures in the column and in the manometer limbs. Therefore for a liquid mixture in the column;

$$P_1 = \rho g (1 - \epsilon) H_b + P_{atm} \qquad \ldots B2$$

$$P_2 = \rho g (1 - \epsilon) (H_b - \Delta h) + P_{atm} \qquad \ldots B3$$

Where H_b is the height of the liquid mixture above point 1 and Δh is the distance between the ends of the manometer limbs. For the manometer limbs,

$$P_1 = \rho g Z_1 + P_{m1} \qquad \ldots B4$$

$$P2 = \rho g Z_2 + Pm_2 \qquad \ldots B5$$

Where Z_1 and Z_2 are liquid height in the manometer limbs and P_{m1} and P_{m2} are pressures above the liquid levels in the manometer limbs as indicated in Figure B1. Hence, combination of the

equations B1 and B5 gives;

$$\epsilon = \frac{\Delta Z}{\Delta h} + \frac{\Delta P_m}{\rho g \Delta h} \qquad \ldots B6$$

Where $\Delta Z = Z_2 - Z_1$ and $\Delta Pm = P_{m2} - P_{m1}$

ΔP_m was read from digital manometer whilst ΔZ was calculated by considering the change in the gas volume trap in the manometer limbs before and after areation. This was achieved by the adoption of the following procedure.

If P^o_{m1} and P^o_{m2} are the initial pressures in the manometer limbs then

$$P^o_{m1} = P^o_{m2} = P_{atm} \qquad \ldots B7$$

After aeration the liquid level inside the manometer tubes will rise as the pressure increases. Then applying the ideal gas law one can write

$$P^o_{m1} A.H_t = P_{m1}.A.(H_t - \delta Z_1) \qquad \ldots B8$$

$$P^o_{m2} A.H_t = P_{m2}.A.(H_t - \delta Z_2) \qquad \ldots B9$$

Where H_t is the total length of the manometer and tubing filled with air and A is the cross sectional area of the manometer limbs. δZ_1 and δZ_2 are the increase of liquid level in the manometer limbs due to aeration. Therefore from B8 and B9 one gets;

$$P_{m1} = \frac{P^{o}_{m1}}{1 - \frac{\delta Z_1}{H_t}} \approx P^{o}_{m1}\left(1 + \frac{\delta Z_1}{H_t}\right) \qquad \ldots B10$$

$$P_{m2} = \frac{P^{o}_{m2}}{1 - \frac{\delta Z_1}{H_t}} \approx P^{o}_{m2}\left(1 + \frac{\delta Z_2}{H_t}\right) \qquad \ldots B11$$

From B10 and B11 one obtains;

$$P_{m2} - P_{m1} \approx P_{atm}\frac{\Delta Z}{H_t} \qquad \ldots B12$$

where $\Delta Z = \delta Z_2 - \delta Z_1$ ...B13

Substitution for ΔZ from equation B12 into equation B6 and subsequent simplifications gives an expression for local gas holdup in the bubble column.

$$\epsilon = \frac{(P_{m2} - P_{m1})}{\rho g \Delta h}\left(1 + \frac{\rho g H_t}{P_{atm}}\right) \qquad \ldots B14$$

Where $P_{m2} - P_{m1}$ is the digital pressure gauge readings and H_t and Δh are the length of the manometer tubing and the distance between the ends of the manometer limbs ,respectively.

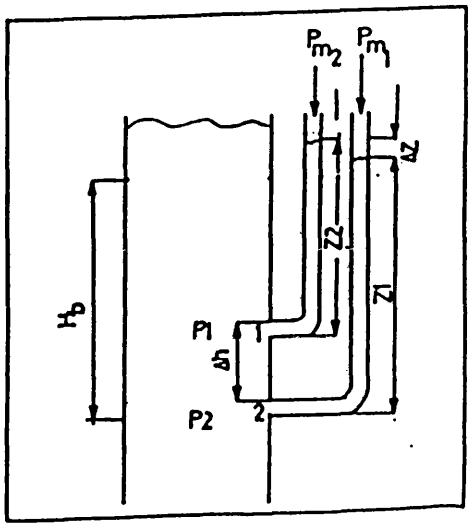

Figure B1

Manometer tubes are connected to the digital pressure gauge. External limbs drawn to illustrate the theoretical basis of the calculation. In the experimental set up the manometers, shown in Figure4.1(d), were placed inside the column.

APPENDIX C

DATA USED TO TEST NEW MODEL

This appendix gives the experimental data of several investigators for air- water and a number of organic liquids. These data were used to test the present model. The results with a sample calculation for Table C1.1 are given below. The results of Tables C1.1- C1.8 and C2.1- C2.7 are for water and organic systems, respectively.

C1- Comparison of the Prediction of the Present Model with the Experimental Values for Air- Water System.

Sample calculation for data of Table C1.1 :

Data of Fair(1962) for water,

t_b = 27 ^oC D= 0.477 m H= 3 m

density=	997	kgm^{-3}
heat capacity=	4179	$J(kg\ K)^{-1}$
Thermal conductivity=	0.609	$W(m\ K)^{-1}$
viscosity=	0.85	cP

$$U_{cJs}= 1.31(2 \times 9.81 \times 0.477\ U_g \varepsilon)^{1/3} \quad ms^{-1}$$

$$1/h_p= [\ (\pi \times 0.031)/(4 \times 997 \times 4179 \times 0.069\ U_{cJs})\ ]^{1/2}$$

$$1/h_f= [\ 1.49 \times 10^{-3} \times (0.85 \times 10^{-3})^{0.567}\ ] / 0.609$$

$= 4.442 \times 10^{-5}$ $(m^2K)W^{-1}$

$1/h_{pred.} = 1/h_p + 1/h_f$

$\%error = (h_{pred.} - h_{exp.}) / (h_{exp.}) \times 100$

Table C1.1.- Data of Fair for air water system.

$t_b = 27\ ^oC$ D= 0.477 m

U_g mms^{-1}	holdup	$h_{exp.}$ $W(m^2K)^{-1}$	$h_{pred.}$ $W(m^2K)^{-1}$	%error
6.38	0.02	2708	3256	21
13.70	0.048	3529	4029	14
14.30	0.045	3617	4078	13
27.90	0.087	4238	4873	15
28.80	0.090	4379	4914	12
39.70	0.124	4678	5338	14
43.60	0.136	4866	5399	11
49.40	0.154	4977	5640	13
49.40	0.154	4625	5640	22

Table c1.2.- Data of Fair for air - water system.
t_b= 27 °C D= 1.067 m H=3 m

U_g mms^{-1}	holdup	$h_{exp.}$ W(m^{2}K)$^{-1}$	$h_{pred.}$ W(m^{2}K)$^{-1}$	%error
3.58	0.0125	2078	3141	51
5.97	0.0209	2506	3631	45
8.32	0.0291	3078	3981	30
10.75	0.037	2701	4259	57
11.9	0.0417	3829	4388	15
13.90	0.0487	3892	4574	18
16.08	0.563	3307	4753	44

Table C1.3.- Data of Xavier(1974) for air water system.

t_b= 20 °C D=0.292 m H= 0.90 m

U_g mms^{-1}	holdup	$h_{exp.}$ W(m^{2}K)$^{-1}$	$h_{pred.}$ W(m^{2}K)$^{-1}$	%error
25.24	0.08	3889	4105	6
30.97	0.09	4128	4282	4
36.71	0.10	4303	4436	3
42.44	0.11	4384	4572	4
48.95	0.12	4512	4704	4
55.06	0.13	4638	4821	4
60.8	0.14	4740	4925	4
66.92	0.145	4838	5003	3
76.48	0.155	4925	5124	4
86.04	0.165	4981	5240	5
96.36	0.170	5102	5327	4
106.30	0.175	5093	5409	6
116.63	0.180	5130	5488	7

Table C1.4.- Data of Ruckenstein and Smigelschi(1965) for air water system.
t_b= 30 °C D= 0.085 m

U_g mms^{-1}	holdup	$h_{exp.}$ W(m^{2}K)$^{-1}$	$h_{pred.}$ W(m^{2}K)$^{-1}$	%error
7.8	0.045	2208	2930	32
12.6	0.078	2316	3397	47
15.70	0.094	2748	3598	31
17.4	0.098	3066	3688	19
21.8	0.106	3178	3831	20
26.1	0.114	3205	3963	23
31.8	0.117	3394	4088	20
37.5	0.120	3502	4199	20
42.7	0.122	3555	4280	20

Table C1.5.- Data of Hart(1970) for air water system.

t_b= 71 °C D= 0.099 m H= 0.86 m

U_g mms^{-1}	holdup	$h_{exp.}$ W(m^{2}K)$^{-1}$	$h_{pred.}$* W(m^{2}K)$^{-1}$	%error
0.0485	0.00103	1960	1200	-39
0.885	0.00188	2256	1450	-36
1.336	0.00284	2693	1664	-38
2.36	0.00502	3011	2024	-33
4.45	0.00947	3489	2512	-28
6.49	0.0138	3790	2844	-25
8.550	0.0182	4006	3122	-22
11.06	0.0235	4296	3394	-21
15.65	0.0333	4574	3824	-16
20.60	0.0438	4688	4184	-11

* film resistance excluded.

Table C1.6.- Data of Present work.

t_b= 10 ^oC D= 0.292 m H= 0.90 m

U_g mms^{-1}	holdup	$h_{exp.}$ $W(m^2K)^{-1}$	$h_{pred.}$ $W(m^2K)^{-1}$	%error
20.8	0.066	3949	3805	-4.0
26.6	0.084	4183	4029	-4.0
34.3	0.105	4508	4276	-5.0
40.6	0.118	4743	4276	-10.0
50.1	0.126	4889	4575	-6.0
56.9	0.133	5005	4673	-7.0
68	0.141	5253	4806	-9.0
76.1	0.145	5296	4886	-8.0
82.8	0.159	5226	4983	-5.0
93.1	0.159	5557	5054	-9.0
103.5	0.194	5626	5231	-7.0
112.9	0.187	5624	5261	-6.0

Table c1.7.- Data of Present Work. air water system.

t_b= 20 ^oC D= 0.292 m H= 0.90 m

U_g mms^{-1}	holdup	$h_{exp.}$ $W(m^2K)^{-1}$	$h_{pred.}$ $W(m^2K)^{-1}$	%error
21.2	0.075	4197	4198	0
27.1	0.092	4441	4453	0
34.9	0.112	4839	4715	-3
41.3	0.124	4917	4881	-1
51.4	0.129	5263	5041	-4
58.1	0.134	5381	5147	-4
69.3	0.159	5770	5371	-7
77.6	0.163	5770	5459	-5
84.4	0.172	5913	5553	-6
94.9	0.178	5975	5653	-5
106	0.186	5975	5761	-4

Table C1.8.- Data of Present Work for air water system.

t_b= 30- 32 ^oC D= 0.292 m H= 0.90 m

U_g mms^{-1}	holdup	$h^{exp.}$ $W(m^2K)^{-1}$	$h_{pred.}$ $W(m^2K)^{-1}$	%error
12.4	0.047	4238	3786	-11
21.6	0.075	5085	4355	-14
27.6	0.080	5341	4541	-15
35.6	0.113	5725	4920	-14
52.0	0.137	6229	5298	-15
70.7	0.151	6831	5579	-18
79.0	0.162	7281	5710	-21
86.6	0.186	7385	5878	-20
96.6	0.189	7385	5969	-19
108.8	0.189	7652	6055	-21
118.6	0.204	7938	6179	-22

C2.-Comparison of the Model Predictions with the Experimental Values for Several Organic Liquids.

Table C2.1.- Data of Lewis et al (1982) N_2-glycol system.

tb= 18 °C D=0.292 m H=1.0 m

U_g mms^{-1}	holdup	$h_{exp.}$ $W(m^2K)^{-1}$	$h_{pred.}$ $W(m^2K)^{-1}$	%error
12.12	0.035	925	913	-1
17	0.052	1025	959	-6
21.2	0.085	1062	1000	-8
27	0.069	1100	1004	-9
36.3	0.079	1175	1029	-13
48.5	0.105	1200	1046	-13
82.5	0.148	1325	1110	-16

Table C2.2.- Data of Lewis et al (1982) for N_2- glycol system.

t_b= 48 °C D= 0.292 m H=0.10 m

U_g mms^{-1}	holdup	$h_{exp.}$ $W(m^2K)^{-1}$	$h_{pred.}$ $W(m^2K)^{-1}$	%error
12.94	0.048	1250	1284	3
17.24	0.067	1357	1358	-1
23.53	0.07	1400	1397	-2
34.12	0.103	1525	1486	-3
50.59	0.133	1575	1561	-1
64.5	0.144	1650	1597	-3
77	0.152	1675	1624	-3
86.5	0.160	1725	1643	-5

Table C2.3.- Data of Lewis et al(1982) for N_2-glycol system.

tb= 82 °C D= 0.292 m H= 1.0 m

U_g mms^{-1}	holdup	$h_{exp.}$ $W(m^2K)^{-1}$	$h_{pred.}$ $W(m^2K)^{-1}$	%error
20	0.077	1642	1726	5
31.76	0.112	1738	1883	8
43	0.138	1880	1980	5
57.6	0.156	1905	2061	8
71.76	0.178	2000	2130	7

Table C2.4.- Data of Hart(1976) for air- glycol system.

tb= 83 °C D= 0.099 m H=0.1 m

U_g mms^{-1}	holdup	$h_{exp.}$ $W(m^2K)^{-1}$	$h_{pred.}$ $W(m^2K)^{-1}$	%error
1.38	0.0065	654	799	22
2.75	0.0128	681	966.5	42
4.8	0.0219	937	1110	19
6.45	0.089	1022	1193	17
8.70	0.0383	1050	1283	22
11.4	0.049	1107	1368	24
12.6	0.0536	1135	1397	23
21	0.0823	1249	1556	25

Table C2.5.-Data of Deckwer(1980) for Paraffin .

tb= 143 ^{o}C D= 0.10 m

U_b= 1.53 (29.1 x10^{-3} x 9.81/0.73)$^{0.25}$= 0.215 m

holdup= U_g / (2U_g + 0.215)

U_g mms^{-1}	holdup	$h_{exp.}$ $W(m^2K)^{-1}$	$h_{pred.}$ $W(m^2K)^{-1}$	%error
5	0.044	500	634	27
7	0.031	550	634	27
10	0.043	660	671	2
15	0.061	710	713	0
20	0.078	790	742	-6

Table C2.6.- Data of Deckwer(1980) for xylene.

Tb=143 ^{o}C D=0.1 m U_b= 0.192 ms^{-1}

U_g mms^{-1}	holdup **	$h_{exp.}$ $W(m^2K)^{-1}$	$h_{pred.}$ * $W(m^2K)^{-1}$	%error
5	0.025	1260	806	-36
7	0.034	1318	899	-32
10	0.047	1380	1007	-27
15	0.068	1500	1143	-24
20	0.086	1585	1246	-21

* film resistance excluded.
** hold up was predicted by equation 2.

Table C2.7.- Data of Deckwer(1980) for kogasin

t_b= 143 °C D= 0.10 m U_b= 0.194 ms^{-1}

U_g mms^{-1}	holdup **	$h_{exp.}$ $W(m^2K)^{-1}$	$h_{pred.}$ * $W(m^2K)^{-1}$	%error
5	0.025	790	838	6
7	0.034	900	935	4
10	0.047	1100	1048	-5
15	0.067	1200	1187	-1
20	0.085	1380	1297	-6

* film resistance excluded.
** hold-up was predicted by equation 2.7

Table C2.8.- Data of Deckwer(1980) for decaline.

t_b= 143 °C D=0.10 m U_b=0.197 ms^{-1}

U_g mms^{-1}	holdup **	$h_{exp.}$ $W(m^2K)^{-1}$	$h_{pred.}$ * $W(m^2K)^{-1}$	%error
5	0.024	900	740	-18
7	0.033	1047	827	-21
10	0.046	1148	927	-19
15	0.066	1259	1050	-17
20	0.084	1220	1149	-5

* film resistance excluded.
** hold-up predicted by equation 2.7

APPENDIX D

CALCULATION INVOLVED CMC DATA

D1.- Calculation of Heat transfer Coefficient .

The following procedure was adopted to calculate heat transfer coefficient of CMC solutions at a given superficial gas velocity.

1.- The experimental values of heat transfer coefficent at the given superficial gas velocities are tabulated and the apparent viscosities of CMC solutions were obtained from the following equations,

$$\mu = K(\gamma)^{n-1} \qquad \text{Pa.s}$$

where $\gamma = 0.195\ U_g^{5}$ s^{-1} $U_g < 4$ cms^{-1}

$\gamma = 50.0\ U_g$ s^{-1} $U_g > 4$ cms^{-1}

The results are presented in tables D1 to D7.

2.- From tables D1 to D7 tables D8 to D14 were constructed. These tables give the variation of heat transfer coefficient with the viscosity of CMC solution at selected superficial gas velocities. Hence the coefficents , A and B, of the following equation were obtained.

$h = A\ \mu^{B}$ heat transfer coefficient in $W(m^2K)^{-1}$; viscosity in cP

The coefficients are given in table D1.15.These were used to obtain values that are presented in table 7.6 .

Table D1.- Apparent viscosity and heat transfer coefficient for 100 ppm CMC solution.

$$\mu = 0.002(\gamma)^{-0.143}$$

U_g cms^{-1}	viscosity cP	hold-up	h $W\ (m^2K)^{-1}$
1.2	2.21	0.036	3158
2.14	1.47	0.065	3467
2.72	1.24	0.079	3704
3.54	1.02	0.105	4054
5.21	0.902	0.128	4656
7.02	0.865	0.152	5257
8.75	0.838	0.183	5781

Table D1.2- Apparent viscosity and heat transfer coefficient for 500 ppm CMC solution.

$$\mu = 0.004\ (\gamma.)^{-0.167}$$

U_g cms^{-1}	viscosity cP	hold-up	h $W\ (m^2K)^{-1}$
1.2	4.25	0.038	2502
2.14	2.772	0.064	2801
2.73	2.257	0.085	2921
3.57	1.779	0.111	3248
5.17	1.567	0.143	3699
7.15	1.481	0.165	4263
9.00	1.425	0.185	4554

Table D1.3- Apparent viscosity and heat transfer coefficient for 500 CMC solution.

$$\mu = 0.008 (\gamma)^{-0.126}$$

U_g cms^{-1}	μ cP	holdup	h $W (m^2K)^{-1}$
1.2	9.02	0.039	2149
2.14	0.0581	0.069	2387
2.73	4.560	0.088	2567
3.55	3.667	0.109	2700
5.19	3.179	0.139	2978
7.19	3.013	0.161	3192
8.93	2.905	0.185	3378

Table D1.4.- Apparent viscosity and heat transfer coefficient for 1500 ppm CMC solution.

$$\mu = 0.011(\gamma)^{-0.123}$$

U_g cms^{-1}	μ cP	holdup	h $W(m^2K)^{-1}$
1.2	12.023	0.033	2065
2.15	8.522	0.063	2297
2.78	7.172	0.081	2391
3.59	6.128	0.105	2534
5.28	5.540	0.128	2852
8.40	5.233	0.158	3245

Table D1.5.- Apparent viscosity and heat transfer coefficient for 2000 ppm CMC solution.

$$\mu = 0.018(\gamma)^{-0.167}$$

U_g cms^{-1}	μ cP	holdup	h $W(m^2K)^{-1}$
1.21	20.17	0.037	1724
2.14	12.53	0.066	1957
2.74	10.193	0.076	2012
3.59	8.135	0.095	2136
5.21	7.109	0.118	2426
7.20	6.736	0.139	2644
8.86	6.506	0.159	2872

Table D1.6.- Apparent viscosity and heat transfer coefficient for 3000 CMC solution.

$$\mu = 0.028(\gamma)^{-.19}$$

U_g cms^{-1}	μ cP	holdup	h $W(m^2K)^{-1}$
1.20	32.124	0.035	1458
2.15	18.46	0.057	1642
2.78	14.461	0.071	1775
3.59	11.343	0.092	1856
5.27	9.70	0.106	2092
7.31	9.125	0.130	2313
8.81	8.807	0.135	2394

Table D1.7.- Apparent viscosity and heat transfer coefficient for 10,000 ppm CMC solution.

$$\mu = 0.158 (\gamma)^{-0.19}$$

U_g cms^{-1}	viscosity cP	hold-up	h $W(m^2K)^{-1}$
1.25	181.48	0.034	851.5
2.17	105.256	0.049	947
2.74	82.735	0.061	1072
3.59	64.0	0.068	1078
5.44	54.46	0.079	1269
6.13	53.24	0.076	1350
8.60	49.923	0.087	1450

Tables D1.8 to D1.14 give variation of heat transfer coefficient with viscosity of CMC solution at a selected values of gas superficial velocity.

Table D1.8 U_g= 1.2 cms^{-1}

	concentration ppm	μ cP	hold-up	h $W(m^2K)^{-1}$
1	100	2.210	0.036	3158.0
2	500	4.520	0.038	2502.0
3	1000	9.020	0.039	2149.0
4	1500	12.023	0.039	2065.0
5	2000	20.170	0.038	1724.0
6	3000	32.124	0.035	1458.0
7	10000	181.480	0.034	851.5

Table D1.9 U_g= 2.14 - 2.17 cms^{-1}

	consentration ppm	μ cp	hold-up	h $W(m^2K)^{-1}$
1	100	1.470	0.036	3469.0
2	500	2.772	0.064	2801.0
3	1000	6.581	0.069	2387.0
4	1500	8.522	0.063	2297.0
5	2000	12.530	0.066	1957.0
6	3000	18.460	0.057	1642.0
7	10000	103.200	0.049	947.0

Table D1.10 U_g =2.72 -2.78 cms^{-1}

	concentration ppm	μ cP	hold-up	h $W(m^2K)^{-1}$
1	100	1.240	0.079	3704.0
2	500	2.257	0.085	2921.0
3	1000	4.560	0.088	2567.0
4	1500	7.172	0.081	2391.0
5	2000	10.193	0.076	2012.0
6	3000	14.461	0.071	1775.0
7	10000	82.735	0.061	1072.0

Table D1.11 U_g= 3.54- 3.59 cms^{-1}

	concentration ppm	μ cP	hold-up	h $W(m^2K)^{-1}$
1	100	1.020	0.105	4054.0
2	500	1.779	0.111	3248.0
3	1000	3.667	0.109	2700.0
4	1500	6.128	0.105	2534.0
5	2000	8.135	0.095	2136.0
6	3000	11.343	0.092	1856.0
7	10000	64.000	0.068	1078.0

Table D1.12 U_g= 5.17- 5.44 cms^{-1}

	cocentration ppm	μ cP	hold-up	h $W(m^2K)^{-1}$
1	100	0.902	0.128	4656.0
2	500	1.567	0.143	3699.0
3	1000	3.179	0.139	2978.0
4	1500	5.540	0.128	2852.0
4	2000	7.109	0.118	2426.0
6	3000	9.700	0.106	2092.0
7	10000	54.460	0.079	1269.0

Table D1.13 U_g= 7.02- 7.31 cms^{-1}

	concentration ppm	μ cP	hold-up	h $W(m^2K)^{-1}$
1	100	0.865	0.152	5257.0
2	500	1.481	0.165	4268.0
3	1000	3.013	0.161	3192.0
4	1500	5.328	0.158	3102.0
5	2000	6.736	0.139	2644.0
6	3000	9.125	0.130	2313.0
7	10000	53.240	0.760	1350.0

Table D1.14 U_g =8.40- 9 cms^{-1}

concentration ppm	μ cP	hold-up	h $W(m^2K)^{-1}$
100	0.838	0.183	5781.0
500	1.425	0.183	4554.0
1000	2.905	0.185	3378.0
1500	5.233	0.158	3245.0
2000	6.506	0.159	2872.0
3000	8.807	0.135	2394.0
10000	49.923	0.087	1450.0

Table D1.15.- Coefficients, A and B, of equation, $h = A(\mu)^B$.

U_g cms^{-1}	μ cP	A	B
1.2	2 - 182	4067	-0.295
2.14- 2.17	1.47- 1.03	4045	-0.303
2.72- 2.78	1.24- 82	3928	-0.290
3.54- 3.59	1.02- 64	4087	-0.315
5.17- 5.44	0.90- 55	4422	-0.311
7.02- 7.31	0.865- 53	4901	-0.325
8.45- 9.0	0.838- 49	5215	-0.331

D2.- Determination of the Best Values of Coefficients of Equation 2.47

The estimated data of heat transfer coefficent that are given in Table 7.6 are correlated according to

$$\frac{1}{h} = A + B(\epsilon U_g)^{\frac{-1}{6}}$$

using Minitab statistical package.The coefficients A and B for a given viscosity were summarised in Table 7.7.

The followings are the results of linear regression analysis of the CMC data in which c5=$(U_g.\epsilon\ .)^{-1/6}$ and Coef gives coefficients.

Viscosity = 1 x 10^{-3} Pa.s

The regression equation is
1/h =0.000144 +0.000032 c5

Predictor	Coef	Stdev	t-ratio
Constant	0.00014421	0.00002916	4.95
c5	0.00003218	0.00001063	3.03

s = 0.00001576 R-sq = 64.7% R-sq(adj) = 57.6%

Analysis of Variance

SOURCE	DF	SS	MS
Regression	1	0.0000000023	0.0000000023
Error	5	0.0000000012	0.0000000002
Total	6	0.0000000035	

Viscosity = 5 x 10^{-3} Pa.s

The regression equation is
1/h =0.000271 +0.000041 c5

Predictor	Coef	Stdev	t-ratio
Constant	0.00027078	0.00004931	5.49
c5	0.00004142	0.00001850	2.24

s = 0.00002500 R-sq = 50.1% R-sq(adj) = 40.1%

Analysis of Variance

SOURCE	DF	SS	MS
Regression	1	0.0000000031	0.0000000031
Error	5	0.0000000031	0.0000000006
Total	6	0.0000000063	

Viscosity = 10 x 10^{-3} Pa.s

The regression equation is
1/h =0.000341 +0.000048 c5

Predictor	Coef	Stdev	t-ratio
Constant	0.00034111	0.00006073	5.62
c5	0.00004832	0.00002244	2.15

s = 0.00002860 R-sq = 48.1% R-sq(adj) = 37.7%

Analysis of Variance

SOURCE	DF	SS	MS
Regression	1	0.0000000038	0.0000000038
Error	5	0.0000000041	0.0000000008
Total	6	0.0000000079	

Viscosity = 20 x 10^{-3} Pa.s

The regression equation is
1/h=0.000466 +0.000043 c5

Predictor	Coef	Stdev	t-ratio
Constant	0.00046575	0.00007398	6.30
c5	0.00004344	0.00002715	1.60

s = 0.00003614 R-sq = 33.9% R-sq(adj) = 20.6%

Analysis of Variance

SOURCE	DF	SS	MS
Regression	1	0.0000000033	0.0000000033
Error	5	0.0000000065	0.0000000013
Total	6	0.0000000099	

Viscosity = 50 x 10^{-3} Pa.s

The regression equation is
1/h =0.000624 +0.000053 c5

Predictor	Coef	Stdev	t-ratio
Constant	0.0006242	0.0001043	5.99
c5	0.00005349	0.00003707	1.44

s = 0.00004341 R-sq = 29.4% R-sq(adj) = 15.3%

Analysis of Variance

SOURCE	DF	SS	MS
Regression	1	0.0000000039	0.0000000039
Error	5	0.0000000094	0.0000000019
Total	6	0.0000000133	

Viscosity = 100 x 10^{-3} Pa.s

The regression equation is
1/h =0.000799 +0.000053 c5

Predictor	Coef	Stdev	t-ratio
Constant	0.0007992	0.0001847	4.33
c5	0.00005340	0.00006183	0.86

s = 0.00005445 R-sq = 13.0% R-sq(adj) = 0.0%

Analysis of Variance

SOURCE	DF	SS	MS
Regression	1	0.0000000022	0.0000000022
Error	5	0.0000000148	0.0000000030
Total	6	0.0000000170	

Viscosity = 180 x 10^{-3} Pa.s

The regression equation is
1/h = 0.00105 +0.000032 c5

Predictor	Coef	Stdev	t-ratio
Constant	0.0010517	0.0002478	4.24
c5	0.00003228	0.00008178	0.39

s = 0.00006500 R-sq = 3.0% R-sq(adj) = 0.0%

Analysis of Variance

SOURCE	DF	SS	MS

Regression	1	0.0000000007	0.0000000007
Error	5	0.0000000211	0.0000000042
Total	6	0.0000000218	

****

D3.- Model Prediction of Heat Transfer Coefficient for CMC Solutions.

The following minitab programme was used in order to calculated data required in Figures 7.17 to 7.19.

```
MTB > let 'delta'=1.82e-3*('vis'**0.567)
MTB > let '1/hf'='delta'/0.60
MTB > let 'Uc'=1.31*(2.6*0.292*9.81*'ug'*'hold-up')**(1/3)
MTB > let '1/hp'=(3.14*0.016/(4*998*4181*0.6*'Uc'))**0.5
MTB > let 'hcal'=1/('1/hf'+'1/hp')
MTB > let 'hcal.'=1/('1/hf'+'1/hp')
MTB > let '%error'=('hcal.'-'hexp.')*100/'hexp.'
MTB > print c1-c9
```

The following results (SI units) were obtained.

	ug	vis	hold-up	hexp.	delta	1/hf	1/hp
100 ppm							
1	0.0120	0.002210	0.036	3158.0	0.0000568	0.0000947	0.0001611
2	0.0214	0.001470	0.065	3467.0	0.0000451	0.0000751	0.0001325
3	0.0272	0.001240	0.079	3704.0	0.0000409	0.0000682	0.0001233
4	0.0354	0.001020	0.105	4054.0	0.0000366	0.0000611	0.0001125
5	0.0521	0.000902	0.128	4656.0	0.0000342	0.0000570	0.0001021
6	0.0702	0.000865	0.152	5257.0	0.0000334	0.0000556	0.0000944
7	0.0875	0.000838	0.183	5781.0	0.0000328	0.0000546	0.0000882
500 ppm							
8	0.0120	0.004520	0.038	2502.0	0.0000852	0.0001420	0.0001596
9	0.0214	0.002772	0.064	2801.0	0.0000646	0.0001076	0.0001329
10	0.0273	0.002257	0.085	2921.0	0.0000575	0.0000958	0.0001217
11	0.0357	0.001779	0.111	3248.0	0.0000502	0.0000837	0.0001113
12	0.0517	0.001567	0.143	3699.0	0.0000467	0.0000779	0.0001003
13	0.0715	0.001481	0.165	4268.0	0.0000453	0.0000754	0.0000928
14	0.0900	0.001425	0.183	4554.0	0.0000443	0.0000738	0.0000878
1000 ppm							
15	0.0120	0.009020	0.039	2149.0	0.0001261	0.0002101	0.0001589
16	0.0214	0.006581	0.069	2387.0	0.0001054	0.0001757	0.0001312
17	0.0273	0.004560	0.088	2567.0	0.0000856	0.0001427	0.0001210
18	0.0355	0.003667	0.109	2700.0	0.0000757	0.0001261	0.0001118
19	0.0519	0.003179	0.139	2978.0	0.0000698	0.0001163	0.0001007
20	0.0718	0.003013	0.161	3192.0	0.0000677	0.0001129	0.0000931

continued..

	ug	vis	hold-up	hexp.	delta	1/hf	1/hp
1500 ppm							
21	0.0893	0.002905	0.185	3378.0	0.0000663	0.0001105	0.0000877
22	0.0120	0.012023	0.039	2065.0	0.0001484	0.0002473	0.0001589
23	0.0215	0.008522	0.063	2297.0	0.0001221	0.0002035	0.0001331
24	0.0278	0.007172	0.081	2391.0	0.0001107	0.0001845	0.0001223
25	0.0359	0.006128	0.105	2534.0	0.0001013	0.0001688	0.0001123
26	0.0528	0.005540	0.128	2852.0	0.0000956	0.0001594	0.0001018
27	0.0729	0.005325	0.158	3102.0	0.0000935	0.0001559	0.0000932
28	0.0840	0.005233	0.158	3245.0	0.0000926	0.0001543	0.0000910
2000 ppm							
29	0.0121	0.020170	0.037	1724.0	0.0001990	0.0003317	0.0001601
30	0.0214	0.012530	0.066	1957.0	0.0001519	0.0002532	0.0001322
31	0.0274	0.010193	0.076	2012.0	0.0001351	0.0002252	0.0001239
32	0.0359	0.008135	0.095	2136.0	0.0001189	0.0001982	0.0001141
33	0.0521	0.007109	0.118	2426.0	0.0001102	0.0001836	0.0001035
34	0.0720	0.006736	0.149	2644.0	0.0001069	0.0001781	0.0000943
35	0.0886	0.006506	0.159	2872.0	0.0001048	0.0001746	0.0000901
3000 ppm							
36	0.0120	0.032124	0.035	1458.0	0.0002591	0.0004318	0.0001618
37	0.0215	0.018460	0.057	1642.0	0.0001892	0.0003154	0.0001354
38	0.0278	0.014461	0.071	1775.0	0.0001648	0.0002746	0.0001250
39	0.0359	0.011343	0.092	1856.0	0.0001436	0.0002393	0.0001148
40	0.0527	0.009700	0.106	2092.0	0.0001314	0.0002190	0.0001051
41	0.0731	0.009125	0.130	2313.0	0.0001269	0.0002115	0.0000962
42	0.0881	0.008807	0.135	2394.0	0.0001244	0.0002073	0.0000927
10,000 ppm							
43	0.0125	0.181480	0.034	851.5	0.0006916	0.0011526	0.0001615
44	0.0217	0.103256	0.049	947.0	0.0005023	0.0008372	0.0001386
45	0.0274	0.082735	0.061	1072.0	0.0004430	0.0007383	0.0001285
46	0.0359	0.064000	0.068	1078.0	0.0003830	0.0006383	0.0001207
47	0.0544	0.054460	0.079	1269.0	0.0003495	0.0005825	0.0001098
48	0.0613	0.053240	0.076	1350.0	0.0003450	0.0005750	0.0001084
49	0.0860	0.049923	0.087	1450.0	0.0003327	0.0005544	0.0001001

continued..

	hcal.	%error
100 ppm		
1	3910.42	23.8257
2	4815.39	38.8921
3	5222.16	40.9872
4	5761.03	42.1073
5	6288.36	35.0593
6	6666.82	26.8180
7	7001.24	21.1077
500 ppm		
8	3315.12	32.4987
9	4157.53	48.4304
10	4597.55	57.3965
11	5127.44	57.8645
12	5610.76	51.6833
13	5943.29	39.2523
14	6187.90	35.8783
1000 ppm		
15	2709.48	26.0810
16	3257.57	36.4712
17	3791.52	47.7024
18	4203.23	55.6752
19	4606.61	54.6882
20	4854.81	52.0931
21	5043.14	49.2938
1500 ppm		
22	2461.46	19.1988
23	2970.73	29.3308
24	3258.95	36.3008
25	3558.27	40.4212
26	3827.84	34.2159
27	4015.30	29.4423
28	4075.98	25.6081
2000 ppm		
29	2033.50	17.9524
30	2594.69	32.5853
31	2864.08	42.3500
32	3201.69	49.8919
33	3483.43	43.5875
34	3671.36	38.8564
35	3777.59	31.5316

	hcal.	%error
3000 ppm		
36	1684.55	15.5385
37	2218.39	35.1026
38	2502.09	40.9630
39	2824.41	52.1772
40	3085.31	47.4815
41	3249.39	40.4840
42	3333.27	39.2342
10000 ppm		
43	760.98	-10.6306
44	1024.83	8.2183
45	1153.57	7.6090
46	1317.56	22.2224
47	1444.46	13.8269
48	1463.28	8.3910
49	1527.71	5.3594

****

NOMENCLATURE

A	intercept in equation 2.47 , constant.
A	surface area of heater in equation 3.2.
A	the shortest distance between the axis of symmetry and the eye of the vortex in equation 2.20. This is shown in Figure 2.2 by distance AA.
A_k	constants of equation 2.18.
A_r	Archimedes number defined by equation 1.55.
B	constants of equation 2.18 that can be put equal to 1 by a suitable choice of ω_o .
B	slope of line in equation 2.47.
C_p	heat capacity of liquid.
c ,C	Constant.
D	column diameter.
D_p	coil diameter.
D_R	impeller diameter.
d_o	orifice diameter.
d_b	average bubble diameter.
d_H	heater vertical length.
d_{vs}	Sauter mean bubble diameter.
E	energy available for liquid circulation in equation 2.14.
E	energy input rate per unit mass in equation 1.42 to 1.46.
E_i	energy input rate in equation 2.11.
E_1	energy dissipiation in the wakes behind the bubble.
E_2	energy dissipation in the hydraulic jump at the liquid surface.
f	friction factor.

Gr	Grashof number.
g	gravitaional constant.
H	initial liquid height.
H_o	aerated liquid height.
H_t	total length of manometer limbs including tubing.
H_d	heater diameter.
h	average heat transfer coefficient.
h_f	film heat transfer coefficient.
h_p	packet heat transfer coefficient.
h_i	instantanous heat transfer coefficient.
h_{max}	maximum heat transfer coefficient.
h_l	heat transfer coefficient of unaerated liquid.
K	flow consistancy index.
k	constant in equation 2.15.
k	thermal conductivity of liquid.
L_c	heater characterictic length.
l	liquid movement length in equation 1.5 and 1.16.
l	length of micro eddies movement.
N_{row}	number of rows in tube bundle.
Nu	Nusselt number.
n	a measure of liquid circulatioin intensity in equations 2.25 and 2.26.
n	flow behaviour index.
n	stirring speed equation 1.5.
P_1	pressure at the column base.
P_2	pressure at the column top.
P_{m1}	pressure above the liquid level in the manometer limb 1.

P_{m2} pressure above the liquid level in the manometer limb 2.

Pe Peclet number.

Pr Prantl number.

P_{atm} atmospheric pressure.

Q power input tothe heater.

q heat flux per unit area.

$R(r^*)$ radial component of dimensionless stream function.

Re Reynold number.

r_o column radius.

r Radial coordinate.

r^* dimensionless radial coordinate.

r_s heater radius.

St Stanton number.

St_f film Stanton number.

St_p packet Stanton number.

T Temperature

t time.

t_b liquid temperature.

t_R distance between tubes.

t_s heater surface temperature

U liquid circulation in equation 1.19.

U_b bubble rise velocity.

U_c average liquid circulation.

U_{cF} average liquid circulation given by Field.

U_{cFs} average liquid circulation given by Field simplified version.

U_{cJ} average liquid circulatin given by Joshi and Sharma.

U_{cJs}	average liquid circulation velocity given by Joshi and Sharma ,simplified.
U_g	superficial gas velocity.
U_L	superficial liquid velocity.
U_s	slip velocity.
u_i	local circulation velocity in equation 2.20.
V	constant in equation 2.18.
V	volumetric gas flow rate.
y	vertical distance from wall
y^+	dimensionless distance
z	axial coordinate.
$Z(z^*)$	axial component of dimensionless stream function.
(P/V)	power input to mechanically stirred column.
α	thermal diffusivity.
β	coefficient of thermal expansion.
θ	temperature difference between the heater surface and the bulk temperature.
δ	velocity boundary layer thickness.
δ_t	thermal boundary layer thickness.
ΔP	pressure difference. Hydrostatic pressure head.
ΔT	temperature difference t_s-t_b
Δh	distance between manometer tapping.
ΔZ	manometer reading.
$\frac{\Delta P}{\Delta h}$	pressure gradient.
$\Delta\rho$	density difference.
ρ_g	gas density
σ	surface tension.
ν	kinematic viscosity.

ψ_o liquid circulation strength.

ψ stream function defined by equations 2.16.

ω vorticity defined by equation 2.17.

τ contact time.

γ shear rate.

τ_w shear stress at the wall

μ_w viscosity at wall.

μ viscosity.

ϵ gas hold-up.

Dimensionless Ratios

Fr	Froude number	$\frac{U_g^2}{gD}$
Gr	Grashof number	$\frac{\beta g \Delta T l}{\nu^2}$
Nu	Nusselt number	$\frac{hD}{k}$
Pe	Peclet number	$\frac{\rho U_g C_p D}{k}$
Pr	Prandtl number	$\frac{\mu C_p}{k}$
Re	Reynolds number	$\frac{\rho U_g D}{\mu}$
St	Stanton number	$\frac{h}{\rho U_g C_p}$
y^+	dimensionless distance	$\frac{y\sqrt{\frac{\tau_w}{\rho}}}{\nu}$

Subscript

g,G gas

l,L liquid

REFERENCES

Akita,K. and Yoshida,F. (1973) Ind. Eng. Chem. Process Des. Dev. 12 No. 1.

Akita,K. and Yoshida,F.(1974) Ind. Eng. Chem. Process Des. Dev. 13 No. 1.

Anderson, J.L. and Quinn, J.A. (1970) Chem. Sci. 25 373.

Armstrong,G.P. (1968) "Modern Chemistry in Industry ", Sci London.

Bach, H.F. and Pilhofer,Th.(1978) Ger. Chem. Eng. 1 270.

Batchelor, G.K.(1967) "An Introduction to Fluid Mechanics" CUP.

Bridge, A.G., Lapidus, L. and Elgin, J.C.(1964) AIChE J. 10 819.

Burkel, W(1972) Chem. Ing. Tech. 44 265.

Calderbank, P.H.(1967) Chem. Engr. 45 CE 209.

Carslaw, H.S. and Jaeger, J.C.(1959) "Conduction of heat in Solids" OUP 2nd ed.

Chen, J.J.J.(1987) Chem. Eng. Res. Des., 65 115.

Clift, R., Grace, J.R, Weber, M.E(1978) "Bubbles, Drops and Particles", AP , New York.

Davidson,L. and Amick, E.H.(1956) AIChE. J 2 337.

Davidson, J.F. and Schuler, B.O.G.(1960, a and b) Tran. IChemE 38 144-153 and 335-342.

Davidson, J.F. and Harrison, D.(1966) Chem. Eng. Sci. 21 731.

Davis, J.T.(1972) "Turbulence Phenomena" AP 49.

Davis, R.M. and Taylor, G.I.(1950) Proc., Roy. Soc. 200A, 375.

Deckwer, W.D.(1980) Chem. Eng. Sci. 35 1341.

Deckwer, W.D.(1981) "Access of Hydrodynamics Parameters Required in the Design and Scale Up of Bubble Column Reactors" Chemical Reactors, ACS Sym. Ser. 168.

Eissa, S.H. and Schugerl K.(1975) Chem. Eng. Sci. 30 1251.

Fair, J.R Lambright, A.J. and Anderson J.W.(1962) Ind. Eng. Proc. Des. Dev. 1 33.

Fair, J.R (1967) Chem. Engng. July 3 67-74 and July 17 207-214.

Field, R.W. and Davidson J.F.(1980) Trans. IChemE 58 228.

Field, R.W.(1980) "Gas Hold-Up and Mixing in Bubble Column" Thesis Univ. Cambridge.

Filed, R.W.(1987) Private communications.

Filed, R.W. and Rahimi, R.(1987) "Hold-Up and Heat Transfer in Bubble Column" Chem. Eng. Symp. Ser No.108 257.

Freedman, W. and Davidson J.F.(1969) Trans. IChE 47 T257.

Goar, B.G.(1968) Hydrocarbon Processing 47 No. 9 251.

Godbole, S.P. Honath, M.F. and Shah, Y.T.(1982) Chem. Eng. Commun. 16 119.

Godbole, S.P. Schumpe, A and Shah, Y.T.(1984) AIChe J 30, No. 2 213.

Grace, J.R. et al (1976) Trans. IChem.E 54 167.

Gupta, R.K. and Sharma, M.M (1967) Indian Chem. Engr. 9 Trans. 100.

Guy, C. Carreau, P.j. and Paris, J.(1986) Can. J. Chem. Eng. 64 23.

Hart, W.F.(1976) Ind. Eng. Chem. Proc. Des. Dev. 15 109.

Haque, M.W Nigma, K.D.P. Viswanathan, K. and Joshi, J.B.(1987) The Chem. Eng. J. 33 63.

Heijnen, J.J and Van't Riet K.(1984) "Mass Transfer, Mixing and Heat Transfer Phenomena in Low Viscosity Bubble Column Reactors" The Chem. Eng. J. 28 B21.

Hikita, H et al (1980) The Chem. Eng. J 20 59.

Hikita, H and Kikukama, H(1974) Chem. Eng. J. 8 191.

Hills, J.H.(1974) Trans. IChE 52 1.

Hills, J.H.(1976) The Chem. Eng. J. 12 89.

Hughmark, G.A.(1967) Ind. Eng. Chem. Proc. Des. Dev. 6 218.

Joshi, J.B and Sharma, M.M.(1976) Tran. IChE. 54 42.

Joshi, J.B and Sharma, M.M.(1979,a) Tran IchE 57 244.

Joshi, J.B and Sharma, M.M.(1979,b) Can. J. Chem. Eng. 57 357.

Joshi, J.B.(1980) Trans. IChE 58 155.

Joshi, J.B. and Sharma,M.M.(1980) Chem. Eng. Commu. 6 257.

Joshi, J.B. and Shah Y.T.(1981) Chem. Eng. Commu. 11 165.

Kast,W.(1962) Int. J. Heat and Mass Transfer 5 329.

Kawase, Y. and Moo- Young, M.(1987) Chem. Eng. Res. Des. Dev. 65 121.

Kay,J.M. and Neddermam, R.M.(1974) "Fluid Mechanics and Heat Transfer" CUP 3rd. ed.

Kelkar, B.G. Phulgaonkar and Shah Y.T(1983) The Che. Eng. J 27 125

Kelkar, B.G. and Shah, Y.T.(1985) AIChE 31 No.4 700.

Kolbel, H., Borchers, E. and Martins,J (1960) Chem. Ing. Tech. 32 84, through Deckwer(1980).

Konsetov, V.V.(1966) Int. J. Heat and Mass Transfer 9 1103.

Kostyak, N.G. et al(1962) J.Appl. Chem USSR 35 1939. through Shah et al (1982).

Kumar et al (1976) Can. J. Chem. Eng. 54 504. through Shah et al (1982).

Kubie, J.(1974) IChe Symp. Ser. No. 38 H1.

Lapidus,L. and Elgin, J.C.(1957) AIChE J 3 63.

Lewis(1980) Unpublished work obtained through Field(1987)

Lewis, D.A. Field, R.W. Xavier, A.M. and Edwards, D.(1980) Trans. IChE 60 40.

Lewis, D.A. Nicol, R.S. and Thompson(1984) Chem. Eng. Res. Des. 62 334.

Lockett, M.J. and Kirkpatrick, R.D(1975) Tras. IChE 53 267.

Louisi, Y.(1979) Dr. Ing. Thesis. Tu Berlin 1972. through Deckwer(1980).

Marrucci, G.(1965) Ind. Chem. Fundamentals 4 224.

Mashelkar, R.A.(1970) Bri. Chem. Eng. 15 1297.

Mersmann, A(1977) Int. Chem. Eng. 17 No.3 385.

Michael,R. and Reichert, K.H.(1981) Can. J. Chem. Eng. 59 602.

Moo-Young, M. Kawase, Y(1987)Canadian J. Chem. Eng. 65 113.

Nicklin, D. J. Wilkes,J.O. and Davidson, J.F(1962) Trans. Instn Chem Engrs. 40 61.

Nishikawa, M. Kato, H. and Hashimoto, K.(1977) Ind. Eng. Chem. Process Des. Dev. 16 133.

Nottenkamper, R. Steiff, A. and Weinspach, P. M.(1983) Ger. Chem. Eng. 6 147.

Novasade, Z.(1954) Chem. Listy 48 946.

Pavlov, V.P(1965) Khim Prov. No. 9 698.

Peebles and Garber (1953) Chem. Eng. Prog. 49 88.

Peroleum Process Handbook (1965)

Pozin, L.S., Aerov, M.E and Bystrova, T.A(1969) Theoretical Foundation of Chemical Engineering. English Translation; Through Hills(1974).

Rosenzeig, M. and Ushio, s.(1974) "Protein from Methanol " Chem. Eng. 81 Jan. 7 62.

Ruckenstein, E.(1958) Chem. Eng. Sci. 7 265.

Ruckenstein, E. and Smigelschi(1965) Trans. Instn. Che. Engrs. 43 T334.

Shah, Y.T. Joshi, J.B, Sharma, M.M (1981) Chemical Reactors, ACS, Symp. ser. 168.

Shah, Y.T. Kelkar et al (1982) AIChE J 28 n0.3 353.

Shaykhutdinov, N.U. Bakirov, A.G.(1971) Int. Chem. Eng. 11 No.4 641.

Smith, T.L and Greenshield(1982) "Tower Bioreactores" Chem. Eng. 81 28 : through Shah et al(1982).

Sittig,M(1967)"Organic Chemical Process Encyclopedia" Noyes. Corp. USA.

Sittig, M and Heine,H(1977) Chem. Ing. Tech.,49 595 : through Shah et al(1982).

Steiff,A and Weinspach, P.M(1978) Ger. Chem. Eng. 1 150.

Towell et al(1965) AIChE. Inst. Chem. Eng. Symp. Ser. No. 10 10.

Turner, J. C.R(1966) Chem. Eng. Sci. 21 971.

Whalley, P.B.(1971) PhD Thesis, Univ. Cambridge.

Whalley, P.B. and Davidson, J.F.(1974)"Liquid Circulation in Bubble Column." Chem. Engrs. Sym. Ser. No.38 J5

Vatai, G.Y Tekic, M.N(1987) Chem. Eng. Sci. 42 No.1 166.

Wallis,G.B(1969) "One Dimensional Two Phase Flow" McGraw Hill.

Wendt, R. Deuerler,F Steiff, A and Weinspach, P.M.(1984) Chem. Ind. Tech. 56 No. 12 946.

Wendt,R. Steiff,A. Weinspach,P.M. (1984) Ger. Chem. Eng. 267.

Xavier, A.M.(1979) Communication through Field, R.W.

Yamashita, F.(1978) J. Chem. Eng. Japan 20 No.2 204.

Yamashita, F.(1987) J. Chem. Eng. Japan 20 No.2 201.

Yau, A.V. et al (1987) Paper at Int. Symp. Co- Current Gas-Liquid Flow, Water 100.

Yoshitoma, H.M.(1965) Kagaku Kogaku 29 No.1 19 ; through Hart(1976).

Zehner, P. and Schuch, G.(1985) Ger. Chem. Eng. 8 282.

Zehner, P.(1986) " Momentum, Mass and Heat Transfer in Bubble Column" Int. Chem. Eng. 26 NO.1 22.

Zuber,N and Findley, J.A(1965) Tra. ASME, J of Heat Transfer, 87 453.